To diversity and beyond

Rozema, Patrick Dennis

To diversity and beyond

Shifting Antarctic microbial communities along environmental gradients

Patrick Dennis Rozema

The research reported in this thesis was carried out at the department of Ocean Ecosystems, which is part of the Energy and Sustainability Research Institute Groningen (ESRIG) of the University of Groningen (the Netherlands), according to the requirements of the Graduate School of Science and Engineering. Funds for this research were obtained by A.G.J. Buma through the Netherlands Polar Programme of the Netherlands Organisation for Scientific Research (NWO; grant: 866.10.105).

The printing of this thesis was partly funded by the Central Library and the Faculty of Science and Engineering.

Cover design and artwork:	Karlien Meijer
Layout:	Patrick Rozema
Printed by:	Gildeprint - Enschede
ISBN:	978-94-034-0254-3
ISBN (electronic version):	978-94-034-0255-0

university of groningen

To diversity and beyond

shifting Antarctic microbial communities along environmental gradients

PhD thesis

to obtain the degree of PhD at the
University of Groningen
on the authority of the
Rector Magnificus Prof. E. Sterken
and in accordance with
the decision by the College of Deans.

This thesis will be defended in public on

Friday 1 December 2017 at 12.45 hours

by

Patrick Dennis Rozema

born on 13 June 1985
in Groningen

Supervisor
Prof. A.G.J. Buma

Co-supervisors
Dr. H. Bolhuis
Dr. W.H. van de Poll

Assessment Committee
Prof. H.J.W. de Baar
Prof. M.S. Clark
Prof. O.M.E. Schofield

Table of contents

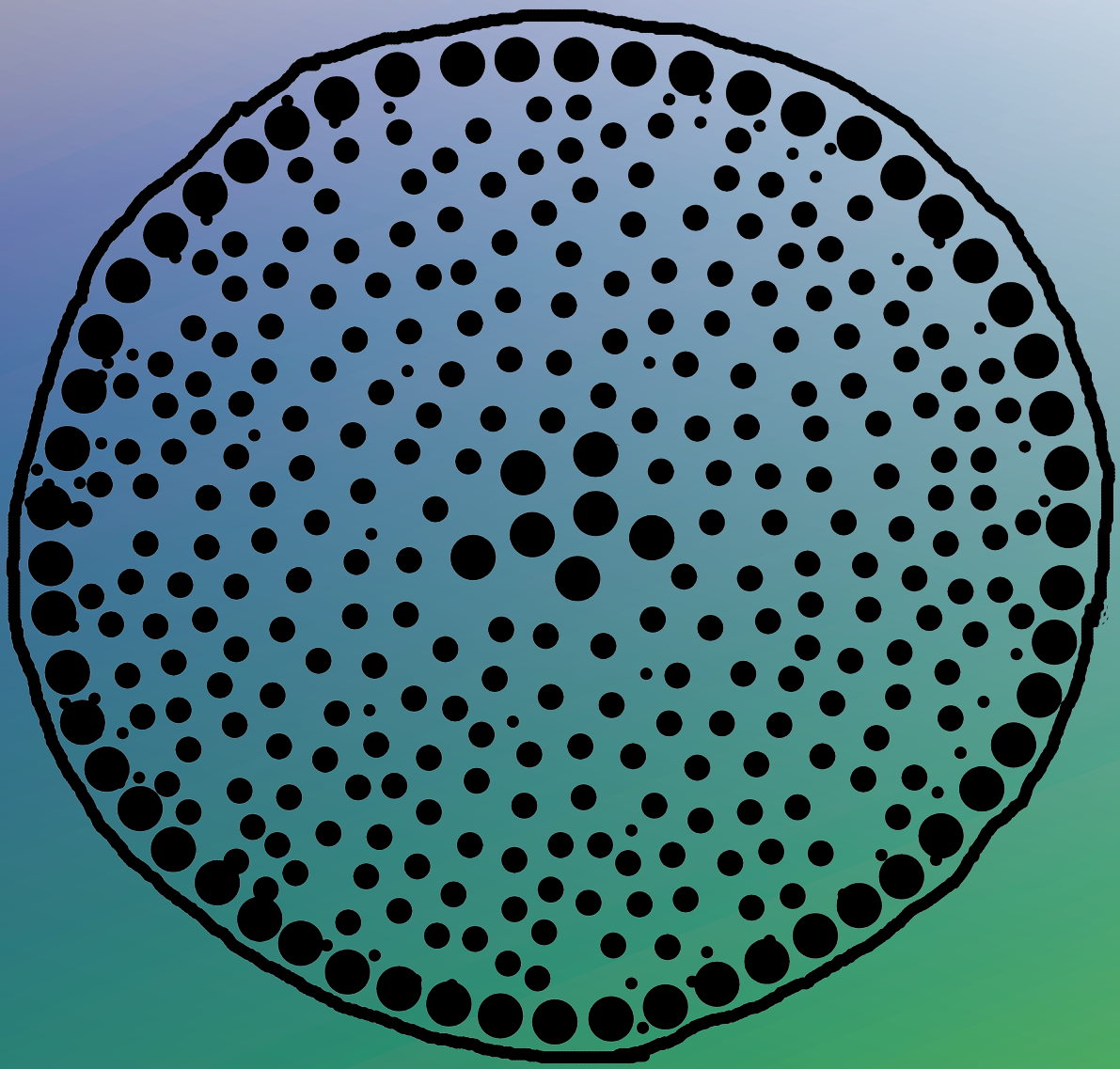

Chapter 1

Introduction and synthesis

The microbial community is strongly governed by bottom up controls, thus environmental forcing has an important impact. Yet, these forcings are often driven by larger processes. Therefore, I first introduce bottom up control, physical and (geo)chemical processes, of microbial diversity. Environmental forcing is rapidly changing due to of climate change. As such, these environmental factors are discussed quite extensively. Thereafter, I focus more on the biology, the main focus of the work in this thesis, namely the phytoplankton and bacterial community in the coastal Southern Ocean near the west Antarctic Peninsula (WAP, Fig. 1). This is followed by an introduction into the top-down control of microbial diversity, namely the grazers. Finally, there is a description of the site where all of the work in this thesis has been conducted.

Environmental influences and climate change at the WAP

Climate change affects the physical environment of many regions on our planet. One of the regions affected most profoundly is the WAP. During the past 50 years, the mean air temperatures over the WAP have increased by 2-3°C (Turner *et al.*, 2005). More specifically, mid-winter atmospheric surface temperatures have increased by an unprecedented 6°C during the latter period due to tropical teleconnections (Vaughan *et al.*, 2003; Ding *et al.*, 2011). Yet, the increase in air temperatures over the WAP has paused since the beginning of the 21st century (Turner *et al.*, 2016). The increase in air temperatures in the WAP region has been associated with changes in the atmospheric circulation, a shortening of the ice season and an increase in glacial and perennial ice melt. Furthermore, ocean (surface) temperatures have increased providing a positive feedback to regional (and global) warming (Meredith & King, 2005).

Atmospheric changes

While the strong rise in mean annual temperatures over the WAP is not fully understood, several relations to climatic modes have been suggested. A positive trend in the Southern Annular Mode (SAM) is observed through monitoring the atmospheric pressure distribution over the Antarctic continent (Thompson & Solomon, 2002). A positive SAM event is characterized by an increase in low pressure systems along the coast which effectively tightens the circulation around the continent. Overall, during the past 50 years, air pressure dropped along the coast and increased at the centre of

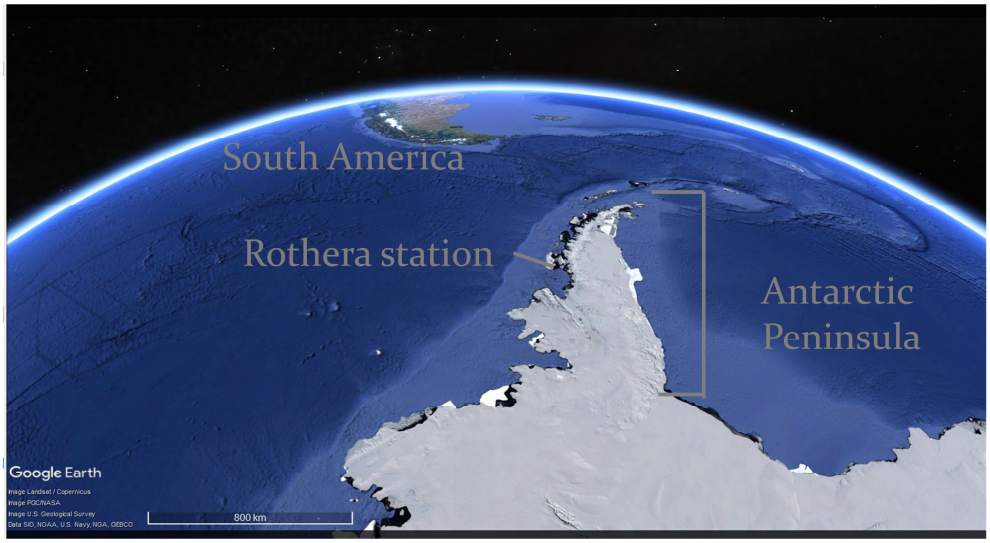

Figure 1: This map shows the Antarctic Peninsula extending into the Southern Ocean where the Drake Passage separates Antarctica from South America. Marked is Rothera Research station, where the research for this thesis was conducted.

the continent, shifting the SAM into a more frequent positive mode. The positive trend in the SAM index is associated with a strengthening of the circumpolar westerlies (Marshall *et al.*, 2006), most likely due to stratospheric ozone depletion and increasing greenhouse gases (Korhonen *et al.*, 2010). Consequently, the loss of atmospheric ozone cools the Antarctic stratosphere which in turn increases the strength of the cyclonic atmospheric circulation, called the polar vortex (Turner *et al.*, 2005).

The strength of the polar vortex is partly dependent upon the temperature difference between the warm middle/upper troposphere and stratosphere (Thompson & Solomon, 2002). Thus, as ozone depletion cools the stratosphere, the temperature difference increases which results in a strengthening of the polar vortex. Also affecting the temperature distribution in the atmosphere are greenhouse gases such as CO_2 (Turner *et al.*, 2009; Korhonen *et al.*, 2010). These gases increase the temperature in the troposphere but further decrease stratospheric temperatures thus enhancing the effect of ozone depletion on the westerlies. Of these two processes, ozone depletion seems to have the strongest influence on the strength of the polar vortex.

The increased strength of the westerlies and the observed shift to a frequently more positive SAM anomaly influenced the regional atmospheric circulation over the Antarctic Peninsula (Thompson & Solomon, 2002). Warm north-westerly winds crossing the Antarctic peninsula greatly affect the northern and western parts of the peninsula by increasing the atmospheric temperatures (Turner *et al.*, 2009; Dixon *et al.*, 2012). Moreover, these strong and warm winds shield the interior part of Antarctica by absorbing moisture which in turn decreases regional atmospheric temperatures in the Antarctic interior (Turner *et al.*, 2009; Russell & McGregor, 2010). Also, ozone depletion is strongest during spring and therefore influences summer air temperatures (Marshall *et al.*, 2006).Thus, atmospheric warming in Antarctica is strongly driven by these atmospheric processes (Thompson & Solomon, 2002; Polvani *et al.*, 2011).

The current pause in the rise of the air temperatures at the WAP started in the late 1990s, most likely due to a greater frequency of east to south-eastern winds which resulted from more cyclonic conditions over the Weddell Sea (Turner *et al.*, 2016). These conditions negated the warming effect generally observed from El Niño-events through tropical teleconnections (Ding *et al.*, 2011; Clem & Fogt, 2013). The increase in eastern winds has also pushed the sea ice in the Weddell Sea against the peninsula, increasing sea ice cover and thereby reducing the heat loss of the ocean. Long term records further suggest that the temperature trends observed since the 1950s fall within the expected climatic variability and do not correlate to any anthropogenic driver apart from the aforementioned increase in positive SAM index (Steig *et al.*, 2013).

Sea ice

Sea ice expand around Antarctica has, as opposed to sea ice in the northern hemisphere, increased by about 1% per decade during the past three decades (Parkinson, 2014). This positive trend applies to the entire Southern Ocean except for the Bellingshausen/Amundsen Sea region. Here, sea ice extent is significantly decreased by 6.8% per decade (Parkinson & Cavalieri, 2012; Stammerjohn & Maksym, 2017). The decrease in the latter region is in sharp contrast with the 4.3% increase in surface coverage in the nearby Ross Sea. Since these two regions are adjacent to each other, it is thought that these opposing trends are partly caused by advection of ice

between the two regions (Stammerjohn & Maksym, 2017). Additionally, this pattern is likely to be caused by the earlier discussed loss of ozone and consequently the increased strength of the westerlies.

In the Antarctica Peninsula region, the duration of sea ice cover has decreased by 40% over a 26-year period which opposes the general trend of increasing sea ice in the Antarctic (Smith & Stammerjohn, 2001; Montes-Hugo *et al.*, 2009; Stammerjohn & Maksym, 2017). Given the north-south orientation of the WAP, these trends are strongest towards the north (Stammerjohn *et al.*, 2008a; Ducklow *et al.*, 2013). Delayed onset of sea-ice formation in the WAP region has also been associated with increased north-westerly winds (Stammerjohn *et al.*, 2008a). These warm winds continuously push sea-ice southward along the peninsula preventing the build-up of sea- ice over the ocean. Without the insulating property of sea-ice, the ocean heat flux to the atmosphere has increased dramatically (Venables & Meredith, 2014). Thus, the increased ocean heat flux further increases air temperatures along the WAP by venting ocean heat to the overlying atmosphere (Vaughan *et al.*, 2003; Meredith & King, 2005; Harangozo, 2006). This positive feedback to regional warming strengthens further as seasonal sea-ice cover becomes shorter. In contrast, sea ice cover at the eastern Antarctic Peninsula, thus the Weddell Sea, has increased over the recent years (Turner *et al.*, 2016).

Sea ice dynamics are strongly affected by the changes in air temperatures over the WAP, and vice versa, as sea ice cover governs the heat lost by the ocean to the atmosphere. Due to the increasingly warmer winters, the period of sea ice growth is shortened by almost 90 days (Stammerjohn *et al.*, 2008a) while the number of days with temperatures above freezing temperature has increased (Barrand *et al.*, 2013). Stammerjohn et al. (2008) showed that the decrease in the duration of the WAP sea-ice season is primarily due to a strong trend towards a later autumn advance and a somewhat weaker trend towards an earlier spring retreat. These shifts in timing of the advance and retreat of sea ice lead to an increasingly longer ice free period during summer. Furthermore, the period of solar heating is extended and leads to an increase in the mean annual temperatures of the Antarctic surface waters (AASW) (Meredith & King, 2005).

Ice sheets and glaciers

Several ice sheets adjacent to the Antarctic Peninsula have collapsed in the past ~40 years. These ice sheet losses are not necessarily gradually, as illustrated by the sudden loss of the Larsen B ice sheet (3.250 square kilometres) in just over 30 days. Moreover, the loss of these ice shelves implies loss of the natural resistance for outflow of glaciers from the land, hence tends to increase glacial discharge and promote further retreat of glaciers behind the former ice shelf (Rignot *et al.*, 2004). Furthermore, most of the glaciers on the WAP are retreating and the rate of glacial melt is still increasing (Cook *et al.*, 2005; Rignot *et al.*, 2013). Most marine terminating glaciers along the WAP are melting from below in contact with underlying seawater, and/or at the glacial front at ~200 m depth (Cook *et al.*, 2016). Yet, as with most parameters along the WAP, there is a difference in response between the northern and southern regions. Glaciers in the south of the WAP region are predominantly melting because of intrusion of warm modified circumpolar deep water (mCDW). These intrusions are not present in the north, where cold water originating from the Weddell Sea is prevents glacial melting (Cook *et al.*, 2016). The increased melting of marine terminating glaciers causes additional fresh water influx into the coastal WAP.

Light availability for phytoplankton

The most important abiotic factor regulating phytoplankton growth is light. The extremely low light conditions during the polar winter strongly limit phytoplankton growth (Venables *et al.*, 2013). During spring and summer when waters are ice-free, strong vertical density stratification of the water column promotes phytoplankton growth by establishing a favourable, stable irradiance regime. Physical density of seawater is a function of salinity and temperature, at low salinity and/or higher temperature, seawater density is low. There are several processes which govern stratification in these coastal regions. Firstly, freshwater input from sea ice, and/or glacial melt, may cause water column stabilization due to low salinity upper waters .(Meredith *et al.*, 2013). While temperature driven stratification is important in many marine systems, it is less so in the Antarctic given the quite uniformly low temperatures. The freshening of seawater due to melting sea ice is considered to be more episodic, since it primarily occurs in spring when the sea ice retreats. Glacial melt

water increases in importance over the spring and summer seasons as air and sea temperatures rise. Both melting sea ice and glacial melt water provide a potential source of stabilization. Secondly, wind mixing events can cause rapid destabilization of the water column. As such, winter sea ice cover preconditions the water column (Venables *et al.*, 2013). When ice cover during winter is high, less wind mixing occurs. Moreover, stratification is further promoted as melting sea ice provides a large source of fresh water during spring. In contrast, when the sea ice is absent, the deeply mixed column requires more energy to restabilize while less meltwater is available (Venables *et al.*, 2013). Yet, meltwater lenses can still occur over this more unstable water column providing a shallow mixed layer (Moline *et al.*, 2004). Mixed layer depths in the northern WAP section have increased in the past ~40 years as opposed to those in the southern section (Montes-Hugo *et al.*, 2009). This discrimination is most probably linked to a difference in sea ice cover and wind forcing.

Nutrients

The Southern Ocean is known as a High Nutrient, Low Chlorophyll region where trace metals, predominantly iron, limit primary productivity while macronutrients (N, P and Si) are abundant (de Baar *et al.*, 1995, 2005). Here, phytoplankton have adapted their trace metal requirements to align with the low environmental concentrations. Adaptation occurs on both short (adaptation: photoplasticity) and long time (evolution: genes) scales, their trace metal requirements with light harvesting capabilities (e.g. Peers & Price, 2006; Alderkamp *et al.*, 2010). In contrast, along the WAP and especially the coastal regions thereof, iron and trace metal concentrations are considered to be higher given the close proximity to potential sources such as bottom sediments, glacial run off and sea ice (De Jong *et al.*, 2012; Sherrell *et al.*, 2015; Annett *et al.*, 2017 and references therein). Yet, the impact of trace metal availability on phytoplankton growth and community composition along the WAP is not yet fully elucidated as glacial melt can vary greatly in trace metal composition (Annett *et al.*, (2015) and references therein).

Macronutrients at the WAP originate primarily from upwelling of and mixing with mCDW (Henley *et al.*, 2017 and referecens therein). Wind mixing events appear to govern the nutrient supply through the deepening of the mixed layer. Additionally,

melting sea ice is also a source of nutrients, as it accumulates organic and inorganic matter during winter and spring (Fripiat *et al.*, 2017). Evidently, macronutrient supply is large enough to sustain high phytoplankton biomass in the coastal WAP (Clarke *et al.*, 2008). Additionally, remineralization of organic matter by bacteria provides an important source for replenishing nutrients during the summer (Ducklow *et al.*, 2007; Kim & Ducklow, 2016; Henley *et al.*, 2017). Therefore, given the large number of sources in the coastal WAP, limitation by macronutrients is rare and short lived when occurring (Henley *et al.*, 2017). If such short periods do exist, than these are most likely in the (glacial) melt water lenses (Dore *et al.*, 1992).

Biology and changes therein

Biological activity is above all shaped by the physical-chemical environment, thus changes in the latter are likely to change the species diversity on a micro and macro scale, from bacterial cells to penguins. The previously mentioned changes in all of the environmental forcings, either directly or indirectly, influence the physical and chemical characteristics of the water column. As such, the phytoplankton within the water column are strongly affected which is likely to hold long-term consequences for the marine ecosystems along the WAP (Schofield *et al.*, 2010; Ducklow *et al.*, 2012a; Saba *et al.*, 2014).

Since there is no substantial primary production in the terrestrial realm on Antarctica, Antarctic biological activity is almost completely dependent on marine primary production. An important physical feature in the marine environment is the presence of sea ice and the inter- and intra-annual variability therein holds a large influence over the ecosystem. Therefore, changes in sea ice dynamics might result in changes in the phytoplankton community which could cause a cascading effect throughout the Antarctic marine ecosystem.

Phytoplankton

Seasonal succession of phytoplankton species is strongly regulated by light and thus sea ice dynamics, of which the dates of sea ice retreat and sea ice formation are most important for two reasons (Ackley & Sullivan, 1994; Ducklow *et al.*, 2012a, 2013). First,

sea ice acts as a vector for seeding phytoplankton into the water column when it melts. Secondly, sea ice is an important fresh water source in spring.

In sea ice, phytoplankton communities are typically found in the bottom layer and/or in a surface slush layer (as reviewed in Arrigo, 2016). These dense communities harbour the same taxonomic groups as the water column communities: diatoms and *P. antarctica* are found to be the most dominating groups within the ice while during winter nano- and picoplankton dominate the water column (Tison *et al.*, 2010). The high resemblance between the spring/summer phytoplankton communities and the autumn/winter sea ice communities indicate a coupling between these two habitats. Presumably, sea-ice algal communities seed the water column during the spring sea-ice retreat (Ackley & Sullivan, 1994) Flooding events of sea ice at the snow-ice interface (slush) will further seed the sea ice from the top, where *P. antarctica* is often observed (Arrigo, 1997). Algal communities developing here are likely to differ in species composition from the bottom communities due to differences in irradiance, nutrients and salinity (e.g. Tison *et al.*, 2010). Entrapment of the phytoplankton occurs during sea ice formation in autumn and this restarts the annual cycle (Garrison & Mathot, 1996).

Austral spring marks the beginning of significant phytoplankton growth in the water column. During this season and the subsequent summer the water column stabilizes because of warming but mainly freshening due to the melting of sea and glacial ice. Stabilization of the water column results in a decrease in mixed layer depth (MLD) and consequently increases light availability for photosynthesis (Sverdrup, 1953). Generally, the subsequent initial phytoplankton blooms consist of diatoms that profit from the relatively high-light conditions (Garibotti *et al.*, 2005). During sudden wind mixing events dominance may shift towards the common and widespread haptophyte *Phaeocystis antarctica* (Arrigo *et al.*, 1999; Annett *et al.*, 2010). The latter species prefers a highly variable light regime, as found when strong wind events increase the MLD (Arrigo *et al.*, 1999). Although *Phaeocystis* species are most recognizable during its colonial form, they are mostly recorded in the flagellated form in the coastal WAP (Annett *et al.*, 2010). Additionally, cryptophytes are observed in relatively high abundance in the northern section of the WAP during the summer (Moline *et al.*,

2004; Mendes *et al.*, 2013). Abundance and distribution of this group are suggested to be controlled by reduced salinity derived from glacial melt, in regions where sea ice is becoming less important (Moline *et al.*, 2004; Saba *et al.*, 2014). Contrasting these suggestions is an observation of cryptophyte dominance east of the Antarctic Peninsula, in the marginal ice zone of the Weddell Sea (Buma *et al.*, 1992). A transition from the initial diatom-dominated bloom to smaller phytoplankton species has been also been attributed to sedimentation (Castro *et al.*, 2002), advection (Moline & Prezelin, 1996) and grazing (Garibotti *et al.*, 2003). Total Chlorophyll *a* levels during an austral summer primarily attributed to diatoms, cryptophytes and haptophytes. However two more groups are numerically abundant in the WAP region. Photosynthetic dinoflagellates and prasinophytes are often found at relative constant absolute abundances (Kozlowski *et al.*, 2011).

Rapid regional warming along the WAP has resulted in substantial changes in the phytoplankton communities (Montes-Hugo *et al.*, 2009). As discussed above, sea ice, air temperature, sea surface temperature (SST) and wind speed have all changed towards a warmer, more temperate climate. In response to these changes, remotely sensed chlorophyll a (Chl a; a proxy for phytoplankton biomass) along the northern part of the WAP have decreased by 89% during the summer months over the past three decades while those in the southern part have increased by 66% over the same period. This decrease in phytoplankton standing stock in the northern sector is thought be to a result of a deeper MLD leading to a decrease in mean light levels for phytoplankton (Mitchell & Holm-Hansen, 1991; Montes-Hugo *et al.*, 2009). In contrast, biomass has increased in the southern section due to favourable light conditions by the retreat of sea ice. Increases in MLD along the WAP occur because of greater surface wind stress (Mitchell & Holm-Hansen, 1991), during ice-free conditions. Since photosynthesis is directly coupled to light availability, a change in mean light levels will influence phytoplankton accordingly. When phytoplankton growth does not exceed loss terms (e.g. due to grazing and sinking) phytoplankton biomass accumulation in surface waters will cease and stocks will decrease. Montes–Hugo *et al.* (2009) therefore suggested that, given the scenarios presented by the IPCC (IPCC, 2007), the warmer polar climate in the northern WAP region might expand to the

south. These ongoing changes will continue to shape phytoplankton growth and community composition and consequently the entire ecosystem of the WAP.

Higher trophic levels

Microzooplankton along the WAP forms an important link in the Antarctic food web. They are significant grazers of bacteria and phytoplankton and affect the composition of microbial assemblages due to selective grazing (Banse, 1992; Sherr & Sherr, 1994, 2002). At the WAP, grazing by microzooplankton is higher than macrozooplankton grazing (Garzio *et al.*, 2013). For example, the five dominant macrozooplankton grazers removed 0-3% of the phytoplankton biomass production whereas the microzooplankton community removed between 30 and 70% (up to 116%). Also, microzooplankton remove a large proportion of the bacterial production (often >100%). The most important groups of microzooplankton at the WAP are microflagellates, ciliates, radiolaria, heterotrophic dinoflagellates, and early life history stages of some crustaceans (Ducklow *et al.*, 2012a; Georges *et al.*, 2014). Somewhat understudied in the Southern Ocean is the influence of mixothropy, species which exhibit both an autotrophic and heterotrophic lifestyle (Stoecker *et al.*, 1988, 2017; Johnson, 2015). This strategy is potentially widespread and quantification of their role in carbon cycling is uncertain.

Antarctic krill (*Euphausia superba*) and salps (e.g. *Salpa thompsoni*) are the two most abundant macro-sized phytoplankton grazers (Atkinson *et al.*, 2004). The Antarctic ecosystem largely revolves around krill as a key prey species for many seabirds and mammals (Everson, 2000). In its turn, krill particularly feeds on large phytoplankton species such as diatoms in high densities (Ross *et al.*, 1998; Steinberg *et al.*, 2015). Finally, krill may produce fast-sinking faecal pellets which may contribute to a negative feedback to global warming by storing CO_2 in the deep ocean (e.g. (Belcher *et al.*, 2017). Krill habitat is generally confined within the region between the polar front to the north and the Antarctic ice shelves to the south (Atkinson *et al.*, 2008). Abundance of krill is highest within the sector 10° to 80°W, the south-western part of the Atlantic Ocean, in close proximity to the Antarctic Peninsula (Atkinson *et al.*, 2012). Temporal variability is largely dependent on phytoplankton biomass and sea ice

extent and duration of the previous winter as the sea ice are feeding grounds for overwintering larvae.

Salps, the second most abundant grazers, are not thought to form an important link between trophic levels. High abundances of salps are generally associated with the extensive lower-productivity regions of the Southern Ocean where algal biomass is scarce and where phytoplankton cells are generally smaller. Under high biomass conditions, the feeding apparatus of salps can become irreversibly clogged with negative consequences for their growth and survival (Nishikawa *et al.*, 1995; Perissinotto & Pakhomov, 1998a, 1998b). As a result, these two grazers, krill and salps, are complementary to each other within the Southern Ocean given their different foraging preferences. Overlap in habitat is further prevented because gelatinous salps have a higher temperature tolerance than krill (Atkinson *et al.* (2004) and references therein).

Unfortunately, krill stocks have declined since the 1970's in the Southern Ocean (Atkinson *et al.*, 2004, 2012). Further declines in krill stocks are most likely due to a decrease in sea ice duration and extent, an increase in SST's and a high fishing pressure (reviewed in Atkinson *et al.*, 2008; Flores *et al.*, 2012)). In contrast, salp densities near the Antarctic coast, including the WAP, have more than doubled per decade (Atkinson *et al.*, 2004). Since average phytoplankton cell size is likely to decrease (Montes-Hugo *et al.*, 2009) due to a shift towards haptophyte and cryptophyte dominance during summer and warmer waters, salps might replace krill in coastal regions (Saba *et al.*, 2014). The effects of long term changes in krill standing stocks might have devastating effects on the Antarctic ecosystem because of the central position of krill in the Antarctic food web.

Typical Antarctic birds which are greatly affected by the decrease in krill availability are the several species of penguins. Previous studies have suggested an increase in sea ice-avoiding Chinstrap penguins and a decrease in sea ice-loving Adélie penguins due to the changes in sea ice along the WAP. However, recent insights into Adélie and Chinstrap penguin community dynamics have shown a decline in both species (Trivelpiece *et al.*, 2011). Therefore, instead of the demise in sea ice controlling the

abundance of these two species it has been put forward that food availability might control the abundance of these penguins. The diet of these penguins consists largely of krill while only a mere 1-2% of the gut contents of both Adélie and Chinstrap penguins is fish. As a consequence, changes in the availability of krill as food could affect the fitness of both species. In addition to a decline in krill abundance, competition for this resource has increased over the past few decades. The ban on whaling allowed for recovery of the baleen whale populations. Whales are largely dependent on krill consumption, further stressing the importance of krill within the Antarctic food web. The increasingly stronger competition for the already decreasing stocks of the ecological important krill is likely to further increase the stress on higher trophic levels in the WAP region.

Bacteria and remineralization

Polar marine bacterial diversity during winter is higher than during summer (Ghiglione & Murray, 2012; Ladau *et al.*, 2013). The dominant phyla in marine systems are (Alpha- and Gamma-) Proteobacteria, Actinobacteria and Bacteroidetes (also known as the Cytophaga-Flavobacterium-Bacteroides group)(Abell & Bowman, 2005; Gentile *et al.*, 2006; Caron *et al.*, 2011; Piquet *et al.*, 2011; Delmont *et al.*, 2014; Luria *et al.*, 2014, 2016; Landa *et al.*, 2016). Bacterial production is largely driven by the remineralization of dissolved organic matter (DOM) released by phytoplankton and other bacteria (Moran *et al.*, 2001). These compounds are either excreted directly by the phytoplankton, or indirectly through either sloppy feeding by zooplankton or cell death by e.g. viral lysis (Brum *et al.*, 2015). As DOM is produced primarily by phytoplankton, a relation with primary production and/or Chl a was hypothesized. Early studies investigating the coupling between primary and bacterial production did not provide sufficient evidence for such a relationship (as reviewed in Ducklow et al. 2012). For example, the Research on Coastal Antarctic Ecosystem Rates (RACER) project focused on this coupling in the waters off the northern Antarctic Peninsula and Drake Passage (Bird & Karl, 1991, 1999; Karl *et al.*, 1991). Here, low bacterial biomass (<2% of the total plankton biomass) and low bacterial productivity was found, with bacterial production averaging ~3% of primary production. These results are 10-fold lower than those observed in the temperate ocean (Cole *et al.*, 1988). The results from

the RACER project did not suggest a correlation between Chl a and bacterial activity, nor did it demonstrate an immediate response of bacterial activity to the spring phytoplankton bloom. Finally, Bird & Karl (1999) did recognize that the uncoupling of primary and bacterial production might not be valid for the entire Southern Ocean nor for different seasons. Yet, a more recent, extensive dataset, both spatial and temporal, did reveal a significant correlation between bacterial production, measured through Leucine incorporation rates, and primary production (Ducklow *et al.*, 2012b).

Rothera - Past, current and future research

Coastal regions of the WAP are scarcely studied with respect to inter- and intra-annual variability in microbial species composition (reviewed in Ducklow *et al.* 2007). One of the sites where studies do span more than a few months is Ryder Bay where Rothera station (67°34'S 68°08'W, British Antarctic Survey, BAS) is located (Fig. 1). These longer time series elucidate seasonal phytoplankton dynamics and annual variability therein (Buma *et al.*, 2001; Clarke *et al.*, 2008; Annett *et al.*, 2010; Piquet *et al.*, 2011). Algal biomass at the Rothera Oceanographic and Biological Time-Series (RaTS) during the summer period is on average 14 mg m^{-3} (Clarke *et al.*, 2008) and peaks over 20 mg m^{-3} are not uncommon (Clarke *et al.*, 2008; Annett *et al.*, 2010). These high Chl a concentrations illustrate the high productivity at this coastal site in the WAP region.

During a typical summer season at Rothera, different phytoplankton species contribute relative to total Chl a. Early spring blooms consist of small (<10µm) diatom species such as *Minidiscus chilensis*, *Chaetoceros* spp., *Fragilariopsis* spp. and *other* small centric diatoms (Annett *et al.*, 2010; Piquet *et al.*, 2011). Mid-summer season diatom assemblages are typically dominated by species of moderate size (+-20µm) although species composition is highly variable (Buma *et al.*, 2001; Clarke *et al.*, 2008; Annett *et al.*, 2010; Piquet *et al.*, 2011). Species attributing to this size fraction are *Odontella weissflogii, Actinocyclus curvulatus, Thalassiosira tumida* and various *Chaetoceros* species (Buma *et al.*, 2001; Clarke *et al.*, 2008; Annett *et al.*, 2010; Piquet *et al.*, 2011). Finally, diatom communities during the last part of the summer season are dominated by larger (+-30-50µm) species such as *Proboscia inermis* and *Eucampia antarctica* (Annett *et al.*, 2010; Piquet *et al.*, 2011). Silicate is generally not reported limiting (with concentrations exceeding 1 µM) for diatom growth in this bay (Clarke *et al.*, 2008).

Wind mixing events may cause stratification breakup after which the phytoplankton community may shift to a different assemblage. Piquet *et al.* (2011) reported two strong mixing events in Ryder Bay during the summer season (early 1998) where the 10m (water depth)-community was mixed up to the surface. The near-surface phytoplankton community was initially dominated by diatoms and prasinophytes. Only 1% of the surface irradiance was observed at a depth of 6.5m while surface salinity was low, suggesting a shallow turbid meltwater lens (Buma *et al.*, 2001; Piquet *et al.*, 2011). The wind mixing event caused a quadrupling in diatom numbers, suggesting that the community at 10m depth was light or nutrient limited beforehand. During the 1998 summer, no dominance of any kind of haptophyte or cryptophyte, including *P. antarctica,* occurred (Buma *et al.*, 2001; Piquet *et al.*, 2011). Even the two strong wind mixing events did not trigger a haptophyte bloom, as opposed to other studies where deep wind mixing events were followed by a dominance of *Phaeocystis antarctica* (Arrigo *et al.*, 1999) including in Ryder Bay (Annett *et al.*, 2010).

In the WAP region, interannual variability in the onset, duration and magnitude of the phytoplankton bloom can be significant. Here, differences in physical parameters between years (i.e. sea ice) have extensive effects on phytoplankton biomass (Venables *et al.*, 2013). Interannual differences in water column physics are strongly associated with El-Niño/Southern Oscillation (ENSO) and Southern Annular Mode (SAM) impacts on sea ice dynamics. More specifically, the studies in 1998 (Buma *et al.*, 2001; Piquet *et al.*, 2011) and a large part of the study done by Annett *et al.* (2010) were executed during El-Niño events. Exceptional observations, such as the lack of a haptophyte bloom after a wind mixing event (Buma *et al.*, 2001; Piquet *et al.*, 2011), might be related to large-scale processes such as ENSO and SAM. Inconsistent observations of phytoplankton community composition have been reported, for example the 2006-2007 season at Rothera when the phytoplankton biomass was low and largely consisted out of haptophytes (Annett *et al.*, 2010). These unexpected deviations from the classical Antarctic foodweb revolving around diatoms and krill illustrate the need for long-term, in-depth monitoring of algal diversity to improve our insight in environmental factors affecting the marine Antarctic ecosystem at large.

Thesis outline

In this thesis I will present findings based on data collected in Ryder Bay, near Rothera Research station on Adelaide Island. The general aim of my thesis was to unravel inter- and intra-annual variability in the microbial community, with an emphasis on phytoplankton. We strived to improve our understanding of how environmental conditions control the phytoplankton diversity and productivity. Ultimately, we want to contribute to the understanding of how the currently observed trends can be projected onto future climate scenarios. To this end, five sample and data sets were obtained and analysed, each focusing on particular environmental, or temporal/spatial scales, as follows:

I: Interannual variability in phytoplankton biomass and species composition in northern Marguerite Bay (West Antarctic Peninsula) is governed by both winter sea ice cover and summer stratification.

II: Assessing drivers of coastal primary production in northern Marguerite Bay, Antarctica.

III: Summer microbial community composition governed by upper-ocean stratification and nutrient availability in northern Marguerite Bay, Antarctica.

IV: : Bioactive trace metal time series during Austral summer in Ryder Bay, Western Antarctic Peninsula.

V: Niche partitioning in Antarctic haptophyte and cryptophyte ecotypes.

Interannual variability in phytoplankton dynamics

The marine phytoplankton community in the WAP region has been suggested to shift from a diatom to a cryptophyte dominated system (Moline *et al.*, 2004; Montes-Hugo *et al.*, 2009). This suggestion is to a large extent based on two different time series, one at Palmer station (Anvers Island) and the other involving a number of transects along the Peninsula visited every January (LTER station grid). Furthermore, a recent study at the RaTS suggested that summer phytoplankton abundance is linked to winter sea ice cover (Venables *et al.*, 2013). In **chapter 2**, a perspective on the year-round

phytoplankton community composition from the southern-most WAP time series is presented. More specifically we addressed the following question:

Does winter sea ice cover and summer water column stability govern phytoplankton biomass and community composition in Ryder Bay?

This was investigated using seven years (2005-2011) of weekly year-round phytoplankton pigment samples analysed (provided by BAS) using high-pressure liquid chromatography. The resulting pigment fingerprints were taxon resolved into absolute and relative abundances of phytoplankton groups using CHEMTAX. These results were supplemented with data regarding the size class distribution of phytoplankton Chl-a from 1997 to 2011. Finally, information about sea ice cover, water temperature, salinity, and water column stability were added to obtain a long-term data set running from 1997 to 2011 with the last 7 years complemented by relative abundances of major taxonomic groups.

Previous findings linked high or low summer phytoplankton biomass to winter sea ice cover through water column stability (Venables *et al.*, 2013). Here, we updated the previously published findings to test if our full set (1997-2011) and subset (2005-2011) adhered to the conclusions drawn previously, which was found to be the case. Yet, we add a nuance to the previous findings as not all low ice winters were followed by low biomass summers, and not all high sea ice winters resulted in extensive phytoplankton blooms during spring/summer. Crucial in establishing high water column stability in summer was indeed winter sea ice cover, and consequently the MLD, but the spring conditions were also found to be important. High air and water temperatures and/or strong winds during spring acted as second preconditioner for summer biomass accumulation. For example, the effects of high winter ice cover were partly negated if wind mixing in spring, was high. To facilitate the influence of this second preconditioner we introduced summers of medium productivity, and summarized the results in a conceptual model.

Secondly, our dataset included taxon resolution obtained with HPLC. These results suggested that summers with a more unstable water column maintained the increased (absolute and relative) abundances of the smaller flagellated cryptophytes and

haptophytes from winter. In contrast, summers characterized by medium or high average biomass levels were dominated by diatoms. We concluded that winter sea ice cover and summer water column stability govern the phytoplankton community composition. Previous studies advocated the importance of cryptophytes along the WAP, here we observed a similar importance of haptophytes (Moline *et al.*, 2004; Saba *et al.*, 2014). The long time span of our size-fractionated phytoplankton biomass data set allows for the extrapolation of our conceptual model to 1997. Indeed, smaller cells were found to be more abundant during years that were overall characterized by deep vertical mixing. This confirms previous findings of downsizing within phytoplankton assemblages in response to current climatic trends (Montes-Hugo *et al.*, 2009). However, we did not observe a convincing relationship between summer MLD and relative abundances of haptophytes and cryptophytes whereas previous studies have (Arrigo *et al.*, 1999; Moline *et al.*, 2004).

Finally, although based on a relatively limited amount of winter data, we observed relatively high contributions of cryptophytes and haptophytes to the phytoplankton community during winter. This pattern was regardless of mixed layer depth during winter. The strong similarity between phytoplankton community composition during low biomass summers and preceding winters strongly suggests a persistence of winter communities during these summers. Apparently, a lack of water column stability and sea ice delayed strong diatom growth, instead allowing the relative and absolute increase of flagellated species. Moreover, melt water lenses resulting from glacial melt might be easier to colonize for these flagellated species as opposed to diatoms, possibly explaining the phytoplankton dynamics observed at the central and northern WAP (Mendes *et al.*, 2013, in press; Saba *et al.*, 2014; Schofield *et al.*, 2017).

Estimating and modeling primary production

Phytoplankton diversity is high along the WAP, and so is their capacity to fix carbon. Given the widespread application of HPLC-CHEMTAX to estimate phytoplankton diversity in this region (Vernet *et al.*, 2008; Kozlowski *et al.*, 2011; Mendes *et al.*, 2013; Schofield *et al.*, 2017), the observed differences in photophysiology between the major taxonomic groups, haptophytes and diatoms (e.g. Kropuenske *et al.*, 2009; Arrigo *et al.*, 2010; Alderkamp *et al.*, 2012), and the potential shift to a non-diatom dominated

system (Montes-Hugo *et al.*, 2009; Saba *et al.*, 2014; **chapter 2**), the following question was addressed:

What are the main drivers of marine primary production in Ryder Bay?

and specifically:

Does the addition of taxonomic information at the class level significantly improve a primary production model?

To answer these questions, we executed a spring to summer field campaign (late November 2013 to mid-March 2014) where bi-weekly experiments (16 in total) were performed by measuring photosynthesis-irradiance (P-E) relationships based on ^{14}C incorporation (after Lewis & Smith, 1983), see **chapter 3**. These data were fitted using a mechanistic model and linearly interpolated through the season to obtain carbon primary production (PP) estimates for the full summer (Platt *et al.*, 1980). Our second approach used a Random Forest model that does not assume any particular mathematical relation between parameters (Breiman, 2001). This statistical model used machine learning to establish relations between all parameters and PP.

Our first computational experiment used all available environmental and biological parameters, thus including HPLC-CHEMTAX phytoplankton composition, to model a subset of the P-E measurements. Results of this approach suggest that data about phytoplankton composition, at least at the broad taxonomic scale, added limited information for predicting PP. While phytoplankton species composition at the resolution of HPLC-CHEMTAX was of limited influence, we showed that a high relative abundance of diatoms was positively correlated with PP while cryptophytes and haptophytes were not. This last observation aligns well with previous findings along the WAP (e.g. Vernet *et al.*, 2008). Additionally, we established that none of the parameters approached a linear relationship with (log) PP, thus suggests that non-traditional approaches might need to be used in the model.

As we established the influence for each parameter on PP, we then conducted a second computational experiment to optimize the random Random Forest model. We defined optimization as reducing the number of included parameters still increasing the fit of

the model. This reduced, optimal model included only light, nitrogen concentration and chlorophyll a. Noteworthy, and somewhat surprisingly, is that sea water temperature explained nearly as much variance in PP as nitrogen concentration. Given the current climatic trends, sea water temperature might thus become a more important parameter for modelling PP.

Based on these modelling efforts we conclude that future models should be cautious to assume any traditional type of mathematical relation between parameters and PP. Moreover, although we acknowledge that different taxonomic groups differ in their photophysiology, apparently all variability is already covered by the inclusion of merely three key parameters. The major taxonomic groups also prefer strongly different water column conditions, thus including the three key parameters already captures the variability in taxonomic composition. As such, our reduced model potentially overestimates the importance of certain environmental parameters but we do not consider this a problem when modelling only PP. Perhaps including phytoplankton community composition at a better taxonomic resolution would have allowed captivating the subtle differences in photophysiology between species.

Seasonal variability in phyto- and bacterioplankton dynamics

Studies investigating microbial dynamics at the WAP are widely distributed in space and time, especially before the breakthrough of high-throughput sequencing. The high diversity in microorganisms at the WAP and strong variation in succession during summers result in a challenging environment to unravel patterns and relationship as a function of environmental conditions. Three previous studies at the RaTS employed microscopy, pigment or DNA fingerprinting techniques or a combination thereof to characterize the microbial community (Buma *et al.*, 2001; Annett *et al.*, 2010; Piquet *et al.*, 2011). In **chapter 4**, we present the first molecular analysis at RaTS, using high-throughput sequencing to characterize the microbial community and understand how environmental variability affects the composition thereof. We combined these sequencing data with both DNA and pigment fingerprinting to investigate differences and similarities between current and traditional approaches to describe (parts of) the microbial community. Moreover, this is, to our knowledge, only the fourth effort to bring phytoplankton taxonomy to the genus level and the second for the bacterial

community at the long-term monitoring site (Buma *et al.*, 2001; Annett *et al.*, 2010; Piquet *et al.*, 2011). Importantly, we aimed to understand the relationship between microbial and environmental variability during the course of summer. Therefore, our main research question was:

What are the dominant environmental parameters shaping the summer microbial community in northern Marguerite Bay?

Samples were collected over a period of ~2.5 months to ensure a sufficient temporal and environmental resolution. The DNA samples were analysed using denaturing gradient gel electrophoresis (DGGE) and MiSeq sequencing of the microeukaryal 18S rRNA gene. For DGGE, we employed an approach using general and group-specific primers to elucidate different dynamics within the eukaryotic community. Moreover, we supplemented this set with an array of environmental parameters as well as pigment fingerprinting.

The 2010-2011 summer was a typical and diatom dominated summer with a strong presence of glacial melt and a medium summer biomass. Short wind mixing events increased the MLD and apparently governed phytoplankton species composition. Opposing these mixing events was stratification and thus a warming of the surface layer. As such, water column stability shaped the summer microbial community most strongly. Additionally, we found indications of (macro)nutrient limitation, suggested by strong deviations from the Redfield ratio (Redfield, 1958). An increased N/P ratio is observed under mild micronutrient limitation (Takeda, 1998), while a lowered ratio combined with low nitrogen availability is indicative of nitrogen limitation. Diatoms dominated the season and rRNA sequencing revealed a succession from pennate diatoms, often observed at the sea ice edge, to *Thalassiosira* sp.. Photosynthetic dinoflagellates, as estimated with HPLC-CHEMTAX, were rarely observed suggesting that the high dinoflagellate richness in the DNA dataset is derived from heterotrophic species. Bacterial diversity was strongly associated with phytoplankton dynamics albeit with a short lag phase. Such dependencies confirmed earlier observations in Ryder Bay and suggests that substrates originating from phytoplankton regulate bacterial dynamics.

While the major parameters that shape the phytoplankton community appeared to be MLD, wind speed and sea water temperature and are in good agreement with a previous study despite a 13 year interval (Piquet *et al.*, 2011), dynamics within all phytoplankton groups left a lot of variability unexplained. A major challenge during this study was the annotation of the 18S rRNA gene sequences was challenging given the complex taxonomy of eukaryotes. Curating the taxonomy of the sequence database to which we annotate, improving sampling resolution to better cover the different, sometimes short lived succession phases, and improving the taxonomic resolution to at least species level appeared to be the most important methodological steps that need to be taken in order to advance our knowledge of microbial dynamics.

Variability in nutrient availability

The Southern Ocean is strongly limited by a lack of iron and occasionally by lack of other trace metals and/or vitamins. In **chapter 4** we observed an increase in the N/P ratio, suggesting limitation by trace nutrients (also known as micronutrients) e.g. iron, as phosphate was not depleted at that time. Moreover, melt water input into the system is an important process occurring at the coastal WAP, yet these waters contain no, or very little, measurable major nutrients (also known as macronutrients). In **chapter 5** we aimed to understand how variable nutrient concentrations relate to phytoplankton community composition in Ryder Bay. Therefore, the following question was formulated:

Does (micro)nutrient availability control phytoplankton bloom magnitude and composition in northern Marguerite Bay?

Over two summer seasons (2012-2014), we investigated concentrations of the trace metals including iron, manganese, zinc, cadmium, copper and labile cobalt, as well as the macronutrients nitrate, phosphate and silicate. These data were complemented with data on phytoplankton biomass as well as the relative abundance of the major taxonomic groups estimated with HPLC-CHEMTAX. During these summers, highly variable concentrations of the aforementioned nutrients were observed. Moreover, a strong difference between the first and second summer was observed with regards to

relative and absolute abundances of phytoplankton species abundance and trace metals.

During the first season, the water column was initially dominated by cryptophytes and to a lesser extent haptophytes. After mid-February an increase in relative diatom abundance coincided with an increase in phytoplankton biomass. Linear regression of the micronutrients (Fe, Mn, Zn, Cd, Cu and Co) versus phosphate and nitrate did not hint at limitation by micronutrients before depleting phosphate or nitrate up to 75 m water depth. Yet, similar regressions against silicate concentrations suggested that zinc, cadmium and manganese could become limiting under diatom dominated conditions. However, silicate concentrations were nowhere being depleted. Interestingly, we did observe an increase of N/P ratios in the surface layer (15 m) during this phase which could be related with decreased concentrations of iron, zinc, cobalt and/or cadmium. Moreover, at the end of the campaign (mid-March), surface phosphate concentrations were around the detection level. Actually, linear regressions of phosphate or nitrate against iron, zinc, cobalt and cadmium for this surface layer strongly suggested that phosphate was, or could become, the limiting nutrient during this phytoplankton bloom. This could suggest two controlling mechanisms. Diatom species utilized more phosphate than based on the Redfield ratio. Or, and perhaps more likely, growth was sub-optimal due to low concentration of some trace metals, most probably iron and/or zinc.

The second season was more strongly influenced by sea ice melting than the preceding year. Changes in diatom biomass may be affected by diatoms released from ice sheets in the second half of December (**chapter 3 and 5**). After mid-January, diatom biomass decreased by 10-20% of the total biomass and in favour of haptophytes and cryptophytes. After the beginning of February, diatom abundance decreased further while both hapto-and cryptophytes increased in numbers. In contrast to the first season, silicate stocks were much more variable and even declined to the detection limit. This silicate depletion was highly unexpected given the near vicinity to the coast with potential silicate input but may be explained by the input of nutrient starved phytoplankton from the sea ice since all macronutrients became strongly depleted. The scarcity of bioavailable micronutrients yet high biomass in the sea ice at the end of

spring presumably drained the cellular reserves of nutrients in the phytoplankton cells. Furthermore, the high silicate requirements were most likely due to the development of algae in the sea ice which generally have thicker siliceous cell walls. A coupling between iron and silicate is often suggested as trace metals might be involved in the formation of diatom cell walls or otherwise strongly couple to silicate uptake (Takeda, 1998; Brzezinski, 2008; Armbrust, 2009). Further supporting a coupling between the low iron and depleted silicate is the strong rise in N/P ratio (Takeda, 1998). We therefore conclude that cellular reserves were replenished when the cells entered the water column, resulting in an imminent local micronutrient depletion.

After mid-January 2014, diatom biomass (mostly *Proboscia* sp. **chapter 3**) increased again and low zinc concentration could have induced increased uptake of cadmium and cobalt. Moreover, the N/P ratio was low after a few days with strongly reduced concentrations of phosphate and especially nitrate suggesting that the halt in phytoplankton biomass accumulation was due to some extent of macronutrient limitation. After this period, the water column was strongly mixed, nutrients were replenished and flagellated phytoplankton became more abundant.

Niche partitioning among hapto- and cryptophytes ecotypes

A shift from a diatom dominated to a phytoflagellate dominated system appears to occur along the WAP for the past decades (Montes-Hugo *et al.*, 2009). Often hypothesized is a positive relation between glacial melt water input and cryptophyte abundance (Moline *et al.*, 2004; Saba *et al.*, 2014) while a deep mixed layer facilitates haptophyte abundance (Arrigo *et al.*, 1999). However, in none of our investigations a convincing relationship between glacial melt water and cryptophytes was found (data not shown but in the framework of **chapters 2, 4** and **6**). While we did see a positive correlation between shallow MLDs and cryptophyte abundance, this relation also existed for haptophytes albeit to a weaker degree (**chapter 2**). Given the lack of clear patterns regarding cryptophyte and haptophyte dynamics at our study site, we applied 18S rRNA sequencing to answer the following question:

Do different haptophyte and cryptophyte species and/or ecotypes exist in Ryder Bay and, if so, can we identify their niches?

This might resolve some of the complexity in the relationship between these phytoflagellates and environmental drivers. Furthermore, identifying the bottom-up controls on these ecotypes, when present, would strongly increase our understanding of future WAP phytoplankton dynamics. As phytoplankton dynamics are a delicate balance between top-down (e.g. grazing) and bottom-up (e.g. preference for a set of environmental conditions i.e. niche) controls, we also aim to identify specialist grazers. Grazing on specific phytoplankton groups or species can keep these phytoplankton abundances limited, thus despite that small, flagellated species can have high growth rates under the right conditions, abundance might still be lower than expected. Thus, in addition to identifying specific niches, we additionally asked:

Can we identify specialist grazers that assert a top-down control of specific haptophyte and cryptophyte species and/or ecotypes?

To answer these two questions, we exploited Ryder Bay as a natural laboratory during two summers (2012-2014) where we took bi-weekly samples on a small transect consisting of three stations sampled at three depths, 2 and 15 m in the sunlit surface layer and 75 m in the winter water (**chapter 6**). This design maximized the environmental variability in between our samples while it was still possible to collect all samples on one and the same day. The latter was important given the strong dependency of, and variability in, irradiance and wind induced mixing (**chapters 3** and **4**) and these conditions therefore needed to be comparable between samples. We used high-throughput sequencing of the 18S rRNA gene in DNA samples. These sequences were compared to pigment fingerprint data (HPLC-CHEMTAX) to ensure comparability to previous research (**this thesis** and references therein). To identify potential niches we measured water temperature and salinity, calculated MLD, and sampled for the macronutrients.

Before assigning taxonomy to our sequences, we established the different oligiotypes using minimum entropy decomposition (Eren *et al.*, 2015). This approach alleviates us from determining an arbitrary cut off in defining taxonomic units by segregating sequences that have small variations in their 18S gene, which are occurring more frequently than the sequencing error rates in our data set. These oligiotypes were then

compared to a sequence database with curated protist taxonomy (Guillou *et al.*, 2013). A comparison of HPLC-CHEMTAX and 18S rRNA sequencing yielded convincing linear relations between relative abundance estimates of the major taxonomic groups but presented an over- and underestimation of haptophytes and diatoms, respectively. This difference is most probably due to the large range of diatom size classes, and thus the 18S rRNA gene copy number (Godhe *et al.*, 2008). The co-occurrence of diatoms with haptophytes would thus also affect the estimates of this latter group.

Our technique did increase the taxonomic resolution and yielded the hypothesized diversity within species (often >99% identity). Firstly, in addition to *Phaeocystis* we observed a second haptophytes genus, *Chrysochromulina*, which contributed up to ~50% of the highly abundant haptophyte community. Moreover, we identified a second species within the *Phaeocystis* genus, namely *P. cf. jahnii*. This is important as it is generally assumed that *P. antarctica* is the only dominant species in the WAP region. Yet species level information did not suffice to allow for the identification of specific niches for the species. For example, the sole cryptophyte species *Geminigera cryophila*, cannot be linked to specific niches beyond the environmental parameters previously established by e.g. HPLC-CHEMTAX as it is the only cryptophytes species. Therefore, the taxonomic resolution needed to be improved further and beyond the species level. Ecotypes, defined as clusters of oligiotypes within a species, show highly similar spatial and temporal dynamics (Cohan, 2002). Thus, different clusters within a species would per definition show different occurrence patterns, assuming that that these different patterns result from contrasting preferences for a combination of environmental parameters. As such, we postulated that these sets of environmental conditions corresponded to different niches. Based on this definition, ecotypes were observed within all of the investigated phytoflagellates.

The differences between ecotypes were most evident in the species belonging to *Phaeocystis* and *Geminigera*. For the latter, we identified three *G. cryophila* ecotypes that differed most strongly in their preferences for MLD and temperature, thus not necessarily salinity (Moline *et al.*, 2004). Shallow melt water lenses over otherwise unstable water columns and cool, deeply mixed columns appear to be discriminating the cryptophyte ecotypes. Furthermore, there appears to be a distinction between the

two ecotypes which prefer a deep MLD, one of which preferring high temperatures whereas the second is more abundant at low temperatures. For the *Phaeocystis* species, *P. antarctica* appears to be the generalist which prefers more open ocean conditions characterized by high salinities and low temperatures but not a deep MLD. *P. cf. jahnii* ecotypes were found to be more specialist, associated with increased sea ice melt and high turbidity, or high nutrient, deeply mixed open oceans conditions. In contrast, *Crysochromulina* also preferred a deep MLD with a high SST.

After having identified specific niches for the ecotypes, a co-occurrence network was created under stringent conditions to identify potential grazers that benefited from the increase in abundance. We could not identify specific grazers on the most abundant *P. antarctica* ecotype. For *Chrysochromulina* and *P. cf. jahnii*, a complex interaction between many nano- and microzooplankton species was found. In contrast, *G. cryophila* was strongly tied to *Prorocentrum* sp., a genus containing known cryptophyte grazers and facultative toxin producers (Johnson, 2015; Ajani *et al.*, 2017). *Prorocentrum* abundance increased after the increase in cryptophytes and peaked just after the maximum in cryptophyte abundance. This suggests that that this dinoflagellate actively grazes on the cryptophyte abundance, and could act as a top-down control. Analysis of the two most abundant cryptophyte did not reveal significant difference in responds to *Prorocentrum* sp..

We conclude that multiple different ecotypes exist and that improving the taxonomic resolution is essential to better understand the complexity of phytoplankton dynamics. Moreover, we suggest different niches for most ecotypes allowing for more comparability between e.g. geographical locations when discussion dynamics in these groups. Finally, we report a potential cryptophyte specific grazer that may assert top-down control on this phytoflagellate, potentially influencing the Antarctic food web.

Considerations and perspectives

Control mechanisms of phytoplankton community composition

Understanding variability in the microbial community is a major question for environmental microbiologists worldwide. At the west Antarctic Peninsula a plethora of parameters could govern the variability in the microbial community composition.

This control can either be top-down, by e.g. grazing or viruses or bottom-up, by for example light or nutrient availability, or temperature. Moreover, the strength of these controls depends on the timescale of interest where multiple parameters are influencing the community simultaneously. This leads to questions such as: What ends a phytoplankton bloom period during summer? Did the winter phytoplankton biomass change through the past decades? These two examples are meant to illustrate how both top-down and bottom-up processes affect microbial community composition on all time scales, yet not necessarily in an identical way.

From this thesis we learnt that winter sea ice cover preconditions the water column for summer and therefore governs both phytoplankton growth and species composition, in turn regulating bacterial community composition (**chapter 2** and **4**). Some of the variability in sea ice cover is governed by large scale climate indices, such as SAM and ENSO, which therefore indirectly govern microbial community. Sea ice coverage is also an important factor in krill recruitment success, which in turn asserts a top-down pressure on the phytoplankton community. The large scale variability is set on decadal time scales. Studying these long term trends is challenging as the WAP monitoring programs have only been running for 20-25 years. Sediment cores could be used to understand some of the microbial variability over the past centuries but it remains challenging to bridge the gap between these cores and field observations as some genera are preserved better than others. Yet, this appears to be the only method to understand patterns in long-term variability. Perhaps the imminent rise of highly sensitive sequencing techniques allows for a fresh approach of these cores.

Seasonal dynamics are becoming better understood. The early spring community resembles that of the preceding winter, consisting in nearly equal parts of cryptophytes, haptophytes and diatoms (**chapter 2** and **4**). At the southern WAP, the subsequent dynamics are governed by sea ice. The presence or absence of sea ice strongly outlines the summer season, as discussed above. Yet, more often than not, the sea ice starts to melt and sheds its accumulated biomass bottom layer to form a, what is considered typical, Antarctic sea ice edge bloom consisting small pennate diatoms late December (**chapter 4**). A strong increase in turbidity suggested large quantities of dissolved and particulate organic matter (**chapter 3**) fuelling and shaping the bacterial

community (**chapter 4**). This period is the most productive in terms of carbon fixation and standing phytoplankton stocks (**chapter 2**, **3** and **5**). These periods are ended by wind induced sea water mixing, and depending on the duration and strength of these winds, the subsequent phytoplankton community is either dominated by medium sized centric diatoms such as *Thalassiosira* species or flagellated species belonging to cryptophytes and/or haptophytes (**chapter 4** and **6**). Which of these major phytoplankton groups dominates strongly depends on the SST and the presence or absence of a melt water lens. Moreover, we observed that within the phytoflagellate groups, ecotypes exist that occupy distinguishable niches (**chapter 6**). Total phytoplankton biomass in this phase is strongly dependent on the presence of diatoms, while a high contribution of flagellated species is strongly associated with a lower standing biomass stock (**chapter 5** and **6**). As such, this period could persist for a relatively long time. A disruption in the stability of the system by e.g. grazing and/or disturbance of water column stability at this stage (around February) could again alter the phytoplankton community. Frequently observed is the dominance of large diatom species such as *Proboscia* and *Corethron*, possibly escaping grazing due to their size. These large species only occur near the end of summer, possibly due to their lower growth rates as a result of unfavourable volume-to-surface ratio. In autumn, when storms are becoming more frequent, the flagellated community again increases in relative abundance in the deepened mixed layer. Strongly decreased light availability as is inherent to the geographical location and time of the year, likely prevents a significant build-up of further phytoplankton biomass. Additionally, many members of the aforementioned flagellates are known to maintain mixotrophic lifestyles (as discussed in **chapter 6**). Therefore, grazing on bacteria, organic particles, and/or small eukaryotes could act as an alternative energy source. Unfortunately, knowledge about the extent of such a strategy in the Southern Ocean is understudied. Additionally, very little data and knowledge exist regarding the autumn-winter-spring seasons due to the challenges and costs involved in sampling during these harsh periods.

On shorter time scales, e.g. weeks to months, we aimed to understand the influence of macronutrients and trace metals on phytoplankton performance. We observed frequent yet short lived periods of nitrogen limitation, nitrogen+phosphorus

limitation, and/or zinc and iron limitation (**chapter 4** and **5**). While these depleted nutrient stocks possibly influenced the maximum capacity of phytoplankton biomass in this system, it did not appear to influence phytoplankton community composition. Moreover, while dissolved concentrations were at or near the detection limit this does not imply that nutrients were not available (**chapter 3, 4** and **5**). We observed a strong connection between the bacterial and eukaryotic community. The bacterial community changed within about two weeks to the new source of organic matter, and continued remineralization of the organic matter. This might have provided a continuous source of nutrients, allowing phytoplankton to maintain growth and compensate the phytoplankton loss terms (**chapter 4**).

Another potentially large influence on microbial community composition is episodic melt events. Above we discussed the influence of sea ice, but the coastal regions are also strongly influenced by glacial melt. However, no episodic events of glacial melt were observed during our field seasons, glacial melt input gradually increased during the summer (**chapter 3** and **4**). As such, the influence of fresh water input did strongly increase over the course of the summers. This glacial melt water, combined with melt of brass sea ice which had already shed its algal biomass, still created melt water lenses during periods of low wind speeds. Wind mixing was the stronger factor governing water column stability and nutrient dynamics (**chapter 5**). Given the rather stable glacial influx during summer, despite slight interannual variability, we do not (yet) consider this the major driver of phytoplankton dynamics. Perhaps with a further decrease of sea ice melt, water column stability derived from glacial melt might become more important.

Necessity to increase resolution

Based on the present thesis, we advocate the need to increase the taxonomic resolution of the identification of microbial communities in the WAP region. This can be considered a key to understand long and short term changes in phytoplankton communities along the WAP, whether or not caused by climate change indicators. Distinct niche partitioning in the crypto- and haptophyte ecotypes revealed several patterns, which were previously found to be unclear or only partly understood. Also of key importance is a better understanding of nano- and microzooplankton, their prey

specificity as well as their grazing rates. These issues provide keys to further understand carbon and energy fluxes in the system. Moreover, understanding the most relevant loss factors is actually vital when conclusions regarding environmental change are under investigation. The most abundant species in a system is not necessarily the most important; others might be more productive and therefore sustain the system to a greater extent. Finally, species diversity is not the same as functional diversity; the latter is yet another level of resolution that is scarcely studied in marine pelagic communities. Therefore, investigations should couple both top-down and bottom-approaches when aiming to understand the dynamics in the microbial community.

A further increase in resolution would actually be to not use species, or even ecotypes, as the smallest taxonomic unit. Yet distinction based on size, mobility, functional genes, and other characteristics could and should be exploited to describe the community, and its climate related changes. Moreover, such approaches should preferably be included in all the major investigations and monitoring programs along the WAP. Finally, in this thesis we established that summer microbial community composition is strongly regulated by winter conditions and community. As such, increasing the sampling resolution in winter is an obvious recommendation from such an observation.

Chapter 2

Interannual variability in phytoplankton biomass and species composition in northern Marguerite Bay (West Antarctic Peninsula) is governed by both winter sea ice cover and summer stratification.

P. D. Rozema
H. J. Venables
W. H. van de Poll
A. Clarke
M. P. Meredith
A. G. J. Buma

Published in:
Limnology and Oceanography (2017)

Abstract

The rapid warming of the West Antarctic Peninsula region has led to reduced sea ice cover and enhanced glacial melt water input. This has potential implications for marine ecosystems, notably phytoplankton growth, biomass and composition. Fifteen years (1997-2012) of year-round size fractionated chlorophyll a, phytoplankton pigment fingerprinting and environmental data were analyzed to identify the relationship between sea ice cover, water column stability and phytoplankton dynamics in northern Marguerite Bay, Antarctica. Over the investigated period, both summer (December–February) and winter biomass declined significantly, 38.5 and 33.3% respectively. Winter phytoplankton biomass was low (<0.25 µg Chlorophyll a l^{-1}) and consisted on average of 69% diatoms, 5% cryptophytes, and 20% haptophytes. Summers following winters with low (<65 days) sea ice cover were characterized by decreased stratification strength and relatively low (median <4.4 µg chlorophyll a l^{-1}) phytoplankton biomass, as compared to summers preceded by high winter sea ice cover. In addition, the summertime microphytoplankton (>20 µm) fraction was strongly decreased in the low biomass years, from 92% to 39%, coinciding with a smaller diatom fraction in favor of nanophytoplankton (<20 µm), represented by cryptophytes and haptophytes. In contrast, diatoms dominated (>95%) during summers with average-to-high biomass. We advance a conceptual model whereby low winter sea ice cover leads to low phytoplankton biomass and enhanced proportions of nanophytoplankton, when this coincides with reduced stratification during summer. These changes are likely to have a strong effect on the entire Antarctic marine food web, including krill biomass and distribution.

Apendices are available online and/or upon request.

Introduction

Climate change strongly affects the physical environment in many different regions of our planet. One of the regions most profoundly affected is the West Antarctic Peninsula (WAP). Annual mean air temperatures over the WAP have increased by 2 - 3°C over the past 50 years (Turner *et al.*, 2005), whilst summertime sea surface temperatures increased by more than 1°C (Meredith & King, 2005). The increase in temperatures in the WAP region is associated with a shortening of the sea ice season and an increase in glacial ice discharge (Depoorter *et al.*, 2013; Rignot *et al.*, 2013). These large-scale changes are strongly affecting the physical and chemical properties of the water column and may thereby affect marine food webs as well (Constable *et al.*, 2014). Pronounced changes in sea ice cover have been observed in the coastal WAP region (Vaughan *et al.*, 2003; Meredith & King, 2005; Harangozo, 2006). Sea ice duration has decreased by almost 90 days in the 1979-2004 period. This decrease contrasts with the general trend of modestly increasing sea ice extent around Antarctica as a whole, which is driven in particular by major advances in the Ross Sea with much slower rates of change elsewhere (Stammerjohn *et al.*, 2008b; Montes-Hugo *et al.*, 2009). The reduction of sea ice at the WAP is primarily due to a strong trend towards a later autumn advance and a somewhat weaker trend towards an earlier spring retreat (Stammerjohn *et al.*, 2008b). As a consequence, mean annual sea ice cover in the WAP area has decreased by 40% over a 26-year period (Smith & Stammerjohn, 2001).

Another effect of warming of the WAP region is the enhanced influx of glacial melt water during summer, due to accelerated glacial retreat (Cook *et al.*, 2005). Marguerite Bay, a major embayment in the central part of the WAP, is surrounded by retreating glaciers and is strongly influenced by the changing sea ice dynamics (Cook *et al.*, 2005; Montes-Hugo *et al.*, 2009; Meredith *et al.*, 2010). In Marguerite Bay, decreased ice cover has been linked to a deepening of the winter mixed layer (Venables *et al.*, 2013). Occasional strong winds during summer can cause well-described mixing events and can lead to a relatively short-term change in mixed layer depth (MLD). However, recent findings from northern Marguerite Bay have associated decreased winter ice cover to reduced stratification during the following spring and summer (Venables *et*

al., 2013). Strong winds and decreased buoyancy during winter can mix the water column to greater depths during periods of low ice cover. These waters then require more buoyancy to be stabilized to the same level during the subsequent spring and summer, thus potentially leading to persistently weaker stratification. Additionally, the production of less sea ice in winter can lead to smaller volumes of ice being available to melt the following spring and summer, thus reducing the potential buoyancy input to restratify the upper ocean.

Seasonal dynamics of phytoplankton are strongly regulated by the timing of sea ice retreat. Austral spring marks the beginning of significant phytoplankton growth after a period of near darkness during winter, in particular when coinciding with water column stabilization caused by warming or freshening due to melt water input from melting sea ice or glaciers. Stabilization of the water column leads to a decreased MLD, thus light conditions become favorable for phytoplankton growth and bloom formation (Sverdrup, 1953). Deep mixing due to periods of strong wind or convection can reduce the light available for photosynthesis. Even though the timing of the onset of the phytoplankton bloom may not change with a deeper mixed layer (Venables *et al.*, 2013), it can influence the phytoplankton community through total biomass and/or species composition.

In coastal Antarctic waters, phytoplankton spring blooms under stratified conditions typically consist of large (>20 µm) diatoms that are favored under relatively high irradiance conditions (Arrigo *et al.*, 1999; Clarke *et al.*, 2008; van de Poll *et al.*, 2009; Annett *et al.*, 2010). In well-mixed waters around Antarctica, dominance can shift to the common and widespread haptophyte *Phaeocystis antarctica* (Arrigo *et al.*, 1999; Alderkamp *et al.*, 2012b). The periods of dominance by nanophytoplankton other than *Phaeocystis*, mainly cryptophytes, seem to be associated with glacial melt water stratification during summer, decreased nutrient stocks after spring and summer blooms (Buma *et al.*, 1992; Moline *et al.*, 2004; Kozlowski *et al.*, 2011; Mendes *et al.*, 2012), and low irradiance conditions during winter (Clarke *et al.*, 2008). Other phytoplankton groups frequently observed, although often in relative low and constant absolute abundances, are chlorophytes, dinoflagellates and prasinophytes (Kozlowski *et al.*, 2011). A negative trend in microphytoplankton biomass in the northern WAP

region, as observed by satellite, was linked previously to a deeper mixed layer and decreased ice cover (Montes-Hugo *et al.*, 2009). This trend is opposite to that observed along the southern most sections of the WAP, where microphytoplankton is increasing due to the opening up of areas previously covered by sea ice.

Shifts within the size class distribution of phytoplankton have the potential to alter the Southern Ocean food web drastically (Atkinson *et al.*, 2004). Krill abundance, pivotal within this ecosystem, has shown a strong dependence on sea ice-associated phytoplankton biomass (Saba *et al.*, 2014). Declining phytoplankton stocks, mainly the microphytoplankton that is the preferred food for krill, are causing decreased success in krill recruitment north of Anvers Island (northern WAP; Montes-Hugo et al. 2009; Saba et al. 2014). So far, krill stocks in January-February in the southern section of the WAP appear to be stable (Steinberg *et al.*, 2015). But juvenile krill depends on sea ice algae during winter, and are therefore affected negatively by the disappearance of sea ice (Trivelpiece *et al.*, 2011; Flores *et al.*, 2012; Reiss *et al.*, 2015). As a result, future krill stocks in the southern WAP could be affected. Thus, the already observed changes within the Southern Ocean food web could be propagated to the region of the WAP (Schofield *et al.*, 2010; Constable *et al.*, 2014).

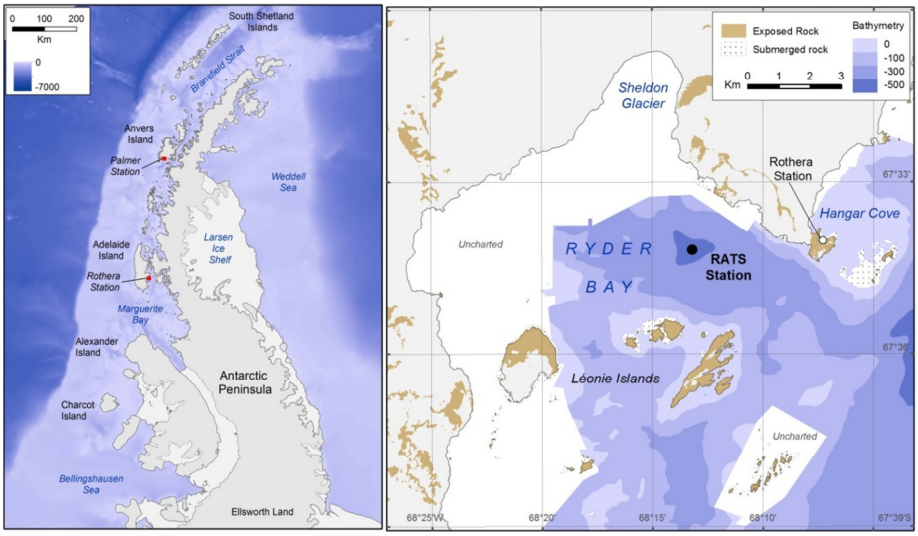

Figure 1: Left a map showing the West-Antarctic Peninsula marked with both the Rothera and Palmer stations. Secondly, a close up of the vicinity of Rothera Research Station with the long-term RaTS site is shown on the right.

In northern Marguerite Bay, phytoplankton biomass estimated by remote sensing has been declining recently in comparison to the 1978-1986 period (Montes-Hugo *et al.*, 2009). A clear example of reduced sea ice cover is the winter of 1998, which led to deeper mixing that persisted through to the subsequent summer (Meredith *et al.*, 2004; Stammerjohn *et al.*, 2008a) and which was associated with a decrease in phytoplankton biomass (Clarke *et al.*, 2008; Venables *et al.*, 2013). While data describing phytoplankton species composition in Marguerite Bay are sparse, available data are comparable to those of the larger WAP region (Garibotti *et al.*, 2005; Kozlowski *et al.*, 2011), showing the dominance of microphytoplankton (> 20 um; Clarke et al. 2008). Diatoms dominate this size class, however there is large variability with respect to species composition (Garibotti *et al.*, 2003, 2005; Annett *et al.*, 2010; Piquet *et al.*, 2011). No long-term year-round phytoplankton studies are available for the area. Data from the adjacent Palmer Long-Term Ecological Research (LTER) grid spans ~20 years, however these are limited to the summer period (Kozlowski *et al.*, 2011).

In the present study we analyzed phytoplankton dynamics in northern Marguerite Bay as a function of winter sea ice conditions and summer stratification, obtained from a long-term ocean monitoring site adjacent to the British Antarctic Survey's Rothera Research Station. Phytoplankton dynamics were elucidated using 15 years of year-round size-fractionated chlorophyll a (Chl a) supplemented with 7 years of pigment fingerprinting (HPLC-CHEMTAX). We aim to propose a conceptual model that allows us to understand the large variability in observed phytoplankton biomass. The almost unique year-round nature of this dataset is valuable in explaining some of these large variations in phytoplankton biomass and composition, not only related to summer stratification, but also to winter ice dynamics.

Materials and methods

Samples for the monitoring of biological and physical oceanographic variables were collected at the RaTS site (Rothera Oceanographic and Biological Time Series; 67.570°S 68.225°W, details in Clarke et al. (2008) and Venables et al. (2013)) located near Rothera Research Station on the WAP (Fig. 1). The monitoring site is situated in Ryder Bay, which is part of the northern Marguerite Bay region. Venables & Meredith (2014)

showed that the RaTS location in Ryder Bay is representative of the broader physical environment across northern Marguerite Bay. The distance between the nearest shore and the RaTS site is ~2 km, and the maximum depth is ~520 m. Data were collected between April 1997 and October 2012. Desired sampling frequency during the summer was twice per week, and once per week in winter. Samples were collected by small boat, unless sea ice precluded accessing of the sampling site. Under these conditions, an alternative site (67.581°S 68.156°W) was used in ~300 m of water and located

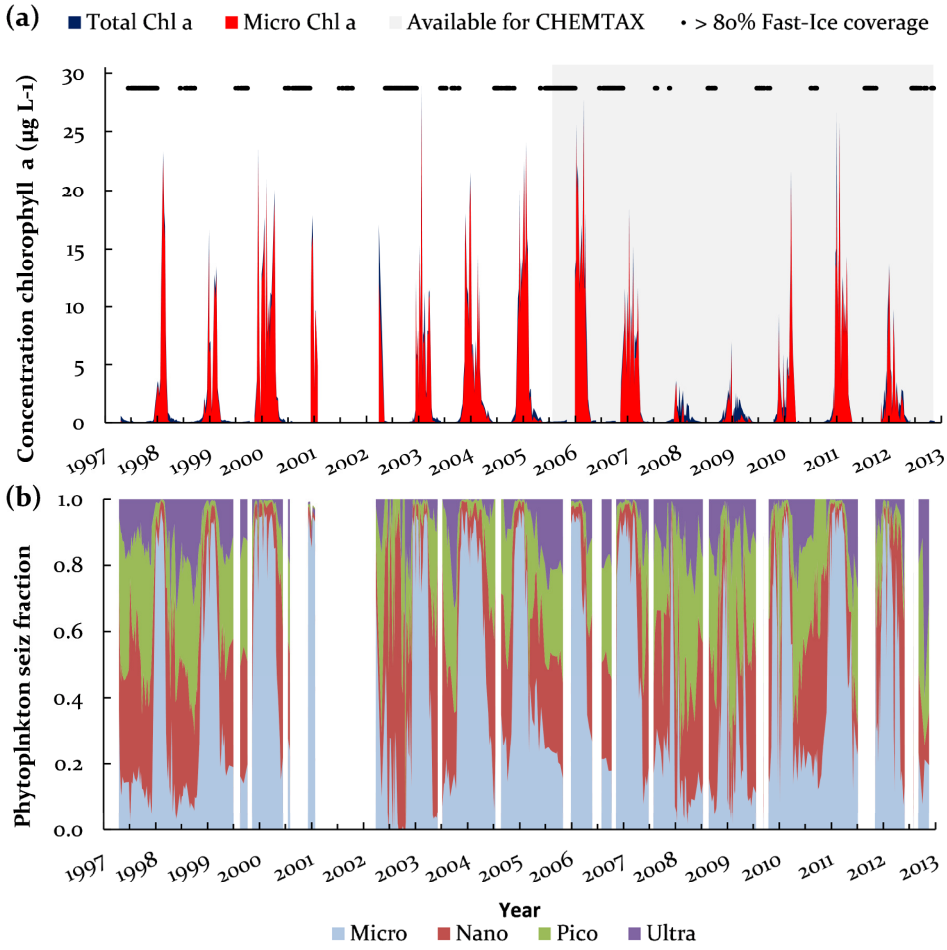

Figure 2: (a) Time series of total and microphytoplankton biomass relative (both in Chlorophyll a) at the RaTS site. Years within the grey area were available for pigment analysis by HPLC. (b) Relative abundance of micro-, nano-, pico- and ultraphytoplankton, based on size-fractionated chlorophyll a. Gaps within both time series mark periods where the RaTS site was not sampled for 30 days or more.

approximately the same distance from the shore. During periods of heavy land-fast-ice, samples were collected through a hole cut in the ice. A gap in the series of measurements was defined if no samples were collected for a period of 30 days or longer (Fig. 2b).

Depth profiles of temperature, conductivity, pressure and fluorescence were obtained using a conductivity-temperature-depth (CTD) instrument. Initially, a Chelsea Instruments Aquapak CTD and fluorometer was used, with a maximum depth rating of 200 m. This instrument was replaced in January 2003 by two CTDs, one SeaBird 19+ CTD and a SeaBird 19 CTD both with a WetLabs in-line fluorometer enabling full depth (500 m) profiles. Variables measured using the CTD were averaging into 1 m bins. Calibration of the CTDs between years and with the Palmer LTER program measurements are discussed in Venables et al. (2013).

Phytoplankton samples were collected at 15 m depth using 2 to 10 L Niskin bottles. This fixed depth was used since it is the depth of the fluorescence maximum, and was reasonably representative of the total biomass in the water column (Clarke *et al.*, 2008). While in transit from the sampling location, samples were stored in insulating blankets and/or boxes to prevent freezing.

Sea ice cover and type were characterized as described in Venables et al. (2013). In short, daily observations were made from an observation tower and considered sea ice conditions in three bays around the research station. We define fast-ice cover as days with ≥ 80% coverage of the area by fast-ice. Even though multiple observers throughout the years can introduce internal heterogeneity in the series due to the observations' subjective nature, such errors were still smaller than the large interannual variability in physical changes within the region (Venables & Meredith, 2014).

MLD was defined as the depth at which the difference between the observed density and surface (1 m) density was ≥ 0.05 kg m^{-3}. Stratification was quantified by calculating the potential energy required to homogenize the water column from the surface to 30 m. This metric of stratification is the negative of the potential energy anomaly, in J m^{-2} (Simpson *et al.*, 1978).

The onset of summer melt was defined as the Julian day on which salinity at 15 m was 0.05 lower on the practical salinity scale than the highest salinity observed during the previous winter at 15 m. Also, if salinity at 15 m increased by > 0.025 on the practical salinity scale during spring, generally as a result of wind mixing, the day of summer melt was defined after this event. Our rational for using these measurements as a possible proxy for median summer biomass was that spring conditions were influenced by the previous winter conditions (sea ice cover, date of retreat, MLD, etc.) as well as current spring conditions (temperature, melt, wind speed, etc.). This could be reflected by the time point during spring when stratification started. We therefore chose to investigate the relationship between the Julian day showing the first significant decline in salinity (15 m) and subsequent median summer biomass. Determination of such a date proved challenging as data collection during spring was frequently hindered by unfavorable sea ice conditions. No data were collected for 1.5 months due to sea ice conditions during the spring 2006-2007 and therefore this spring period was excluded from the analysis.

For size-fractionated Chl a analysis, triplicate samples (250 – 2000 mL each) were filtered through sequential 47 mm filters into microphytoplankton (>20 µm, Nylon mesh filter), large nanophytoplankton (20-5 µm, membrane filter), small nanophytoplankton (5-2 µm, membrane filter) and picophytoplankton (2-0.2 µm, membrane filter) fractions. Filtrations were conducted in the dark and at 4° C, and were started immediately after return to the laboratory (within 60 minutes after sampling). Chl a analyses were conducted as described in Clarke et al. (2008) and based on Wood (1985); in short, pigment extractions were performed overnight at 4° C in chloroform/methanol (2:1 v/v) and Chl a was determined before and after the addition of 0.1 N HCl using a fluorimeter (AU-10, Turner). Total Chl a concentrations were calculated by summing the four size fractions.

Collection of samples for pigment analysis by high-pressure liquid chromatography (HPLC) on GF/F (47 mm, Whatman) started in October 2005, and was conducted by filtering 1 L of seawater using a moderate vacuum. The results presented here are based on 268 GF/F filters collected from September 2005 until November 2012. Filtering started immediately after the return to the laboratory, and was conducted under low

light. Filters were snap frozen in liquid nitrogen and stored at -80°C until further processing. Samples for pigment analysis using HPLC were not taken or analyzed if no liquid nitrogen was available.

Prior to extraction, the filters were freeze dried for 48 h in the dark. To extract the pigments, the filters were incubated in 90% acetone (v/v) at 4° C in the dark for 48 h (van Leeuwe *et al.*, 2006). Pigments were separated on a Waters 2695 HPLC system using a Zorbax Eclipse XDB-C8 column (3.5 µm particle size) as described by Van Heukelem & Thomas (2001) and modified by (Perl, 2009). Diode array spectroscopy type 996 (Waters, US) and retention times were used for manual pigment identification and quantification. Calibration of the system was performed against standards (DHI LAB PRODUCTS) for chlorophyll c3, chlorophyll c2, peridinin, 19'-butanoyloxyfucoxanthin, fucoxanthin, neoxanthin, prasinoxanthin, 19'-hexanoyloxyfucoxanthin, alloxanthin, lutein, chlorophyll b and chlorophyll a1.

Calculation of the abundance of various phytoplankton groups based on their pigment signatures was conducted using CHEMTAX v1.95 (Mackey *et al.*, 1996). This program uses a factor analysis and steepest descent algorithm to find the best fit based on initial pigment ratios. Eight different phytoplankton classes were chosen to be representative of the marine Antarctic ecosystem (Wright *et al.*, 2009, 2010; Higgins *et al.*, 2011); prasinophytes, chlorophytes, dinoflagellates, cryptophytes, two types of haptophytes and two types of diatoms. Microscopic observations from two summer seasons at the RaTS station were taken into account when determining which classes to include in our CHEMTAX matrix (Annett *et al.*, 2010).We distinguished between two haptophyte groups because the dominant haptophyte *Phaeocystis antarctica* can show high variability in ratios of 19-butanoyloxyfucoxanthin, fucoxanthin and 19-hexanoyloxyfucoxanthin to Chl a ratios under varying light conditions and iron concentrations (reviewed in van Leeuwe et al. (2014)). Also, two types of diatoms (Diatoms 1 and 2) were included. Diatoms 2 include species such as *Pseudonitzschia sp*. and *Proboscia sp.*, often observed in sea ice ecosystems and at RaTS, and contain chlorophyll c3 whereas most other diatom species (Diatoms 1) do not (Annett *et al.*, 2010). The initial ratios for the different phytoplankton classes were constructed using

published results from various sources describing pigmentation of Antarctic phytoplankton (Tab. S1).

Pigment concentration data were sorted in 8 bins; 7 bins for the 7 different summer seasons (2005-2012) and one bin for all winter samples combined as these samples were taken less frequently. Summer and winter bins were defined using a cluster analysis on all pigment concentrations. City-block distances were calculated and samples clustered according to Ward's method (Latasa *et al.*, 2010). Samples with very low biomass clustered together. The limit of low biomass (< 0.25 µg l^{-1} Chl a) was found to be distinctive between the summer and winter samples. Thus, samples with low biomass were considered a winter sample if no increase in biomass occurred within 14 days after the sample was taken. The initial ratio's matrix was separately optimized for the summer and winter bins. Using two classes for haptophytes and diatoms greatly improved the residual mean square error (RMSE). Exclusion of chlorophyll c2, neoxanthin and prasinoxanthin in the winter bin resulted in a strong decrease in RMSE during the initial exploratory CHEMTAX analyses (Tab. S1). Low values for the RMSE for the 8 summer bins resulted in the inclusion of all 12 pigments for the summer samples. As the algorithm of CHEMTAX is prone to being stuck at local minima, we ran CHEMTAX 60 times (reviewed in Kozlowski *et al.* (2011)). The first run used the initial ratio matrix as taken from the literature while the ratios for the subsequent runs were varied randomly by +-35% of the initial ratios (Wright *et al.*, 2009). Chl a was always defined as 1. After the 60 runs, the run with the lowest RMSE per bin was checked to ensure that the final ratios were ecologically realistic. If so, then those results were considered the best possible result. Final ratios are included in Table S1. Settings for the CHEMTAX program were as described in Kozlowski et al. (2011) with all the elements varied.

Classification of winter samples in the size-fractionated Chl a time series, as needed for statistical purposes, was as used for defining the winter bin for the CHEMTAX analysis (see above). We refrained from using a fixed period as sampling effort during winter was variable due to inaccessibility of the site. Summer samples were defined as all the samples collected in December, January and February. These classifications were

employed to discuss long term trends in the relative abundance of phytoplankton size fractions and total Chl a during summer and winter using linear regressions.

To differentiate between the different summers and winter relative phytoplankton species composition we used a non-parametric multivariate analysis of variance (NPMANOVA) with the Bray-Curtis distance measure and 9999 permutations. This was supplemented by post-hoc pairwise Hotelling's tests if the initial analysis was found significant (Anderson, 2001) and corrected with a Bonferroni correction (alpha 0.05) to avoid type 1 errors (Holm, 1979). Further exploration of the relative phytoplankton composition and its interannual variability was tested by using a Non-metric multidimensional scaling (NMDS). The NMDS scores were rotated using a Principal Component Analysis (PCA) to maximize the case scores along the two axes. The PCA shows how the various phytoplankton groups characterize the different summers and which summers were similar to one another.

To understand the relationship between winter MLD, duration of fast-ice cover and summer stratification strength, we used second PCA-rotation of NMDS scores with Euclidian distances. Before the NMDS, the data were log-transformed and their means subtracted to correct for differences in the scale of the variables. A minimum spanning tree of the initial NMDS scores depicts how the years were oriented within the initial three-dimensional space of the NMDS. The exclusion of biological parameters allowed us to test if the water column properties differed significantly between the years. Stress of the initial NMDS, as calculated by Shepard's plots, was ~0.05.

A correlation table was used to assess linear relationships between winter MLD, duration of fast-ice cover, median summer Chl a and summer stratification strength as our phytoplankton data do not cover the full duration of the time series (Venables *et al.*, 2013). The correlation table was expanded with the median relative abundances of the different phytoplankton groups. Spearman's rank coefficients were calculated to test for correlations both between the environmental parameters (winter MLD, duration of fast-ice cover, median summer Chl a and summer stratification strength) and phytoplankton abundance and between the various abundances of the phytoplankton groups. We opted for a rank-based approach due to the non-linear

nature of phytoplankton responses to changing environmental conditions. The correlations were assumed significant if $p \leq 0.05$. For $p \leq 0.1$ but > 0.05, correlations were reported as indicative of a possible relationship.

To classify the productivity of summers based on median summer Chl a, we used the results of the NMDS analyses. Grouping of years based on the winter MLD, duration of fast-ice cover and summer stratification strength was used to construct a conceptual model that predicts summer phytoplankton biomass and composition depending on winter and summer water column properties.

All statistical tests were conducted using PAST 2.17c (Hammer *et al.*, 2001) except for the PCAs on the NMDS scores which were created using CANOCO 5.02.

Results

Winter sea ice duration has been highly variable during the lifetime of the RaTS programme, 1997 to 2013 (Ducklow *et al.*, 2013; Venables & Meredith, 2014). Sea ice cover at the RaTS site was described in detail by Meredith et al. (2008, 2010) and updated in Venables & Meredith (2014). A greatly decreased presence of fast-ice (24-64 days) was observed during the winters of 1998, 2001, 2003 and 2007-2010 (Fig. 2a; Venables & Meredith, 2014). These reductions were linked to an increase in northerly winds driving the ice out of Ryder Bay (Meredith *et al.*, 2010). In comparison to Adelaide Island, both Charcot Island and Anvers Island (Palmer Station; Fig. 1) displayed sea ice anomalies of the same sign but with a different scale (Ducklow *et al.*, 2013). Anvers Island lies north of Adelaide Island, while Charcot is to the south, hence these locations are on a north-south climatic gradient along the WAP. When comparing the satellite-derived data to the direct observations of sea ice cover at Adelaide Island, good agreement is generally found (Ducklow *et al.*, 2013; Venables & Meredith, 2014).

An exception was the winter of 2003, when there was little fast-ice detected by satellite yet direct observations made at Rothera indicated 89 days of fast-ice coverage (Ducklow *et al.*, 2013; Venables & Meredith, 2014). Also, winter MLD during 2003 was relatively deep (75 m) suggesting an overestimation of sea ice cover in the direct

observations. The average duration of fast-ice cover throughout the time-series was 76 days.

As a result of the high variability in winter sea ice presence, variation in winter MLD was also large. Mean winter MLD was >= 75 m during the years in which fast-ice coverage was low, with the exception of 2009 (Venables *et al.*, 2013). In contrast, mean winter MLD averaged < 42 m during the remaining years, with 2000 being the shallowest at only 16 m. Mean summer upper-ocean (30 m) stratification strength varied between 462 J m^{-2} (2010-2011) and 124 J m^{-2} (2007-2008). The results on winter MLD and summer stratification strength as used in the correlation analysis were updated from Venables et al. (2013).

During the full sequence of RaTS, variability in total phytoplankton biomass was high (Fig. 2a). Winter concentrations were low, averaging just 0.061 µg Chl a l^{-1} with stocks never exceeding 0.194 µg Chl a l^{-1}. Lowest winter biomass levels were found to be less than 0.001 µg l^{-1}. Winter biomass levels decreased at a rate of 0.023 µg l^{-1} per decade or 33.3% over the duration of the time series (df = 203, p = 0.022). The average contribution of microphytoplankton to total biomass during winter was 18.5%, and increased by 8.0% per decade (df = 203, p < 0.001) and varied between 0.00% and 64.9% (Fig. 2b), yet absolute microphytoplankton biomass remained unchanged. The three remaining smaller phytoplankton size classes decreased in absolute and relative abundance over the 1997-2012 winter periods.

Average summer (Dec – Feb) Chl a concentration was 8.53 µg l^{-1} with frequent peaks of more than 20 µg l^{-1}. The highest measured value was 28.92 µg l^{-1} in January 2003. The summers of 2007-2008 and 2008-2009 were exceptional due to their extremely low maximum biomass maximum of 6.96 Chl a µg l^{-1}. Over the complete period (1997-2012), total summer (Dec – Feb) biomass decreased significantly by 38.5% or 2.88 µg Chl a l^{-1} per decade(df = 224, p = 0.006). On average, 75.0% of the summer Chl a stock was contained in microphytoplankton. This fraction was lower for 2007-2008 and 2008-2009 respectively, 32.2% and 30.9%.

Pigment fingerprinting followed by CHEMTAX analysis revealed that diatoms were the dominant group and relative abundances of this group rarely dropped beneath 50%

(Fig. 3a). Median abundances of diatoms were 91.0% in summer and 71.4% for winter. Medians for the other phytoplankton groups during winter were 19.0% for haptophytes and 2.6% for cryptophytes with prasinophytes, dinoflagellates and chlorophytes remaining below 0.5%. Medians were used as they are less sensitive to extreme values, but this has the consequence that the values do not always add up to 100%. This

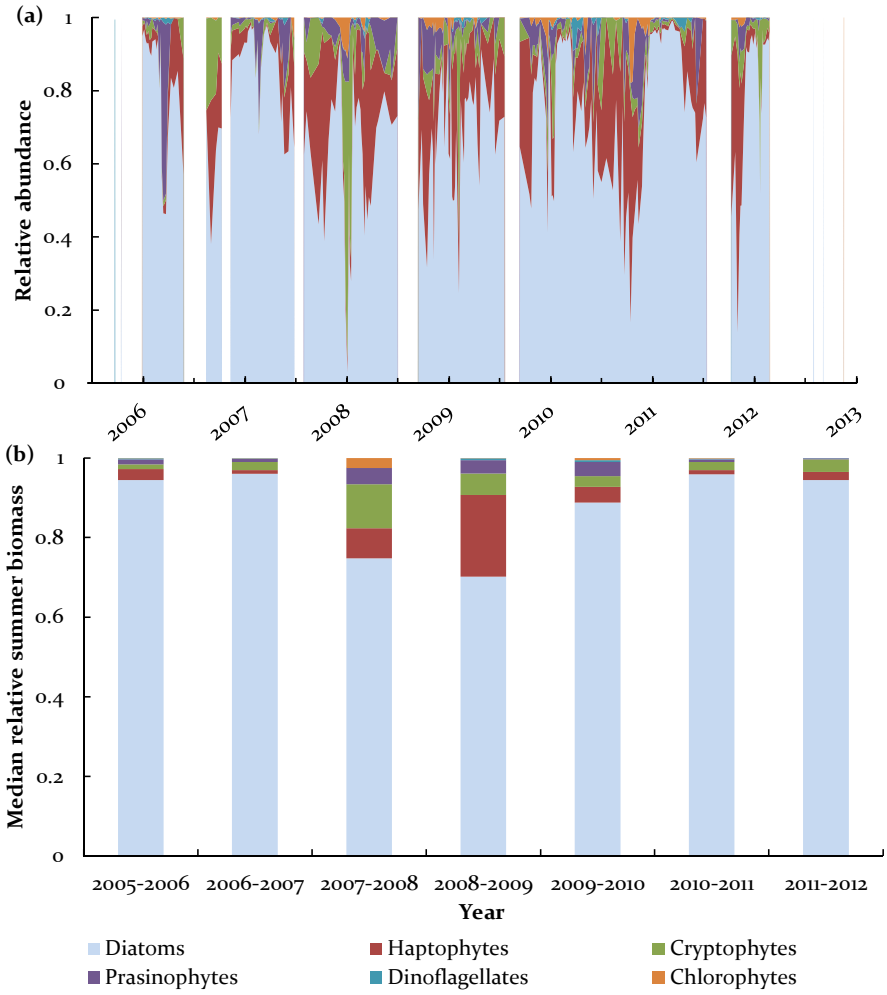

Figure 3: (a) Relative abundance for the six most important phytoplankton groups based on CHEMTAX for the 2006-2012 period. Diatoms and haptophytes sub groups were combined after the analysis. Interruptions in the dataset indicate a gap in the dataset of more than 30 days. Year labels on the x-axis are at January (b) Median fractions per summer (December- February) of the CHEMTAX results. Data in both a and b were standardized to 100%.

illustrates that prasinophytes, chlorophytes and dinoflagellates were observed less frequently but could occasionally contribute to the winter community. In particular prasinophytes could be relatively abundant during winter with a mean of 4.9% yet a low median. Exceptionally high prasinophyte abundances were observed during the late summer of March 2006, when they dominated phytoplankton stocks with a relative abundance of 40.2 - 48.8%. On average, samples with an overall phytoplankton biomass higher than 0.25 µg Chl a l^{-1} were dominated by diatoms resulting in medians (mean in brackets) of: 1.6% (3.0%), 2.4% (7.3%) and 2.8% (6.8%) for prasinophytes, cryptophytes and haptophytes respectively. Chlorophytes and dinoflagellates represented less than a median of 0.1% (average < 1.23%) of the summer biomass. The large difference between the medians and means for haptophytes and cryptophytes shows that these groups were more skewed in their variability. Also, dynamics within the summer season, which are lost by just means and/or medians, show that cryptophyte relative abundance increased to 76.0% in January 2008, 58.9% in February 2009 and 23.2% in January 2010 (Fig. 3a). Haptophyte abundances reached 21.5% in February 2008, 40.3% in January 2009 and 29.9% in January 2010 (Fig. 3a).

As phytoplankton absolute abundance can be highly variable due to various environmental parameters, we choose to rely mainly on the relative abundances. A change in relative abundance does not necessarily mean that one group was increasing or decreasing in absolute numbers as relative abundance is highly dependent on the variability of the other phytoplankton groups. Thus, to validate any possible trend in cryptophyte and haptophyte absolute abundances with respect to relative abundance of diatoms we needed to validate our choice for the latter. When diatom relative abundance was low, cryptophyte absolute abundance was up to 11.8-fold higher than when diatoms were the dominating fraction (≥ 0.9; Fig. 4a). Also, haptophyte absolute abundance was a maximum of 5.7-fold higher with a decreased relative abundance of diatoms (Fig. 4b).

Medians for the summer periods showed significant differences in group-specific abundances between years (Fig. 3b). In the years 2007-2008 and 2008-2009, both haptophytes and cryptophytes were relatively more abundant at the expense of

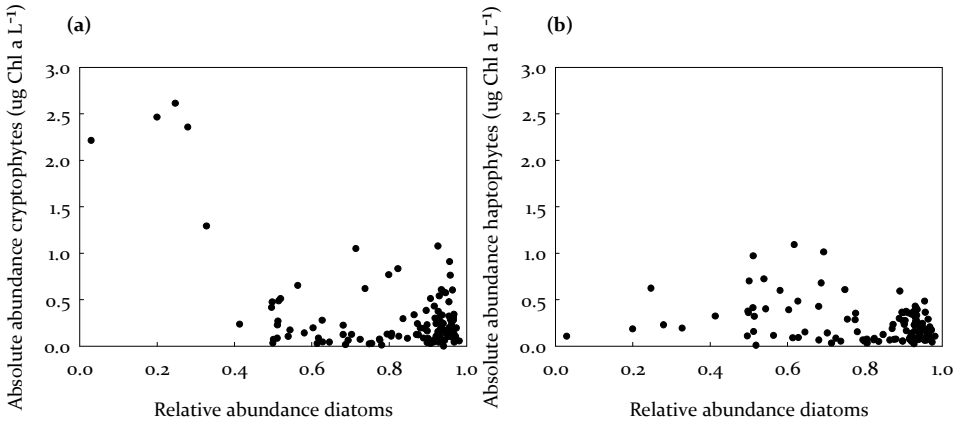

Figure 4: Relative abundance of diatoms versus absolute abundance of (a) cryptophytes and (b) haptophytes. A decrease in the relative abundance of diatoms coincided with a large increase in absolute numbers of cryptophytes and haptophytes.

diatoms. In addition, absolute diatom abundance was decreased while haptophytes and cryptophytes remained stable or showed higher abundances in comparison to periods of diatom dominance (>90 %). Following two low biomass summer seasons, 2009-2010 started with low biomass during the first half of summer, more haptophytes and cryptophytes and fewer diatoms in comparison to 2005-2006, 2006-2007, 2010-2011 and 2011-2012 (Fig. 3a). Yet, the 2009-2010 summer biomass levels reached average concentrations during the second half of summer, although median biomass remained low for the summer (Fig. 2a; 4.42 µg Chl a l^{-1}) . In contrast to these low biomass years, the summer seasons of 2005-2006, 2006-2007, 2010-2011 and 2011-2012 were highly similar with respect to relative abundances of the various phytoplankton groups.

Results from the NPMANOVA on the relative abundances of the phytoplankton groups revealed that the summers were not similar (pseudo-$F_{7, 187}$ = 14.46, p < 0.0001). Firstly, pairwise comparisons (Tab. 1) show that the pooled winter samples were different from all the summer assemblages except for 2008-2009. Secondly, the summers of 2007-2008 and 2008-2009 were significantly different in comparison to the other years. The third low biomass summer, 2009-2010, was similar to all summers except 2010-2011. In addition, 2007-2008, 2008-2009 and 2009-2010 were considered equal to each other.

Table 1: Post-Hoc testing after a NPMANOVA analysis on the relative species abundances from CHEMTAX for the summers (December-February) and the winter showed significant difference between the groups (pseudo-$F_{7, 187}$ = 14.46, p < 0.0001). The winter includes all winter samples of the 2005-2012 period pooled together as sample size was low. The table shows the Hotelling's p values after a Bonferroni correction for multiple testing (α = 0.05). Only values below 0.05 are shown and indicate significant differences between periods. The p-values are based on 9999 permutations.

		2005-2006	2006-2007	2007-2008	2008-2009	2009-2010	2010-2011	2012-2013	2005-2013
2005-2006	**Dec-Feb**	-							
2006-2007	**Dec-Feb**		-						
2007-2008	**Dec-Feb**	0.008	0.036	-					
2008-2009	**Dec-Feb**	0.003	0.003		-				
2009-2010	**Dec-Feb**					-			
2010-2011	**Dec-Feb**			0.003	0.003	0.020	-		
2011-2012	**Dec-Feb**			0.022	0.003			-	
2005-2012	**Winter**	0.003	0.003	0.003		0.031	0.003	0.003	-

Thirdly, the summer seasons of 2005-2006, 2006-2007, 2010-2011 and 2011-2012 were found to be similar. The NMDS scores supported the results obtained from the NPMANOVA (Tab. 1, Fig. 5b). Here, the winter samples clustered close to the 2008-2009 samples which were related with high haptophyte abundance. In contrast, 2007-2008 was governed more by cryptophytes and overlapped only slightly with the winter samples. The results from the NPMANOVA for 2009-2010 were confirmed by the NMDS as this year overlapped with all other summers. Finally, 2005-2006, 2006-2007, 2010-2011 and 2011-2012 were clustered together indicating a highly similar phytoplankton community in terms of group-specific abundances.

The sudden increase of diatoms in the second half of January of 2010 could be related to melting sea ice from outside the bay. The summer of 2009-2010 was characterized (at 15 m) by a high average salinity (~33.4), an average sea water temperature and a

*Table 2: Correlation table for the taxonomic groups were checked for correlation amongst themselves and with; mean winter mixed layer depth (MLD), Median summer Chlorophyll a, days of fast-ice cover and summer top 30m stratification strength. Significance values are (*) p < 0.1 show a trend but no significant correlation, ** p < 0.05 and *** p < 0.001. Values and direction of the slope of the correlation (if p < 0.1) are shown below the diagonal. Seven years of phytoplankton relative abundances were included (df = 5). Bray-Curtis distance and Spearman's rank coefficients were used for the comparisons between the phytoplankton groups and between the phytoplankton groups and physical parameters. Euclidian distances and linear correlations were used for comparisons of the physical parameters.*

	Mean winter MLD (m)	**Median chlorophyll a (µg l^{-1})**	**Fast-ice cover (days)**	**Mean summer stratification top 30 m (J m^{-2})**	**Prasinophytes**	**Chlorophytes**	**Dinoflagellates**	**Cryptophytes**	**Haptophytes**	**Diatoms**
Mean winter MLD (m)	-	**	***	(*)				**		
Median chlorophyll a (µg l^{-1})	-0.86	-	**	**				***	(*)	**
Fast-ice cover (days)	-0.95	0.83	-	(*)				(*)		
Mean summer stratification top 30 m (J m^{-2})	-0.71	0.84	0.67	-				***	**	**
Prasinophytes					-	(*)			(*)	
Chlorophytes					0.68	-				
Dinoflagellates							-			
Cryptophytes	0.79	-0.96	-0.68	-0.93				-	(*)	**
Haptophytes		-0.75		-0.86	0.75			0.68	-	**
Diatoms		0.86		0.82				-0.82	-0.82	-

very low contribution of glacial melt water (Fig. 9 & 10 in Meredith et al. 2013). However, after January 18th (Fig. S1a) there was a 0.5 °C decrease in sea water temperature at 15 m and a small increase in salinity (~0.15). These changes coincide with a large increase (from 51.4 to 87.3%; Fig. 3a) in the relative contribution of diatoms. Also, after the sudden change on January 18th there was increased sea ice melt at the RaTS site which remained throughout February (Fig, S1b; Meredith et al. 2013).

To explore which physical characteristics could drive variability in phytoplankton composition, the medians of the relative summer abundances per group and year were correlated with previous winter mean MLD, summer chlorophyll median, number offast-ice days in the previous winter and mean summer upper-ocean (top 30 m) stratification strength (Tab. 2). Firstly, relative abundances of prasinophytes, haptophytes and cryptophytes were strongly negatively correlated with diatoms. This effect was strongest for cryptophytes and haptophytes. Secondly, weaker summer stratification was found to be directly correlated with a lower relative abundance of diatoms. In contrast, abundances of prasinophytes, haptophytes and cryptophytes were positively influenced by a weakening of stratification in summer. Also, a weak positive relationship was found between the relative contribution of diatoms and total phytoplankton biomass (Tab. 2). Lower median summer Chl a was found to be associated with a larger proportion of cryptophytes. Finally, a significant and positive trend between winter MLD and cryptophyte abundance was observed.

Results of a PCA on NMDS scores for winter mean MLD, number of fast-ice days and mean summer upper-30m stratification strength suggested a high similarity for these physical parameters between years with medium and low biomass (Fig. 5a). Also, the minimum spanning tree shows that the medium biomass years were closer to the low biomass years than to the high biomass years. Furthermore, 2010, a medium biomass year, was more similar to the low biomass years than to the other medium biomass years.

Even though both haptophytes and cryptophytes showed a negative relation with stratification strength they did not necessarily co-occur (Tab. 2). A further investigation of the summer MLD versus the relative abundance of both haptophytes

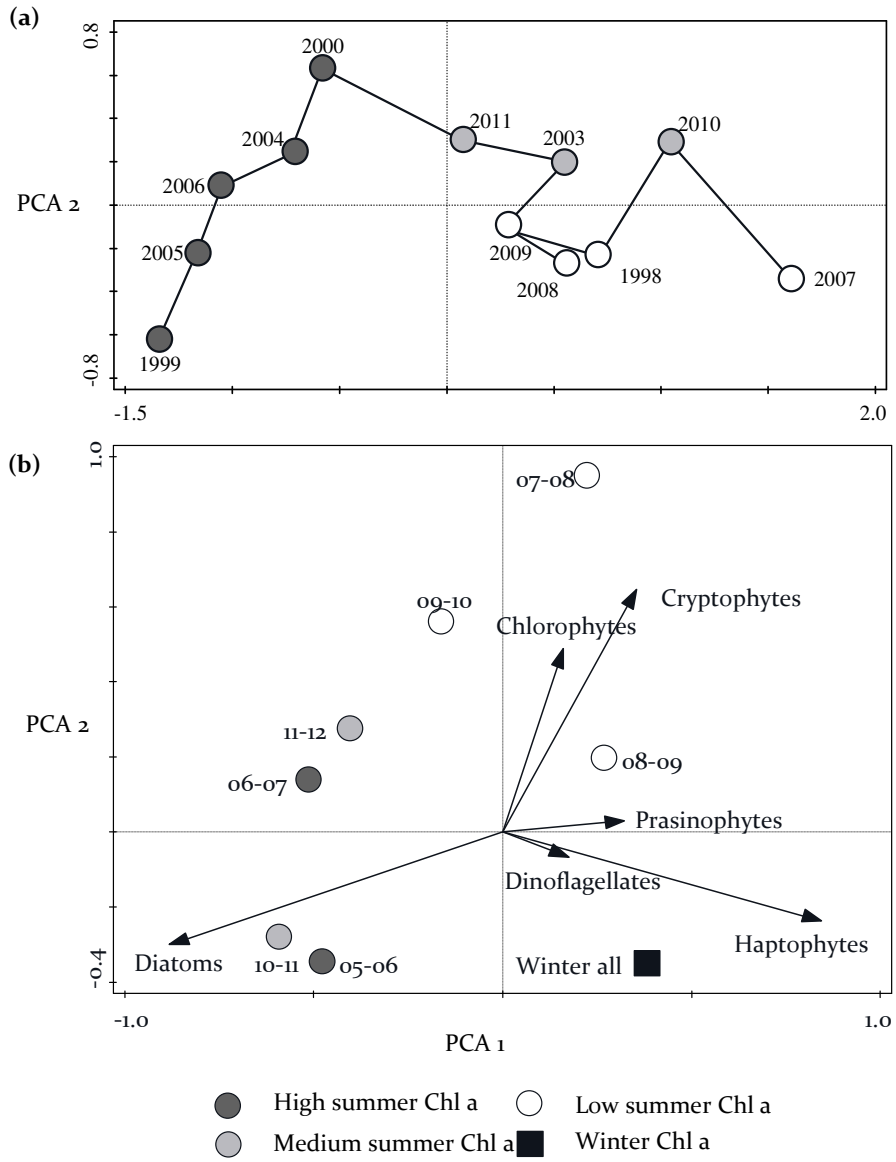

Figure 5: Principal Component Analysis (PCA) on the scores of a Non-metric Multidimensional Scaling (NMDS) analysis. Data points are colored based on median summer biomass The top graph (a) shows how the different years were related based on winter mean MLD, number of fast-ice days and mean summer upper-ocean (top 30 m) stratification strength. The lines connecting the years show the minimum spanning tree. The bottom graph (b) show how strongly and to which season the relative abundance of different phytoplankton groups was related. Also, all pooled winter samples are plotted to compare the winter community to that of the different summers.

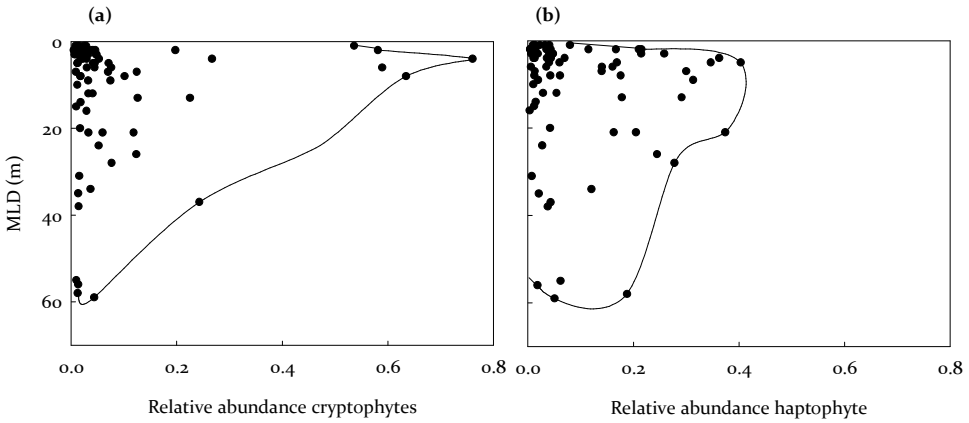

Figure 6: Mixed layer depth (MLD) at the time of sampling plotted against the relative abundance of (a) cryptophytes or (b) haptophytes during the low biomass period (2007-2010). Cryptophytes preferred a relative shallow MLD while haptophytes were more diverse in their occurrence at variable MLDs. Convex hulls show the maximum relative abundance at various MLDs.

and cryptophytes showed high abundances of cryptophytes during a shallow MLD (10 - 20 m), as could be deduced from the shape of the convex hull (Fig. 6a). No such relations (data not shown) were observed when relative abundances of haptophytes or cryptophytes were plotted against 0 or 15 m salinity, major nutrients (nitrogen, phosphate, silicate) or oxygen isotopes (indicative of melt water origin). Haptophytes do not seem to have a preferred MLD (Fig. 6b), occurring in similar relative abundances at various MLDs. Thus, even though the water column was, when averaged over the summer, unstable in comparison to medium/high biomass summers, short-term stratification events still occurred and seemed to have been associated with cryptophytes.

Median summer biomass appeared to be highly predictable (p = 0.002; r^2 = 0.68) when using the day when water column stabilization by fresh water input started to have a significant effect (Fig. 7). The difference between the earliest and latest start of the salinity decrease was 126 days (~ 4 months). This large difference in onset of the melt period resulted in a 16-fold difference in median biomass between the highest and lowest summer biomasses. The negative correlation suggests that an early onset of melt results in a highly productive summer or low productivity when melt is delayed.

Spread of the observations for the high biomass summers is relatively large as sample collection was hindered more frequently by unfavorable sea ice conditions.

Discussion

Our study showed large interannual variability in phytoplankton bloom magnitude and composition, related to winter sea ice cover and summer stratification strength. Microphytoplankton (> 20 µm) dominated the summers between 1997 and 2013 except for 2007-2008 and 2008-2009 (Fig. 2a, b). Earlier observations by remote sensing linked an increase in MLD due to declining sea ice cover and an increased wind strength to a dominance of microphytoplankton > 20 µm (Montes-Hugo *et al.*, 2009). This is in line with our direct observations as microphytoplankton abundances in 2007-2008 and 2008-2009 were significantly decreased (Fig 2b). The HPLC data at the RaTS station

(7 out of the 15 years) showed that the observed decreasing trends in microphytoplankton were associated with a decline in diatoms (Annett *et al.*, 2010). Our combination of size-fractioned Chl a with HPLC pigment fingerprinting appears to be a strong tool and can unravel the phytoplankton community responsible for the observed decrease in summer and winter phytoplankton biomass.

In contrast to summer, microphytoplankton did not contribute much to the winter and spring biomass (< 20%) while picophytoplankton (< 2 µm) represented > 48%. The 2007-2009 summers were more similar to the winter composition with regard to their size class distribution. These summers experienced steep increases of the microphytoplankton fraction when compared to the winter community. Yet, these increases lasted for a period significantly shorter than summers with a high biomass. Moreover, a summer with low biomass due to a decrease in (large) diatoms, does not necessarily imply a low microphytoplankton fraction. Colonies of *Phaeocystis antarctica* or large cryptophytes (> 20 um) would be included in the microphytoplankton fraction. Both were observed frequently at the RaTS site by studying *in vivo* microscopy samples and revealed a high variability in cryptophyte cell sizes, ranging from < 10 um to > 20 um in cell length (A. Buma, unpublished results). Hence, the low biomass in 2009-2010 but average microphytoplankton fractions can

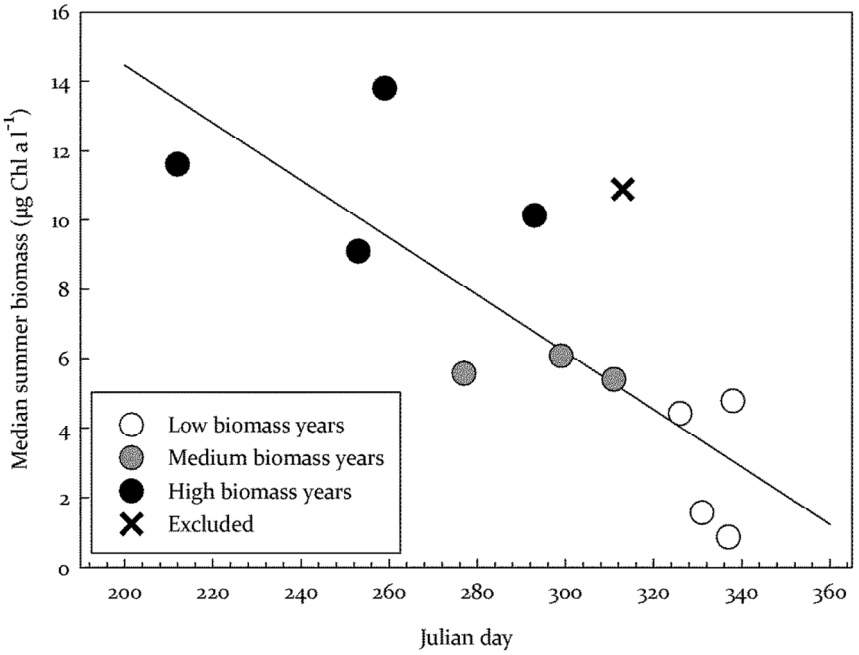

Figure 7: Onset of summer melting in comparison to median summer biomass. The date of the salinity decrease is negatively correlated with median summer biomass ($p = 0.002$; $r^2 = 0.68$). The cross stands for a summer season for which no CTD data were collected for 1.5 months during the spring period. The colors indicate median summer concentrations of phytoplankton biomass (white: low, grey: medium and black: high).

explain the low relative abundance of diatoms as observed by CHEMTAX (Fig. 3a, b). This could also apply to 1997-1998, yet no HPLC data were available for this year.

Low light availability during winter due to deep mixing and the polar night limited phytoplankton growth and maintained a stable community with predominantly haptophytes (24%), cryptophytes (5%) and (small) diatoms (71%) (Fig. 2a, 3a and 8). Differences in composition between winters were not tested due to a high variability in number of available samples per year. Pigment data suggest a dominance of diatoms during winter while size-fractionated Chl data suggested a low contribution of microphytoplankton, thus diatoms in winter were smaller than those in summer. This winter community would have experienced the first available light during spring and formed the base for the summer community. The seven years of HPLC data show the

persistence of haptophytes and cryptophytes during spring (Fig. 3b). The spring phytoplankton assemblages in this study were all highly similar to those of winter.

Classical, well-described Antarctic diatom blooms propagate after spring when the water column has stabilized due to e.g. glacial melt water input, surface warming and/or melt of fast-ice. However, a deeply-mixed winter water column takes more buoyancy input (and, for a given rate of energy input, more time) to stabilize. This delay in stratification due to the lack of sea ice may have prevented the formation of classical diatom blooms in some years. Delayed onset of increased light availability caused the winter and spring communities to persist longer.

Our results show a highly similar and diatom-dominated composition between most summers (Tab. 1 and Fig. 5b). Diatom abundance and summer stratification were positively correlated (Tab. 2), in agreement with earlier observations at various Antarctic sites (Arrigo *et al.*, 1999; Clarke *et al.*, 2008; van de Poll *et al.*, 2009; Annett *et al.*, 2010; Piquet *et al.*, 2011). However, we observed a larger presence of haptophytes (max. 40.3%) and/or cryptophytes (max. 76.0%) during summer periods with low biomass (2007-2010, Fig. 3a). Summers such as 2007-2008 and 2008-2009 showed that weak mean summer stratification, due to the absence of fast-ice during winter, experience low diatom abundances. Although 2009-2010 shifted towards delayed diatom dominance, the median summer biomass remained low. The sudden change in water column conditions, an increase in salinity and decrease of the temperature, on January 18th 2010 could suggested lateral advection bringing in sea ice from elsewhere, as there was not much sea ice during winter (Fig 2a, S1), altered the phytoplankton community. This is further supported by the exceptionally high contribution of sea ice melt observed during this period (Fig. S1b; Meredith et al. 2013). This late increase of sea ice melt illustrates why 2009-2010 was placed in between two years belonging to two different classifications, namely 2007-2008 (low) and 2011-2012 (medium; Fig. 5b). In contrast, the two summers of 2007-2009 remained low in both biomass and diatom abundance. These two summers (and the first half of 2009-2010) suggest a persistence of the winter/spring community during years with weak summer stratification. This persistence was further strengthened by the lack of a significant difference between the summer of 2008-2009 and the pooled winter samples (Tab. 1). Not only did the relative

abundances of cryptophytes and haptophytes increase when diatoms were less abundant, also absolute numbers increased (Fig. 4).

While both haptophytes and cryptophytes occasionally dominated, they did not necessarily co-occur (Tab. 2). Both groups were linked to unstable water column conditions, suggesting similar strategies for maintaining their presence (Tab. 2). Previous studies often associated *Phaeocystis* with well-mixed water columns in which average irradiance levels were low (Arrigo *et al.*, 1999; Alderkamp *et al.*, 2012b). Different strategies to cope with non-photochemical quenching following high irradiance exposure seems to be a major difference between diatoms and *Phaeocystis* (Kropuenske *et al.*, 2009; Alderkamp *et al.*, 2012a, 2013). Cryptophytes were often associated with low salinity and observed in the surface layer (Moline *et al.*, 2004; Kozlowski *et al.*, 2011; Mendes *et al.*, 2013).Yet, our pigment data show a strong positive correlation with winter MLD and negative with summer stratification strength suggesting the opposite (Tab. 2). Also, cryptophytes were more abundant than haptophytes during periods in summer with a shallower MLD (Fig. 6). These two opposing observations suggest that surface stratification over an unstable and uniformly mixed water column favored cryptophytes. These conditions were possibly indicative of surface melt water stratification after periods of deep mixing. Apparently, cryptophytes cannot out-compete diatoms during years where water column stability is promoted earlier in the season. Prasinophytes were only present in high numbers during a small period at the end of the summer of 2005-2006. It is possible that this peak represents a small incursion of more open ocean waters, as prasinophytes were generally observed at depth at offshore stations (Kozlowski *et al.*, 2011).

Limitation of phytoplankton growth by macronutrients during summer was unlikely due to generally high concentrations within the region, especially as low phytoplankton biomass was related to deeper (winter) mixing (Clarke *et al.*, 2008). While micronutrients such as iron might limit phytoplankton growth, structural limitation is unlikely due to the coastal nature of the bay (Bown et al. 2017; Alderkamp et al. 2012b; Annett et al. 2015). Temporary limitation of phytoplankton by low concentrations micronutrients might incidentally occur at RaTS although reported minimum concentrations are still higher than observed in open Southern Ocean

(Bown et al. 2017). In contrast, limitation by light (de Baar *et al.*, 2005) or photoinhibition (Alderkamp *et al.*, 2010) could not be excluded due to frequent changes in MLD and very high biomass concentrations (Venables *et al.*, 2013). Yet none of these factors appeared to be limiting factors during the years of low biomass. Moreover, top down control on phytoplankton biomass cannot be excluded although it does not appear to govern phytoplankton growth rates in Ryder Bay (Venables *et al.*, 2013). A shift from grazers preying on large (by krill) to small phytoplankton (e.g. by ciliates or salps) could have an impact in low biomass years as small grazers can increase their numbers more rapidly than e.g. krill. Thus, small phytoplankton growth rates might be controlled more efficiently (Behrenfeld, 2010). Also, while this paper focusses on 15 m Chl a, depth-integrated Chl a has been published previously and showed highly similar trends (Venables *et al.*, 2013).

To assess the combination of our long term observations of the physical and biological conditions, we constructed a conceptual model. Analysis of the total number of winter fast-ice days revealed two clusters, high (89-124 days) and low (24-64 days) fast-ice winters, with a gap of 25 days separating the two clusters (Fig. 5a). Venables et al. (2013) suggested that this parameter is ultimately driving summer bloom magnitude. This grouping of years was used as a starting point for our conceptual model (Fig. 8). Summer stratification of the top 30 m was used as a second conditioner as diatoms, traditionally associated with high biomass, favor strong stratification (Tab. 2). Three different bins partitioned the summer into years of strong (283-264 J m^{-2}), intermediate (209-264 J m^{-2}) and weak (123-198 J m^{-2}) stratification. Finally, the years for which a full summer was covered were partitioned into three classes by median biomass based on the 15 years of Chl a measurements: high (9-14 µg Chl a l^{-1}), medium (5-7 µg Chl a l^{-1}), and low (0-5 µg Chl a l^{-1}). The minimum spanning tree in Figure 5a further suggests that the low biomass conditions were a starting point at which the water column was still in a minimum, winter-like state. A more stable water column would improve the conditions for biomass growth to medium or higher levels. The grouping of high, medium and low biomass years suggests a strong dependence on the physical environment, further confirming the results from the correlation analyses (Tab. 2) and NPMANOVA (Tab. 1).

Most years within our time series followed the classification by the model as proposed. The only exception was 1999-2000, where strength of summer stratification was intermediate while biomass was high (9.01 µg Chl a l^{-1}). The preceding winter MLD (mean 15.7 m) was much shallower than during any other winter in our time series, most likely due to a high number of fast ice days (114), thereby promoting exceptionally strong post-winter stratification and an early onset of phytoplankton growth. Also, at the end of November, Chl a concentrations were 3.89 µg l^{-1} (Fig. 2a) while one week later it had increased to 23.71 µg l^{-1}. This is the highest concentration observed in any of the 15 years of December observations apart from one sampling event on the 31st of December (2010).

Our conceptual model identified three different categories of summers based on phytoplankton biomass. To understand how the phytoplankton community was composed within these categories, we pooled the years within the same category (Fig. 8). This resulted in three fingerprints showing that the high and medium biomass years were identical in their community composition. Cryptophytes, haptophytes and diatoms represented the bulk of the biomass, respectively 1.63%, 1.85% and 95.22% for summers with high biomass and 2.59%, 1.56% and 95.15% for medium biomass summers. Thus, there was little to no difference in relative contribution of the major groups between years categorized as high or medium summer biomass. However, low biomass years showed more cryptophytes (6.36%) and haptophytes (10.72%) while the diatom fraction (77.90%) decreased. These last fractions were highly similar to those observed in winter. Thus, supporting our suggestion of summers preceded by winters with strong mixing may exhibit a persisting winter phytoplankton community.

We furthermore investigated if our conceptual model could explain the phytoplankton biomass and composition on the coastal WAP, mainly north of Marguerite Bay. The summertime phytoplankton community near Palmer station on Anvers Island experienced an increase of the relative contribution of cryptophytes related to event of increased melt water input (Moline *et al.*, 2004; Saba *et al.*, 2014). In contrast, in Marguerite Bay haptophytes and cryptophytes were seen to replace diatoms during low biomass years. Winter sea ice cover was low at Anvers Island and its duration shorter than in northern Marguerite Bay (Ducklow *et al.*, 2013). Therefore, winters at Anvers

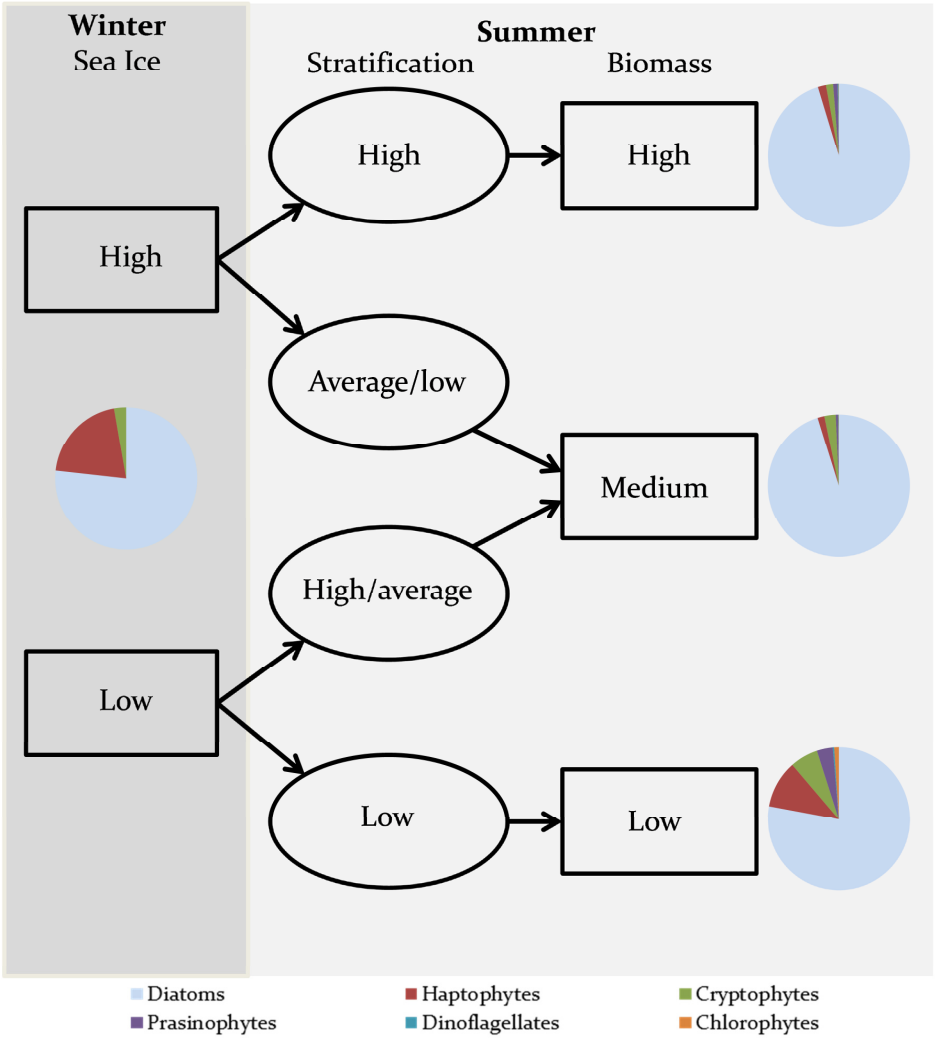

Figure 8: Conceptual model linking the number of ice days to the strength of summer top 30m stratification. Two different sea ice modes (>76 and <76 days) can lead to three different stratification strength bins weak (283-264 J m^{-2}), intermediate (209-264 J m^{-2}) and weak (123-198 J m^{-2}). Consequently, three classifications of median summer biomass (Chlorophyll a concentrations of 0-5, 5-7 and 9-14 µg Chl a l^{-1}) allow the labeling of summers as low, medium or high biomass years. Also, median relative abundances for six phytoplankton groups during the winter and three summer classifications are shown.

island can be classified as low sea ice winters and, consequently, summer biomass can only reach low or medium values if following our conceptual model. A comparison of the Chl a measurements from Palmer Station sites B or E at Anvers Island and from RaTS revealed on average threefold higher Chl a at RaTS. The years in which the RaTS

biomass approached that of Palmer Station were after winters with low ice cover, in agreement with our model. Also, the lack of winter sea ice and polynya-like properties of the northern WAP were likely to cause a deeper MLD during winter (Ducklow *et al.*, 2013; Turner *et al.*, 2013; Venables *et al.*, 2013).

However, average summer MLD near Palmer station (1993-2012) was significantly shallower (~20 m) than in northern Marguerite Bay (~32 m; Ducklow et al. 2013). Thus, the deeper winter MLD and lower sea ice cover during spring suggests that meteoric water input, presumably predominantly of glacial origin, promotes stratification during summer and causes the shallow MLDs (Ducklow *et al.*, 2013). We suspect low biomass summers can have elevated haptophytes, cryptophytes or a mixture thereof in agreement with satellite observations that suggest a decline in phytoplankton sizes (Montes-Hugo *et al.*, 2009). To our knowledge, this study is the first to present high resolution, multi-year, year-round and direct observations on how changes in size-class distribution and composition of the phytoplankton community at the coastal WAP relate to the changes in the physical environment. Earlier studies based on indirect satellite observations have estimated size-class distribution and/or total biomass over longer timespans (Montes-Hugo *et al.*, 2008a, 2008b, 2009).

Satellite derived biomass observations confirm our findings of declining summer phytoplankton biomass in the northern Marguerite Bay region (Fig. 2a in Montes-Hugo et al. 2009). This trend is dictated by two summers of extremely low biomass and decreased abundances of diatoms. While biomass at the southern WAP in the open ocean might be increasing (Montes-Hugo *et al.*, 2009), coastal regions in the area do not follow this trend. Current trends of delayed sea ice formation and strengthening wind are likely to cause deeper MLDs and weaker and later summer stratification (Meredith & King, 2005; Montes-Hugo *et al.*, 2009; Meredith *et al.*, 2013). Even though there is a projected increase in glacial melt water which might add stability and thus partially counteract MLD deepening, oxygen isotope data at the RaTS site showed that this is not the dominant effect in determining changes in upper ocean stratification at this location (Meredith *et al.*, 2013). Further delays in stratification onset due to the increasing winter MLD and lack of sea ice melt is likely to result in decreased productivity (Fig. 7). The deep mixing that causes unfavorable conditions for large

diatom blooms is likely to become more frequent and the microphytoplankton fraction will most likely further decrease in abundance. We expect cryptophytes and (colonial forms of) *Phaeocystis* to be observed more frequently and become more important in the Antarctic ecosystem, in concert with declining phytoplankton biomass.

Conclusions

Well-described trends over the northern WAP can now be projected further south as we connect our and previous observations into a conceptual model. Decreased (winter) sea ice cover will result in less abundant and smaller phytoplankton. We suggest that periods in the summer during low biomass years with a deeper MLD promote haptophytes (Arrigo et al. 1999). When MLDs become shallow, e.g. a shallow melt water lens of glacial origin on top of a relatively unstable water column, cryptophytes are likely to increase their presence (Moline et al. 2004; Mendes et al. 2013). A combination of these two mechanisms hold when compared to satellite observations that suggest a decline in phytoplankton sizes (Montes-Hugo et al. 2009). Our results nuances earlier suggestions of a cryptophytes dominated coastal WAP as haptophyte contributions were also observed to vary in relation to environmental changes (Saba et al. 2014).

Phytoplankton communities will have a different composition when current trends are projected forwards under global warming scenarios. Export of anthropogenic CO_2 by heavy diatoms might be diminished if the phytoplankton community will shifts towards a flagellate-based systems (Weston *et al.*, 2013). Further declines in krill and penguin stocks, as observed along the northern WAP, are likely to occur in Marguerite bay (Atkinson *et al.*, 2008; Schofield *et al.*, 2010; Constable *et al.*, 2014; Saba *et al.*, 2014), as diatom abundance declines. These projections will hold extensive consequences on the Antarctic ecosystem and biogeochemical cycling.

Acknowledgements

We thank all the Marine Assistants and other staff at Rothera and in Cambridge who have contributed to the collection of the samples and data used here. Also, we thank Ronald Visser, who assisted with HPLC measurements and Simon Wright for providing an original version of CHEMTAX. Gemma Kulk and two anonymous reviewers are

thanked for valuable discussions. This research was funded by the Netherlands Polar Programme (866.10.105). RaTS is funded by the Natural Environment Research Council, and is a component of the BAS Polar Oceans programme.

Apendices are available online and/or upon request.

2

Chapter 3

Assessing drivers of coastal phytoplankton productivity in northern Marguerite Bay, Antarctica.

P. D. Rozema
G. Kulk
M. P. Veldhuis
A. G. J. Buma
M. P. Meredith
W. H. van de Poll

Published in:
Frontiers in Marine Science (2017)

Abstract

The coastal ocean of the climatically-sensitive west Antarctic Peninsula is experiencing changes in the physical and (photo)chemical properties that strongly affect the phytoplankton. Consequently, a shift from diatoms, pivotal in the Antarctic food web, to more mobile and smaller flagellates has been observed. We seek to identify the main drivers behind primary production (PP) without any assumptions beforehand to obtain the best possible model of PP. We employed a combination of field measurements and modeling to discern and quantify the influences of variability in physical, (photo)chemical and biological parameters on PP in northern Marguerite Bay. Field data of high-temporal resolution (November 2013 – March 2014) collected at a long-term monitoring site here were combined with estimates of PP derived from photosynthesis-irradiance incubations and modeled using mechanistic and statistical models. Daily PP varied greatly and averaged 1764 mg C m^{-2} d^{-1} with a maximum of 6908 mg C m^{-2} d^{-1} after the melting of sea ice and the likely release of diatoms concentrated therein. A non-assumptive random forest model (RF) with all possibly relevant parameters (M_{RFmax}) showed that variability in PP was best explained by light availability and chlorophyll *a* followed by physical (temperature, mixed layer depth and salinity) and chemical (phosphate, total nitrogen and silicate) water column properties. The predictive power from the relative abundances of diatoms, cryptophytes and haptophytes (as determined by pigment fingerprinting) to PP was minimal. However, the variability in PP due to changes in species composition was most likely underestimated due to the contrasting strategies of these phytoplankton groups as we observed significant negative relations between PP and the relative abundance of flagellates groups. Our reduced model (M_{RFmin}) showed how light availability, chlorophyll *a* and total nitrogen concentrations can be used to obtain the best estimate of PP (R^2 = 0.93). The resulting estimates from our models suggest summer PP to have been between 214.4 and 176.1 g C m^{-2}. Through the employment of a modeling technique without any assumptions apart from a representative sampling strategy, we showed and estimated how PP in this climatically sensitive and changing region can best be predicted and described.

Apendices are available online and/or upon request.

Introduction

The western Antarctic Peninsula (WAP) is a region where changes in climate have been most pronounced over recent decades, with strong variability superposed on a long-term warming trend (Vaughan *et al.*, 2003; Meredith & King, 2005; Turner *et al.*, 2005, 2016). These changes include shifting patterns in wind direction and speed, a strong reduction sea ice extent and marked glacial retreat (Marshall *et al.*, 2006; Montes-Hugo *et al.*, 2008a; Stammerjohn *et al.*, 2008b; Rignot *et al.*, 2013; Turner *et al.*, 2013; Stammerjohn & Maksym, 2017). As a result, the physical characteristics of adjacent marine waters are changing. Increasing wind speeds and the diminution of sea ice have resulted in deepening of mixed layers along the northern WAP region (Montes-Hugo *et al.*, 2009). Moreover, the decrease in sea ice extent removes an important source of freshwater which would otherwise enhance salinity stratification of the water column upon melting in spring. In contrast, an increase in glacial melting is observed, due to enhanced upwelling of relatively warm Circumpolar Deep Water (Cook *et al.*, 2016). These changes may have significant consequences for irradiance and nutrient availability. On the one hand, the increase in glacial meltwater promotes stratification and consequently improves light availability. On the other, more frequent and/or deeper mixing could increase the availability of macro- and micronutrients, whereas glacial meltwater is generally poor in macronutrients but potentially rich in trace metals such as iron (Alderkamp *et al.*, 2012b). This interplay between climate change related impacts is likely to have an effect on both the composition and productivity of the phytoplankton community.

The classical Antarctic food web revolves around highly productive sea ice edge blooms consisting of diatoms, where krill can feed and transfer energy up the food chain (reviewed in Ducklow et al. 2012a). These blooms are instigated by the melting of sea ice and increase in light availability after the polar winter. With the appearance of deeper mixed layers, the phytoplankton community has reoriented itself towards higher proportions of smaller flagellates such as haptophytes (generally *Phaeocystis*) and cryptophytes (Arrigo *et al.*, 1999; Montes-Hugo *et al.*, 2009; Kozlowski *et al.*, 2011; Trimborn *et al.*, 2015; Rozema *et al.*, 2017a). In the WAP region, this shift in phytoplankton community seems further fueled by the replacement of sea ice melt by

glacial melt as the major source of freshwater (Moline *et al.*, 2004; Mendes *et al.*, 2013). While diatoms are still the major contributor to phytoplankton biomass, cryptophytes and haptophytes are increasing in the coastal WAP region (Saba *et al.*, 2014; Rozema *et al.*, 2017a). Our current understanding suggests an association of haptophytes with more unstable water columns, while cryptophytes show increased abundances when these water columns are restabilizing due to glacial meltwater injection.

The occurring shift in the phytoplankton community seems to coincide with changes in the primary productivity (PP) of the coastal WAP ecosystem. Physical properties of the water column, for example stability, influence PP directly and indirectly. A less stable water column means less available light for photosynthesis, but also promotes growth of different phytoplankton groups. Phytoplankton biomass accumulation is limited in years following winters with a more unstable water column due to low sea ice cover during winter (Venables *et al.*, 2013). This potential effect is further strengthened due to the changing species composition as productivity per biomass unit of small flagellates is different to that of diatoms (reviewed in Petrou et al. 2016). For example, *Phaeocystis antarctica* is thought to be more productive per chlorophyll a (Chl-a) and per captured photon than *Fragilariopsis cylindrus*, a small diatom associated with the sea ice edge (Arrigo *et al.*, 2010; Alderkamp *et al.*, 2012a). In contrast, data suggest a decreased potential for productivity in cryptophytes than in haptophytes or diatoms due to a smaller photosynthetic cross section (Claustre *et al.*, 1997). A study examining cultured Arctic representatives of these three groups suggest a dependency on temperature; haptophytes only grew faster under higher temperatures (Van de Poll, unpublished data).

Few field-based studies have assessed the relationship between phytoplankton community composition and PP in the Southern Ocean (Uitz *et al.*, 2009; Takao *et al.*, 2012) or the WAP (Claustre *et al.*, 1997; Vernet *et al.*, 2008; Huang *et al.*, 2012). All these studies observed a significant effect of species composition on water column PP. The most extensive study in the coastal WAP observed a positive relation between diatom abundance and water column PP (Vernet *et al.*, 2008). In contrast, a negative relation was observed between cryptophytes and water column PP. Vernet et al. (2008) further estimated that phytoplankton species composition explained 11% of the variability in

primary production. Yet relative phytoplankton species abundances are currently not used when modeling PP at the WAP. Estimates of daily depth-integrated PP over 1995-2006 along the WAP ranged from 250 to 1100 mg C m^{-2} d^{-1}. The coastal regions and Marguerite Bay were most productive, reaching maxima of ~5000-7200 mg C m^{-2} d^{-1} in highly productive years (Ducklow *et al.*, 2012b; Weston *et al.*, 2013; Stukel *et al.*, 2015). A study modeling weekly PP measurements used a simple, but often used, model which fits their data reasonably and leaving room for improvement (Behrenfeld & Falkowski, 1997; Vernet *et al.*, 2012). This model did not take the composition of the phytoplankton or macro nutrient availability into account, parameters previously known to be affected by the observed changes in climate. Investigating these relations will help tuning current global biogeochemistry models, which already incorporated a crude mechanism to describe phytoplankton community composition (e.g. Aumont et al., 2015).

This study aims to understand and model PP in a climatically variable, coastal region of the WAP where large changes in phytoplankton species composition and meltwater dynamics occur. Our main objective is to reassess the relations between PP, phytoplankton biomass and species composition, light, macronutrient concentrations, and water column properties. Thereby, we study if parameters not traditionally used to model PP, such as variability in phytoplankton species composition and macro nutrient concentrations, would need to be included given rapid changes currently unfolding in the WAP and improve current models (Behrenfeld & Falkowski, 1997; Vernet *et al.*, 2012). Most previously used models are appropriate for open ocean applications and not necessarily coastal systems. To this end, we used a non-assumptive model (Random Forest, (Breiman, 2001)) based on *in situ* measurements to discern the contributions of different biological and environmental parameters governing PP. In addition, we seek a minimalistic but optimized model of PP unbiased by our previous understanding of phytoplankton productivity. This optimized model was then used to estimate PP during one austral summer in a region where PP was studied previously to ensure a good validation of our findings with independent studies. Finally, we seek to compare a statistical approach with a more traditional mechanistic method of estimating PP (Platt *et al.*, 1980; Weston *et al.*, 2013).

The basis for our modeling approaches was formed by field measurements collected at the British Antarctic Survey's Rothera Research Station in northern Marguerite Bay. Here, the year-round Rothera Oceanographic and Biological Time Series (RaTS) program, representing the larger northern Marguerite Bay region, provides the infrastructure and scientific context to understand the dynamics in phytoplankton productivity (Venables & Meredith, 2014). Previous studies have shown a variable, yet generally high, level of phytoplankton biomass dominated by diatoms during summers in this region (Annett *et al.*, 2010; Kozlowski *et al.*, 2011; Rozema *et al.*, 2017a). Phytoplankton biomass, both total and per major taxonomic group, was shown to be related to summer water column stability which, in turn, was driven by winter sea ice cover (Venables *et al.*, 2013; Rozema *et al.*, 2017a). Typically, persistence of summer biomass appears to be regulated by wind mixing events, meltwater input and nutrient availability (Piquet *et al.*, 2011; Rozema *et al.*, 2017b). The variability at this coastal site, where PP has occasionally been studied, will allow our models to cover a large variability in environmental conditions and phytoplankton community dynamics. Also, the RaTS allows for sufficient context of our estimates on which we can build and validate our non-traditional modeling approach.

Materials and methods

Site, sample collection and RaTS program

The sampling site was situated in northern Marguerite Bay near Rothera Research Station and is part of the RaTS-program (Fig. 1; 67.570°S 68.225°W). Year-round observations of biological and physical processes at this site (15m depth) started in 1997 (Clarke *et al.*, 2008; Venables *et al.*, 2013; Rozema *et al.*, 2017a). The RaTS site is situated in water ~520m deep and ~2km from the nearest shore. Our extensive summer campaign (Nov 2013-Mar 2014) was run in parallel to the RaTS program. CTD and fluorescence measurements to a maximum depth of ~95m were obtained using a live-feed from the CTD package (SeaBird 19+) equipped with an in-line fluorometer (WS3S, WETLabs), turbidity sensor measuring at 700 nm (ECO NTU, WETLabs) and a spherical sensor (SPQA, LICOR) for Photosynthetically Active Radiation (PAR). Multiple fixed (2, 15 and 75m) and one variable (depth of fluorescence maximum; F_{max}) depths were sampled for pigment analysis by HPLC, macronutrients (N, P and Si) and

maximum quantum yield of photosystem II (PSII). Phytoplankton production through ^{14}C incorporation was measured at F_{max}. Surface oxygen isotopes (om) used in this study were part of the RaTS program supplemented with a small number (n = 7) of samples collected at 2m. Desired sampling frequency during summer was twice per week, and once per week for photosynthetic parameters with ^{14}C incubations (P-E). The fluorescence profiles were calibrated against Chl-a measured by HPLC and collected at 15m and F_{max}. All samples were collected by deploying a 12-24L Niskin bottle with a hand or electric winch on a small boat. After collection, the samples were transported in dark and insulated boxes to the laboratories for further processing. Daily wind speed data from Rothera station was obtained from the British Antarctic Survey (http://www.antarctica.ac.uk/met/metlog/).

PAR and light attenuation

Year-round measurements of PAR were collected every half hour at Rothera station using a fixed sensor (SKP215, Quantum Skye, UK). These measurements were integrated to estimate the daily irradiance dose at the surface (PAR_{daily}, in µmol photons m^{-2} s^{-1}). Attenuation in the water column (K_d in m^{-1}) was derived from linear regression of natural log-transformed, PAR values as measured with the sensor on the CTD (Kirk, 1983). Estimates of K_d were based on the observations between 5 and 50m

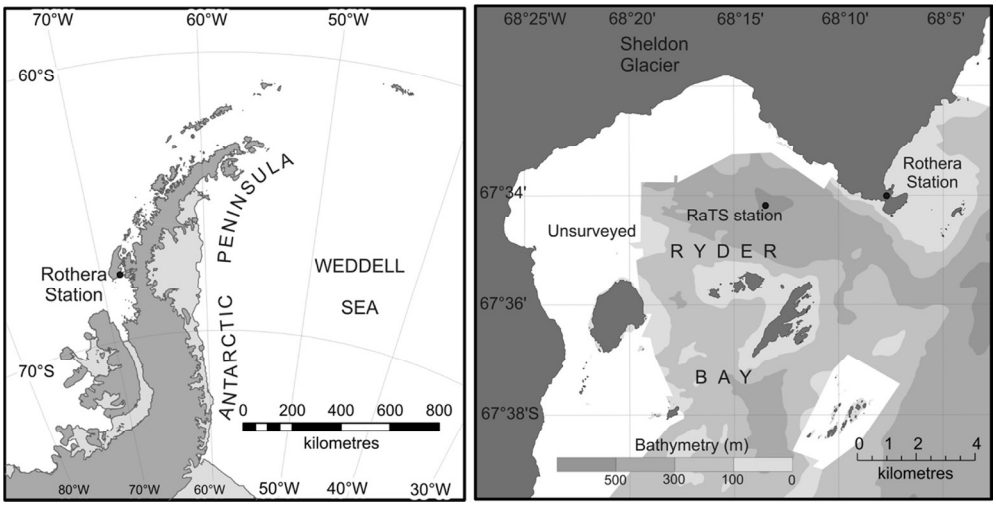

Figure 1: Left: map of the western Antarctic Peninsula, marked with the location of Rothera Research Station on Adelaide Island in northern Marguerite Bay. Right: An expanded view of the immediate vicinity of Rothera, including Ryder Bay where the RaTS long-term monitoring station is situated.

unless PAR was below detection levels at depths shallower than 50m. The first 5m were excluded due to frequent shading by the sampling boat. Also, strong deviations in PAR within the water column during a cast, most likely due to changing cloud cover, resulted in a skewed estimate of K_d. Therefore, these casts were split and K_d was calculated by using the curve which had the majority of measurements. These estimates were linearly interpolated to obtain estimates for K_d on days between CTD casts and subsequently used to obtain daily light dose estimates for every depth for every half hour using (eq. 1):

$$E = PAR_{daily} \cdot e^{-K_d z} \qquad \text{(eq. 1)}$$

where E (µmol quanta m^{-2} s^{-1}) is the daily irradiance dose at depth z (m) (Kirk, 1983).

Water column stability and stable oxygen isotopes

Mixed layer depth (MLD) was defined using the depth at which the Brunt–Väisälä frequency (BVF) was highest, as recommended recently for the WAP (Carvalho *et al.*, 2017). Ocean Data View v4.7.8 was used to calculate the BVF (Schlitzer, 2016). Oxygen isotope samples ($\delta^{18}O$) were analyzed as described in Meredith et al. (2008). We used the $\delta^{18}O$ and salinity data to derive quantitative estimates of the freshwater contributions from sea ice melt and meteoric water, which is possible since freshwater of meteoric origin is isotopically lighter than that originating from sea ice melt. The two sources of meteoric water are precipitation and glacial meltwater (Craig & Gordon, 1965). Simple budget calculations have shown that glacial discharge is the largest contributor to the meteoric water prevalence in the coastal WAP environment, however this glacial melt may be injected over a broader depth range than direct precipitation, which necessarily impacts the ocean directly at the surface (Meredith *et al.*, 2017).

Macronutrients

Nutrient samples were collected as described earlier (Bown et al., 2017) or as described below. A cross comparison of these two different collection methods during the 2012-2013 season did not yield major differences. Subsamples (2x 5 mL) for macronutrient analysis were filtered (prefilter: 0.8 µm, membrane: 0.2 µm, Acrodisc Supor PF, Pall,

US) and stored in the dark at -20°C (nitrate, nitrite, and phosphate) or 4°C (silicate). Analyses for samples collected using both collection methods were conducted using a Technicon TRAACS 800 Auto-analyzer at the Royal Netherlands Institute for Sea Research, The Netherlands (Bown *et al.*, 2017). Nitrite and nitrate were summed and are presented as N_{Tot}.

Phytoplankton pigments

Collection for and measurement of phytoplankton pigments were done using the standard RaTS protocol (Rozema *et al.*, 2017a). In short, phytoplankton cells were collected on GF/F filters (Whatman, US) under low light and at ~2°C using a mild vacuum (<0.2 mbar) generated with a water jet pump. After filtration, the filters were snap frozen in liquid nitrogen and stored at -80°C until analysis. For analysis, samples were freeze dried for 48h prior to extraction in 90% acetone (v/v) at 4°C in the dark for another 48h. The pigments were separated using a Waters 2695 HPLC system equipped with a Zorbax Eclipse XDB-C8 column (3.5 µm particle size) as described by van Heukelem and Thomas (2001) and modified by Perl (2009). Pigments were manually identified using retention times and diode array spectroscopy (type 996, Waters, US) before quantification. Calibration of the system was performed using standards (DHI LAB PRODUCTS, Denmark) for chlorophyll c_3, peridinin, 19'-butanoyloxyfucoxanthin, fucoxanthin, neoxanthin, prasinoxanthin, 19'-hexanoyloxyfucoxanthin, alloxanthin, lutein, chlorophyll b and Chl-a.

CHEMTAX (v1.95) was used to estimate the abundance of various phytoplankton groups (Mackey *et al.*, 1996). This program employs a factor analysis and steepest descent algorithm to find the best fit using initial pigment ratios from previous studies for eight different phytoplankton classes, namely prasinophytes, chlorophytes, dinoflagellates, cryptophytes, two types of haptophytes and two types of diatoms (Appendix Table 1, Wright et al. 2009, 2010; Rozema et al. 2017). Haptophytes were included as two separate groups since *Phaeocystis*, the most abundant haptophyte in our system, has shown great plasticity in cellular pigment ratios with iron and light availability (as reviewed in van Leeuwe et al. (2014). Also, two diatom groups were included to allow for differentiation in chlorophyll c_3 containing diatoms such as

Proboscia spp. and *Pseudonitzschia* spp. and non-c_3 containing species (unpublished data).

A total of 139 samples were divided over 3 bins. We calculated from city-block distances and clustered the samples according to Ward's method as suggested by Latasa et al. (2010) using Past 2.17c (Hammer *et al.*, 2001). This dendrogram suggested binning of the samples collected at 0-7m, 8-49m and 50-75m bins and the smallest bin size was 40. The initial ratios were as used previously with the RaTS data (Appendix Table 1; Bown et al., 2017; Rozema et al., 2017). Neoxanthin and prasinoxanthin were excluded for the 50-75m bin. Further CHEMTAX settings were as described previously (Kozlowski *et al.*, 2011; Rozema *et al.*, 2017a). CHEMTAX was run 60 times using randomized pigment:Chl-a ratios (+- 35% of the initial matrix) to obtain the best possible result per bin (Appendix Table 1; Wright et al., 2009). Both haptophyte and diatom groups as used with CHEMTAX were pooled and renamed to "pooled haptophytes" and "pooled diatoms", respectively.

Estimating phytoplankton biomass

A quenching correction was applied to the upper water column fluorescence, as collected during the CTD casts, to allow for an accurate estimate of the water column biomass. This correction was based on linear regression of Chl-a concentration at 2m and 15m or F_{max} (the sample collected at the shallowest depth was used) as estimated from HPLC analysis. If F_{max} was >>15m (start summer campaign: late November 2013 – Early December 2013) then Chl-a measured at F_{max} and 2m were used. The slopes of these regressions were then used to estimate biomass in relation to the calibrated CTD fluorescence for the top layer. We present the corrected phytoplankton biomass estimates as Chl-a_{corr}. Additionally, standing phytoplankton stocks were calculated by integrating the first 80m of the water column using Chl-a_{corr}. The depth of 80m was chosen as this is generally in the layer of winter water, near the deepest sample for HPLC (75m) and light does not penetrate this deep during summer (Clarke *et al.*, 2008).

Maximum quantum yield of PSII

Triplicate measurements of maximal quantum yield of PSII (F_v/F_m) using a WATER-FT PAM (Walz, Germany) in dark-adapted subsamples (40 mL) allowed for the assessment of the photophysiological state of the phytoplankton community (reviewed in Maxwell and Johnson 2000). F_v/F_m values <0.5 are generally indicative of exposure to stress due to e.g. exposure to excess PAR and/or ultraviolet radiation or nutrient limitation.

Dissolved inorganic carbon

Dissolved Inorganic Carbon (DIC) concentrations were used in the calculation of primary production from ^{14}C measurements. Samples for the analysis of DIC were collected on eight sampling days (January 15, 25, 30, February 3, 10, 17, 25 and March 3, 2014) in borosilicate glass bottles and analyzed within 20h of sampling as presented in Jones et al. (2017). DIC concentrations were determined by coulometric analysis according Johnson et al. (1987) and Dickson et al. (2007) using a VINDTA 3C instrument (Versatile INstrument for the Determination of Total Alkalinity, Marianda, Germany). A power function was used to described the relationship between DIC and HPLC derived chlorophyll *a* concentrations (R^2 = 0.94, p <0.001) to estimate DIC concentrations for the calculation of primary production on missing sampling days.

Photosynthesis-Irradiance measurements

Water collected at the depth of F_{max} was used to estimate phytoplankton productivity. PP was estimated by constructing P-E curves (n = 16) based on a modified protocol from Lewis and Smith (1983). Seawater subsamples (20 mL) were incubated in a photosynthetron for 4h under 21 different light intensities (8 – 713 µmol quanta m^{-2} s^{-1}; Osram Powerball HCl-TT 250W in a Jolly symmetrical armature) at *in situ* (+-0.5°C) temperature after the addition of 0.37 MBq ^{14}C-bicarbonate (PerkinElmer, The Netherlands; >1.7 TBq $mmol^{-1}$) in clear 60 mL polyethylene terephthalate (PET) bottles (Qorpak, US). After incubation, the samples were filtered onto polycarbonate membrane filters (Millipore, US; 25 mm, 0.4 µm pore size) using a gentile vacuum (<0.1 bar) on a filtration carousel (Millipore, US). After filtration, the filters were acidified with fuming HCl for ~20 min to vent off unincorporated ^{14}C-bicarbonate. Filters were placed into 20 mL PET scintillation vials (Wheaton, US) and supplemented with 10 mL

scintillation cocktail (Ultima Gold, PerkinElmer, The Netherlands). For time zero activity, triplicate samples were prepared, filtered over polycarbonate membrane filters and immediately acidified. For total activity, 10 µL Ethanolamine was added to 100 µL ^{14}C spiked subsamples in triplicate in 20 mL PET scintillation vials containing a clean polycarbonate membrane filter. Time zero activity and total activity were then treated identically to the other samples. All samples were vortexed and left for two days to ensure maximum dispersal of activity throughout the scintillation cocktail before counting activity on a Tri-Carb 2900TR (Packard Instrument Company, US).

The data were converted to DPM after correction for time zero activity (Nielsen, 1952), and normalized to Chl-a, as derived from the HPLC analyses, and DIC (see above), and corrected for metabolic discrimination (5%) between ^{12}C and ^{14}C (Nielsen & Bresta, 1984). These data were fitted by least-squares nonlinear regression using the model (eq. 2) of Platt et al. (1980), modified by MacIntyre and Cullen (2005):

$$P = P_s\left(1 - e^{-\alpha\left(\frac{E}{P_s}\right)}\right)\left(e^{-\beta\left(\frac{E}{P_s}\right)}\right) + P_0 \qquad \text{(eq. 2)}$$

where P (µg C µg Chl-a^{-1} h^{-1}) is the carbon fixation rate at irradiance E, P_s (µg C µg Chl-a^{-1} h^{-1}) the light-saturated maximum of carbon fixation in the absence of photoinhibition, α (µg C µg Chl-a^{-1} h^{-1} [µmol quanta m^{-2} s^{-1}]$^{-1}$) the initial slope of the P-E curve, β (µg C µg Chl-a^{-1} h^{-1} [µmol quanta m^{-2} s^{-1}]$^{-1}$) is a measure for photoinhibition, and P_o (µg C µg Chl-a^{-1} h^{-1}) is the carbon uptake or release without any irradiance. These parameters were considered characteristic for the phytoplankton throughout the water column at the day of collection.

Constructing and evaluate models

Two different methods of calculating phytoplankton carbon uptake were employed. The classical, mechanistic approach relies on the estimations of the P-E parameters, biomass estimates and total irradiance for days without P-E incubations (MPlatt; Platt et al., 1980). These estimates were obtained as discussed below and run through M_{platt} for every 1m. Our second statistical approach method uses Random Forest (RF) regressions. RF is a machine learning method which constructs a large number of

regression trees by randomly taking subsets of the data and input variables (Breiman, 2001). The major benefits of using such a tool over more traditional (mostly linear) models are: Regression trees allow for (1) non-linear relationships between input and output variables, (2) non-additive interactions between predictor and response variables and (3) correlations between different input variables (Breiman, 2001; Shi & Horvath, 2006). The relevant variables included were phytoplankton biomass, macronutrients, MLD, temperature, salinity, total irradiance and the relative abundance of the three most important phytoplankton groups, namely diatoms, haptophytes and cryptophytes (Behrenfeld & Falkowski, 1997; Arrigo *et al.*, 1999; Dierssen & Smith, 2000; Vernet *et al.*, 2012, 2008; Montes-Hugo *et al.*, 2009; Piquet *et al.*, 2011; Venables *et al.*, 2013; Williams *et al.*, 2016; Bown *et al.*, 2017; Rozema *et al.*, 2017a, 2017b).

For the RF approach, we modeled the log of the PP estimates from the 16 P-E experiments (see above) using the depths for which all the aforementioned variables were available (n = 62). We constructed a model in which all the parameters (M_{RFmax}) were included and one reduced, optimized model (M_{RFmin}). During the construction we grew 2000 trees, and four (M_{RFmax}) or two (M_{RFmin}) variables were used at every split. Variables least important in M_{RFmax} were removed individually until the fit of the new model no longer improved and this became M_{RFmin}. Partial dependence plots were generated for each variable per model to understand to the relationship with PP. These plots have the input parameter on the horizontal axis and give the range of impact of the input variable on PP. We discussed the importance of each variable to the models above but here we used the shape (and direction) of the curve to understand how this parameter influenced PP in our RF models. Partial dependence plots show the effect of the predictor on the response variable after accounting for the average effects of the other predictors. Therefore, it is the trend, not the actual values, that describes the dependence between both variables.

To assess the predictive power of both RF models, the data were split randomly into a training (80%) and test set (20%). This was repeated 10 times resulting in slightly different models of each type (M_{RFmax} and M_{RFmin}). These 10 slightly different models were subsequently tested against the randomly generated test sets using linear

regression. We included the mean *p* and R^2 values of these assessments. The "randomForest" package in R (v3.3.1) was used to build our models (Liaw & Wiener, 2002; R Core Team, 2016).

Constructing input matrices and estimating phytoplankton productivity

After the construction of the minimal RF model, we aimed to calculate the PP in the water column (0-80m) over the full course of the season using M_{platt} and M_{RFmin}. For this, we needed to obtain full matrices for all parameters used in the models. We used anisotropic ordinary kriging to interpolate both in depth and time using the "gstat" package in R (Pebesma, 2004). First, we optimized the kriging function to best fit the autocorrelation per variable for the depth component using variograms. This function was then used for the interpolation through time. We chose a weighing factor of 0.3 for the time component to allow for the required sensibility needed during short, sudden events such as wind mixing. The matrix for PAR data was constructed as described above. Values for α, β, P_o and P_s were linearly interpolated from days with P-E incubations. Thus identical biomass and PAR estimates were used for all modeling approaches.

PP was calculated for every half hour, due to the resolution of the light measurements, and every depth (0-80m) using M_{platt} and M_{RFmin}. The values were summed to obtain daily values. We chose to use a resolution of half an hour as light was highly variable throughout the day and our model included the potential for photoinhibition. Secondly, our RF model included the aforementioned parameters and was run using the constructed matrices. For light in M_{RFmin} used the summed daily irradiance for all depths. We summed all data for December, January and February as this is traditionally the most productive period and define this as the summer productivity estimates.

Results

Light

PAR availability in the water column was higher during spring (November) than during summer (Fig. 2a). Also, PAR in the water column was lowest from December 15th to December 21th. This was related to high turbidity, increasing K_d to >0.30 m^{-1} as

well as low surface irradiance dose (December 23rd and 24th; Fig. 2b, c). In contrast, surface irradiance dose peaked at the end of December before gradually decreasing. A brief and sharp increase of PAR at 15m occurred on January 15th when K_d was low. Not until February 14th had PAR penetrated >50 µmol quanta m^{-2} s^{-1} beyond 15m again and thereafter remained above this level (Fig. 2a). The dynamics in K_d strongly coincided with standing phytoplankton biomass. The only major exception was after the short break (December 23rd and 24th) in our sampling effort due to hindrance of drifting sea ice sheets. During these casts, K_d was far higher (>0.30 m^{-1}) than observed at other times in our campaign.

Water column physics

Our field campaign started (November 26th) during a period where SSTs started to increase slightly while MLD and surface salinity decreased (Spring, Fig. 3a, b and 4a). Above zero surface temperatures first occurred on and persisted onwards from December 6th (start of period 1). The MLD during the first half of December was shallow (1m) while salinity kept decreasing. After a brief period of elevated wind speed and a deepening of the MLD (December 23rd), the water column surface salinity restabilized while the SST increased further (Fig. 3a, b and 4a). Maximum SST at 1m during this summer was 2.7°C on January 6th and 11th. The period of high SSTs was interrupted by an increase of wind speed and deepening of the MLD in mid-January ending period 1 and homogenizing water column temperature and salinity (Fig. 4a). This increase in MLD was of a short duration as the water column restabilized within a week. Thereafter, surface temperature increased again with positive temperatures up to a depth of ~30m and a stable surface salinity (~32.6). These conditions lasted until mid-February when strong winds occurred more frequently, salinity started to increase and SST decreased which resulted in the end of period 2. As in spring, the water column temperature dropped and stayed below 0ºC and was more homogenous throughout the water column after February 10th, labeled as period 3.

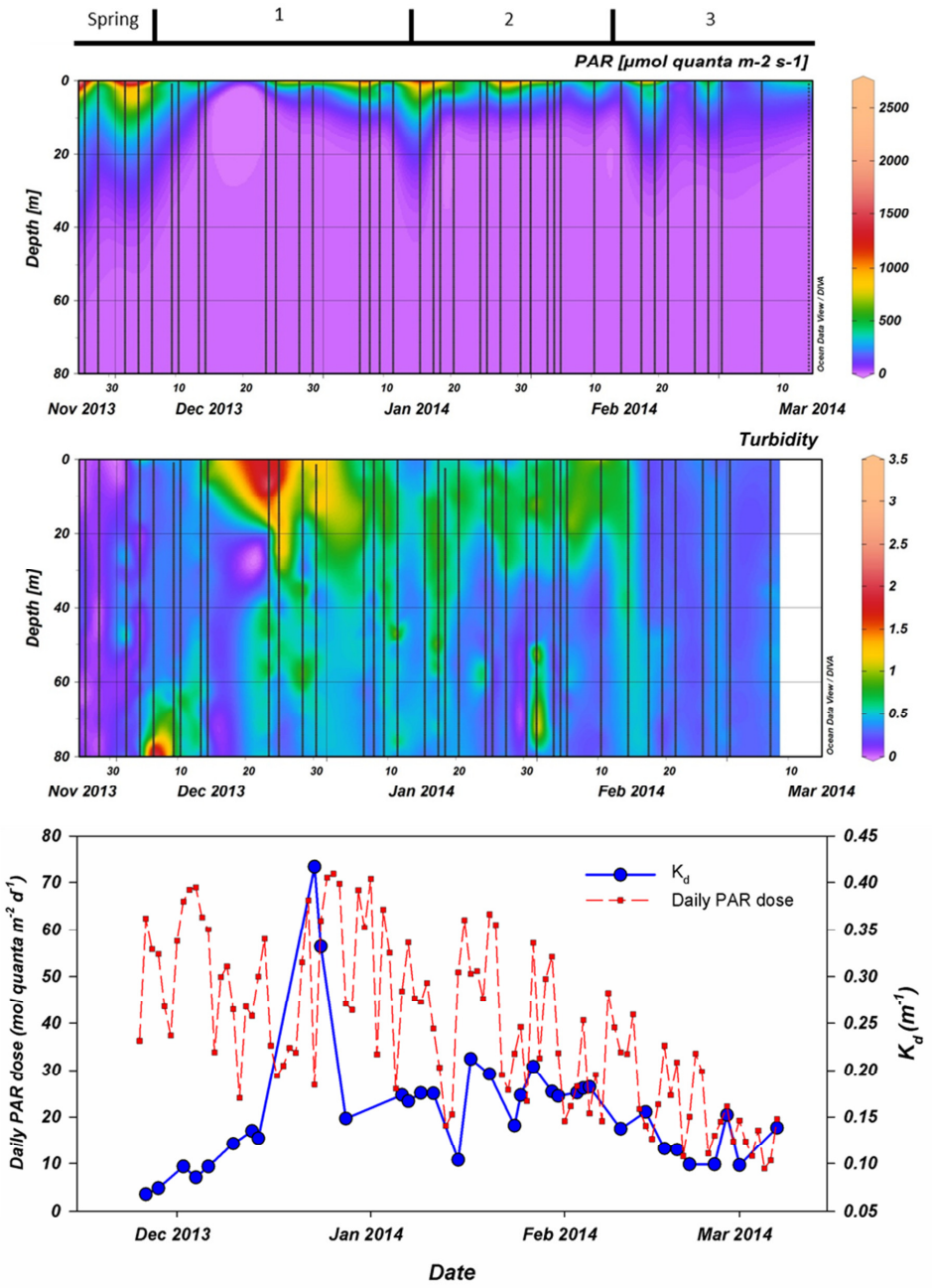

Figure 2: Top: Photosynthetically active radiation (PAR) as measured during CTD casts (vertical casts). Middle: Turbidity as also measured during the CTD casts. Bottom: First, the extinction coefficient (K_d in blue) as calculated using the PAR data collected by CTD. Also, the daily irradiance dose for PAR (red) integrated from continuous measurement at Rothera station. All data were collected during the 2013-2014 season. Period 1 starts on December 6th, period 2 on January 15th and period 3 on February 10th.

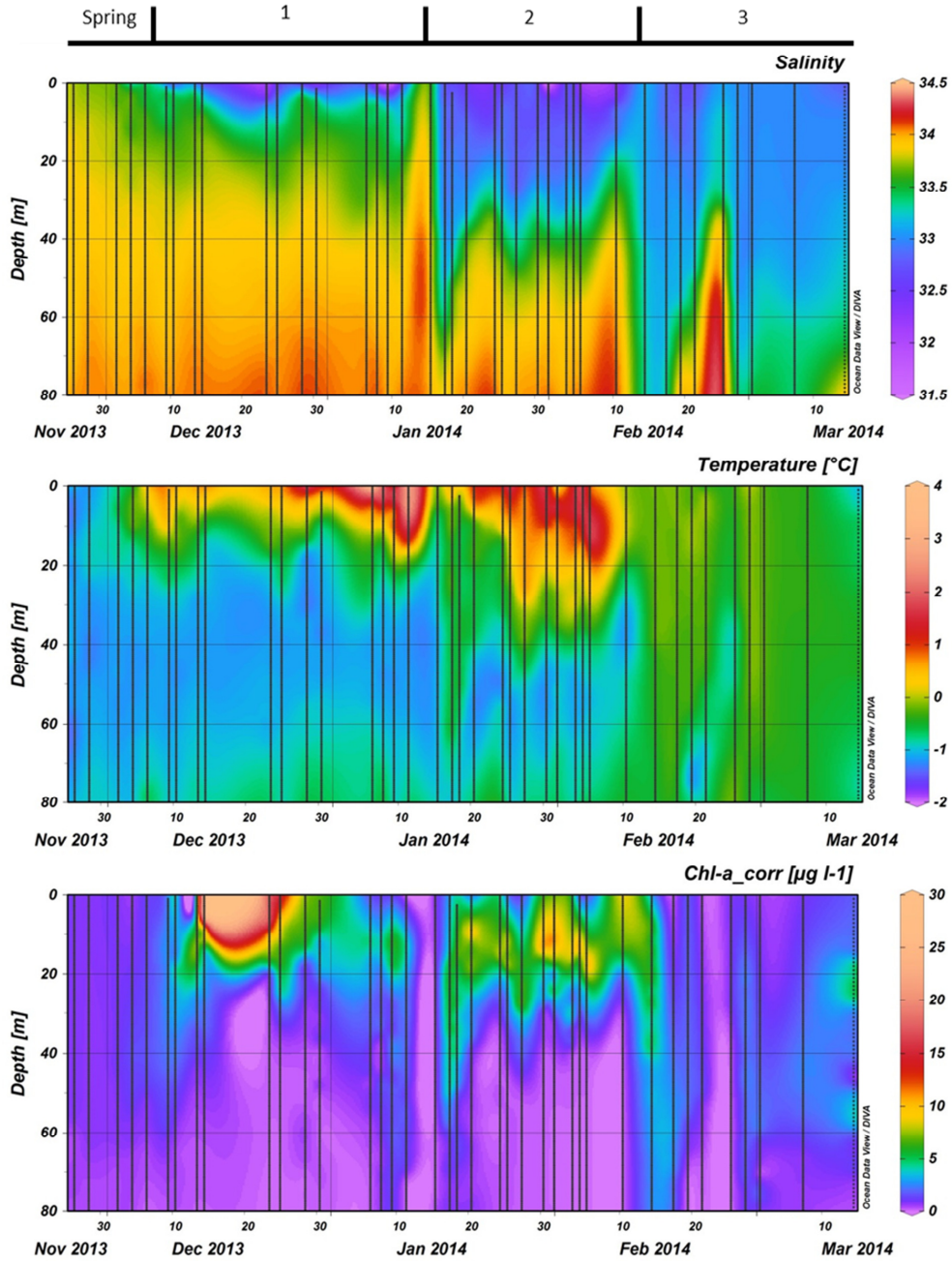

Figure 3: Top: Salinity, middle: Temperature, and bottom: Phytoplankton biomass as measured by fluorescence during the vertical CTD casts. Phytoplankton biomass fluorescence was calibrated against chlorophyll a measurements with HPLC and corrected for quenching in top layer using the chlorophyll estimates. All data were collected during the 2013-2014 season at the RaTS site. Period 1 starts on December 6th, period 2 on January 15th and period 3 on February 10th.

Freshwater origin

Sea ice retreat from the preceding winter was late and the contribution of sea ice meltwater to the water column during summer was, although modest at all times, the highest (2.8%) recorded in the RaTS program (Appendix Fig. 4b; Legge *et al.*, 2017; Meredith *et al.*, 2017). Oxygen isotope data from the surface and at 2m depth showed an influx of sea ice melt after December 13th, continuing to at least the end of February. The contribution of glacial melt was higher than sea ice melt (mean 4.4%), but also more variable. After an initial increase, freshwater of meteoric origin peaked at 8.3% (also a record for the RaTS program) before dropping to just 3.1% on January 15th as an increase in wind speed mixed the water column (Fig. 4a). Both freshwater components increased rapidly after the period of MLD deepening, after which the meteoric freshwater contribution at 2m depth remained relatively stable at ~4% while the contribution of sea ice melt slowly decreased towards the end of summer.

Macronutrients

Macronutrient concentrations at the end of spring were high with water column averages of 29.0, 1.8, and 83.5 µM for N_{Tot}, phosphate, and silicate, respectively (Fig. 5). These values were characteristic of the Antarctic winter water, as concentrations at 75m were only slightly higher. During period 1, the vertical distribution of the macronutrients strongly followed the patterns observed in SSTs. Nutrient concentrations were generally lowest at the surface (2m). Nutrient concentrations in the first ~15m strongly decreased over a 10-day period after December 13th. On December 23, all macronutrients were virtually depleted with only 0.01 µM phosphate, 0.06 µM N_{Tot}, and 0.70 µM silicate left at 2m depth. This period of depletion lasted until the end of period 1, when nutrients throughout the water column were mixed, restoring 2m values to the levels similar to those observed before December 13th. Low nutrient concentrations were observed in period 2 with minimum values at 2m depth on February 5th (13.6 µM silicate, 0.07 µM nitrate and no detectable nitrite or phosphate). This depletion of nutrients persisted to a depth of ~20m. Period 3 was characterized by a gradual increase in surface nutrient levels.

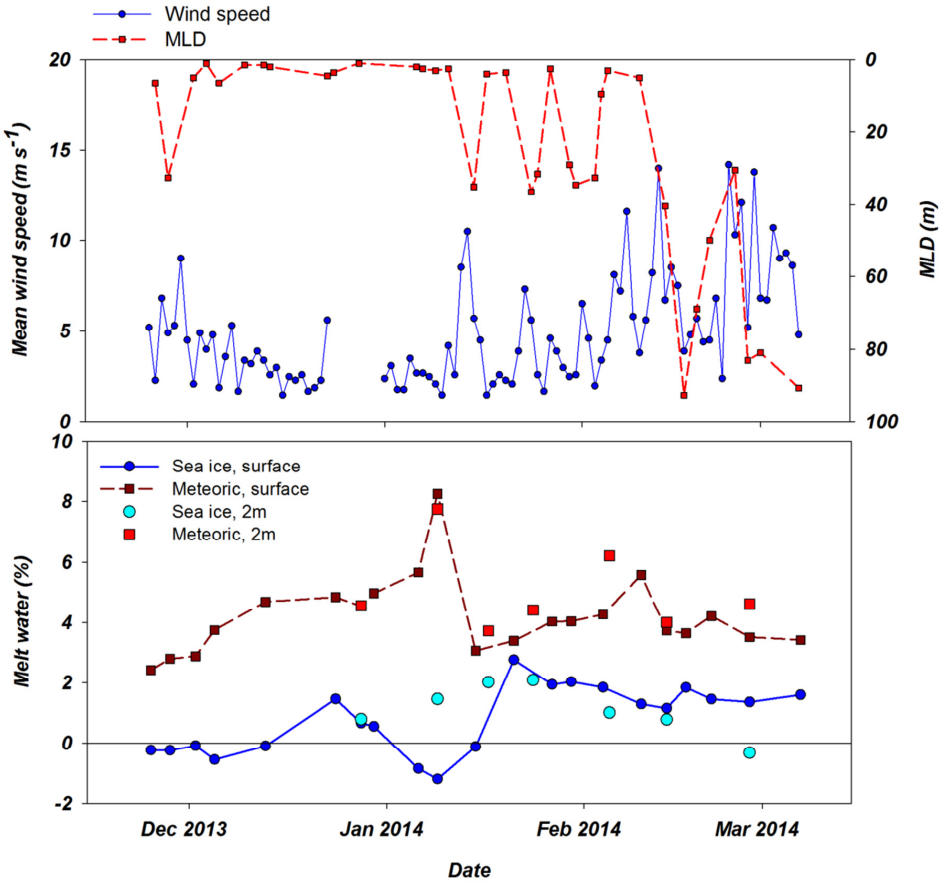

Figure 4: Top: Daily average wind speed (blue) and mixed layer depth (MLD) calculated using the depth of the maximum Brunt–Väisälä frequency. Bottom: Different fractions of meltwater with different origins. Firstly, samples collected at the surface as part of the RaTS program are divided into the fraction of meteoric origin (dark red) and sea ice origin (dark blue). Additionally, a number of samples collected at the same site, but at 2m depth also show the two fractions (light red and blue, respectively) and illustrates the effect of very shallow meltwater lenses. All data were collected during the 2013-2014 season. Period 1 starts on December 6th, period 2 on January 15th and period 3 on February 10th.

Phytoplankton biomass and species composition

Phytoplankton biomass accumulated during period 1 (Fig. 3c). Relative abundances of diatoms increased at the cost of haptophytes during the start of this period (Fig. 6). A sudden increase in phytoplankton biomass (up to 26 µg Chl-a l^{-1}), mainly consisting of small diatoms (Buma et al. unpublished microscopy data; Fig. 6 and Appendix Fig. 1), coincided with the occurrence of sheets of sea ice in the bay on December 14th. This biomass peak lasted until December 28th after which values dropped to ~5 µg Chl-a l^{-1}.

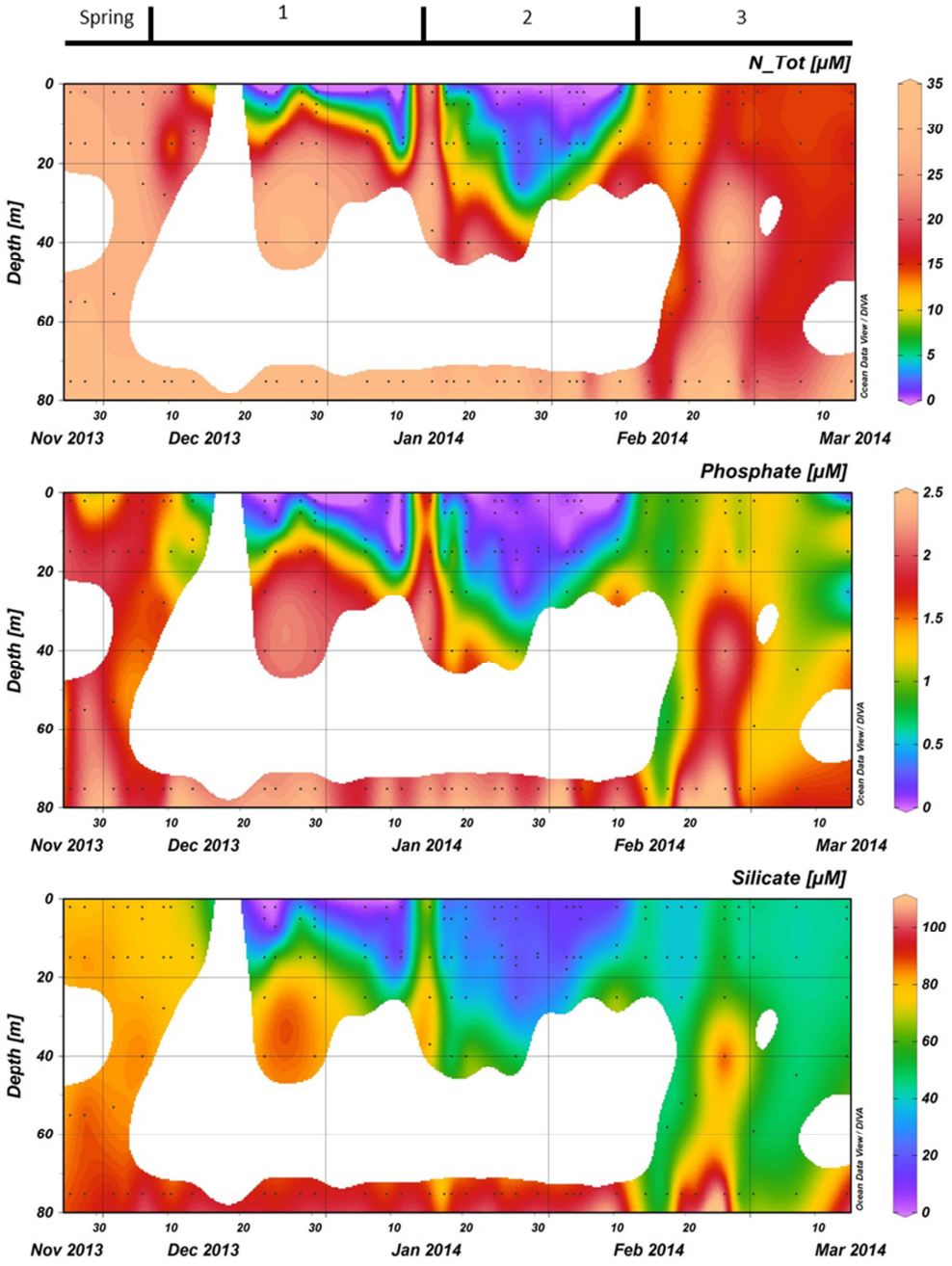

Figure 5: Top: Total nitrogen (nitrate + nitrite), middle: Phosphate, and bottom: Silicate concentrations in the water column at the RaTS site. Black dots illustrate the sampling depths. Period 1 starts on December 6th, period 2 on January 15th and period 3 on February 10th.

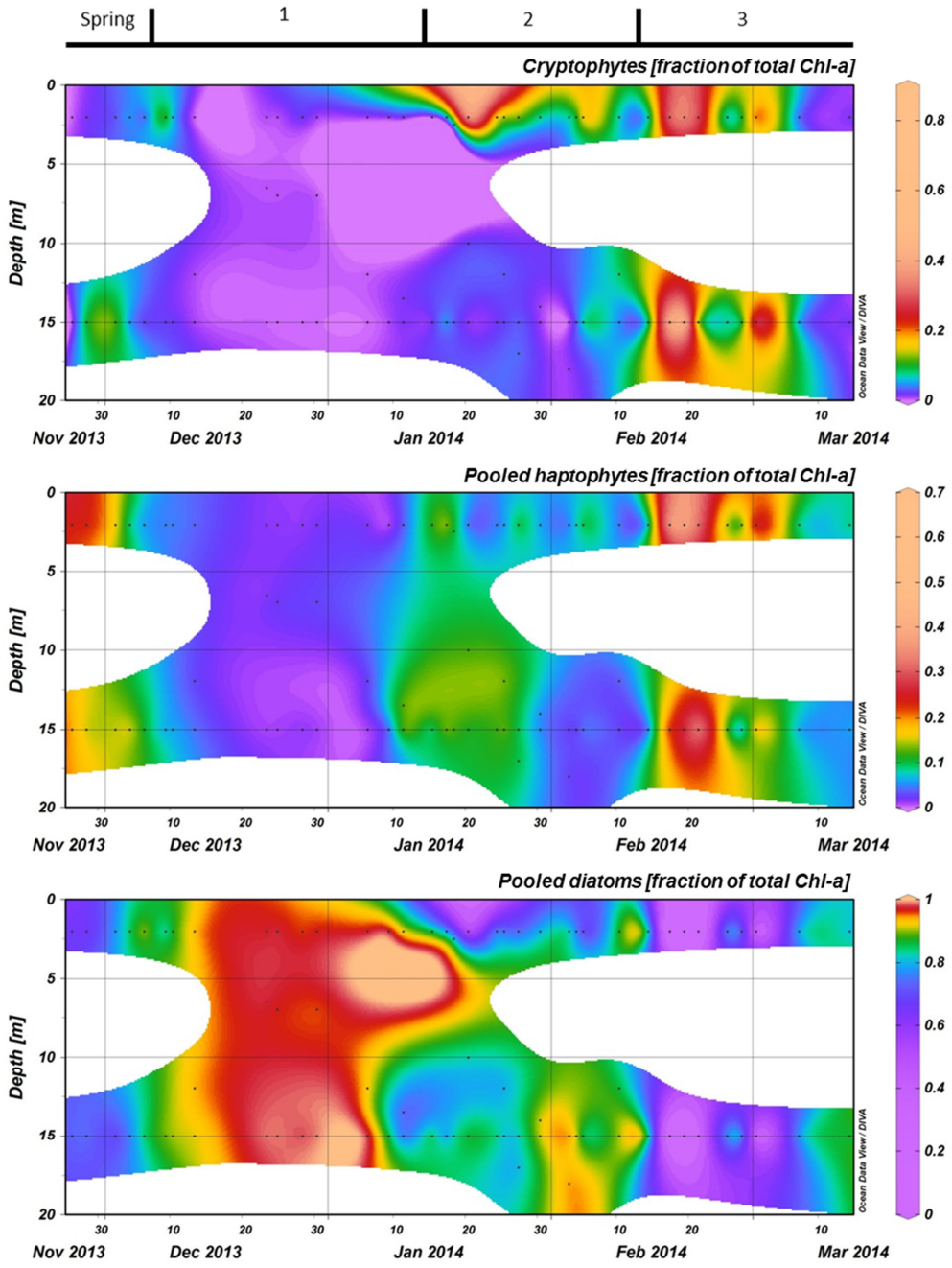

Figure 6: The relative abundances of the three most important phytoplankton groups, as calculated with CHEMTAX using HPLC measurements of pigments, are shown for the top 20 meters at the RaTS site. Top: Pooled diatoms, middle: Pooled haptophytes, and bottom: Cryptophytes. Black dots illustrate the sampling depths.

Integrated phytoplankton stocks (0-80m) followed a similar trend: a large increase between December 10th and 14th, and a steady decrease thereafter (Fig. 7). Moreover, F_v/F_m in the top 10m during the short, yet sharp increase in biomass was lower than expected for the *in situ* light intensities when compared to the rest of the summer (p < 0.001; appendix Fig. 2). After the biomass peak, phytoplankton stocks remained stable until the end of period 1. During period 2, diatoms remained the most important taxonomic group although cryptophyte proportions increased (max. 40%) in the surface layer (2m; Fig. 4a and 6). Also, haptophytes increased at 15m (~15%) until January 30th. Phytoplankton biomass was more evenly distributed over the first 30m during this period, reaching a maximum concentration of 11 µg Chl-a l^{-1} and suggested three short periods where biomass increased and decreased (Fig. 7). The first was associated with the increase in haptophytes at 15m, the second and third with diatoms. In period 3, relative abundances of haptophytes and cryptophytes were both elevated in comparison to the previous periods (max. 38 and 47%, respectively) and both phytoplankton groups co-occurred in the first 15m (Table 2). Diatoms were more abundant at the deep fluorescence maxima. Phytoplankton biomass at 75m was low and only increased during the two occasions where strong winds caused a deepening of the MLD. Relative group abundance matched those observed in the surface, albeit with a delay of ~30 days (Appendix Fig. 1).

P-E measurements

Variability in photosynthetic parameters as obtained from the P-E experiments (n = 16) changed over the course of the summer. At the end of spring (November-early December), α, P_s and P_o were low in comparison to the summer values (Table 1). At the end of December, both α and P_s increased >50%. P_s appeared to reach an average of ~4 µg C µg Chl-a^{-1} h^{-1} for the rest of the summer (January – March) while P_o increased further to 0.68 - 0.85 C µg Chl-a^{-1} h^{-1}. The α also increased further to 0.068 - 0.083 µg C µg Chl-a^{-1} h^{-1} [µmol quanta m^{-2} s^{-1}]$^{-1}$. In contrast, β was very low and only increased to a maximum average of 0.004 µg C µg Chl-a^{-1} h^{-1} [µmol quanta m^{-2} s^{-1}]$^{-1}$, suggesting that photoinhibition was of minor importance.

Using these P-E parameters, we calculated integrated PP for the water column on the days of the experiments (Fig. 7). These values ranged from 92.5 (end of November) to

*Table 1: Shown below are the mean values (±standard deviation) for photosynthetic parameters P_s and P_o (both in µg C µg Chl-a^{-1} h^{-1}), and α and β (both in µg C µg Chl-a^{-1} h^{-1} [µmol quanta m^{-2} s^{-1}]$^{-1}$) as calculated from the ^{14}C experiments at F_{max}. Also presented are Chl-a (µg l^{-1}) as a proxy for phytoplankton biomass and DIC_{calc} (µmol kg^{-1}) during these experiments. The values below are averages of n experiments conducted between Nov 2013 and Mar 2014. Only 1 experiment was run at the end of November and was pooled with the early December values (up to the 9th and indicated by *). The values for December 24 or later are therefore shown separately (as indicated by #). We did not use these averages for our calculations but the measurements per time point.*

	n	Chl-a	DIC_{calc}	P_s	P_o	α	β
Nov-Dec*	3	1.1±0.9	1.1±0.9	1.347±1.177	0.486±0.438	0.040±0.027	0.000±0.000
Dec#	3	12.6±4.8	12.6±4.8	3.803±3.409	0.569±0.501	0.059±0.047	0.002±0.003
Jan	4	4.6±2.9	4.6±2.9	3.521±0.589	0.797±0.435	0.080±0.030	0.002±0.002
Feb	4	4.1±2.4	4.1±2.4	4.228±1.174	0.633±0.592	0.068±0.040	0.004±0.004
Mar	2	2.80±0.3	2.80±0.3	3.950±0.191	0.847±0.454	0.082±0.026	0.001±0.002

*Table 2: Spearman rank order correlations where log PP estimates (n = 42) for the depths for which pigment samples were collected (with PP > 0) were correlated to the calculated relative abundance of the major phytoplankton groups as calculated with CHEMTAX. The used PP estimates were from the days on which a photosynthesis vs. irradiance experiment was conducted. Significant correlations are indicated by an *.*

	Log PP	**Rel. cryptophytes**	**Rel. haptophytes**	**Rel. diatoms**
Log PP	-			
Rel. cryptophytes	-0.15	-		
Rel. haptophytes	-0.65*	0.57*	-	
Rel. diatoms	0.57*	-0.70*	-0.93*	-

6907.7 (end of December) mg C m^{-2} d^{-1}. While the PP estimates from these experiments showed an increasing trend over the entire month of December, PP on December 23rd was substantially lower. The peak value of 6907.7 mg C m^{-2} d^{-1} occurred on December 30th after which PP decreased reaching a minimum of 438.2 mg C m^{-2} d^{-1} on January 15th. PP during period 2 increased again to a maximum of 3109.5 mg C m^{-2} d^{-1} and lasted until mid-February before stabilizing around 680 mg C m^{-2} d^{-1} during period 3.

Testing importance of species composition

To estimate the potential influence of phytoplankton species composition on PP we compared the log PP at discrete depths where we collected supplementary data (if PP > 0, n = 42) against the relative abundances of the three major phytoplankton groups (Table 2). It appeared that while PP and both diatoms and haptophytes approached a monotonic relation, cryptophytes and PP did not. Linear regressions for these three comparisons yielded r^2 values of 0.01, 0.27 and 0.14 ($p < 0.001$) for cryptophytes, haptophytes and diatoms, respectively. Thus, we opted for spearman rank order analyses, which are less sensitive for non-linear trends (Table 2). We observed a negative relation between PP and haptophytes whereas a larger diatom fraction resulted in higher PP ($p < 0.001$). However, the relation between cryptophytes and PP was no longer significant ($p = 0.36$). The opposing trends between haptophytes and diatoms versus PP were supported by correlations between the phytoplankton groups (Table 2). Haptophytes and cryptophytes were positively related to each other while both were negatively related to diatom abundance ($p < 0.001$).

Creating RF models

Using M_{RFmax} with all the parameters included ($p < 0.001$, $R^2 = 0.91$), we quantified the contribution of the different input parameters on PP using a variable importance plot (Fig. 8). Of these parameters, daily PAR was the most important, increasing the mean square error (MSE) by 50.4%. The other two large components were phytoplankton biomass (26.7%) and water temperature (21.6%). The three macronutrients (N_{Tot}, phosphate and silicate) showed a smaller importance (20.4 to 17.3%). Salinity (15.5%), MLD (13.6%) and the relative contributions of the major phytoplankton species (7.3 to 12.2%) influenced the MSE to a lesser extent. The contribution of some of the 12 included parameters was limited, possibly because some of the variability was already explained by a correlated and more important parameter. Therefore, we reduced our first model (M_{RFmax}) to obtain a more minimalistic model (M_{RFmin}) with only three parameters that explain 93% of the variability: daily irradiance dose throughout the water column, phytoplankton biomass and N_{Tot} (Fig. 8). The second-best option explained only slightly less of the MSE and included seawater temperature instead of N_{Tot}. The inclusion of either seawater temperature or N_{Tot} resulted in highly similar

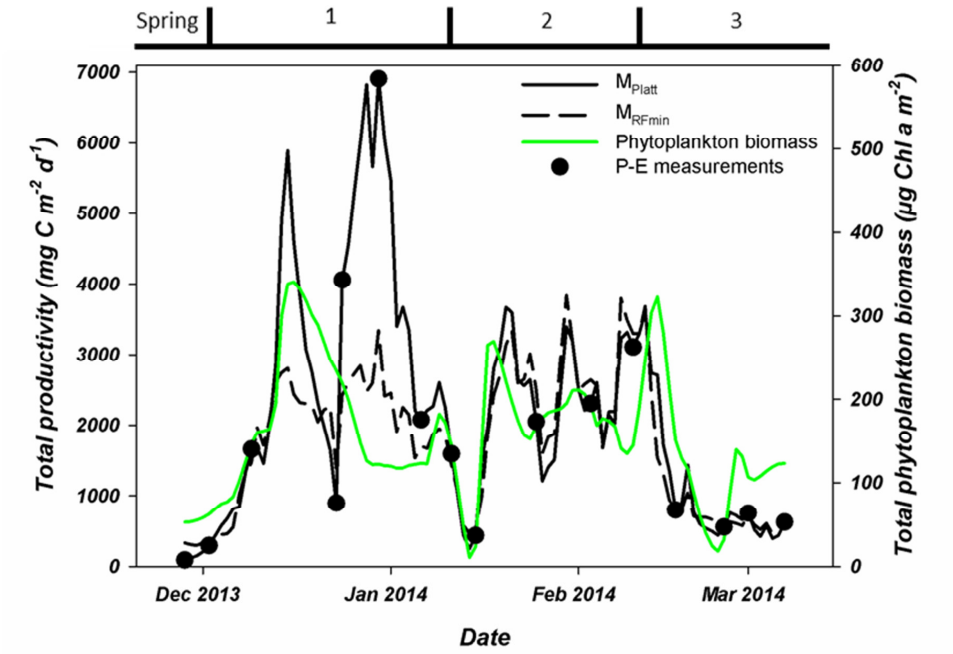

Figure 7: Total, water column integrated primary production as measured during P-E experiments (black dots) or estimated using two modeling approaches. These estimates are based on Platt et al. (1980; solid black line) or the minimal random forest model constructed in this study (dashed black line). Also shown is the water column integrated phytoplankton biomass. All integrations were to a depth of 80 meters. Period 1 starts on December 6th, period 2 on January 15th and period 3 on February 10th.

minimal models. A linear correlation analysis on all the samples in which N_{Tot} was measured (excluding 75m samples) revealed a strong relation between the two parameters ($p < 0.001$, $r^2 = 0.67$).

Partial response of variables

After the construction of our models, we analyzed how each of these parameters influenced PP at the depths where all auxiliary data (generally 2, 15, 75m, and F_{max}) were available using partial dependence plots (Fig. 9). The partial dependence plots for the two different models were highly similar and thus we present M_{RFmax} as it includes all variables, those for M_{RFmin} are included in the supporting information (Appendix Fig. 3). Light was the most important factor in both models, the partial dependence plot suggests that when light is not available, PP is strongly decreased. Also, when light is above a certain threshold (~3 mol quanta m^{-2} d^{-1}), its effect on PP remains

unchanged. Phytoplankton biomass showed a similar trend. PP did not increase further above ~7 µg Chl-a l^{-1}, although the support of this plateau is limited given that it is based on only 10-20% of the data. The three macronutrients had similar trends in relation to PP: the lower the concentration, the higher the PP until it reaches a plateau. Silicate and N_{Tot} dynamics suggest two distinct plateaux in its relation to PP, coinciding with the concentrations in the two different bloom periods (before and after January 15th). Seawater temperature showed a strong bimodal effect where 0°C was pivotal, likely related to the freeze of thaw cycle of glacial and sea ice. In contrast, a decreasing salinity and MLD coincided with a gradual increase in PP. Finally, the contribution of relative species abundances show a strong positive effect on the

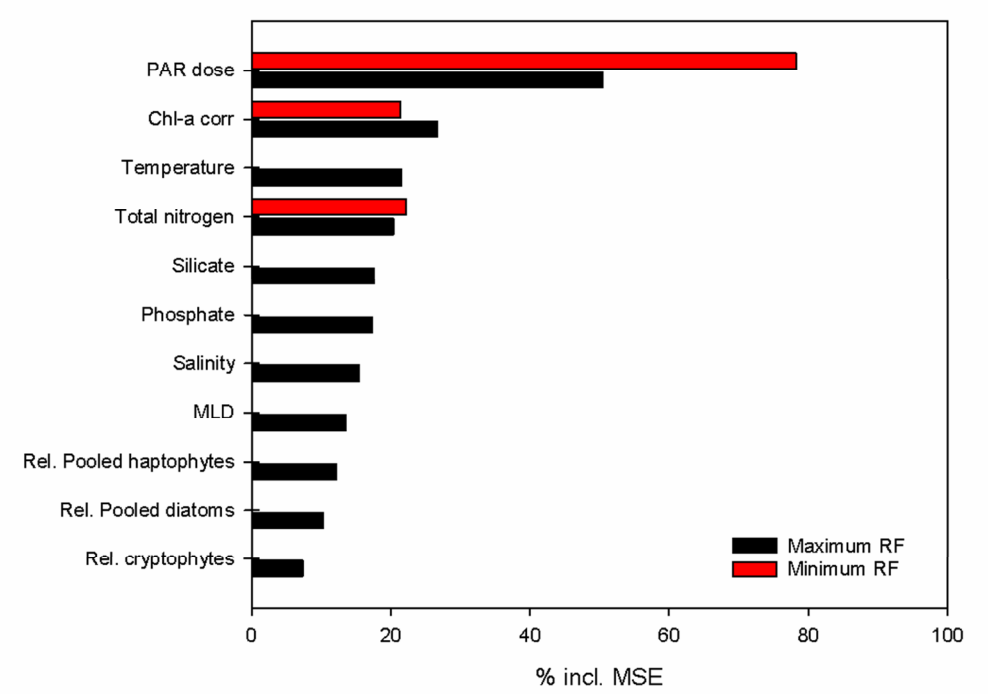

Figure 8: Variable importance plot for the two random forest models build to estimate PP throughout the water column: RF_{max} (black) and RF_{min} (red). The x-axis shows the percentage of reductions in mean square error (MSE) per variable. All variables were included in the maximum model; daily PAR dose in the water column, phytoplankton biomass (chlorophyll a corrected for quenching), temperature, total nitrogen, silicate, phosphate, salinity, mixed layer depth (MLD based on maximum Brunt–Väisälä frequency) and relative abundance of the three most abundant phytoplankton groups. The minimum model excluded variables until a model was reached with the highest possible fit. The importance of the three remaining variables in this model is shown in red.

presence of diatoms as the effect on PP is strongly reduced below ~93% diatoms. Roughly 70% of our data have decreased diatoms abundances suggesting a strong support for this observation. As such, increasing fractions of cryptophytes and/or haptophytes are associated with decreased PP.

Estimating summer PP

PP over the full course of the summer season was estimated using two different approaches, the traditional M_{Platt} and our best RF model, M_{RFmin} (Fig. 7 and 10). Dynamics of both PP estimates were very similar (Fig. 10), and both methods produced near identical values for the period after January 15th (periods 2 and 3). While the patterns in PP for December and early January (period 1) were similar, the magnitude of PP differed greatly (Fig. 10). At most, PP estimated in December was a factor 2.5 higher using M_{Platt} than when calculated using M_{RFmin}. On average, M_{Platt} was 40% higher during the first month of the summer reaching a maximum of 6908 mg C m^{-2} d^{-1} on December 31st (Fig. 7). PP in December peaked twice in both models, namely on December 15th and 31st. After January 15th, three steep increases in PP occurred on January 21st, 30th and February 8th-12th. The maxima of these periods were of the same magnitude at those calculated for December with the M_{RFmin} model. In contrast, using M_{Platt} PP in January and February was only half of the values observed in December. A second noteworthy difference between the two methods of estimation is to which depth PP occurs (Fig. 10). However, these differences contribute little to the summed PP (Fig. 10). Total summer PP (Dec-Feb) was estimated to be 214.4 g C m^{-2} using M_{Platt} and 176.1 g C m^{-2} using M_{RFmin}, or 2.68 and 1.96 g C m^{-2} d^{-1}, respectively.

Discussion

In the present study we measured PP at a coastal monitoring site over one full summer and modeled PP using two approaches (mechanistic and statistical), resulting in three different models (M_{Platt}, M_{RFmax}, and M_{RFmin}). Firstly, we briefly describe how our field site and the summer season dynamics were representative of the wider WAP region and conditions, both past, present and future. Then, we evaluate the M_{RFmax} model to find relations between environmental parameters and PP. The four most important parameters in relation to PP were PAR, phytoplankton biomass, seawater temperature and N_{Tot}. This full model was simplified through the reduction in parameters to obtain

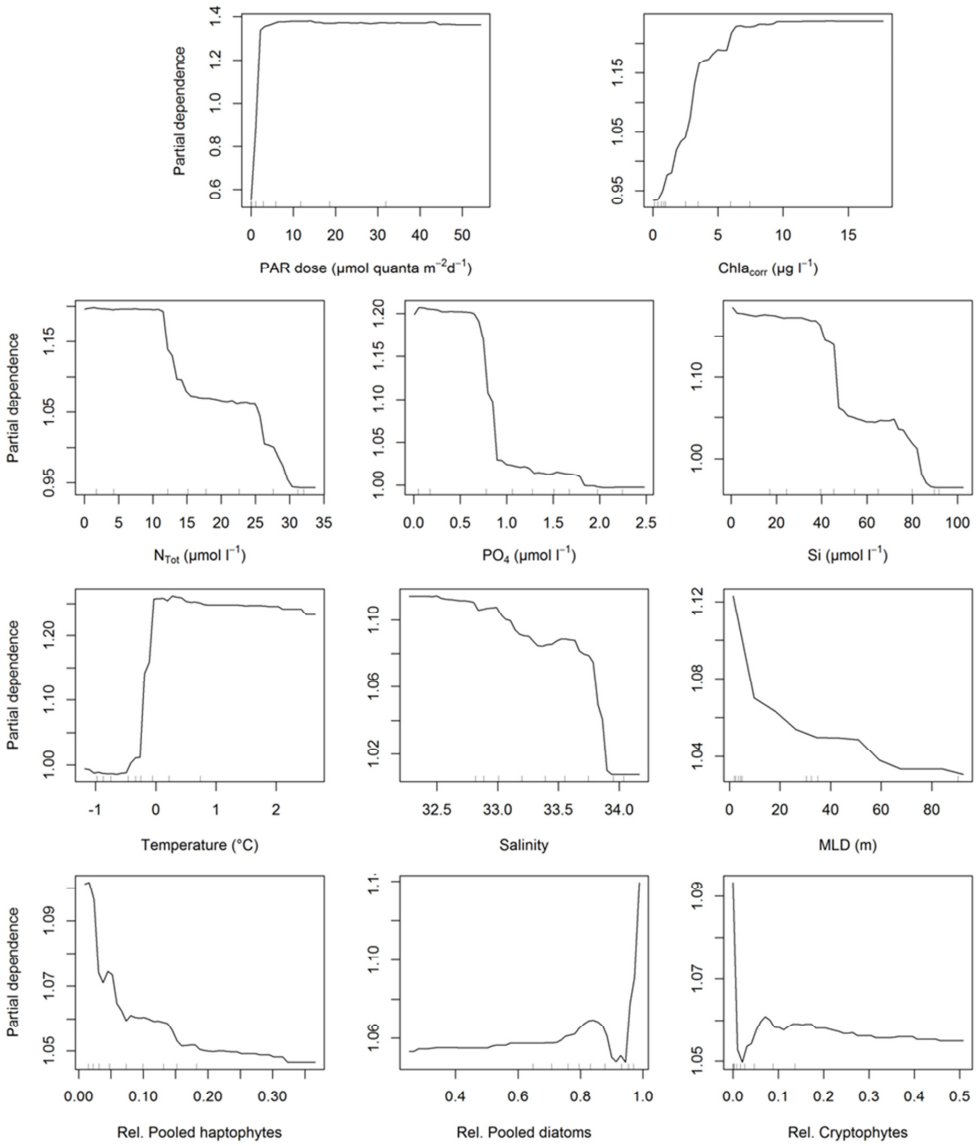

Figure 9: Partial dependence plots for all the variables included in the maximum random forest model to assess the importance of each value in the modeling op PP. The partial dependence plots for the minimal model are shown in appendix Fig. 3. Inner tick marks represent the 10% cohorts.

the minimal representative model capable of predicting PP, M_{RFmin}. The minimal model only included PAR, phytoplankton biomass and N_{Tot}. Finally, we compare both models and discuss the implications of our M_{RFmin} on the current efforts of modeling phytoplankton production in the coastal WAP.From our *in situ* measurement, we

identified four different periods during the 2013-2014 summer season (Fig. 2 & 4 spring, 1, 2 and 3), which were divided by the influx of large sheets of sea ice (period 1) or wind mixing events (ending periods 1 and 2). This suggests an adequate covering of past, current and future conditions in the coast WAP (Ducklow *et al.*, 2007, 2013). Period 1 was strongly influenced by sea ice whereas 2 and 3 were not. Accurately covering of these distinctively different periods is important given the continuously decreasing expand of winter sea ice (Stammerjohn & Maksym, 2017). This summer could be classified as one of medium productivity (median summer biomass at 15m was 4.3 µg Chl-a l^{-1}), slightly elevated SSTs and typical sea ice dynamics (Meredith *et al.*, 2013; Venables *et al.*, 2013; Rozema *et al.*, 2017a). Below we briefly review the characteristics of these different periods and how these are representative for other coastal sites along the WAP to establish the range of conditions to which our models were exposed.

Influence of presence/absence of sea ice on phytoplankton dynamics

During period 1, the sea ice gradually melted and freshened the surface layer thereby reducing MLD and promoting diatom growth, as is typical for the traditional WAP ecosystem (Ducklow *et al.*, 2012a, 2013). Moreover, a strong increase of turbidity indicated the marked presence of non-photosynthetic material, presumably microalgal aggregates released from the bottom of the sea ice (Fig. 2b, Legge *et al.*, 2017). Low F_v/F_m values and relatively low values for α further suggests that the diatoms in these aggregates were low light acclimated which is typical for the sea ice environment (Table 1, Appendix Fig. 2, Arrigo et al. (2014)). The difference in F_v/F_m between the late December community and the rest of the season suggests that the late December community was of a different origin, presumably the sea ice, confirming that period 1 could be deemed representative for the traditional coastal phytoplankton dynamics.

Classical features of the sea ice environment were the sole dominance of diatoms and depleted silicate stocks, the latter unexpected given the coastal nature of the site and never documented prior to the 2013-14 summer (Clarke *et al.*, 2008; Annett *et al.*, 2017b; Bown *et al.*, 2017; Cassarino *et al.*, 2017; Rozema *et al.*, 2017b). Even though macronutrient concentrations in the water column during this period were low and uptake by phytoplankton was likely hampered, nutrients could still have been available

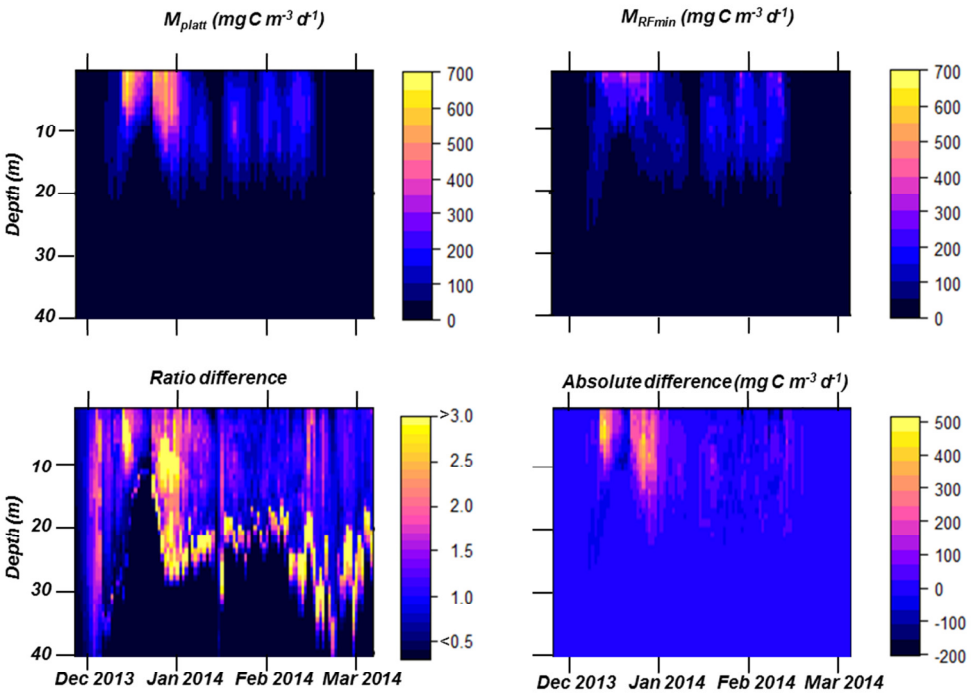

Figure 10: Estimated primary production (PP) in the top 40m based on M_{Platt} (Top left) and on M_{RFmin} (Top right). The ratio of PP between the two models (Bottom left), values >1 indicate a higher estimates using M_{Platt}. This ratio is used to understand the differences in behavior between the two models. Finally, we show M_{Platt} minus M_{RFmin} (Bottom right) to present when and at which depths the two models differ or match.

through high bacterial remineralization, sloppy grazing and/or viral lysis which peaks after the end of the bloom (Ducklow *et al.*, 2012b; Brum *et al.*, 2015). Additionally, the build-up of phytoplankton biomass could also have been ended by strong grazing, as is often observed at the sea ice edge, an attribute not covered in the RaTS program (Ross *et al.*, 2008; Saba *et al.*, 2014; Steinberg *et al.*, 2015).

Brief wind mixing events marked the starts of both periods 2 and 3, two periods uninfluenced by sea ice cover. These mixing events reconfigured the water column, lower SST, and mixed the freshwater to a greater depth, thus changing the conditions for phytoplankton growth, as evident from changes in the community composition and PP. In period 2, the water column was restabilized by a fresh and shallow surface layer, which was populated by cryptophytes which are often associated with glacial meltwater (Moline *et al.*, 2004; Saba *et al.*, 2014). Below this layer, haptophytes and

later large diatoms (mostly *Proboscia* spp.) thrived. Period 3 was characterized by increased wind mixing causing a more homogenous water column and deeper MLDs, typical for conditions at the end of summer and observed more frequently at the WAP (Clarke *et al.*, 2008; Montes-Hugo *et al.*, 2009; Venables & Meredith, 2014; Rozema *et al.*, 2017b). Thereafter, the community consisted of large proportions of haptophytes, diatoms and cryptophytes (Fig. 6).

Evaluation of parameters potentially impacting PP

First and foremost, our statistical model showed the importance of light availability and biomass in the promotion of PP. While completely expected, it does establish further confidence in our statistical model, which needed to establish these relations from the training set as opposed to the mechanistic model where these relations were already established.

Nutrient concentrations during summer can be highly variable and even undetectable near the surface (Fig. 5, Clarke *et al.*, 2008; Bown *et al.*, 2017; Rozema *et al.*, 2017b). Governing of PP (or biomass accumulation) by macronutrients in coastal Antarctic regions have been described previously and suggested a potential limitation of nitrogen (Alderkamp *et al.*, 2012b; Henley *et al.*, 2017; Rozema *et al.*, 2017b). Moreover, the nutrient dynamics are strongly influenced by the source of meltwater. Glacial melt is low in macronutrients and organic matter and dilutes the surface layer (Henley *et al.*, 2017). This opposed to sea ice melt, a prominent source of organic matter and bacteria to remineralized the nutrients (as reviewed in Fripiat et al., 2017). Additionally, deep (wind) mixing replenishes the nutrient concentrations of the euphotic zone. These three different components control MLD in the coastal WAP system and explains why nitrogen is a better predictor for PP than MLD (Meredith *et al.*, 2008; Rozema *et al.*, 2017b). The positive effects of a low salinity, above 0°C water temperature and shallow MLD on PP support the importance of glacial melt in shaping the PP. But in this study, these parameters did not contribute significantly in predicting PP (Fig. 8).

Moreover, our partial dependence plots suggest negative relationships between nutrient concentrations and PP (Fig. 9) when above 12, 0.7 and 42 µM for N_{Tot},

phosphate and silicate respectively and neutral when below these thresholds. We consider these negative relations an effect from the phytoplankton community becoming dominated by only one (or at least very few) species for which the conditions are optimal when the community is blooming (Annett *et al.*, 2010). The blooming species, which contributes most to PP, takes up most of the macro nutrients and dominates. We suspect that the blooming species draws down nutrients to concentrations in line with their uptake kinetics and half-saturation constants and, when reaching these minimum concentrations, form the plateaus in the relations between macronutrients and PP (Huisman & Weissing, 1999; Timmermans *et al.*, 2004).

When we consider all the parameters included in our M_{RFmax} model, the added benefit of including phytoplankton community composition is limited (Fig. 8). However, this does not imply that Chl-a specific production does not vary between the groups in the natural assemblages. The random forest model selects the parameters that explain the statistically highest possible amount of the MSE of PP. Yet, some of the variability explained by the top parameters is also be explained by mechanisms related to lower ranking parameters. Thus, while adding those parameters would not improve the model this does not mean that they are not ecologically or mechanistically important. For example, literature suggests that haptophytes favor a more unstable water column and our results confirm such a relation (Arrigo *et al.*, 1999; Rozema *et al.*, 2017a). However, haptophyte relative abundance is suggested to be of only minor importance in relation to PP by our models, despite a large difference between photosynthesis strategies between haptophytes and e.g. diatoms (Kropuenske *et al.*, 2009; Alderkamp *et al.*, 2012a). However, as we know haptophytes are related to deeper MLDs, and therefore lower SSTs, higher macronutrient concentrations and more variable PAR (Kozlowski *et al.*, 2011; Rozema *et al.*, 2017a). Thus, most of the variability in PP explained by knowing the fraction of haptophytes is already captured by the aforementioned parameters that rank higher. As such, we conclude that adding species information would not significantly improve models of PP in the coastal system. Sufficient knowledge of the physical, (photo)chemical properties and total phytoplankton biomass in the water column will suffice for predicting PP.

PP estimations

Calculation of PP by both approaches (M_{Platt} and M_{RFmin}) was strongly similar except during the second half of December (Fig. 10, period 1). The most important difference between these ~3 weeks and the rest of the season was the presence of melting sea ice. Estimates using M_{Platt} were higher (53%) during period 1 than those using M_{RFmin}. However, integrated biomass during period 1 was not exceptionally high when compared to period 2 or 3. In fact, it was lower than expected given the PP estimates from both models. Apparently, the high PP as measured using the P-E parameters did not result in an increase in total phytoplankton biomass. A difference in Chl-a specific production between taxonomic groups is unlikely to have been played a major role given the low contribution of taxonomic information to PP in M_{RFmax} (Fig. 9). The large discrepancy between productivity and phytoplankton biomass accumulation could be due to a number of reasons. 1) Phytoplankton released from the sea ice are low light acclimated and were lowering their Chl-a:carbon ratio while acclimating to higher irradiance intensities in the water column, thus growth would remain undetected using Chl-a as we used Chl-a as a proxy (Sakshaug & Holm-Hansen, 1986). 2) Phytoplankton Chl-a:carbon ratios remain relatively unchanged, but the phytoplankton mainly replenish their micro- and macronutrient reserves before biomass accumulation by growth (Arrigo, 2005). These two explanations are supported by the lower F_v/F_m, possibly indicative of photo inhibition, and low α observed for this population (Table 1, Appendix Fig. 2). Additional explanations are related to ecosystems dynamics. They assume that the high productivity is translated into phytoplankton biomass, but there is also a large loss factor. 3) Sea ice occurrence is often associated with krill and other grazing which can efficiently lower phytoplankton biomass (Behrenfeld, 2010). 4) Viral lysis as after a period of biomass increase, viruses often lyse which include the bursting of phytoplankton cells and thus lowering biomass (Brum *et al.*, 2015). Finally, the last and possibly most likely option 5) would be fast sedimentation of microalgal aggregates dominated by heavily silicified diatoms (Riebesell *et al.*, 1991). The last three theories are supported by the observation of a very high turbidity in the surface layer (Fig. 2b), not occurring elsewhere in the summer despite similar phytoplankton biomass concentrations. Our fieldwork cannot conclusively exclude any of the five hypotheses mentioned above or combinations

thereof, that created the observed dynamics in phytoplankton biomass and proportions thereof to PP during period 1. Most likely it is a combination of multiple of the aforementioned explanations. Thus, while M_{RFmin} resembles mechanistic models that estimate PP in the marine environment, it would greatly benefit from the inclusions of parameters better explaining the phytoplankton dynamics at the sea ice edge. Also, the relation between N_{Tot} and PP does provide extra information for future efforts modeling PP in the coastal Antarctic ocean.

Our two estimates of 176.1 and 214.4 g C m^{-2} per summer are in fair agreement with multiple different estimates of PP from previous years. Two recent estimates of net PP of 146 g C m^{-2} yr^{-1} for 2009-2010 and an estimate of 192 g C m^{-2} yr^{-1} for 2005-2006 for the RaTS site are comparable to ours (Henley et al., 2017; Weston et al., 2013). The latter estimate also employed P-E experiments with a very similar set up to ours. A slightly lower productivity of 99.4 g C m^{-2} over a 5 month period was observed at a more northerly site near Palmer Station, generally considered less productive than northern Marguerite Bay (Stukel *et al.*, 2015; Rozema *et al.*, 2017a). Furthermore, our estimates are in broad agreement with a multi-year (1995-2006) analysis of PP using ^{14}C along the WAP (Vernet *et al.*, 2008). Another study based on the 2007-2008 summer but also covering the large WAP region estimate a lower productivity (78 g C m^{-2} over four months) although this estimate is from a low biomass summer (Huang *et al.*, 2012; Rozema *et al.*, 2017a). Another estimate derived from calculating NCP from silica isotopes conducted at the RaTS, has calculated a maximum of only 56.4 g C m^{-2} over four months in 2009-2010 (Annett et al., 2017). Such a large discrepancy might be related to the bias of a silica based method to diatoms as haptophytes and cryptophytes also contribute to the carbon drawdown (Fig. 9) and diatom abundance was low in the 2009-2010 seasons (Rozema *et al.*, 2017a).

Implications and perspectives

Our data underline the importance of sea ice for phytoplankton biomass accumulation and PP in the coastal seas. Thus, a decrease in sea ice, as has been observed for the WAP since the start of the satellite record, will have substantial impact on the coastal marine system (period 1; Stammerjohn et al., 2008). Also, the diatoms associated with the sea ice and the related meltwater layer are pivotal in the food web due to the

importance in the krill life cycle (Flores *et al.*, 2012). While the loss of sea ice would result in a decrease in phytoplankton, the influence of meltwater from glaciers is rising (period 2; Moline et al., 2004; Montes-Hugo et al., 2009). While this meteoric meltwater also promotes stratification, which in turn promotes PP, the timing of the establishment of glacial meltwater layers and the phytoplankton communities within are different potentially affecting the entire food web (Moline *et al.*, 2004; Montes-Hugo *et al.*, 2009; Mendes *et al.*, 2013; Saba *et al.*, 2014; Rozema *et al.*, 2017a). While most PP models are designed for ocean regions, the MLD at the coastal ocean is established differently than in the open ocean due to the proximity of glaciers thus are generally not adequately included in these models.

Our minimal model also underlines that dissolved nitrogen and seawater temperature can be used to estimate PP. While we do not infer a causal relation between PP and these parameters, we observe strong relation to PP. Our RF does not fully explain the dynamics in PP, namely only 93%, and we consider this is related to the dynamics occurring in December. The strong reduction in phytoplankton biomass despite a high PP suggests another source which influences phytoplankton stocks, as discussed above. We consider the counterintuitive relation between N_{Tot} and PP evidence of important underlying processes not captured by our accurate yet simple model. Thus, a future improvement would be the measurement and incorporation of these undescribed processes into a model. Also, the near binary effect of above and below 0°C sea surface temperatures only indicates the importance of meltwater and mixing to the winter water layer. No relation to PP was observed with increasing seawater temperature while the strength of the relation between PP and salinity declines strongly when approaching lower values (<32.5).

Conclusions

We presented a phytoplankton PP model in the highly productive northern Marguerite Bay region. We thereby considered the effect of variability in relative phytoplankton group abundances to be adequately covered by the implementation of physical and (photo)chemical properties of the water column. Firstly, we show the challenge of modeling PP in phytoplankton communities from the sea ice. This underlines the importance of the effort to obtain measurements from (below) the sea ice. Secondly,

nitrogen concentrations were a stronger predictor of PP than MLD. Possibly because of the large difference in nitrogen concentrations between glacial and sea ice melt, the main sources for salinity driven stratification. Finally, our statistical models show that relative species abundances do not have to be included in future modeling efforts while maintaining a high level of confidence in the model. This last conclusion greatly simplifies the monitoring efforts required to provide field based measurements needed to estimate PP. The combination of these insights, based on both a classical, mechanistic model and independent, statistical models, should help shape the priorities for modeling efforts to accurately estimate PP in the climatically-sensitive and variable coastal WAP region.

Acknowledgements

We would like to thank Pim Sprong, Ronald Visser, Johann Bown and Libby Jones who have helped with the collection of the samples and data used here. Our research was made possible by and greatly benefited from all the BAS staff at Rothera and Cambridge, to whom we are very grateful. Also, we would like to thank Libby Jones for providing some of the DIC data collected by her and Hugh Venables for sharing PAR data from Rothera Research Station. Furthermore, we thank Arjo Bunskoeke and Mieke Blauw who assisted with the development, testing and implementation of the protocol for our P-E experiments. Sean de Graaf and Wendy Bollen are thanked for their help with running and processing the HPLC samples and data. Additionally, we would like to thank the editor and the reviewers for their valued opinions and suggestions which helped to improve the manuscript. This research was funded by the Dutch Polar Programme (866.10.105). Funding for the RaTS programme is from the Natural Environment Research Council, and is a component of the BAS Polar Oceans programme.

Apendices are available online and/or upon request.

3

Chapter 4

Summer microbial community composition governed by upper-ocean stratification and nutrient availability in northern Marguerite Bay, Antarctica.

P. D. Rozema
T. Biggs
P. A. A. Sprong
A. G. J. Buma
H. J. Venables
C. Evans
M. P. Meredith
H. Bolhuis

Published in:
Deep-Sea Research Part II:
Topical Studies in Oceanography (2017)

Abstract

The Western Antarctic Peninsula warmed significantly during the second half of the twentieth century, with a concurrent retreat of the majority of its glaciers, and marked changes in the sea-ice field. These changes may affect summertime upper-ocean stratification, and thereby the seasonal dynamics of phytoplankton and bacteria. In the present study, we examined coastal Antarctic microbial community dynamics by pigment analysis and applying molecular tools, and analysed various environmental parameters to identify the most important environmental drivers. Sampling focussed on the austral summer of 2009-2010 at the Rothera oceanographic and biological Time Series (RaTS) site in northern Marguerite bay, Antarctica.

The Antarctic summer was characterized by a salinity decrease (measured at 15 m depth) coinciding with increased meteoric water fraction. Maximum Chl-a values of 35 μg l^{-1} were observed during midsummer and mainly comprised of diatoms. Microbial community fingerprinting revealed four distinct periods in phytoplankton succession during the summer while bacteria showed a delayed response to the phytoplankton community. Non-metric multidimensional scaling analyses showed that phytoplankton community dynamics were mainly directed by temperature, mixed layer depth and wind speed. Both high and low N/P ratios might have influenced phytoplankton biomass accumulation. The bacterioplankton community composition was mainly governed by Chl-a, suggesting a link to phytoplankton community changes. High-throughput 16S and 18S rRNA amplicon sequencing revealed stable eukaryotic and bacterial communities with regards to observed species, yet varying temporal relative contributions. Eukaryotic sequences were dominated by pennate diatoms in December followed by polar centric diatoms in January and February. Our results imply that the reduction of mixed layer depth during summer, caused by meltwater-related surface stratification, promotes a succession in diatoms rather than in nanophytoflagellates in northern Marguerite Bay, which may favour higher trophic levels

Apendices are available online and/or upon request.

Introduction

The Western Antarctic Peninsula (WAP) has recently experienced strong atmospheric warming. Between 1957 and 2006 the Antarctic Peninsula warmed by 0.11 ± 0.06 °C per decade and this increase was strongest during winter and spring (Steig *et al.*, 2009; Turner *et al.*, 2016). As a result, sea-ice extent has been decreasing in the WAP region, with potential consequences for phytoplankton bloom dynamics (Montes-Hugo *et al.*, 2009). During spring and early summer, sea-ice melting may induce water column stratification enhancing the light availability for phytoplankton bloom development (Sverdrup, 1953; Ackley & Sullivan, 1994). Stratification in coastal regions is further promoted by increased freshwater supply from glacial melt and precipitation (Dierssen *et al.*, 2002; Cook *et al.*, 2005, 2016, Meredith *et al.*, 2008, 2013, 2017; Depoorter *et al.*, 2013; Rignot *et al.*, 2013). Glaciers in the central and southern regions are affected most pronouncedly due to increasing temperatures of mid-depth (150 m) waters melting glacial fronts (Cook *et al.*, 2016). Decreased cloud cover and increasing wind speeds in the northern WAP are further altering water column properties by changing light availability (Montes-Hugo *et al.*, 2009). These changes are already affecting phytoplankton community dynamics and are likely to become more pronounced in the future (Moline et al., 2004; Montes-Hugo et al., 2009; Rozema et al., 2016; Saba et al., 2014).

Due to variability in regional warming, changes in the phytoplankton community and biomass are not uniform across the WAP (Montes-Hugo *et al.*, 2009). Additionally, the ongoing retreat of glaciers along the WAP exposes new areas to light and consequently an increase in phytoplankton biomass (Peck *et al.*, 2010). Wind speeds in the northern WAP are increasing, resulting in more pronounced mixing leading to lower surface chlorophyll a (Chl-a) levels (Turner *et al.*, 2005; Montes-Hugo *et al.*, 2009). In contrast, phytoplankton biomass is increasing towards the central/southern region of the WAP. In Marguerite Bay, an extensive bay surrounded by glaciers in the central region of the WAP, lower mean summertime sea surface temperatures and higher average Chl-a concentrations were observed when compared to the northern WAP (Clarke *et al.*, 2008; Meredith *et al.*, 2010). The present study was conducted in Ryder Bay, in the

northern part of Marguerite Bay, at the site of the Rothera oceanographic and biological Time-Series (RaTS).

The increase in glacial runoff affects the phytoplankton communities differently in various regions. In Potter Cove on King George Island (northern WAP), phytoplankton biomass remained low despite high nutrient levels (van de Poll *et al.*, 2011). Here, sediment-rich run-off from the glacier increased water turbidity, thereby causing unfavourable irradiance conditions for phytoplankton growth despite salinity stratification. A similar scenario was described for Kongsfjorden on Spitsbergen (Arctic; Piquet et al., 2014). In contrast, glacial meltwater might contain high levels of iron thereby fuelling phytoplankton blooms (Alderkamp *et al.*, 2012b; Bown *et al.*, 2017). In the Amundsen Sea, high levels of phytoplankton biomass were sustained by iron input from the nearby Pine Island Glacier (Alderkamp *et al.*, 2012b).

The phytoplankton community in the central to southern WAP consists mainly of diatoms, the haptophyte *Phaeocystis antarctica* and cryptophytes (Buma *et al.*, 2001; Garibotti *et al.*, 2005; Annett *et al.*, 2010; Kozlowski *et al.*, 2011; Piquet *et al.*, 2011). Diatoms are often dominant in stratified waters due to their adaptation to high irradiance levels while *P. antarctica* is mainly found in waters characterized by strong vertical mixing (Arrigo *et al.*, 1999). Cryptophytes are thought to dominate waters strongly influenced by (glacial) meltwater (Moline *et al.*, 2004). Earlier studies at the RaTS site reported peaks in phytoplankton biomass in December or January, possibly related to sea-ice presence and/or melt (Clarke *et al.*, 2008; Venables *et al.*, 2013). Additionally, a secondary Chl-a peak was frequently observed in March (Clarke *et al.*, 2008). The phytoplankton summer community exhibited a succession of various diatoms (Buma *et al.*, 2001; Clarke *et al.*, 2008; Annett *et al.*, 2010; Piquet *et al.*, 2011). Also, both hetero- and autotrophic dinoflagellates accounted for 27% of the total phytoplankton biomass in Ryder Bay (Annett *et al.*, 2010). Data on the abundance of haptophytes and cryptophytes in northern Marguerite Bay are limited but suggest that events which allow for the dominance of either of these two groups do not necessarily occur every summer (Arrigo *et al.*, 1999; Moline *et al.*, 2004; Annett *et al.*, 2010; Piquet *et al.*, 2011; Rozema *et al.*, 2017a). Previous observations of the physical properties confirmed the representativeness of the RaTS monitoring site for the larger northern

Marguerite Bay area (Venables & Meredith, 2014). This suggests that the previously described dynamics in the phytoplankton community should be applicable to the RaTS site.

The pivotal link between primary producers and higher trophic levels within the Antarctic food web is krill, which prefer grazing on (large) diatoms (Quetin & Ross, 1985; Haberman *et al.*, 2003). Recent studies in the Southern Ocean have shown a decline in krill in favour of salps, presumably related to shifts in the phytoplankton community (Atkinson *et al.*, 2004; Flores *et al.*, 2012). This shift from krill to salps is not (yet) occurring at the WAP although these two grazers are not observed simultaneously (Steinberg *et al.*, 2015). Other frequently observed grazers, yet considered of less importance or less well studied, are copepods, (silico)flagellates, heterotrophic dinoflagellates and tintinnids (Sherr & Sherr, 2007; Atkinson *et al.*, 2012; Ducklow *et al.*, 2012a; Dolan *et al.*, 2013; Steinberg *et al.*, 2015). Potentially, grazers could exert top-down control on the phytoplankton biomass in the WAP ecosystem (Behrenfeld, 2010). A recent investigation into the applicability of this mechanism, the so-called 'dilution-recoupling hypothesis', for the RaTS site suggests that phytoplankton biomass accumulation is more strongly linked to light than grazing pressure (Venables *et al.*, 2013). Yet incidentally strong governance of phytoplankton biomass by grazers during summer periods cannot be excluded.

Bacterial community dynamics seem to be mostly dependent on phytoplankton biomass and composition (Delmont *et al.*, 2014; Kim *et al.*, 2014; Landa *et al.*, 2016). Antarctic marine bacterial biomass correlates with recently produced algal dissolved organic carbon (DOC; Moran et al., 2001) while marine bacterial community composition correlated with the concentration and speciation of dissolved organic matter (DOM; Billen and Becquevort, 1991; Ducklow et al., 2012b; Landa et al., 2016). Furthermore, a shift in bacterial community composition was shown to follow a shift in phytoplankton composition, with a lag phase lasting a few days to one month (Billen & Becquevort, 1991; Piquet *et al.*, 2011; Ghiglione & Murray, 2012). The bacterial community in marine Antarctic habitats consists mainly of the phyla (Alpha- and Gamma-) Proteobacteria, Actinobacteria and Bacteroidetes (Gentile *et al.*, 2006; Piquet *et al.*, 2011; Delmont *et al.*, 2014; Kim *et al.*, 2014; Luria *et al.*, 2014; Landa *et al.*, 2016).

The Bacteroidetes are also referred to as the Cytophaga-Flavobacterium-Bacteroides (CFB) group (Abell & Bowman, 2005; Gentile *et al.*, 2006). One study based on metaproteomics revealed a dominance of Rhodobacterales and Alteromonadales (Williams *et al.*, 2012). The *Sulfitobacter* genus (Rhodobacterales) was observed to increase in relation to DOM of diatom origin (Landa *et al.*, 2016). This genus, and other genera belonging to Rhodobacterales, are known to be able to transform DMSP, observed in high quantities at RaTS (Stefels, personal communication), into DMS (Curson *et al.*, 2008; Reisch *et al.*, 2011). Furthermore, during winter bacterioplankton diversity was found to be higher compared to summer (Ghiglione & Murray, 2012; Ladau *et al.*, 2013).

The aim of this study was to understand how the microbial community in Ryder Bay (Adelaide Island, WAP) responds to changes in environmental conditions. We hypothesized that both phytoplankton and bacteria are governed by enhanced water column stability caused by sea-ice melt during spring and/or glacial meltwater input during summer (Clarke *et al.*, 2008; Meredith *et al.*, 2010). Furthermore, we hypothesized that limitation by macronutrients would be unlikely (Clarke *et al.*, 2008; Venables *et al.*, 2013; Bown *et al.*, 2017). Finally, we hypothesized that the bacterial community changes, albeit with a delay, due to shifts in phytoplankton community composition.

To test our hypotheses, we followed microbial community structure at the RaTS site in northern Marguerite Bay during the summer of 2010-2011. We applied an approach which combined two DNA (Denaturing Gradient Gel Electrophoresis (DGGE) and MiSeq amplicon sequencing) and two pigment-based techniques (High pressure liquid chromatography (HPLC) and size-fractionated Chl-a).

Material and methods

Study site and sample collection

This study was conducted in Ryder Bay, Adelaide Island (Western Antarctic Peninsula) near Rothera research station (Fig. 1). Sampling took place at the RaTS site (67°34.200'S 68°13.500'W, fig. 1), ~4 km from Rothera (Clarke *et al.*, 2008). Sampling (excluding collection of DNA samples, see below) occurred once or twice a week in the

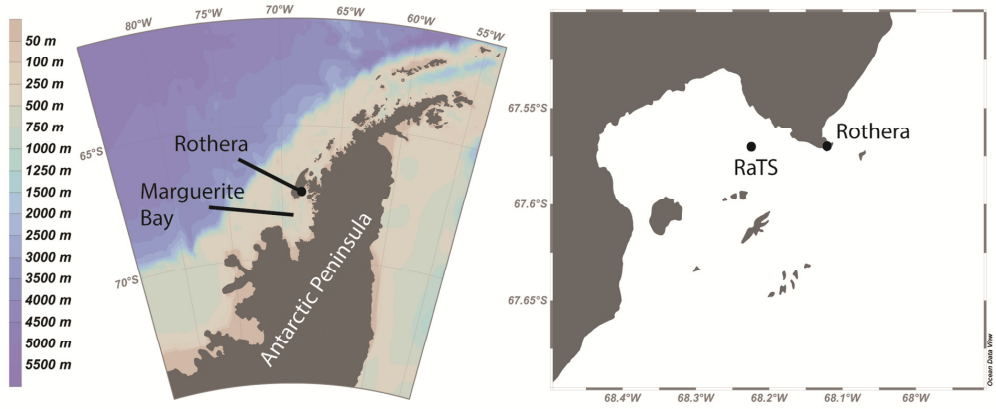

Fig. 1: Map of sampling area: (Left) the position of Rothera research station on Adelaide Island, north of Marguerite Bay and (Right) the RaTS sampling site in Ryder Bay near Rothera research station.

period from October 15, 2010 to March 23, 2011 from a small boat equipped with a hand winch. Full water column profiles were obtained with a CTD (conductivity, temperature, and depth) supplemented with LiCor photosynthetically available radiation (PAR) and fluorescence sensors (WetLabs). Calibration of the CTDs between years and with the Palmer Long-Term Ecological Research (LTER) program (Ducklow *et al.*, 2012a) are discussed in Venables et al. (2013). Samples for HPLC analysis of pigments, nutrients (nitrate, nitrite, phosphate and silicate), size-fractionated Chl-a (>20 µm, 20-5 µm, 5-2 µm and 2-0.2 µm) and $\delta^{18}O$ were taken at water depth (15 m) using a 12 L Niskin bottle as part of the standard RaTS sampling scheme. This depth represents the long-term climatological phytoplankton peak observed using a fluorescence sensor attached to the CTD (Clarke *et al.*, 2008). Sample processing for nutrients, $\delta^{18}O$, and size-fractionation was done according to the RaTS standard protocol (Clarke *et al.*, 2008; Meredith *et al.*, 2008). For HPLC, 1000 mL was filtered over 47 mm GF/F filters (Whatman, US). Filters were snap frozen in liquid nitrogen and stored at -80 °C for later analysis in the home laboratory.

For DNA analysis, seawater samples were taken at 15 m depth on December 9, 2010 and January 13, 24, 27, 31, February 3, 10, 16, and 21 (2011). Between 2 and 4 litres, collected as described above, were filtered on a 47-mm polycarbonate membrane of 0.2 µm pore

size (Millipore, US). Filters were snap frozen in liquid nitrogen and stored at -80 °C until analysis in The Netherlands.

Environmental parameters (RaTS-programme)

Mixed-layer depth (MLD) was calculated as the depth where the density difference ($\Delta\sigma$) relative to the surface was 0.05 kg m^{-3} (Brainerd & Gregg, 1995). Salinity is presented on the practical salinity scale. Five-day averaged wind speed data from Rothera station was retrieved from the British Antarctic Survey (http://www.antarctica.ac.uk/met/metlog/). Nutrient samples were analysed in the UK according to Clarke et al. (2008). Oxygen isotope samples ($\delta^{18}O$) were analysed as described in Meredith et al. (2008) at the Natural Environment Research Council Isotope Geosciences Laboratory (Keyworth, UK).

Pigment analysis (RaTS-programme)

Size-fractionated Chl-a samples were classified and analysed on base as described before (Clarke *et al.*, 2008) following Wood (1985); in short, pigment extractions were performed overnight at 4° C in chloroform/methanol (2:1 v/v) and Chl-a was determined before and after the addition of 0.1 N HCl using a fluorometer (AU-10, Turner). The microplankton (>20 µm) fraction was calculated from the size-fractionated Chl-a data and normalized to HPLC Chl-a values. Samples for HPLC analysis, as part of the RaTS program (Rozema *et al.*, 2017a), were processed as described in van Heukelem and Thomas(2001) and modified by Perl (2009). In short, HPLC filters were freeze dried for 48 hours. Pigments were extracted in 90% acetone for 48 hours in the dark and at 4 °C. Pigment detection was run on an HPLC (Waters 2695 separation module, 996 photodiode array detector) equipped with a Zorbax Eclipse XDB-C_8 3.5 µm column (Agilent Technologies). Quantification was done using standards (DHI, Denmark). Pigments reported in this study are: Chl-a, chlorophyll b, chlorophyll c_3, peridinin, 19'-butanoyloxyfucoxanthin, fucoxanthin, neoxanthin, prasinoxanthin, 19'-hexanoyloxyfucoxanthin, alloxanthin and lutein. Initial and final pigment ratios are presented in Table A.1. Values for Chl-a reported in this study were based on HPLC analysis.

DNA extractions

DNA was extracted from the filters using a modified protocol of Boelen et al. (2000). Microcentrifuge tubes (1.5 mL) containing halved filters were filled with 500 µL DNA extraction buffer (2% [w/v] cetyl trimethylammonium bromide (CTAB), 1.4 M NaCl, 20 mM EDTA, 100 mM Tris-HCl (pH = 8.0) and heated to 60 °C. One µL (beta)-mercaptoethanol was added before incubation for 30 minutes at 60 °C. Samples were centrifuged for 10 minutes at 14k rcf, after the addition of 500 µL CIA (Chloroform/Isoamylalcohol [24:1] v/v). The upper phase was transferred to a clean tube. Subsequently, 335 µL isopropanol was added and the samples were cooled for one hour at 4 °C. The samples were centrifuged for 30 minutes at 14k rcf and 4 °C, after which the liquid phase was discarded. The pellet was cleaned in 800 µL ethanol (80%) before incubation at -20 °C for 10 minutes. The ethanol was discarded after centrifuging for 30 minutes at 14k rcf and 4 °C. Pellets were dried for ~60 minutes at room temperature before resuspension in 100 µL of 0.1x TE buffer (1 mM Tris-HCl, 0.1 mM EDTA, pH 8.0). Finally, the DNA samples were incubated overnight at 4 °C to dissolve and stored at -20 °C.

DNA amplification

PCR reactions (25 µL final volume) were run on a VWR thermo cycler (VWR, US). For every reaction, 2.5 µL of a 10- to 100-fold diluted DNA solution was used as a template. The following primer sets were used: Euk1A and 516R-gc for eukaryotes (Sogin & Gunderson, 1987; Amann *et al.*, 1990; Díez *et al.*, 2001), diatom specific primer Diatom18SR1 and 1209F-GC (Giovannoni *et al.*, 1988; Godhe *et al.*, 2008), Dino 18S F1-GC and Dino 18S R1 for dinoflagellates (Lin *et al.*, 2006) and 968F-GC and 1401R for bacteria (Nübel *et al.*, 1996). The –GC suffix stands for the GC-clamp required for analysis by DGGE. Additional information on the primers used can be found in Table A.2 and reaction mixture composition and reaction conditions are listed in Table A.3. Amplicon yield was estimated by DNA gel electrophoresis on a 1% agarose gel, stained with ethidium bromide (0.002 %). Gels were visualized using an Image Master (Pharma Biotech, UK). DNA amplicon yield and size were estimated by including a DNA Smart Ladder (Eurogentec, Belgium).

DGGE

PCR product was subjected to DGGE analysis using a PhorU system (Ingeny, Netherlands). DGGE analysis was done as described in Piquet et al. (2008). Approximately 60 ng of PCR amplicon was run for each sample as well as in-house developed markers with bands along the gradients of interest. Different denaturing gradients of urea-formamide were used; 20-45% for diatoms and eukaryotes, 20-40% for dinoflagellates and 30-70% for bacteria. All samples were run for 16 hours at 100V in 0.5x TAE buffers, except for the diatom samples, which were run for 20 hours. The gels were stained using silver staining, according to Heuer et al. (2001).

Community sequencing

Analyses of the species composition in both the eukaryotic and bacterial fractions using MiSeq were performed on samples representative of the various periods in microbial succession as judged from DGGE clustering (general Eukaryotes and Bacteria; Fig. 6 & 7). This resulted in three representative DNA samples (December 9, January 27 and February 16) that were shipped on dry-ice to the Research and Testing Laboratory (Texas, United States) for paired-end sequencing on an Illumina MiSeq using their protocols and primers. The EukA7F and Euk555R primers were used to investigate the eukaryotic community while 28F and 519R were used for the bacterial community (Table A.2; Frank et al., 2013; Medlin et al., 1988; Moreno et al., 2010).

Analysis of RaTS parameters

CTD data were visualized in Ocean Data View v4.5.6 (Schlitzer, 2016). Correlations between environmental parameters were calculated in the statistical package PAST v2.17c (Hammer *et al.*, 2001). The CHEMTAX analysis package v1.95 (Mackey *et al.*, 1996) was used to calculate relative and absolute abundances of different phytoplankton groups based on the pigment concentrations as obtained by HPLC. Phytoplankton group abundances were calculated in CHEMTAX by groups using marker pigments and their previously derived ratios. The program then uses a factor analysis and steepest descent algorithm to find the best fit based on initial pigment ratios. The phytoplankton groups used in our analysis were: prasinophytes, chlorophytes, dinoflagellates, cryptophytes, two classes of haptophytes (*P. antarctica* has a variable pigment signature in response to iron conditions (van Leeuwe *et al.*,

2014)), and two classes of diatoms. Diatoms were separated as one class with *Pseudonitzschia*-like species containing chlorophyll c_3 while the other class does not. Initial ratios (Table A.1) were obtained from Wright et al. (2010), except those for *P. antarctica*, which were taken from Wright et al. (2009). After CHEMTAX analysis, abundances for both haptophyte and both diatom classes were pooled and presented as haptophytes and diatoms, respectively.

Calculation of freshwater origin

The ratio of oxygen isotopes ($\delta^{18}O$) in the sea water samples was used to subdivide the freshwater fraction, as calculated from salinity measurements, into quantitative estimates of freshwater contributions from sea-ice melt and meteoric water. This distinction is possible as freshwater of meteorological origin is isotopically lighter than freshwater originating from sea-ice melt. The two sources of meteoric water are precipitation and glacial melt water input (Craig & Gordon, 1965). The relative balance of direct precipitation and glacial discharge is discussed in detail in Meredith et al. (2016); for the period of our data, the latter is inferred to be the dominant freshwater input.

Analysis of community fingerprints from DGGE

The DGGE gels were digitized using a negative photo scanner (Epson Perfection V700 photo). Bionumerics v3.5 (Applied Maths, Belgium) was used for analysis of the DGGE band patterns as described in Piquet et al. (2008). We used the in-house developed markers to ensure correct alignment of bands between samples. Band patterns were transformed to relative band intensities and exported to Past v2.17c (Hammer *et al.*, 2001) to estimate species evenness and richness, and Simpson diversity indices (Simpson, 1949). The Simpson indices were subtracted from 1.

Furthermore, the DGGE data were analysed using the Bray-Curtis similarity coefficient and presented in the form of unweighted pair group method with arithmetic averages (UPGMA) dendrograms. One of the markers used for the DGGE was added as outgroup. Values for the cophenetic correlation were deemed good if >0.85. Each dendrogram underwent bootstrapping (n = 1000). Bootstrap values, the percentage of replicates in which each node was present, were added to the dendrograms. These

bootstrap values were consequently used to propose clusters with a certain degree of confidence. NMDS (Non-metric multidimensional scaling) was chosen to explore how the community data based on DGGE related to each other at the different time points during the Antarctic summer season (reviewed in Ramette (2007)). The relative band intensity was also used for NMDS. The minimum spanning tree was added to show the nearest neighbour of every sample within multidimensional space as we simplified the NMDS to a 2d plot. Stress of the ordination was checked using Shepard plots. Finally, we added vectors to the NMDS for a number of (environmental) parameters to create a biplot to identify which variables potentially influenced the microbial communities. These variables were not included in the ordination and are simply a projection of the variable along a linear vector. The length of the vectors was scaled linearly to improve the visual interpretation of the NMDS biplot, so only their directions and relative lengths should be considered (Ramette, 2007). We used the following environmental variables for the eukaryotes, diatoms and dinoflagellates NMDS's; PAR, MLD, wind speed, salinity, water temperature, total N (nitrite and nitrate summed), phosphate and silicate. Silicate was excluded for the dinoflagellates. For bacteria, Chl-a was added as a proxy for algal biomass.

Community sequence analysis

Amplified 16S and 18S rRNA gene sequence reads were analysed using a number of algorithms within the QIIME microbial community analysis pipeline (Caporaso *et al.*, 2010). Paired reads were pre-processed and joined using PEAR (Zhang *et al.*, 2014). A quality filter step was used to filter out reads with ambiguous bases, unrealistic read lengths and reads with an average quality scores (using a 40 nt sliding window) below 30. Mapping, dereplication, OTU clustering and chimera checking/removal were done using Vsearch 1.1.3 (Torbjørn et al., 2015). For OTU clustering we choose a 95% sequence identity cut off to accommodate for the higher expected variation in the variable regions which would lead to an overestimation of the actual diversity when the traditional 97% cut off would be used. The cluster centroid for each OTU was chosen as the OTU representative sequence and OTU's with an occurrence smaller than 6 in the complete dataset were removed before community analysis. The taxonomic assignment of the representative sequences was carried out using a naïve

Bayesian classifier (Wang *et al.*, 2007) against the SILVA SSU non-redundant database (119 release; Quast et al., 2013). Diatoms in this database are ordered as proposed recently (Medlin & Kaczmarska, 2004). BIOM tables generated by the taxonomic assignment yielded seven taxonomic levels for bacteria and eight for eukaryotes ranging from phyla to family or genus ranks. Nodes representing >1% of the data set with the three samples combined are presented in this manuscript while the full list is included in Table A.4. DNA sequences obtained in this study are deposited in the National Centre for Biotechnology Information (NCBI) Sequence Read Archive under accession number SRP072539.

Results

Environmental variables

Spring (October-November) was characterized by a deep mixed layer (~80 m; Fig. 3) and major nutrients were abundant with phosphate and total nitrogen concentrations around 1.3 and 16 µM respectively (Fig. 4). The deep MLD suggesting that the source of nutrients replenished during winter was deep mixing maintained by strong and persistent winds (Fig. 3). At the start of summer (December), the water column quickly stratified due to a strong decrease in salinity, ranging between 33.1 and 33.8 (Fig. 2). Lowest salinities observed were 33.3 on January 27 and 33.1 on February 21. Density changes were strongly related to changes in salinity (r^2 = 0.98, p < 0.001) and not temperature, as is inevitable given the equation of state for seawater at low temperature. During the period of DNA sampling, the water column slowly warmed from -0.7 °C on December 9 to >1.5 °C at 15 m in the period from January 26 to February 4. PAR decreased during the DNA sampling period (data not shown). Throughout the summer, maximum PAR at 15 m was 111.5 µmol photons m^{-2} s^{-1}. PAR values during the sampling period for DNA analyses were 46.9 µmol photons m^{-2} s^{-1} on December 9 and a maximum of 12.3 µmol photons m^{-2} s^{-1} in January and February. CTD fluorescence signals revealed two peaks during DNA sampling (Fig. 2). Fluorescence values at 15 m reached peak values on December 28 (22 mg Chl-a m^{-3}) and January 17 (27 mg Chl-a m^{-3}). A second fluorescence peak was observed on February 7 (9.3 mg Chl-a m^{-3}). During DNA sampling the MLD was shallow (<10 m; Fig. 3). Fluorescence peaks were therefore found below the MLD except for a short period from December 31

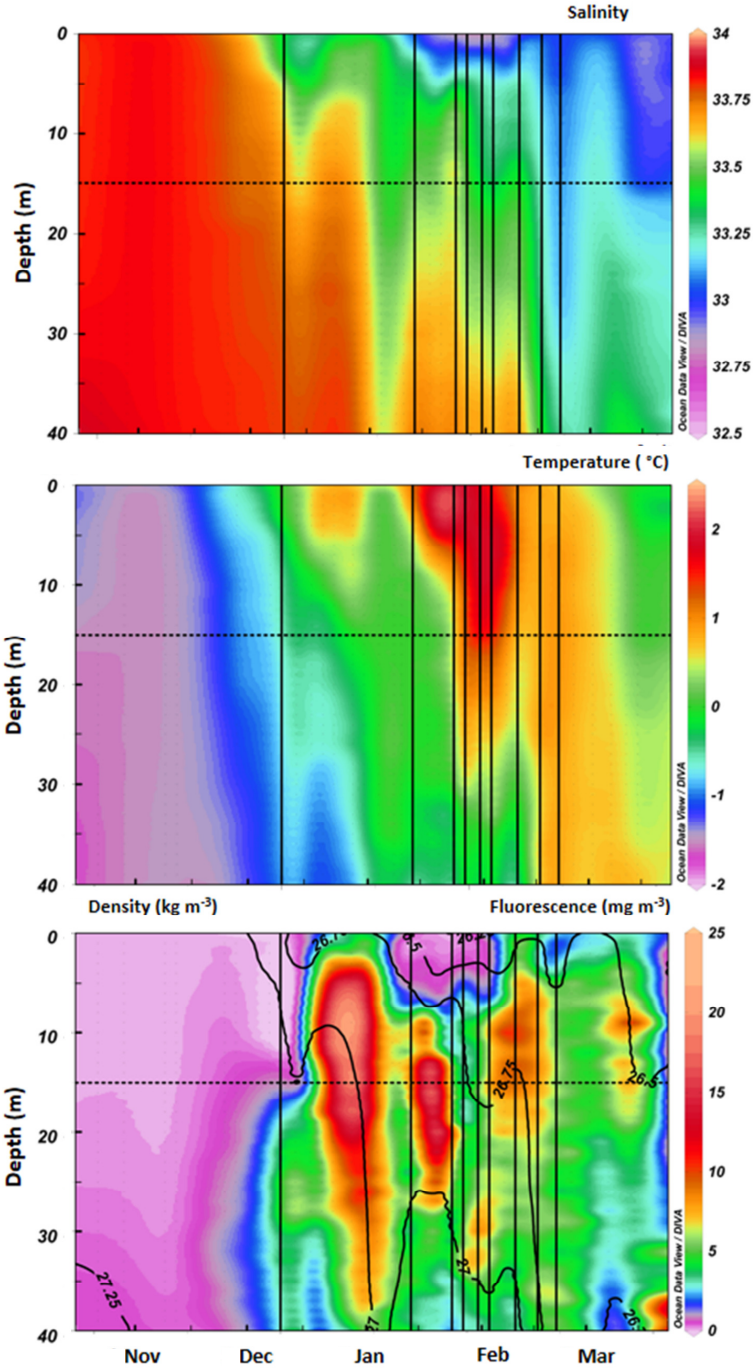

Fig. 2. Plots of the salinity (Top), temperature (Middle), and fluorescence and density (Bottom) during the spring and summer period. Density (Bottom) is marked by the black isobar lines. The horizontal dashed line indicates 15-m depth, whereas the vertical lines indicate sampling days.

to January 8. During this period the MLD deepened to a maximum of 31 m on January 4, coinciding with an increase in wind speed, starting December 11 and decreasing after January 4. A maximum wind speed of 8.0 m s^{-1} was observed on December 28. The decrease in salinity over the season correlated strongly with an increase in meteoric water (glacial melt plus precipitation), based on $\delta^{18}O$ results ($r^2 = 0.74$, $p < 0.001$, Fig. 3). In contrast, no sea ice was present in Ryder Bay during the period of interest (Venables *et al.*, 2013). Only brash ice of glacial origin was observed frequently in December and occasionally in January and February (data not shown). In theory, the increase in meteoric water could represent increased glacial discharge or increased input of precipitation, with the latter including the injection to the ocean of snow that had accumulated on top of sea ice during winter. However, the absence of sea ice from Ryder Bay during the study period precludes this and glacial discharge and the melt of snow accumulated on land is inferred to be the likely dominant source of meteoric water input (Meredith *et al.*, 2017). Total N and phosphate reached minimum values on January 27 (1.1 µM) and February 3 (0.1 µM) respectively (Fig. 4). Silicate showed no clear seasonal pattern. However, two minima were observed: on January 10, (22.2 µM) and on March 7, (23.4 µM). At the end of the season, values returned to those found at the beginning of the season. The average N/P ratio over the summer was 13.0 and was relatively stable apart from two deviations. Firstly, the ratio increased from December 17 to 28 to a maximum of 26.4 before restabilising at the average on the 31st. Secondly, N/P ratios decreased below 10 on January 17 and fell to 5.3 on January 27. Thereafter, the ratio increased back to its average.

Phytoplankton pigments

HPLC based total Chl-a concentration revealed two biomass peaks during the DNA sampling period (Fig. 5) as suggested earlier by the two *in situ* fluorescence maxima (Fig. 2). The main component of total Chl-a consisted of the microplankton fraction: over the entire HPLC sampling period, total Chl-a consisted on average of 78.6% microplankton (Fig. 5). The remaining 21.4% was evenly divided across the three smaller fractions. Phytoplankton community diversity was higher at the start of the HPLC sampling period and decreased over the sampling period.

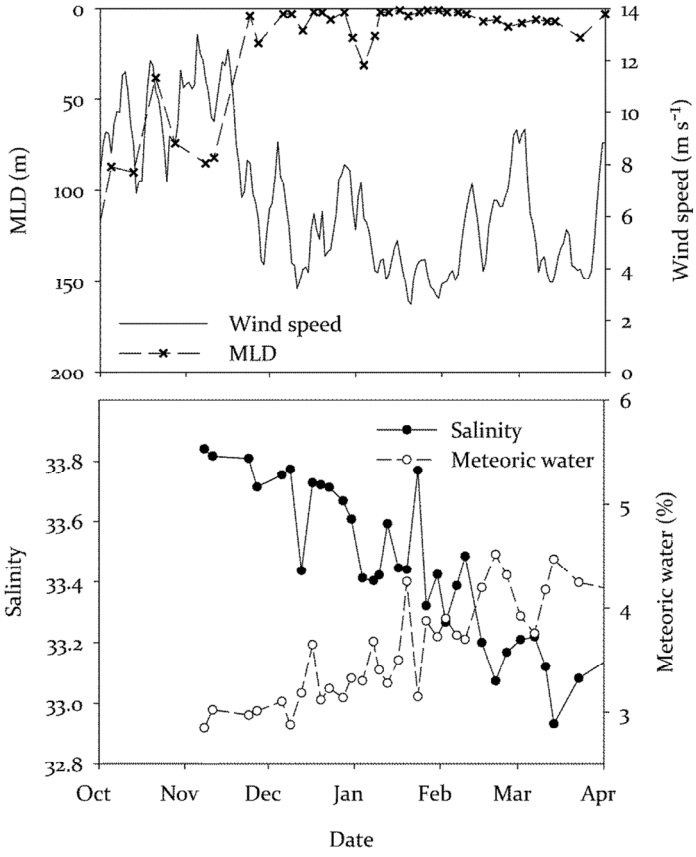

Fig. 3: (Top) Wind speed and MLD during the spring and summer. Wind speed (thin black line) is a 5-day running average. MLD (black dashed line). (Bottom) Salinity (black dots) and meteoric water (white dots) content at 15 m.

The phytoplankton community was diverse during spring (October-November; Fig. 5). Initially, haptophytes were more dominant (46%) than diatoms but these were steadily replaced by diatoms over the course of spring resulting in a relative abundance of <10%. Also, prasinophytes were a major component of the community, contributing on average 16% during spring. Cryptophyte relative abundances were low averaging only 6%.

During summer, dinoflagellates and prasinophytes were not major contributors to the phytoplankton community. Only after January 17 was there a slight increase in absolute and relative abundance of these two groups. Chlorophyte contributions were

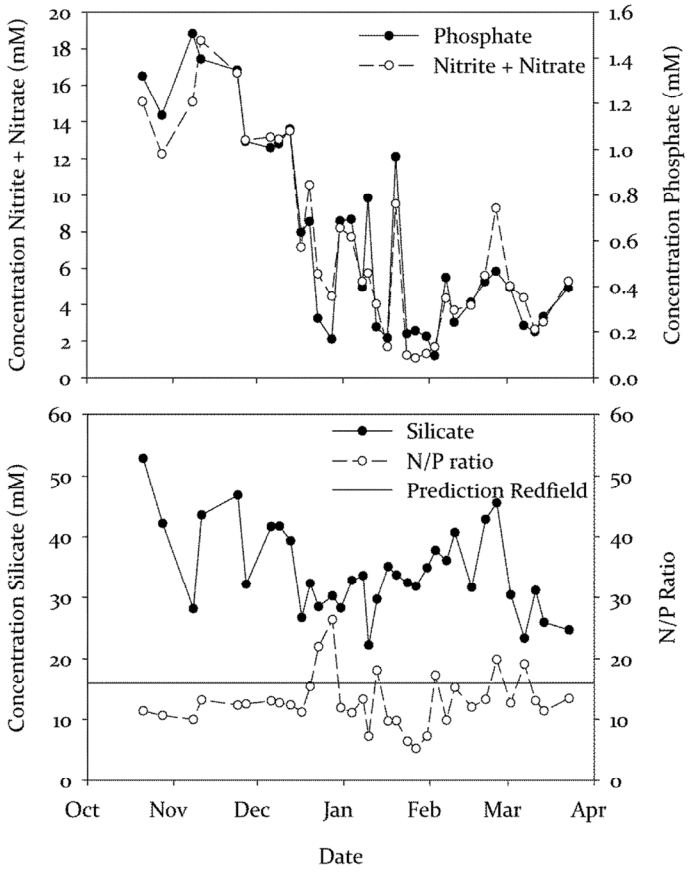

Fig. 4: Concentrations of macronutrients ((Top) Nitrate + Nitrite (black dots), Phosphate (white dots) and (Bottom) Silicate) as measured at 15 m in µM. The bottom graph has the N/P ratios included. N in this ratio is Nitrate + Nitrite. The solid line marks the classical Redfield ratio (Redfield, 1958).

low throughout the season. During the first Chl-a peak, diatoms became the dominant phytoplankton group. This group remained dominant until the end of the summer. Relative contributions of cryptophytes and haptophytes remained low during summer although three modest temporary increases in absolute cryptophyte abundance occurred. These increases coincided with observed dynamics in Chl-a although the contribution of cryptophytes peaked at 1.02 µg Chl-a l^{-1}. Absolute haptophyte abundance only increased once (to 0.28 µg Chl-a l^{-1}) during the period of the highest Chl-a concentration (January 20).

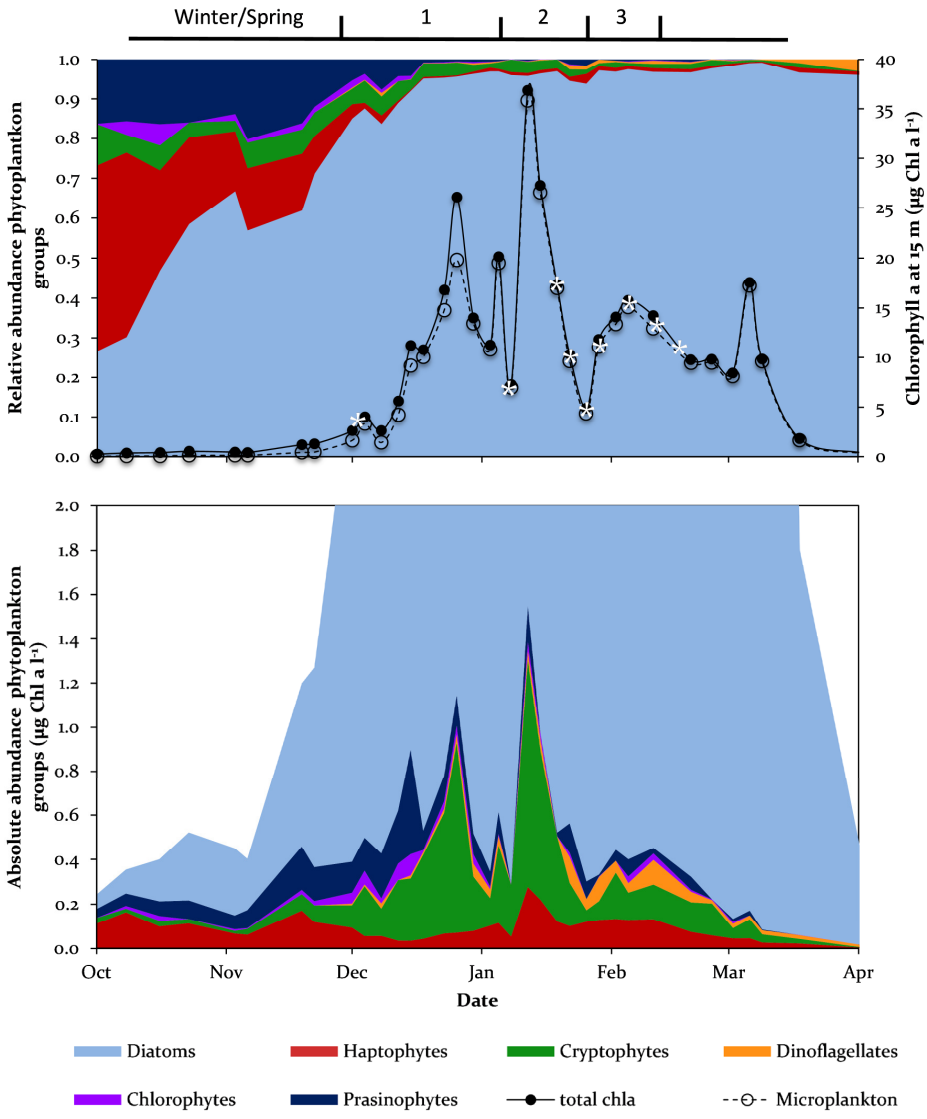

Fig. 5: Phytoplankton biomass and composition based on HPLC measurements analysed with CHEMTAX. Total Chl-a is indicated by the solid line. The fraction microplankton is indicated by the dashed line. Asterisks mark DNA sampling days. The different periods in the Antarctic summer, as discussed in 4.1, are marked above the graph.

Molecular fingerprinting: Eukaryotes

DGGE analysis revealed 21 to 34 bands in each sample (Table 1). Evenness ranged from 0.64 to 0.83, and was lowest at the start of summer or when Chl-a was >8 µg l^{-1}. Values for the Simpson index varied little, from 0.92 to 0.95. The dendrogram showed strong

Table 1: Diversity indices retrieved from the DGGE analysis. The parameters were calculated from the number of bands and relative intensity per band per sample. At the bottom, the averages and standard deviations (Stdev) are presented.

	Eukaryotes			Diatoms			Dinoflagellates			Bacteria		
	# Species	Evenness	Simpson	# Species	Evenness	Simpson	# Species	Evenness	Simpson	# Species	Evenness	Simpson
09 Dec	28	0.64	0.93	16	0.56	0.85	20	0.64	0.90	24	0.64	0.92
13 Jan	29	0.77	0.94	15	0.64	0.86	17	0.55	0.84	25	0.69	0.93
24 Jan	26	0.73	0.93	10	0.60	0.77	21	0.70	0.92	21	0.58	0.86
27 Jan	34	0.70	0.95	16	0.63	0.88	17	0.69	0.89	29	0.62	0.92
31 Jan	29	0.79	0.95	8	0.71	0.79	20	0.78	0.92	23	0.80	0.93
03 Feb	21	0.73	0.92	12	0.65	0.83	21	0.74	0.92	21	0.69	0.91
10 Feb	30	0.69	0.93	12	0.68	0.85	24	0.68	0.92	24	0.61	0.90
16 Feb	25	0.68	0.92	16	0.78	0.91	17	0.75	0.90	22	0.67	0.91
21 Feb	27	0.83	0.95	11	0.64	0.82	20	0.74	0.92	20	0.65	0.89
Average	28	0.73	0.94	13	0.65	0.84	20	0.70	0.90	23	0.66	0.91
Stdev	3	0.06	0.01	3	0.06	0.04	2	0.06	0.02	3	0.06	0.02

separation of the December 9 and February 21 samples: both samples deviated highly from the other samples (Fig. 6). Furthermore, one cluster consisted of January 13, 24, 27, 31 and February 3 samples (Euk1). A second cluster consisted of the February 10 and 16 (Euk2) samples. Similarity between clusters Euk1 and 2 was 0.60. Within Euk1 there was a weak indication of two distinct clusters (January 13 and 25 vs January 27, 31 and February 3) but only 39% of the replicates supported this separation. NMDS results did support the observations made with the UPGMA and the minimum spanning tree suggested a pattern of seasonal succession (Fig. 6). The biplot supported the trends in environmental parameters as water temperature increased during January 24 and February 3. The weak separation within the Euk1 UPGMA cluster was apparent in the NMDS. The wind mixing event during the first half of February, followed by a deepening of the MLD, seemed to be the main driver for the separation of clusters Euk1 and 2. The beginning (December 9) and end of the season (February 21) were opposed in both biological and environmental parameters judging from their opposite positions in the NMDS.

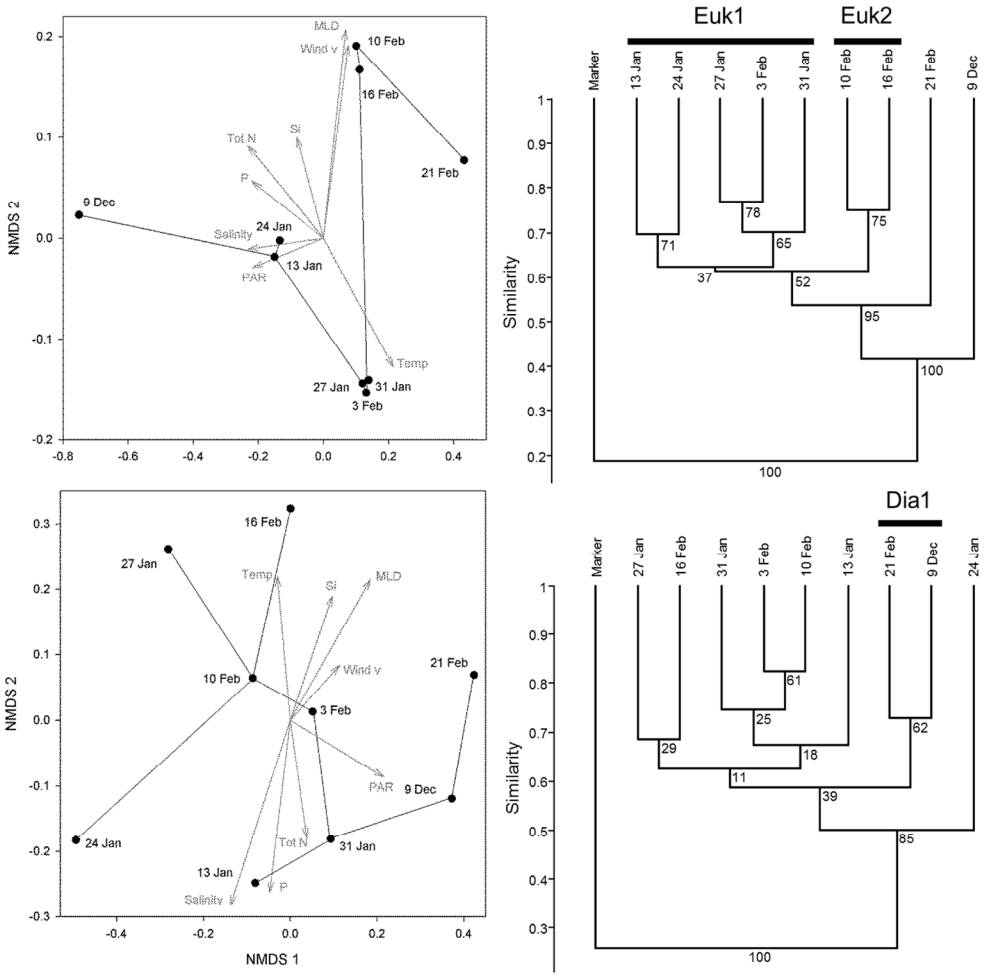

Fig. 6: NMDS biplots (Left) and dendrograms (Right) of eukaryotes (Top) and diatoms (Bottom). Dendrograms and NMDSs' are based on the Bray-Curtis similarity coefficient. Black dots in the NMDS represent the DGGE results for a given sampling event. Grey arrows indicate environmental parameters. Stress according to Shepard plots was 0.20 for eukaryotes and 0.18 for diatoms. Numbers at the branches of the clusters show the bootstrap percentage (n = 1000). Clusters discussed in this paper are marked and named.

Molecular fingerprinting: Diatoms

Each sample contained 8 to 16 diatom-related DGGE bands (Table 1). There was no obvious trend in the Simpson indices but overall values were low (mean = 0.84) and variable (standard deviation = 0.04). The evenness was low, ranging from 0.56 to 0.78, and showed an increasing trend over the duration of the season. The only noteworthy deviation in the average number of diatom species was January 31 (8; mean 12.8). The

diatoms showed weak clustering by date (Fig. 6): only January 24 showed a unique composition. As opposed to the eukaryotes, December 9 and February 21 (Dia1) were moderately similar to each other and dissimilar to the other time points. NMDS supported the weak clustering as observed in the UPGMA as distances between samples appeared to be relatively equal. Of the four NMDSs performed, R^2 (0.71) of the diatoms was lowest. The vectors of the environmental parameters showed no clear trends with the eukaryote fingerprinting results other than salinity and phosphate having the longest vectors.

Molecular fingerprinting: Dinoflagellates

Analysis of the DGGE banding pattern showed a stable community from 17 to 24 species per sample (Table 1). Variability in the Simpson indices was low and thus relatively stable. In contrast, evenness varied more, from 0.55 to 0.78, and slowly increased towards the end of summer. The strongest increase was at the end of January, during the decay of the largest peak in Chl-a and coinciding with an increase in absolute abundance of dinoflagellates as derived from pigment analysis. The dendrogram revealed three unique communities: December 9, January 13 and February 21 (Fig. 7). Community composition was relatively stable during the period from January 24 to February 16, with all communities showing >65% similarity. Most samples were oriented along the vertical axis in the NMDS, where salinity and MLD were found to be most strongly correlated (Fig. 7).

Molecular fingerprinting: Bacteria

The number of bands observed in the DGGE gel ranged from 21 to 29 per sample (Table 1) with the highest number on January 27, slightly decreasing over the course of the summer. Overall, Simpson indices first increased during December and January reaching a peak value on January 31, thereafter diversity decreased slightly (min-max = 0.86-0.93). Interestingly, the lowest diversity was also observed in the second half of January, namely January 24. Evenness ranged from 0.58 to 0.80. The highest value was measured on January 31 and coincided with low phytoplankton biomass. The dendrogram showed clustering of the samples of December 9 and January 13 (Bac1; Fig. 7). Similarity between the two samples was 0.69. A second cluster consisted of January 24 and 27 samples (Bac2) while a third cluster included samples taken on January 31

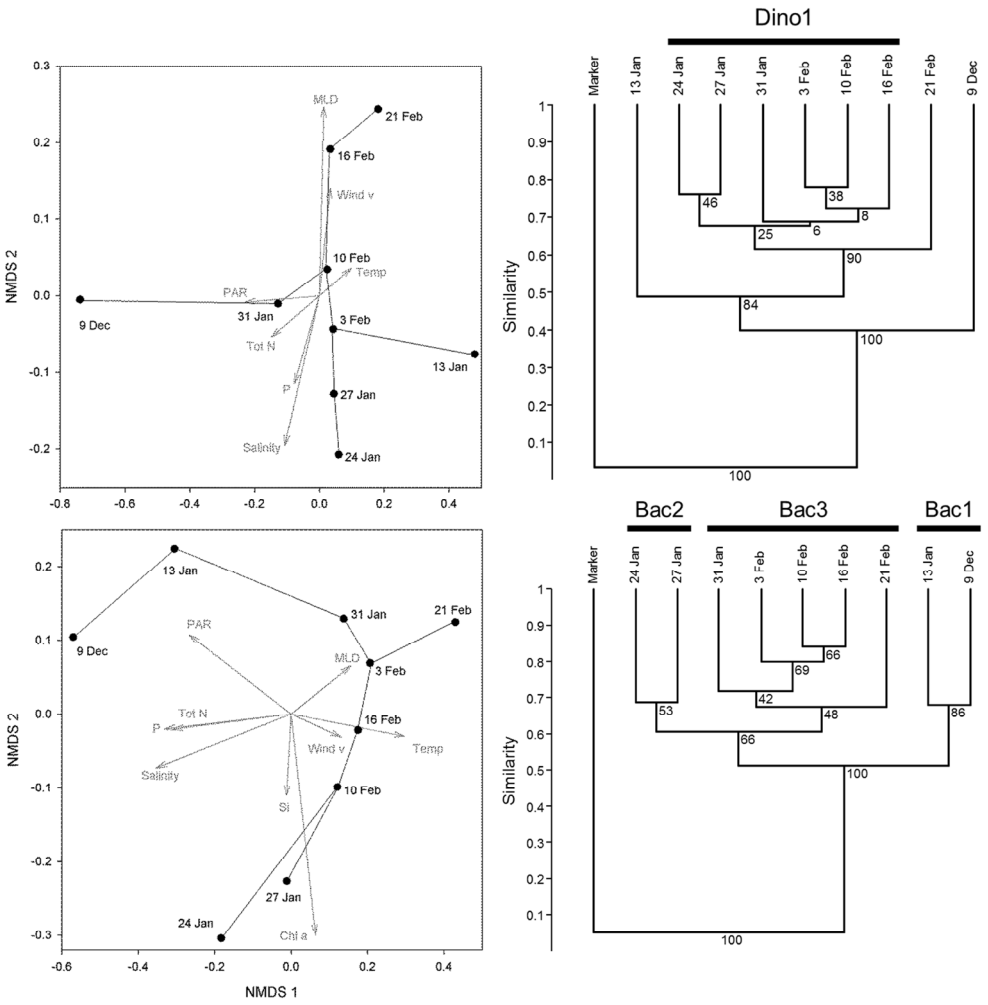

Fig. 7: NMDS biplots (Left) and dendrograms (Right) of dinoflagellates (Top) and Bacteria (Bottom). Dendrograms and NMDSs' are based on the Bray-Curtis similarity coefficient. Black dots in the NMDS represent the DGGE results for a given sampling event. Stress according to Shepard plots was 0.06 for dinoflagellates and 0.10 for bacteria. Grey arrows indicate environmental parameters. Numbers at the branches of the clusters show the bootstrap percentage (n = 1000). Clusters discussed in this paper are marked and named.

and February 3, 10 and 16 (Bac3). February 21 clustered with Bac3 for 48% of the permutations. The similarity between clusters Bac2 and 3 was 0.60. NMDS showed a strong correlation between Chl-a and bacterial community composition. Furthermore, the remaining vectors suggested a similar distribution as observed in the eukaryote NMDS. The minimum spanning tree showed relative large distances between the

sampling dates, fully supporting the clustering proposed in the UPGMA. The biplot showed clustering of January 24 and 27, mainly driven by phytoplankton biomass (Fig. 7). December 9 and January 13 clustered based on high PAR and elevated nutrient concentrations.

Eukaryotic sequences

The total number of observed nodes to which sequences could be assigned with a ≥95% similarity was 45, 49 and 50 in December, January and February respectively. Species evenness was generally low, but highest in December (0.26) with respect to the two later samples (0.20 and 0.15). Simpson indices followed the same trend as evenness and dropped from 0.84 to 0.75. Results of the eukaryotic sequences support the clustering as shown by DGGE analysis. January 27 and February 16 samples were more similar in community composition (73%) in comparison to December 9 (42%, UPGMA, data not shown). December 9 was dominated by unknown pennate diatoms (Bacillariophyceae), which were hardly observed in the two later samples (Table 2). In contrast, polar centrics (Mediophyceae), represented by the genera *Thalassiosira* and *Chaetoceros,* increased in abundance in the three consecutive samples (Fig. 8). Radial centrics (Coscinodiscophyceae) were hardly observed and only represented by *Stellarima microtrias.* Haptophytes were the only representatives of the Prymnesiophyceae. Their abundances were lowest on December 9 (0.6%) and doubled in the following two samples (1.21-1.24%). Also, cryptophytes were only represented by the order of Cryptomonadales and slightly decreased from 1.59 to 0.08% during the summer. Dinoflagellates were observed in high numbers throughout the season. The maximum percentage of sequences allocated for dinoflagellates (or Alveolata, Dinophyceae, Gymnodiniphycidae) was on January 27 with 34.49% while only 20.04 and 21.06% of the sequences were related to dinoflagellates on respectively December 9 and February 16. Both MAST-4 and MAST-1 stramenopiles were observed. The first group had 3.21% of the sequences on December 9 and decreased to <0.25% for the later samples. Mast-1 remained constant at ~0.4% of the sequences.

Apart from heterotrophic dinoflagellates, the non-photosynthesizing community was represented most significantly by species from the order *Maxillopoda* to which the suborder Copepoda belongs (Table 2). While almost absent in December (0.05%) and

Table 2: Dominant eukaryote genera which represent nodes observed >1% of the total number of sequences of the three samples combined. All numbers are percentages and the sum per sample is presented at the bottom.

	Sampling Date		
	9 Dec	27 Jan	16 Feb
Thalassiosira	15.83	36.75	46.36
Unassigned Bacillariophyceae	33.74	0.72	4.03
Unassigned Alveolata	4.73	12.97	8.05
Unassigned Mediophyceae	3.53	5.44	14.07
Unassigned Dinophyceae	10.27	5.54	1.95
Unassigned Gymnodiniphycidae	2.36	10.68	4.38
Unassigned Dinoflagellata	2.68	5.30	6.68
Maxillopoda	0.05	8.44	0.50
Unassigned Eukaryotes	1.24	1.77	3.84
Unassigned Animalia	0.47	2.68	1.11
Chaetoceros	0.52	1.21	2.37
Mast-4 Stramenopiles	3.20	0.15	0.39
Unassigned Stramenopiles	3.44	0.06	0.08
Unassigned Bacillariophytina	3.21	0.10	0.23
Unassigned Prymnesiophyceae	0.60	1.21	1.24
Unassigned Choreotrichia	2.01	0.29	0.11
Protaspa	2.05	0.21	0.11
Unassigned Thecofilosea	1.13	0.60	0.48
Unassigned Cryptomonadales	1.59	0.20	0.08
Stellarima microtrias	0.08	1.38	0.31
Unassigned Diatomea	0.90	0.30	0.55
Unassigned Oligotrichia	1.12	0.19	0.26
Unassigned Syndiniales Group I	1.32	0.07	0.13
MAST-1 Stramenopiles	0.45	0.37	0.43
Sum	**96.52**	**96.63**	**97.74**
Total sequences entire sample	63493	53079	35361

January (0.50%), it was well represented in February where 8.44% of the sequences were allocated to this order. Further potential grazers were ciliates belonging to Oligotrichia and Choreotrichia (possibly including tintinnids), and both groups were most abundant (max 2.01%) on December 9. Finally, two nodes with single-celled

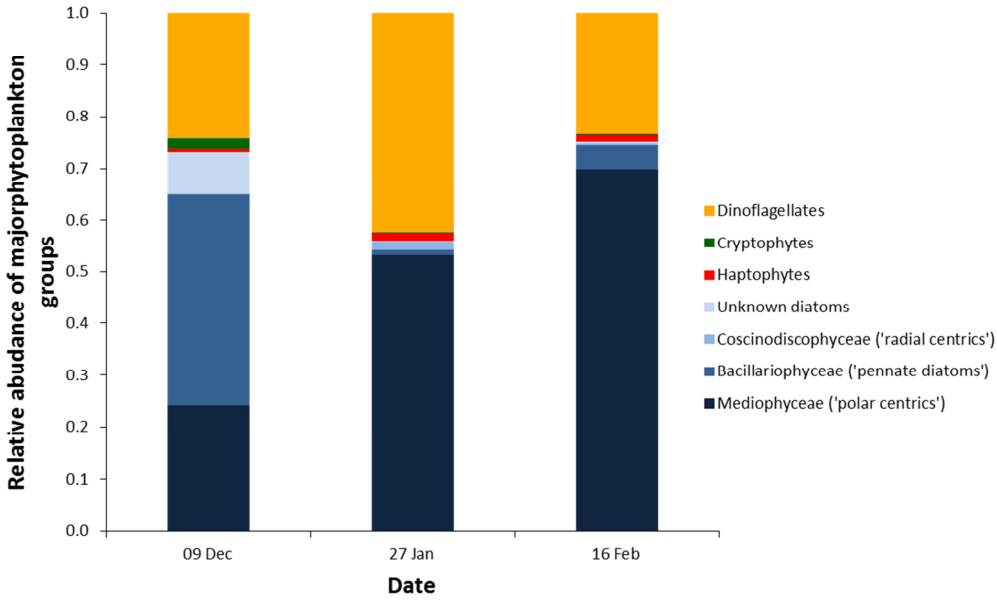

Fig. 8: DNA sequences shown per major phytoplankton group. The diatom groups are segregated into their order when possible. More descriptive names (Polar, pennate and radial centric diatoms) are given in the legend as derived from Medlin and Kaczmarska (2004).

amoeboid protists were observed, including *Protaspa*, belonging to the class of Thecofilosea. The relative abundance of amoebas was highest on December 9 and decreased during the season. A dinoflagellate endosymbiont (Syndiniales group 1) completed the list of nodes with >1% of the sequences but the only noteworthy contribution was on December 9 (1.32%).

Bacterial sequences

The majority (60-75%) of the sequence reads obtained using the Bacteria specific primers could be assigned as chloroplasts and were ignored in further analysis of bacterial diversity. The most abundant groups of the remaining sequences were assigned as Proteobacteria and Bacteroidetes (data not shown). A significant part of the sequences (2-11%) could not be assigned at the phylum level. Actinobacteria, Deferribacter, Firmicutes, BD1-5 and Verrucomicrobia were present in low numbers while Cyanobacteria were not observed in these samples. The contribution of Proteobacteria was highest in early December declining from near 90% of the total

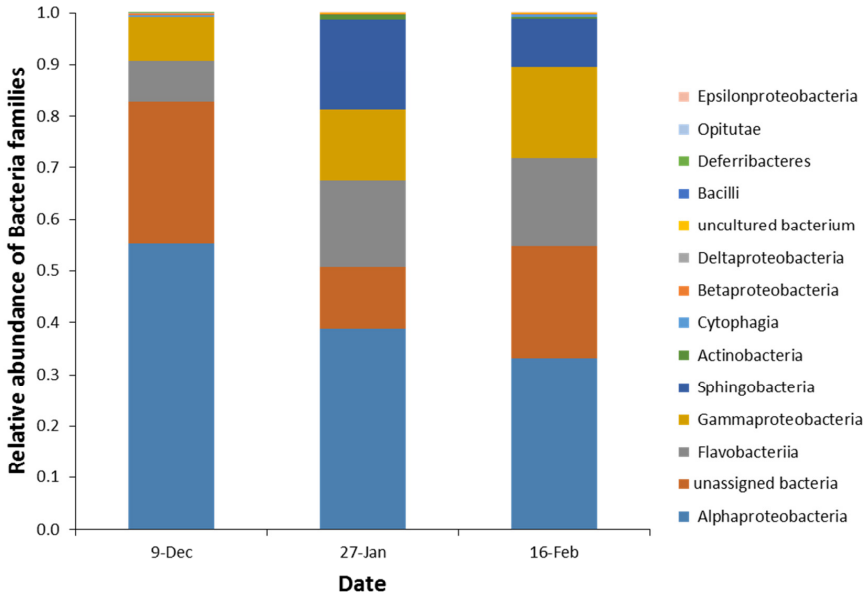

Fig. 9: Bacterial community composition derived from 16S rRNA gene amplicon sequencing analysis. Stacked column graph represents the relative distribution of the dominant classes at the different time points. The total number of sequence reads was 63493, 53079 and 35361 per sample for respectively 9 December, January 27 and February 16.

abundance to 61% while Bacteroidetes increased from 8 to near 30%. At the Class level, the Alphaproteobacteria was the most dominant group at all time points, followed by unassigned bacteria: Flavobacteria, Gammaproteobacteria and Sphingobacteria (Fig. 9). In contrast to the steady decrease in abundance observed in the Alphaproteobacteria, the Gammaproteobacteria nearly doubled their abundance towards the end of summer. Flavobacteria also doubled towards the end of summer, while Sphingobacteria (which were nearly absent in early summer) increased to 17% during mid-summer and declined to 9% at the end of summer. Actinobacteria also peaked during mid-summer (from 0.1% to nearly 1 %). In contrast, the unassigned group of Bacteria revealed a lowest abundance at mid-summer. At the order level, the SAR11 clade of the Alphaproteobacteria was the most abundant decreasing in relative contribution from 19 to 5% during the summer whereas the second most abundant order within the Alphaproteobacteria, the Rhodobacterales, increased from 2.8 to ~5.4% during summer. Among the Gammaproteobacteria, the Oceanospirillales were

most abundant, steadily declining in relative abundance over time (from 3.2, 2.1 to 1.3%).

Discussion

Our study involved the first multi-primer approach to analyse microbial community changes as a function of Antarctic environmental conditions. Molecular fingerprinting methods such as DGGE have their limitations, such as over- or underestimating rRNA gene copy numbers which is further biased when PCR is involved (Muyzer, 1999). There is a limit at which DGGE can successfully separate bands derived from different species and a potential for multiple bands belonging to one species, as discussed in Neilson et al. (2013). Yet even with the known pitfalls it has been successfully used to study microbial communities in polar regions (Díez *et al.*, 2004; Gast *et al.*, 2004; Piquet *et al.*, 2008, 2011; Ghiglione & Murray, 2012). Current high-throughput DNA rRNA amplicon sequencing techniques could potentially analyse microbial communities at a higher resolution and identify organisms at or below the genus level depending on the gene or gene fragment of interest. However, such identification depends on coverage and annotation of the extant diversity, well-chosen primer sets and well maintained, curated databases for reference. The database is especially limited with regards to the oceanic micro-eukaryotes. In addition, shifts in the classical microscope-based phylogeny due to DNA based efforts further amplify the challenge of annotation to the species level (Medlin & Kaczmarska, 2004). Finally, species in extreme environments, such as ours, are often underrepresented in the reference databases. However, if supplemented with the classical taxon-specific pigment markers as proxies for phytoplankton group abundances, sequence results can give additional insights into ecologically relevant processes. For example, the pico-eukaryotes diversity and dynamics can now be studied more accurately (Yu *et al.*, 2015).

Phytoplankton community dynamics

During spring, the observed dominance of haptophytes could have been due to deep mixing of the water column during the winter months (Montes-Hugo *et al.*, 2009) in combination with the absence of sea ice (Venables *et al.*, 2013; Rozema *et al.*, 2017a). Persistence of the winter/spring community was suggested to depend on the timing of water column freshening (Rozema *et al.*, 2017a). In contrast, diatoms dominated during

summer as found earlier (Buma *et al.*, 2001; Garibotti *et al.*, 2005; Clarke *et al.*, 2008; Piquet *et al.*, 2011; Luria *et al.*, 2014). Our finding that stratification mainly governs phytoplankton succession in northern Marguerite Bay is in general agreement with earlier studies at the RaTS site (Piquet *et al.*, 2011; Rozema *et al.*, 2017a). However, the influence of deviations from the expected N/P ratio adds a new perspective to phytoplankton community dynamics in northern Marguerite Bay.

After the first sampling date (December 9th), the observed increase in phytoplankton biomass coincided with enhanced meteoric water input. This increase was likely caused by pennate diatoms, which are more often associated with early season phytoplankton communities and sea-ice melting (period 1; Fig. 5 and 8; Annett et al., 2010; Ligowski et al., 1992; Pike et al., 2009). However, given the absence of sea ice in the period of investigation, it is not likely that the dominance of this group was derived from local sea-ice seeding. Increasing N/P ratios during this stage were possibly indicative of a mild limitation in micronutrients despite sufficient availability of macronutrients (Takeda, 1998). The wind-induced mixing event at the end of December and not a possible limitation in nutrients, was likely to end the period of phytoplankton growth (Bown *et al.*, 2017). Despite this mixing, no shift towards *P. antarctica* (haptophytes as calculated by CHEMTAX (Fig. 5)) or cryptophytes was observed at 15 m. Apparently, relative diatom abundance was high enough to overcome short mixing events and prevented the establishment of groups more commonly associated with an unstable water column (Kozlowski et al ., 2011; Montes-Hugo et al., 2009; Rozema et al., 2016). This was further supported by size-fractionated Chl-a as phytoplankton consisted almost entirely of >20 µm cells until mid-January (Fig. 5).

The second period (Fig. 5) was characterized by a meltwater lens shallower than 5m (Fig. 2). The resultant strongly stratified water column could have stimulated biomass accumulation at 15 m. With 40% of the sequences (Table 2) allocated to the polar centrics, particularly belonging to the genus *Thalassiosira*, the phytoplankton community had changed significantly in contrast to the December sample. *Thalassiosira* species in this area were frequently observed and described in earlier studies (Garibotti *et al.*, 2005; Annett *et al.*, 2010; Piquet *et al.*, 2011). The presence and high abundance of *Thalassiosira* genus was as expected given the global distribution

and frequent observations in the coastal and open regions in the Southern Ocean (Armbrust, 2009; Díez et al., 2004; Ducklow et al., 2012a; Pike et al., 2009; Piquet et al., 2008). As the MLD remained stable after the Chl-a peak, other factors must have caused the collapse of the bloom from January 17. While macronutrient concentrations were low, but not depleted (Fig. 4), N/P ratios decreased strongly (5.3 on January 27) after the peak in phytoplankton biomass. This decrease might suggest that low nitrogen availability prevented the persistence of the phytoplankton bloom. Yet, the NMDS analysis did not support this. Also, limitation by micronutrients or biomass loss due to grazing cannot be excluded (Behrenfeld, 2010; Bown *et al.*, 2017).

During the third period (February 3-21) diatom dominated biomass increased to moderate levels. An increase in wind speed, and thus MLD, coincided with a strong decrease in salinity in the top 15 m due to meteoric water input (Fig. 3 and 5). Pennate diatoms underwent a relatively larger increase in relative abundance (0.72% to 4.03%) than polar centric diatoms (43.4% to 62.8%; Fig. 8), while radial centric diatoms decreased in relative contribution. Possibly, the continuously changing MLD, generally marking the end of summer, strongly shaped this changing community (Venables *et al.*, 2013). There was no indication of limitation by nutrients, thus grazing or, more likely, light limitation prevented the build-up of large phytoplankton stocks.

Grazers and dinoflagellates

Sequencing results showed the presence of various grazers which were also reported in earlier microscopy and molecular (clone libraries) investigations of the eukaryotic community of Ryder Bay (Annett *et al.*, 2010; Piquet *et al.*, 2011) and Southern Ocean (Dolan *et al.*, 2013; Georges *et al.*, 2014). While half of the microplankton biomass in marine systems can consist of heterotrophic dinoflagellates (Sherr & Sherr, 2007), early efforts using pyrosequencing showed that most of the sequences north of the Polar Front were derived from dinoflagellates. South of the Polar Front they decreased in observed frequency and contributed ~30% to the total number of reads (Wolf *et al.*, 2013). In our study dinoflagellate-related pigments were hardly observed throughout the summer season. Possibly, Antarctic dinoflagellates were underestimated by CHEMTAX as many species might have been categorized as haptophytes. Yet, as haptophytes abundances during summer were low, a potentially mislabelled

dinoflagellate component would not alter our conclusions on relative phytoplankton abundances significantly (Fig. 5). In contrast, we found 20 to 35% of our eukaryote sequences to be assigned to dinoflagellates. This discrepancy suggests a dominance of heterotrophic dinoflagellates with only a minor contribution of autotrophs. However we have to keep in mind abundance estimates based on sequences are not easily translated to multicellular organisms or organisms with high copy numbers of the gene used for barcoding, such as dinoflagellates (Zhu *et al.*, 2005). As a result, an overestimation of dinoflagellate abundance based on sequence data is possible. Annett et al. (2010) found that dinoflagellates (auto- and heterotrophic) abundances were low in Ryder Bay. Yet, given the large size of some species and relative high C content they could still contribute significantly to microbial biomass. Therefore, detailed studies on dinoflagellate dynamics might benefit from a combination of chemotaxonomic, microscopic and molecular approaches.

Bacterial community

Community fingerprints of samples collected on December 9 and January 13 clustered and these bacteria most likely originated from the winter/spring community (Fig. 7). The later January (24 and 27) samples appear to have responded to the peak in Chl-a in period 1, while the bacterial samples collected thereafter indicated a response of the bacterial community to the seasonal high in Chl-a during period 2. The February 21 sample was similar to the previous cluster (Jan 31 – Feb 16) mimicking the high similarity between succession in the photosynthetic community, albeit with a delay. The bacterial communities frequently correspond with a lag-phase to phytoplankton biomass and composition (Piquet *et al.*, 2011; Ghiglione & Murray, 2012). The bacterial community in the BAC3 clustered appeared to have played a pivotal role in remineralizing major nutrients as these were increasing despite increasing phytoplankton biomass (Landa *et al.*, 2016). This source of nutrients replenishment, in combination with vertical mixing, presumably allowed for renewed phytoplankton growth after a large bloom. Based on our UPGMA results (grouping of January 13 in BAC and EUK clusters) we estimated a lag phase between phytoplankton peak in Chl-a and bacterial response of 1 to 2 weeks, however, care must be taken given the limited data set. Moran et al., (2001) showed that bacterial production was coupled to recently

produced DOC by algae and thus related to primary production. Ducklow et al. (2012b) also showed the coupling between Bacteria and phytoplankton based on correlations between leucine incorporation rates and both primary production and Chl-a. That study showed a stronger correlation between bacterial biomass and Chl-a than with primary production which confirms our finding of Chl-a concentration being important in bacterial community composition (Fig. 7). Our data are supported by earlier findings of Piquet et al. (2011), where the bacterial community was found be influenced by the factors that also shaped the eukaryotic community, in particular stratification and mixing, although Chl-a was excluded in the previous study.

Alphaproteobacteria and Bacteroidetes dominance (Fig. 9) is in agreement with other studies that confirm their ubiquitous presence in the Southern Ocean and Antarctic coastal sites (Gentile *et al.*, 2006; Straza *et al.*, 2010; Piquet *et al.*, 2011; Ghiglione & Murray, 2012; Luria *et al.*, 2014). Alphaproteobacteria, especially the ubiquitous SAR11 clade were abundant in mid-December in our study. The low light conditions during the transition between Antarctic summer and winter may favour the photoheterotrophic SAR11 group over other bacterial groups. In contrast, during late spring and summer they would be outcompeted for light by eukaryotic phytoplankton (Ducklow *et al.*, 2007; Grzymski *et al.*, 2012; Williams *et al.*, 2012). In addition, relative haptophyte abundance was high after the winter and thus surface waters could be enriched with dissolved low molecular weight compounds such as DMSP. Previous observations have coupled the metabolically diverse generalists of the alphaproteobacterial class with decaying algal blooms releasing dissolved low molecular weight compounds such as DMSP (Malmstrom *et al.*, 2004; Curson *et al.*, 2008; Reisch *et al.*, 2011). The initial abundance of Alphaproteobacteria could be related to the release of low molecular weight carbon sources by haptophytes which is followed by a later response of the Bacteroidetes to diatom dominance in summer. Bacteroidetes relative abundance increased after two periods of high Chl-a dominated by diatoms at the end December and in January (periods 1 & 2; Fig. 5). A proposed preference of Bacteroidetes species for high molecular weight carbon compounds was recently confirmed by genomic analysis of several Bacteroidetes strains (Fernández-Gómez *et al.*, 2013). This might also explain why Actinobacteria, also specialized in the

degradation of high molecular weight carbon, displayed a similar trend as the Bacteroidetes.

Group specific variability

Variability in response times differed between the various groups of microorganism studies here. Not only did we observe a lag phase in the response of the bacteria when confronted with a changing phytoplankton community after the collapse of a bloom but also between different eukaryotic groups. The trends observed for the general eukaryotes were different than those of the diatoms and dinoflagellates (Fig. 6 & 7) while more similarity was initially expected. Variability in these latter two groups was less than observed in the general eukaryotes (Table 1). A possible explanation might be related to the choice of methodology. DGGE (and PCR) is a good, frequently-used technique for describing species represented by more than ~1% of the environmental DNA. Thus, a particular portion of the ecosystem was described when using primers for general eukaryotes as this includes grazers, dinoflagellates, diatoms, and many other groups varying in amounts of DNA. To be present in the DNA the species need to have a large copy number of the gene or be highly abundant ("blooming"). The specific primers for diatoms and dinoflagellates are more likely to include "all" species present, including those with at low abundance (<~1%). The low abundance species might have been missed by the general eukaryote primers. As such, responses to environmental conditions of the specific groups will be less clear as the capabilities of DGGE for quantitative analysis are mediocre. Thus, we conclude that the eukaryotic community changes, from picophytoplankton to large grazers, respond to larger environmental shifts. The decreased variability in the specific groups illustrates the plasticity of the eukaryotic microbial community improving resilience of the ecosystem in an extreme environment (Barton *et al.*, 2010).

Current and future implications

Our hypothesis that phytoplankton succession is governed by periods of enhanced water column stability was confirmed by our study. It is well established that meltwater input affects Antarctic phytoplankton biomass accumulation through the increase in stratification, consequential alteration of the light and mixing regime and potential iron enrichment (Dierssen *et al.*, 2002; Alderkamp *et al.*, 2012b; Saba *et al.*,

2014). Furthermore, as hypothesized, limitation by macronutrients was not observed. Finally, as hypothesized, the bacterial community showed a delayed response to shifts in phytoplankton community composition. The summer of 2010-2011 investigated in the present study was relatively warm compared with previous years, and characterized by the absence of sea-ice cover and high meteoric water input, inferred to be predominantly from glacial origin. These conditions clearly led to a diatom dominated phytoplankton assemblage throughout the summer. In contrast, years characterized by low phytoplankton biomass were found to be dominated by *P. antarctica* and/or cryptophytes, most likely resulting from an unstable water column due to the absence of sea ice in the preceding winter (Rozema *et al.*, 2017a). Our study represented what appeared to be a typical Antarctic summer with average levels of phytoplankton biomass (Rozema *et al.*, 2017a). The discussed dynamics might be different in summers when relative diatom contributions and phytoplankton biomass are low.

The future climatic evolution of the WAP is not easy to predict, however further increases in glacial discharge are likely (Cook *et al.*, 2016). As a result shifts in the phytoplankton community might occur, such as a decrease in average phytoplankton size (Moline *et al.*, 2004; Montes-Hugo *et al.*, 2009; Saba *et al.*, 2014). This shift in size classes might be due to a decrease in diatoms and an increase in cryptophytes and/or haptophytes (Arrigo *et al.*, 1999; Moline *et al.*, 2004; Saba *et al.*, 2014; Rozema *et al.*, 2017a). Yet, despite a steady increase of glacial meltwater, increased cryptophyte abundances during summer stratification were not observed in our study, at least not at the depth of our interest where glacial influences were still observed (Fig. 3 and 5; Table 2). Depth resolved variability in microbial community composition at the RaTS was studied during more recent summer seasons. The shift from diatoms to cryptophytes could affect the bacterial community and important consumers such as krill, since krill prefers diatoms as their primary food source (Haberman *et al.*, 2003). Krill forms the main trophic link to higher levels within the Antarctic food web (Atkinson *et al.*, 2004; Trivelpiece *et al.*, 2011). Thus, changes in the phytoplankton community could affect the entire Antarctic food web. We have shown that the reduction of MLD during summer, as caused by meltwater-related surface

stratification, promotes a succession in diatoms rather than (nano)phytoflagellates in northern Marguerite Bay. This might favour higher trophic levels, in particular after relatively warm winters with low sea-ice cover, where phytoplankton dynamics could otherwise be characterised by lower biomass throughout and the dominance of less-edible phytoflagellate groups (Haberman *et al.*, 2003; Saba *et al.*, 2014).

Acknowledgements

We would like to thank the Marine Assistants and other staff at Rothera and in Cambridge who have contributed to the collection of the samples and data used here. Also, we thank Ronald Visser for his assistance with HPLC analyses. Corina Brussaard is thanked for a valued discussion of an early draft of the manuscript. Finally, we would like to thank the editors, Simon Wright and two anonymous reviewers for their insights and helpful suggestions on improving this paper. This research was funded by the Dutch Polar Programme (866.10.105). Funding for the RaTS programme is from the Natural Environment Research Council, and is a component of the BAS Polar Oceans programme.

Apendices are available online and/or upon request.

4

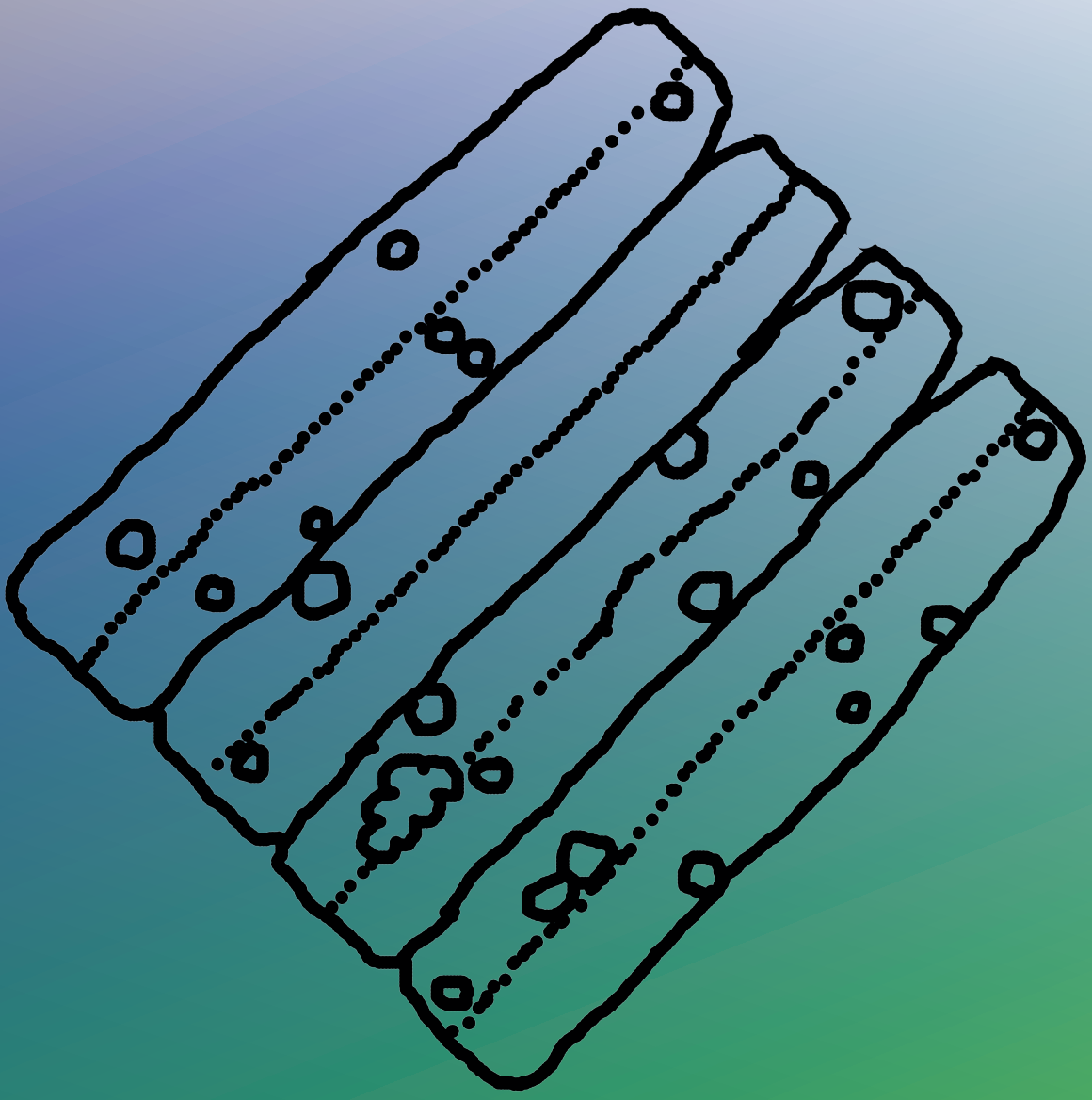

Chapter 5

Bioactive trace metal time series during Austral summer in Ryder Bay, Western Antarctic Peninsula.

J. Bown
P. Laan
S. Ossebaar
K. Bakker
P. D. Rozema
H. J. W. de Baar

Published in:
Deep Sea Research Part II:
Topical Studies in Oceanography (2017)

Abstract

The Western Antarctic Peninsula, one of the most productive regions of the Southern Ocean, is currently affected by the increasing of atmospheric and oceanic temperatures. For several decades, the Rothera Time Series (RaTS) site located in Ryder Bay has been monitored by the British Antarctic Survey and has shown long lasting phytoplankton summer blooms (over a month) that are likely driven by the length of the sea ice season. The dynamics of phytoplankton blooms in Ryder Bay may just as well be influenced by natural fertilization of iron and other bioactive trace metals due to the proximity of land, islands and glaciers. For the first time, temporal distributions in the surface layer (0-75 m depth) of six bioactive trace metals (dissolved: Fe, Mn, Zn, Cd, Cu and dissolved labile Co) have been investigated with high temporal and spatial resolution at the RaTS site during a total of ~2 and 3.5 months respectively, over two consecutive summers. Most of the studied trace elements showed wide ranges of concentrations and this dynamics appears to be driven by phytoplankton uptake, remineralization and occasional vertical mixing associated with storm episodes. The biological uptake of DMn, DZn, DCd, DCo_L and DCu was proportional to uptake of phosphate and silicate, which was associated with weak to strong linear relationships depending on which phytoplankton bloom events was considered. This further suggests that the surface water distributions of these studied bio-active trace metals were mainly driven by biological uptake and remineralization during austral spring and summer in Ryder Bay. Even though DFe didn't show any strong relationship with phosphate, DFe decreasing concentrations during each bloom event suggest that Fe is a key essential element for phytoplankton in the area of study. The consistency of trace metals / nutrient ratios during two consecutive summers indicates that over-winter scavenging removal was slow relative to mixing. The increase of DCd/P and DCo_L/P drawdown ratios during the two consecutive blooms monitored during the second season could reflect the substitution of DZn by trace metals DCd and DCo_L due to lowered DZn concentrations after the first bloom. Relationships of trace elements versus silicate appear to be dominated by diatoms abundances which tend to vary both at the season and bloom time scale.

Simultaneous short-term events of depletions of both nutrients and bio-active trace metals might induce stress in the growth of the phytoplankton assemblage.

Introduction

The Western Antarctic Peninsula (WAP) is a highly productive region that supports high abundances of phytoplankton (Arrigo *et al.*, 2008; Clarke *et al.*, 2008). The WAP is currently affected by increasing temperatures of air and seawater and these changes can impact on primary production, for example via modifying seawater composition and hydrological characteristics. These increased temperatures are indeed associated to shifts in the wind pattern that have affected the length of the sea ice season along the WAP (Venables *et al.*, 2013). This net loss of winter sea ice is likely to drive a downward trend in the magnitude of phytoplankton blooms in Ryder Bay (Venables *et al.*, 2013).

The primary productivity of the WAP coastal waters can also be impacted by supply of trace nutrients due to the presence and the intensity of major local sources. This is in contrast with the offshore Southern Ocean that is a High Nutrient Low Chlorophyll area due to lack of essential trace nutrient iron (Fe) (de Baar *et al.*, 1995). Antarctic continental shelves have been depicted as a significant source of Fe for coastal waters (Ardelan *et al.*, 2010; Hatta *et al.*, 2013) and more offshore areas of the Southern Ocean (De Jong et al., 2012; Dulaiova et al., 2009; Klunder et al., 2014 their Fig. 9). In Pine Island Bay, glacier melt has been shown to be the predominant Fe source that can sustain phytoplankton bloom by lateral advection of Fe over 150 km distance (Gerringa *et al.*, 2012). A recent study conducted in the Amundsen Sea Polynya also showed that meltwater enriched seawater was the dominant source of Fe for surface waters (Sherrell *et al.*, 2015). These results are different from the Ross Sea which is known to be subject to seasonal iron limitation (Sedwick *et al.*, 2000). Recently Gerringa et al. (2015) reported very low dissolved Fe (0.02-0.08 nM) in the upper 100m of the water column of the Ross Sea in austral spring (20 December - 5 January).

In Ryder Bay, one preceding study at RaTS site showed that total dissolvable iron concentrations should be high enough to support primary production (10-50 μmol m^{-3} (nM); Weston et al., 2013) and the other that the dissolved iron concentrations indicate

that Fe supply from deep water is sufficient to meet biological demand relative to macronutrient supply (Annett *et al.*, 2015). Therefore Fe limitation was deemed unlikely in this region even without additional summer Fe inputs from glacial sources (Annett *et al.*, 2015).

In addition to Fe, other trace elements such as Mn, Cd, Zn and Co are known to be involved in biological functions (de Baar & La Roche, 2003) and therefore are essential for phytoplankton growth. Very few studies have been focused on these essential trace elements in coastal waters or nearby the ice shelf of Antarctica (Grotti *et al.*, 2001; Hendry *et al.*, 2008; Saito *et al.*, 2010; Noble *et al.*, 2013; Sherrell *et al.*, 2015). During Austral summer the surface distributions of DMn, DZn, DCd, DCo and DCu have been shown to be mainly driven by distinct sources and sinks depending on the characteristics of the region of study. External sources such as sediments resuspension in Amundsen Sea Polynya and atmospheric inputs in Terra Nova Bay are thought to be important sources for Mn in surface waters (Grotti *et al.*, 2001; Sherrell *et al.*, 2015). In a different manner, Zn and Cu have shown to have small to negligible sources on the shelf (Sherrell *et al.*, 2015) while remineralization is described as the main internal source. In McMurdo Sound region, the sea-ice could also be a source for Mn and Co when associated to water-column mixing occurring faster than scavenging processes (Noble *et al.*, 2013) while when sea ice melt in East Antarctica, the supply to surface waters of trace elements other than Fe is most likely insignificant (Lannuzel *et al.*, 2011). Removal of DCd, DZn, DCu and DCo was generally associated to biological activity in the Ross Sea and in Amundsen Polynya (Saito *et al.*, 2010; Sherrell *et al.*, 2015) but also, in late bloom conditions, with strong scavenging on biogenic sinking particles (Sherrell *et al.*, 2015).

Here we present concentrations of dissolved iron (DFe), manganese (DMn), zinc (DZn), cadmium (DCd), copper (DCu) and dissolved labile cobalt (DCo_L) measured at the RaTS site during the second half of Austral summer 2013 (from January to March) and during summer 2014 (late November - late February). The main objective is to describe the concentration dynamics of DFe, DMn, DZn, DCd, DCo_L and DCu in the 75 m deep surface layer, with an eye to the biological processes that are expected to govern their distribution during different phytoplankton bloom events.

Materials and Methods

Study area

The present study took place during the second half of one austral summer (mid January-March 2013 and referred as season 1, S01) and during most of the next summer season (mid November 2013- end of February 2014, referred as season 2, S02) in Ryder Bay, a shallow (≤~520 m) coastal embayment of Marguerite Bay close to the British Antarctic Survey (BAS) research station Rothera located on Adelaide Island (67°34'S, 68°08'W; Fig. 1). At this time of the year, this region is characterized by phytoplankton blooms dominated by large diatoms (Clarke *et al.*, 2008; Venables *et al.*, 2013) with a magnitude and duration controlled by light, mixing and duration of sea ice (Venables *et al.*, 2013). Net and exportable primary production can be high throughout the summer season (Weston *et al.*, 2013) and can be characterized as a "high recycling, low export" area.

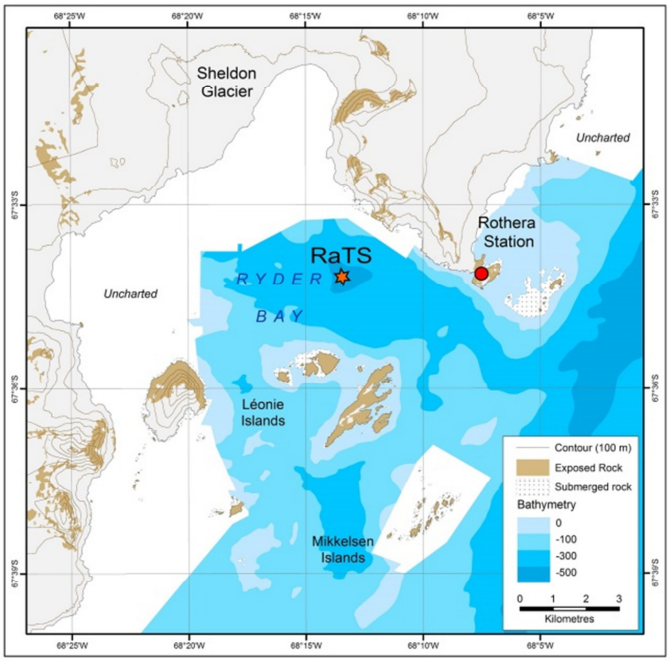

Figure 1: Map of Ryder Bay, Rothera Antarctic Time Series sampling site (RaTS) is marked by an orange star.

Hydrographic features in Marguerite Bay have been previously described (Meredith *et al.*, 2004; Clarke *et al.*, 2008; Martinson *et al.*, 2008; Moffat *et al.*, 2008). Located on the shelf of the Western Antarctic Peninsula, Marguerite Bay is influenced by the warm, salty and high nutrient Circumpolar Deep Water (CDW) that flows around the Antarctic continent in the Antarctic Circumpolar Current (Martinson *et al.*, 2008). This CDW occasionally enters onto the continental shelf following the topography (Clarke *et al.*, 2008; Martinson *et al.*, 2008) and its upper layer, UCDW, is the predominant variety of CDW that can be found in Ryder Bay (referred herein as modified CDW, mCDW). During autumn and winter, the surface waters cool and become saltier during sea ice formation and the mixed layer deepens to ~100 m depth. During summer, its remnant, called Winter Water (WW), is found in the ~75-100 m depth range and is identified by a minimum temperature. Above the WW, the surface layer that has been warmed and freshened by melt water produces the Antarctic Surface Water (AASW). Ryder Bay is also subject to large fluxes of glacial melt water and studies using oxygen isotopes have identified this meteoric water as the main source of freshwater to the AASW during summer (Meredith *et al.*, 2004).

Sampling

Samples have been collected on a weekly basis (sometime twice a week depending on weather conditions) at Rothera Oceanographic and Biological Time Series site (RaTS, Fig.1). Special ultraclean PolyvinylDifluoride (PVDF) plastic samplers of 4 L volume (Fig. 2), were designed and based upon the larger 24 L type used successfully in the deep ocean (Rijkenberg *et al.*, 2015). Each sampler has butterfly type valves at both ends, as well as teflon PTFE spigots at bottom and top for subsampling and air inlet, respectively. The very clean and smooth surface PVDF material does not require any initial cleaning, other than some rinses with MQ water and at each deployment on the downcast the open bottles are flushed by ambient pristine seawater.

Most of the time 6 seawater samples were collected at 6 depths throughout the surface layer (0-75 m depth) from a small open powerboat equipped with a clean all-titanium winch designed by NIOZ (Fig. 2). The winch comprises 600 m length of metal-free Dyneema 6 mm diameter cable with a plastic enclosed bottom weight at the end. The samplers are attached with open position valves to the hydrowire, at desired depth

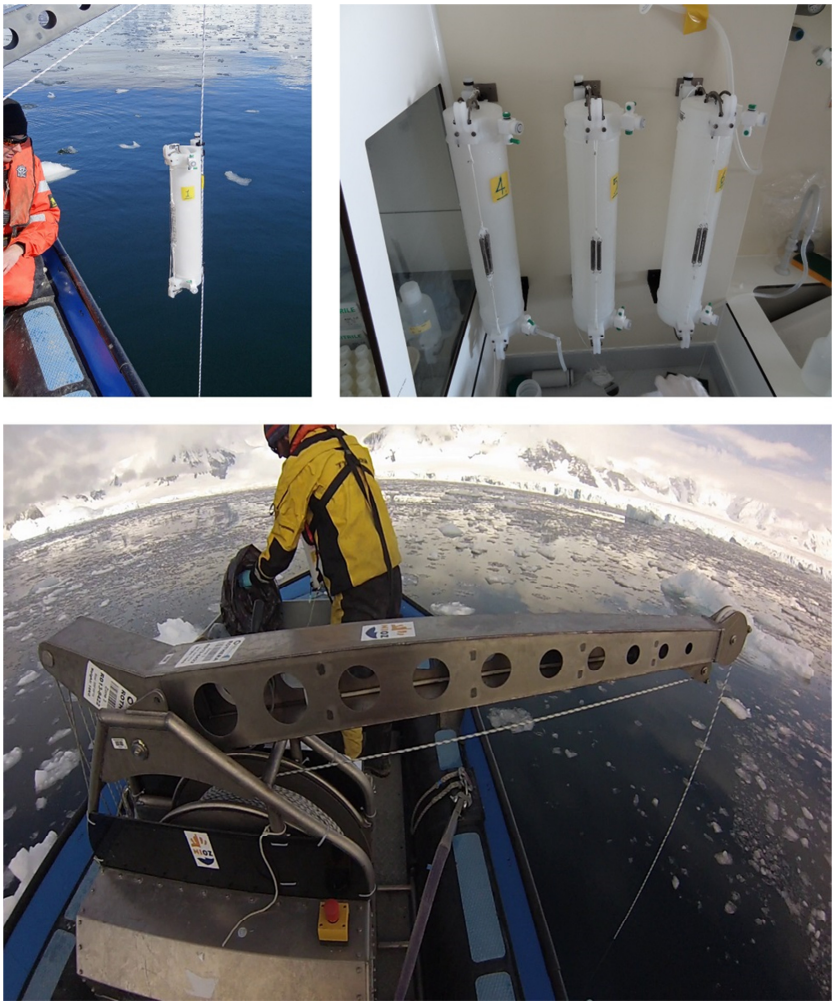

Figure 2: Top left: co-author Patrick Laan inspecting the special designed ultraclean PVDF sampler (4 L) attached to the 6 mm Dyneema hydrowire suspended of the titanium winch arm (top left). Notice the top butterfly valve is in open position (as is the identical lower butterfly valve, not visible here). Two standard teflon PTFE spigots. The messenger has yet to be attached below the sampler. Top right: 4 L PVDF samplers mounted on the wall of the trace metals clean container in the Gerritz Laboratory ready for sub-sampling. Lower panel: the all-titanium winch excludes inadvertent contamination for the trace metals Fe, Mn, Zn, Cd, Co, Cu (Pb) of interest for this study. The round drum holds 600 metres of 6 mm Dyneema cable. The winch arm extends out at starboard side and can be shifted from near horizontal position (as shown here) to more upright position by the simple block and tackle hand-operated string (also 6 mm Dyneema) visible at left side (port). Within the titanium casing at both sides of the drum are at one side the electric motor driving the winch and at other side two large batteries. Upon return at the base the batteries are re-charged overnight.

intervals, and an all-plastic encased drop weight messenger attached below each sampler. Once all samplers are at their desired depths, another messenger is fixed on the wire and dropped down, tripping the first sampler, while releasing the next messenger to travel down to the next sampler. This procedure is well known in classical oceanography but now with ultraclean equipment.

Pressure, temperature, salinity and fluorescence were measured with a Sea-Bird conductivity, temperature and depth recorder (CTD, SBE19plusV2, Sea-Bird Electronics, Inc.) attached 10 m above the bottom end of the Kevlar line. Water samples for analysis of phytoplankton pigments were collected 1-3 times a week at 15 m depth at RaTS using a 16 or 24 L Niskin bottle. Samples for dissolved or labile trace elements (DFe, DMn, DZn, DCd and DCo_L and DCu), and for major nutrients (nitrate, phosphate, silicate) were collected at typical sampling depths of 2, 5, 15, 25, 40 and 75 m. After return to the shore base, the boxes were carried into a trace metal overpressurized clean laboratory container (class 100).

Next each sampler was taken out of the box and mounted vertical on the wall for subsampling from the bottom spigot (Fig. 2). For trace metals sub-sampling, sub-sample bottles (125, 250 and 500 mL Low Density Polyethylene, LDPE, Nalgene), as well as Cryo.S cups (2 mL volume) and all other plastic ware in contact with sample and/or reagents, had been pre-cleaned following a three step procedure (detergent, 6 M HCl, 3 M HNO_3) then filled with 0.35 M QD-HNO_3 (triple subboiled-distilled from 65 % reagent grade, J.T. Baker) and finally stored double bagged. All rinsing was done with Millipore MilliQ deionized water (referred as MQ, 18.2 $M.\Omega.cm^{-1}$) and with the sampled seawater prior final sampling. Trace metals and nutrients sub-samples were filtered on 0.2 µm pore size Sartorius Sartobran cartridges attached directly to the spigot of the PVDF sampler under slight overpressure (Air, 0.5 atm overpressure) to enhance the filtration rate. These filtered trace metals samples were then acidified to pH = 1.8 - 1.9 with ultrapure HCl (1 mL per half liter, Romil, UpA) and double bagged. Filtered seawater was collected into pre-rinsed 5 mL polyethylene vials and stored at 4 °C for silicate analyses and at -20 °C for nitrate and phosphate analyses. After the sub-sampling each PVDF sampler was rinsed with MQ and stored in plastic bags until the next sampling event.

Nutrients analysis

All analyses of the major nutrients were carried out with a Technicon TRAACS 800 Auto-analyzer at the Royal Netherlands Institute for Sea Research, Texel, in August 2014. During each run a daily freshly diluted nutrient internal standard (in-house reference material that we use that is monitored consistently) was measured in triplicate to monitor the performance of the analyzer. The precision, calculated as the standard deviation of the cocktail of 48 measurements for phosphate and nitrate (during 8 different runs) and 34 measurements for silicate (during 7 different runs) for silicate, phosphate and nitrate is determined as 0.6 $\mu mol.L^{-1}$, 0.016 $\mu mol.L^{-1}$, 0.13 $\mu mol.L^{-1}$, respectively.

Phytoplankton pigment analysis

Collection of cells for pigment analysis by high-pressure liquid chromatography (HPLC) on GF/F (47 mm, Whatman) was conducted by filtering 3-8.25 L of seawater using a moderate vacuum (0.2 mbar). The results presented here are based on 56 GF/F filters, 21 for S01 and 35 for S02. Filtering started immediately after the return to the laboratory, and was conducted under low light. Filters were snap frozen in liquid nitrogen and stored at -80 °C until further processing. The analysis of phytoplankton pigments by HPLC is described previously (Rozema *et al.*, 2017b).

The data processing of the measured pigment concentrations with CHEMTAX v1.95 (Mackey *et al.*, 1996) allowed the calculation of relative abundances of the major phytoplankton groups. Included groups were prasinophytes, chlorophytes, dinoflagellates, cryptophytes, two classes of haptophytes, and two classes of diatoms. Haptophyte pigments, which were dominated by *Phaeocystis*, can be highly variable in relation to light and/or iron availability, thus haptophytes were subdivided into two classes for the CHEMTAX analysis (van Leeuwe *et al.*, 2014). The results of the analysis for both haptophytes classes were merged and are presented here as pooled haptophytes. Also, two classes for diatoms were included; one without and one with chlorophyll c3 that accounts for *Pseudonitzschia*-like and *Proboscia* species, both of which have been observed at the RaTS site before (Annett *et al.*, 2010). Results of the two diatom classes were merged and presented as pooled diatoms. Initial pigment ratios used for the haptophyte classes were obtained from Wright et al. (2009). Diatom

pigment ratios were based on a *Proboscia alata* culture, isolated from RaTS in 2014. The initial matrix was further supplemented by ratios from Wright et al. (2010). Both seasons were binned separately and run 60 times with randomized ratios (+-35 %) and settings as recommended in Kozlowski et al. (2011).

Trace elements determination by ICPMS

Sample preconcentration has been performed in the clean room (class 100) of the NIOZ home laboratory. All reagents, standards, samples and blanks were handled in pre-cleaned low density polyethylene bottles (LDPE) according to GEOTRACES program guidelines for trace elements analysis (www.geotraces.org). Samples were preconcentrated off-line using the *seaFAST*-pico preconcentration flow injection system (Elemental Scientific Inc., ESI, Omaha, NE, USA). Detailed description of the beta version of this system can be found in Lagerström et al. (2013). The values presented for Co represents the labile fraction of the total dissolved fraction and will be referred as DCo_L as no UV oxidation step has been performed to destroy strong organic complexes formed between Co and organic matter (Shelley *et al.*, 2010; Bown *et al.*, 2011; Biller & Bruland, 2012) as recommended by GEOTRACES for trace elements analysis.

Reagents and materials

All reagents used were of high purity grade. Clean glacial acetic acid obtained by double sub-boiling quartz distillation of 100 % glacial acetic (AnalR Normapur, VWR) and suprapur ammonium hydroxide 25 % (Merck) were both used for the making of the buffer reagent. All reagents were prepared with deionized water MQ. Two rinsing solutions were made by dilution of QD-HNO_3 with MQ (0.01 and 0.02 M) and used for *seaFAST*-pico cleaning during preconcentration procedure. Elution acid (1.5 M) was also obtained by dilution QD-HNO_3 with MQ water and was spiked with a 1.5 Rh solution to obtain a Rh concentration of 1.5 nM in the to be analyzed sample that is used as internal standard during the two ICPMS runs. The buffer batch used for the *seaFAST*-pico on line pH adjustments of all the samples of the present study was made of acetic acid and ammonium hydroxide (Merck) and adjusted to pH = 6.50 ± 0.10.

Both preconcentration and buffer cleaning columns have been cleaned with the following 100 mL solutions prior use, 1.6 M HCl (Suprapur, Merck), MQ water, acidified seawater (pH = 2), 1.5 M nitric acid and MQ water. Procedure blanks, calibration standards, reference material, laboratory reference samples, and samples (411 samples in total) have been processed over 10 days, and the buffer cleaning column has been cleaned again after 5 days of use. Seawater subsamples have been poured in 30 mL LDPE nalgene bottles and eluted into 2 mL cups (2 mL pp Cryo.S™; Greiner bio-one) which previously have been cleaned with nitric acid. The procedural blank solution consisting of 0.012 M HCl (Seastar) in MQ water with 0.1 % v/v Mediterranean Sea Surface water was freshly prepared every two days in LDPE 125 mL bottle (Lagerström *et al.*, 2013).

Automated offline preconcentration and matrix removal before analysis by ICPMS

The sea*FAST*-pico is an offline preconcentration and matrix removal module. Samples are preconcentrated onto the sea*FAST* built-in column (V=200 µL; ESI) containing the NOBIAS PA1 resin (http://www.icpms.com/PDF/seaFAST-pico-open-ocean%20seawater.pdf). Next the system is rinsed, the autosampler probe moves to the 1st rinsing solution (0.02 M, QD-HNO_3) and the sample loop is over-filled 1.5 times with the 0.02 M QD-HNO_3 using vacuum suction to rinse the loop as well as fill it. Then the second rinse (0.01 M QD-HNO_3) and the buffer solution are pushed through the loop and onto the column, a total of 1.0 mL of the 3:1 mixture of 0.01 M QD-HNO_3 and buffer (pH ~ 7) is used to rinse unchelated major seawater ions from the column (the only difference here is that we used QD-HNO_3 solution instead of HCl as in Lagerström et al. (2013)). The chelated elements are eluted with clean acid into a 2 mL vial on the autosampler for later analysis by ICPMS. In the offline configuration the automated system buffers 10 mL of acidified seawater sample before loading it onto the NOBIAS PA1 column in which both ethylenediaminetriacetic acid and iminodiacetic acid chelating groups are immobilized on a hydrophylic polymer. This resin has high affinity with metal ions over a pH ranging from 5.5 to 7.0 (Sohrin *et al.*, 2008). Seawater matrix is then removed and the concentrated sample is eluted with 750 µL of 1.5 M $QHNO_3$ giving a pre-concentration factor of 13.33. The complete column recovery of the desired elements (Fe, Mn, Zn, Cd, Cu and Co) requires accurate and reproducible

sample buffering at pH ~ 6 (Sohrin *et al.*, 2008; Lagerström *et al.*, 2013; Quéroué *et al.*, 2014). For this reason buffer pH was daily checked and adjusted if needed, in the present study samples were initially acidified to pH = 1.8 – 1.9 and subsequently buffered to pH = 6.0 ± 0.1.

Analysis by ICPMS

A multi element stock standard with natural isotopic abundances of Fe, Mn, Zn, Cd, Co and Cu was made in 0.024 M nitric acid from dilution of individual element standards. This multi element standard was then used to make standard additions to matrix matching seawater collected in the Mediterranean Sea and characterized by relatively low concentrations for the investigated elements. The 6 produced standards were treated in the same manner as all other samples. A total of 5 calibration curves were processed by the sea*FAST*-pico in order to control the reproducibility and the stability of the system during the 10 days of samples preconcentration step. Trace metals concentrations were determined by Inductively Coupled Plasma Mass Spectrometry (Thermo Element 2, Thermo Fisher Scientific) one month after the preconcentration step.

Procedural blank values represent the contributions to the whole sea*FAST* system, bottles, ICPMS and its autosampler and reagents such as the buffer solution and the elution acid. Producing trace metals free seawater is very difficult, instead we have chosen to use acidified MQ water spiked with low trace metals seawater as described above and as also used by Lagerstrom et al. (2013). The mean procedural blanks (n = 23) for each metal of interest are reported in Table 1. For Ni, Cu, Mn, Co, Cd, as well as reported Pb, the blanks are comparable or lower than values presented in other studies using a similar method (Biller & Bruland, 2012; Lagerström *et al.*, 2013; Quéroué *et al.*, 2014). On the other hand, for Fe and Zn the blanks are higher than reported elsewhere, this would need further investigation in the future. Nevertheless, the concentrations of DFe and DZn that we measured in the present coastal region of study (lowest DFe= 0.36 nM and lowest DZn= 0.38 nM; supplementary material) are higher than the procedural blanks of Fe (0.21 ± 0.07 nM, Table 1) and Zn (0.19 ± 0.06 nM, Table 1). The limit of detection of the method for each studied element was estimated as three time

Table 1. Blanks, detection limits and our measured values of SAFe D2 reference sample versus reported consensus values. Latter consensus values of SAFe D2 reference sample of May 2013 are taken from: http://www.geotraces.org/science/intercalibration/322-standards-and-reference-materialsFor labile Co it is mentioned this is ~60 % of total Co, therefore the above listed labile Co consensus value is the calculated 60 % of the total Co consensus value of May 2013.

Element	**Blanks (nmol kg^{-1})**	**Detection limits (nmol kg^{-1})**	**Element (nmol kg^{-1})**	**Measured**	**Consensus**
Fe	0.210	0.201	dFe	0.987 ± 0.070	0.933 ± 0.023
Zn	0.185	0.169	dZn	7.39 ± 0.28	7.43 ± 0.25
Ni	0.030	0.027	dNi	8.69 ± 0.22	8.63 ± 0.25
Cu	0.020	0.018	dCu	1.96 ± 0.14	2.28 ± 0.15
Mn	0.008	0.011	dMn	0.44 ± 0.02	0.35 ± 0.05
SAFe D2 (n=7)	**Blanks (pmol kg^{-1})**	**Detection limits (pmol kg^{-1})**	**Element (pmol kg^{-1})**		
Co	0.929	0.842	Labile Co (DCo_L)	31 ± 2	27.4 ± 1.74
Cd	1.356	1.326	dCd	970 ± 27	959 ± 23
Pb	0.859	1.031	dPb	31 ± 3	28 ± 1

average blanks (n=24) and detection limits (3 times the blank standard deviation)

the standard deviation of the blank and are also reported in Table 1. Accuracy and reproducibility have been assessed by measuring laboratory internal standard (acidified seawater sample from Mediterranean Sea) and SAFe D2 reference material that have been pre-concentrated with the sea*FAST* in between samples, calibration standard and blanks. Results are shown in Table 1.

Results

RaTS site hydrography (0-75m depth)

The CTD data recorded during the two seasons showed that the surface layer at the RaTS site had similar features to those previously described(Meredith *et al.*, 2004; Clarke *et al.*, 2008; Venables & Meredith, 2014; Annett *et al.*, 2015). The present CTD dataset provides a synoptic view of the modifications of the water column throughout the summer season (Fig. 3).

The Winter Water (WW) was found in the upper mixed layer during early summer period and identified by a temperature minimum and salinity minimum (November 2013; Fig. 3, S01 and S02). Within the following spring season, this temperature minimum (remnant WW) was found at increasing depth to finally reach depths below 60 m (~-1.28 °C, Fig. 3, S02). This is because the surface waters are freshened by ice melt (salinity ~32) and warmed by solar radiation (up to 3.0 °C, 17 January, 2013, and 22 January, 2014; Fig. 3) leading to the formation of AASW (Annett *et al.*, 2015). The CTD

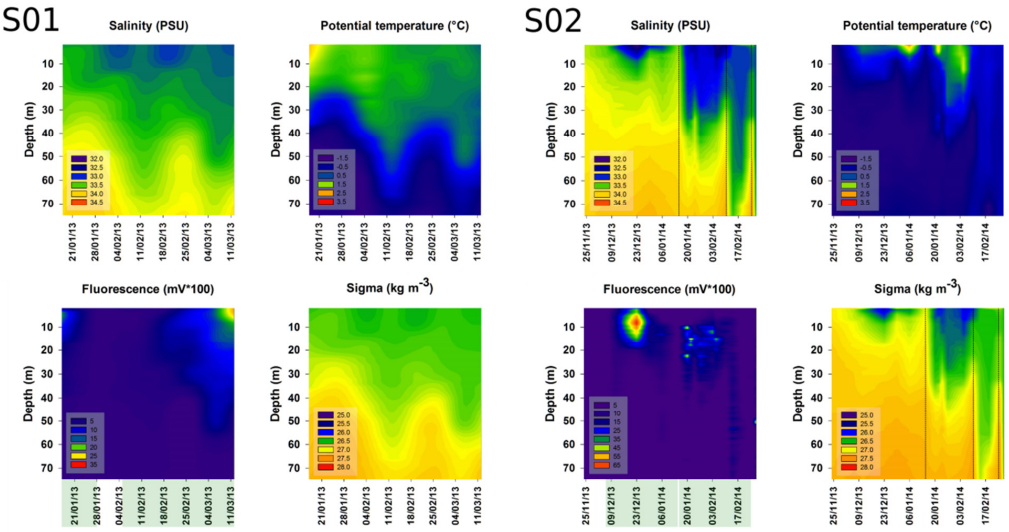

Figure 3: Time series of potential temperature, salinity, fluorescence and potential density during season 1 (S01) and season 2 (S02). The length of each bloom events is illustrated by green shading on the X axis of fluorescence time series. Vertical dotted lines on salinity and potential density time series represents sampling events conducted after storm episodes.

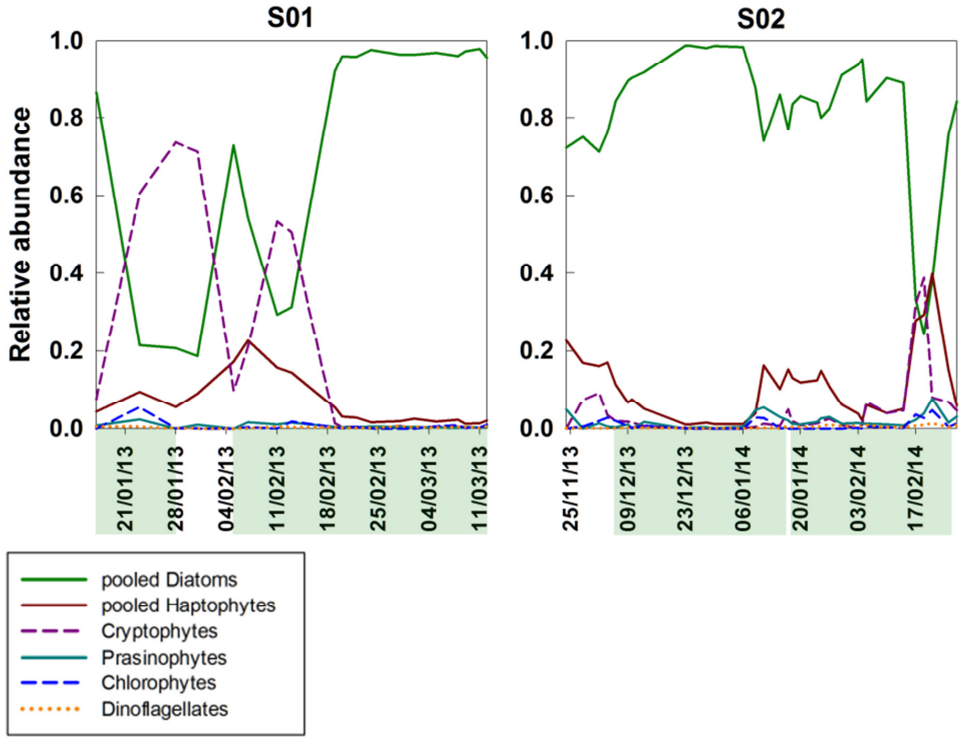

Figure 4: Relative phytoplankton abundances during seasons S01 and S02. The length of each bloom events is illustrated by green shading on the X axis.

data also show that, throughout the summer season, the surface seawater properties can be disturbed by storm episodes during which strong winds can increase the depth of the upper mixed layer from a few metres to more than 40 m in a very short time (i.e. 5 March, 2013, 15 January and 14 February, 2014; Fig. 3) while the deeper (50-85 m) WW layer remains fairly steady (Fig. 3). In addition to storm episodes the euphotic layer can also be influenced by freshwater inputs from meteoric water (glacier ice melt) and/or sea ice melt, which was detected by lower salinity 31.5-33.5 (23 December, 2013, and 5 February, 2014; Fig. 3).

Biogeochemistry

Two main events related to photosynthetic activity were monitored during the first spring season (S01), a diatoms bloom decay (B1) from 17 to 28 January, 2013, depicted by the decreasing of fluorescence peak in the 0-15 m surface layer (from 20 mV*100 to 2.5

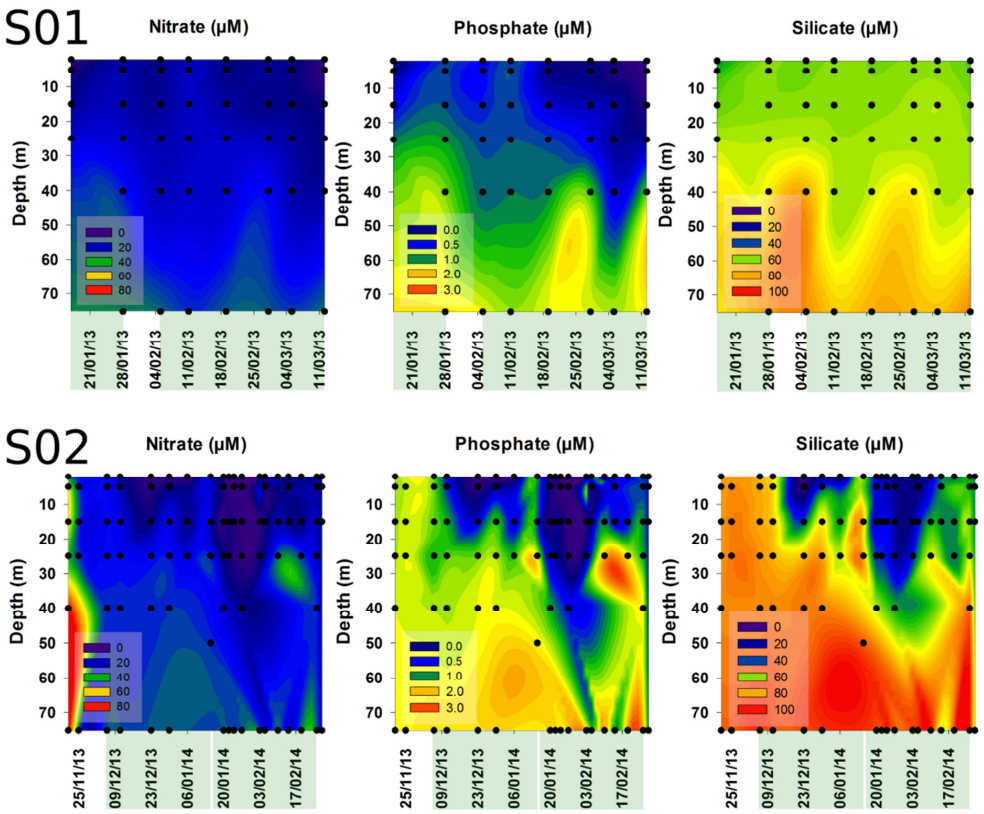

Figure 5: Major nutrient (Nitrate, Phosphate, Silicate) time series at RaTS during S01 and S02. The length of each bloom events is illustrated by green shading on the X axis.

mV*100; Fig. 3) and the decline in the relative abundances of diatoms (Fig. 4), a slight increase of silicate (from 45-50 µM to 60 µM) and a sharper increase of nitrate (from ~0.5 µM to ~30 µM) and phosphate (from ~0.25 µM to >1.75 µM; Fig. 5, S01). The start of another diatoms bloom occurred between 5 February and the 12 March, 2013 (event B2), indicated by the increase of the fluorescence signal (from ~2.5 mV*100 to 28 mV*100; Fig. 3, S01) and decreasing concentrations of the major nutrients (Fig. 5, S01). The early stage of this bloom was marked by low biomass, slow increase of diatoms relative abundance and by the presence of haptophytes and cryptophytes until diatoms dominated (22 February, 2013; Fig. 4). During the time of the fluorescence maximum, the concentrations of nitrate and phosphate were as low as 0.10 µM and 0.02 µM, respectively, while the concentrations of silicate remained fairly constant with concentrations around 55-60 µM (Fig. 5, S01).

During the second spring season (So2), the first phytoplankton bloom extended from 6 December, 2013, to 15 January, 2014, and was dominated by diatoms (Fig. 4). This B3 event can be divided in two stages. Firstly there was a growing phase during which the fluorescence peak increased to the season maximum of 65 mV*100 on 23 December, 2013 (~8m depth; Fig. 3) while major nutrients exhibited decreasing concentrations, for silicate a dramatic decrease from a mean of ~80 µM to 31 µM, accompanied by a decrease from a mean of ~44 µM to ~11 µM for nitrate and from a mean of 1.90 µM to 0.74 µM for phosphate in the 0-25 m depth layer (Fig. 5, So2). During that time the relative abundance of diatoms increased while haptophytes sharply decreased (Fig. 4). Thereafter, the bloom decayed, as shown by the decreasing of fluorescence to low values (~2.5 mV*100) and increasing concentrations of the major nutrients (> 60 µM for silicate, >25 µM for nitrate and >1.25 µM for phosphate; Fig. 5, So2). The development of a second diatom bloom was monitored from 15 January to 25 February, 2014 (B4) and can be described as previous blooms above with two relative fluorescence maxima (~58 mV*100 on 22 January and 40 mV*100 on 5 February) associated with minima of silicate (20-30 µM), nitrate (~2 µM) and phosphate (~0.10 µM) (Fig. 5, So2). As observed during B3, haptophytes were present during the bloom start and slowly decreased while diatoms relative abundance increased. At the end of So2, diatoms abundance dropped down while the relative abundance of haptophytes and cryptophytes sharply increased (Fig. 4).

Distributions of dissolved trace metals

The dissolved Fe, Mn, Zn, Cd, Cu and labile Co displayed increasing concentrations with depth during the first season So1. Relative minima were observed around January 17th when phytoplankton activity decreased, fairly low concentrations were measured for DFe, DMn (1.2 and 0.2 nM, Fig. 6), and DCd and DCo_L (300 pM and 50 pM, Fig. 6). From the beginning of February to the end of summer, trace elements concentrations gradually decreased to their lowest level while fluorescence signal increased to its maximum (Figs. 3 and 6). In that manner, DFe, DMn and DZn was found in the 0.3-0.5 nM range, DCo_L and DCd concentrations were lower than 45 pM and 150 pM, respectively, and DCu slightly decreased below 2.0 nM (Fig. 6).

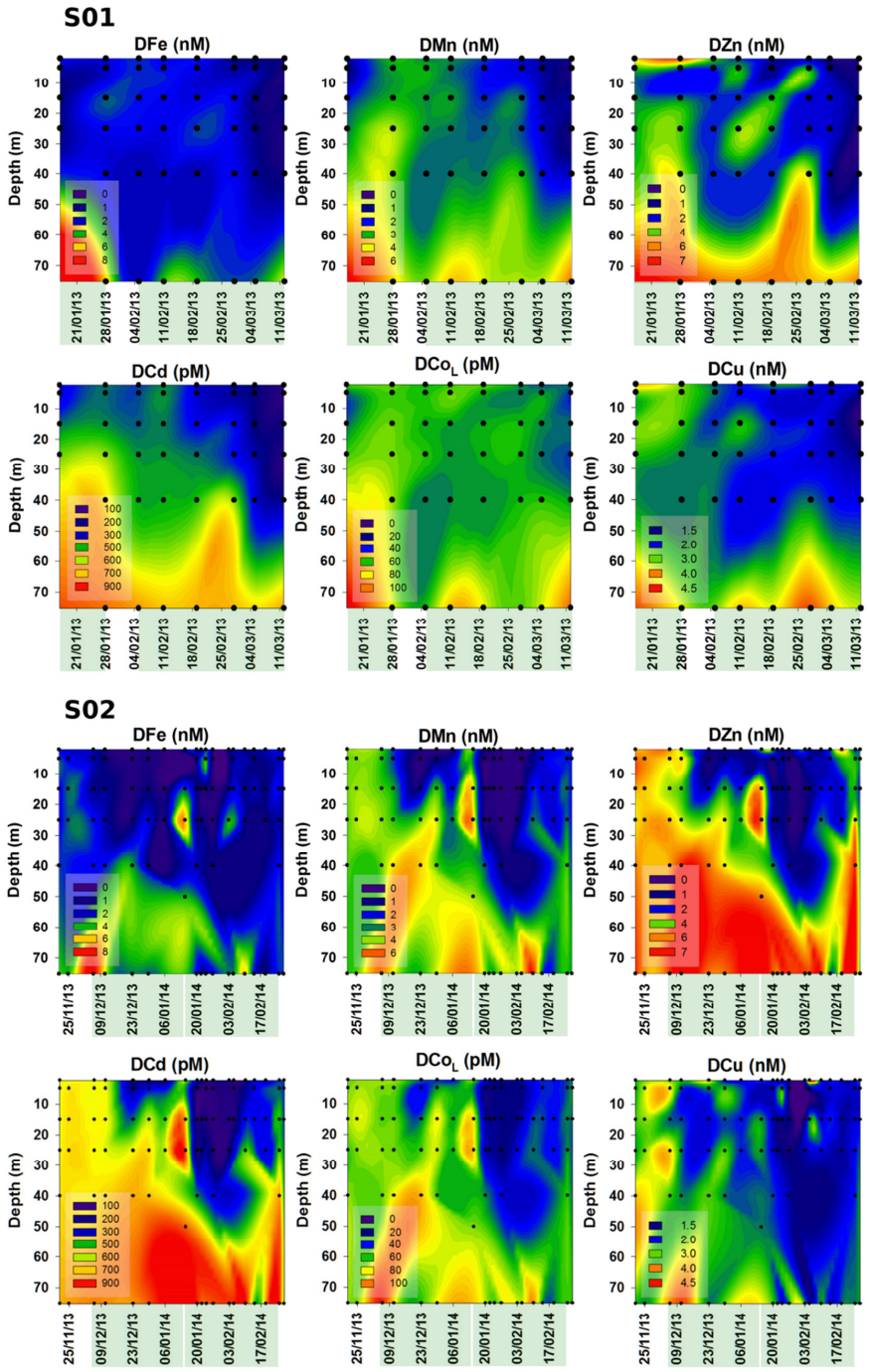

Figure 6: DFe, DMn, DZn, DCd, DCo$_L$ and DCu time series at RaTS during S01 and S02. The length of each bloom events is illustrated by green shading on the X axis.

Table 2. Linear relationships derived for first season S01 for bloom events B1 and B2 and for second season S02 for bloom events B3 and B4. The concentration values of trace metals Mn, Zn, Cu and Fe are in nM, and of Cd, Co in pM. The concentrations of major nutrients P and Si both are in µM. Therefore the slopes of regression are in nmol.µmol^{-1} (i.e. 10^{-3}) or pmol.µmol^{-1} (i.e. 10^{-6}).

	S01	
	B1	B2
Mn vs P	[Mn]= 1.71*[P] + 0.60 (n=11; R^2=0.91; p<0.001)	[Mn]= 1.45*[P] + 0.81 (n=36; R^2=0.75; p<0.001)
Mn vs Si	[Mn]= 0.103*[Si] – 3.51 (n=11; R^2=0.82; p<0.001)	[Mn]= 0.095*[Si] – 3.60 (n=36; R^2=0.52; p<0.001)
Cd vs P	[Cd]= 222*[P] + 230 (n=11; R^2=0.91; p<0.001)	[Cd]= 265*[P] + 120 (n=36; R^2=0.85; p<0.001)
Cd vs Si	[Cd]= 14.3*[Si] – 357 (n=11; R^2=0.94; p<0.001)	[Cd]= 18.3*[Si] - 751 (n=36; R^2=0.66; p<0.001)
Zn vs P	No Linear Relationship	[Zn]= 2.30*[P] + 0.24 (n=36; R^2=0.69; p<0.001)
Zn vs Si	No Linear Relationship	[Zn]= 0.166*[Si] – 7.81 (n=36; R^2=0.59; p<0.001)
Co vs P	[Co]= 7.6*[P] + 53 (n=11; R^2=0.42; p<0.05)	[Co]= 12*[P] + 45 (n=36; R^2=0.44; p<0.001)
Co vs Si	[Co]= 0.491*[Si] + 33.4 (n=11; R^2=0.43; p<0.05)	[Co]= 0.997*[Si] – 0.191 (n=36; R^2=0.40; p<0.001)
Cu vs P	No Linear Relationship	[Cu]= 0.71*[P] + 1.60 (n=36; R^2=0.55; p<0.001)
Cu vs Si	No Linear Relationship	[Cu]= 0.06*[Si] – 1.2 (n=36; R^2=0.55; p<0.001)
Fe vs P	No Linear Relationship	[Fe]= 1.10*[P] + 1.00 (n=36; R^2=0.45; p<0.001)
Fe vs Si	No Linear Relationship	No Linear Relationship
	S02	
	B3	B4
Mn vs P	[Mn]= 1.89*[P] + 0.28 (n=31; R^2=0.85; p<0.001)	[Mn]= 1.48*[P] + 0.17 (n=50; R^2=0.74; p<0.001)
Mn vs Si	[Mn]= 0.05*[Si] - 0.19 (n=31; R^2=0.84; p<0.001)	[Mn]= 0.05*[Si] – 0.60 (n=50; R^2=0.84; p<0.001)
Cd vs P	[Cd]= 241*[P] + 229 (n=31; R^2=0.91; p<0.001)	[Cd]= 270*[P] + 91 (n=50; R^2=0.78; p<0.001)
Cd vs Si	[Cd]= 6.60*[Si] + 156 (n=31; R^2=0.95; p<0.001)	[Cd]= 9.34*[Si] – 65.1 (n=50; R^2=0.96; p<0.001)
Zn vs P	[Zn]= 2.49*[P] + 0.49 (n=31; R^2=0.80; p<0.001)	[Zn]= 2.03*[P] + 0.7 (n=50; R^2=0.63; p<0.001)
Zn vs Si	[Zn]= 0.070*[Si] – 0.47 (n=31; R^2=0.85; p<0.001)	[Zn]= 0.071*[Si] - 0.50 (n=50; R^2=0.81; p<0.001)
Co vs P	[Co]= 16*[P] + 41 (n=31; R^2=0.58; p<0.001)	[Co]= 19*[P] + 19 (n=50; R^2=0.73; p<0.001)
Co vs Si	[Co]= 0.45*[Si] + 35 (n=31; R^2=0.63; p<0.001)	[Co]= 0.65*[Si] + 9.32 (n=50; R^2=0.84; p<0.001)
Cu vs P	No Linear Relationship	[Cu]= 0.29*[P] + 1.68 (n=50; R^2=0.41; p<0.001)
Cu vs Si	No Linear Relationship	[Cu]= 0.01*[Si] + 1.55 (n=50; R^2=0.40; p<0.05)
Fe vs P	[Fe]= 1.76*[P] – 0.51 (n=36; R^2=0.41; p<0.001)	No Linear Relationship

At the beginning of the second spring and summer season (S02), the concentrations of dissolved trace metals were measured in very early summer, when phytoplankton activity still was negligible (end of November 2014, Figs. 3, and 6). At that time, the DFe, DMn, DCu, DZn, DCo_L and DCd were all exhibiting fairly homogeneous vertical distributions with concentrations ranging from 2.0 to 4.0 nM, 3.40 to 4.0 nM, 2.70 to 3.60 nM, 4.90 to 6.70 nM, 60 to 75 pM and 630 to 738 pM respectively (Fig. 6). As surface waters were warmed by insolation (Fig. 3; S02), phytoplankton started to grow and minimum concentrations of trace elements were detected when the fluorescence signal was at its maximum and major nutrients also at their minimum (around 23 December, 2013, 21 January and 5 February, 2014 as described above in 3.1. section, Figs. 3, 5 & 6). During these bloom events, the concentrations of trace metals decreased from 3 to 10 times lower than the late winter levels (Fig. 6). For instance during B4 event on the 27th January 2014, trace metal mean concentrations in the 0-25 m depth

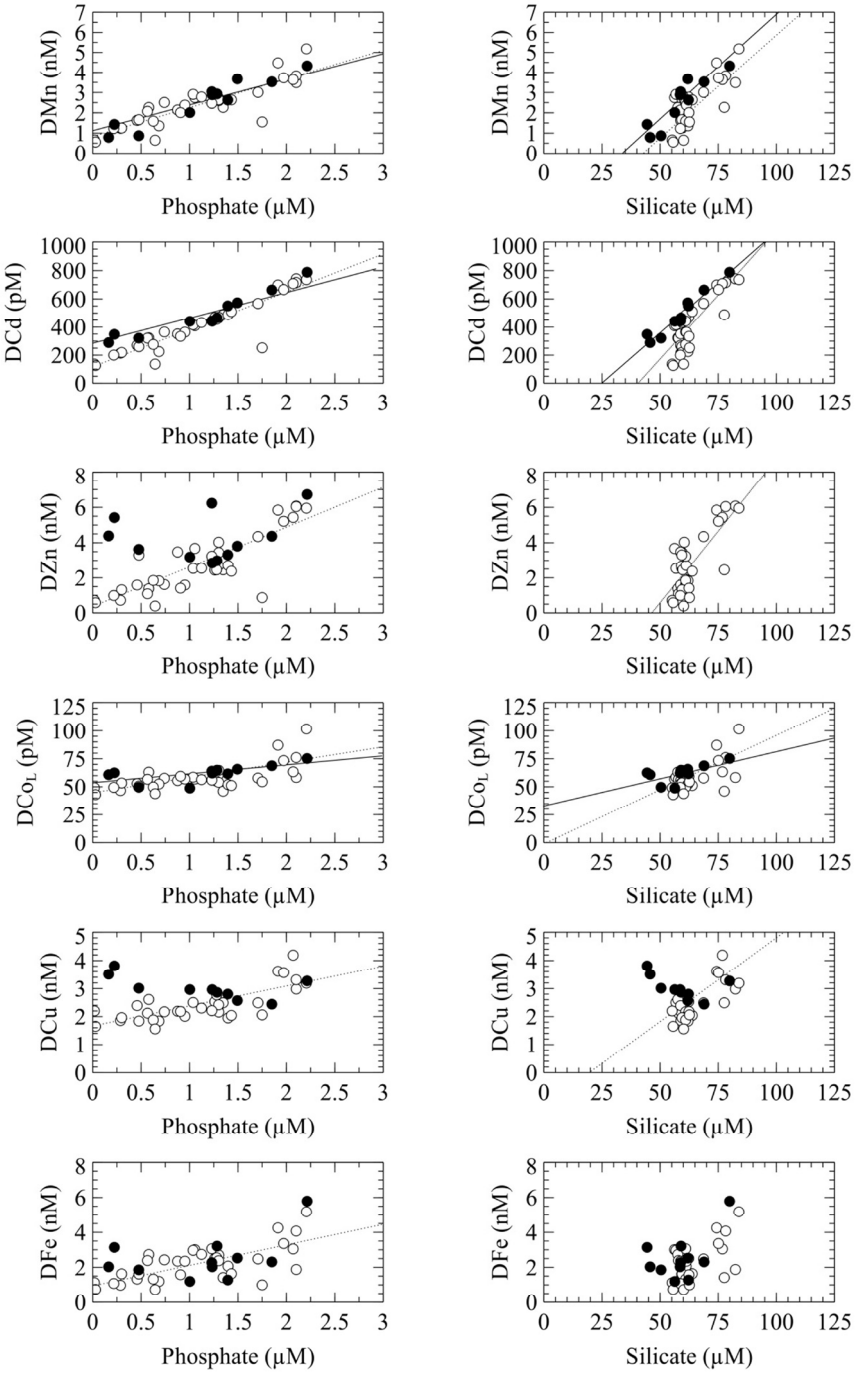

Figure 7: Trace elements concentrations versus phosphate and silicate during S01. Solid lines and dotted lines illustrate linear regression of DMe vs. Nutrient during B1 (black dots) and B2 (white dots). Equations of each linear regression are reported in Table 2.

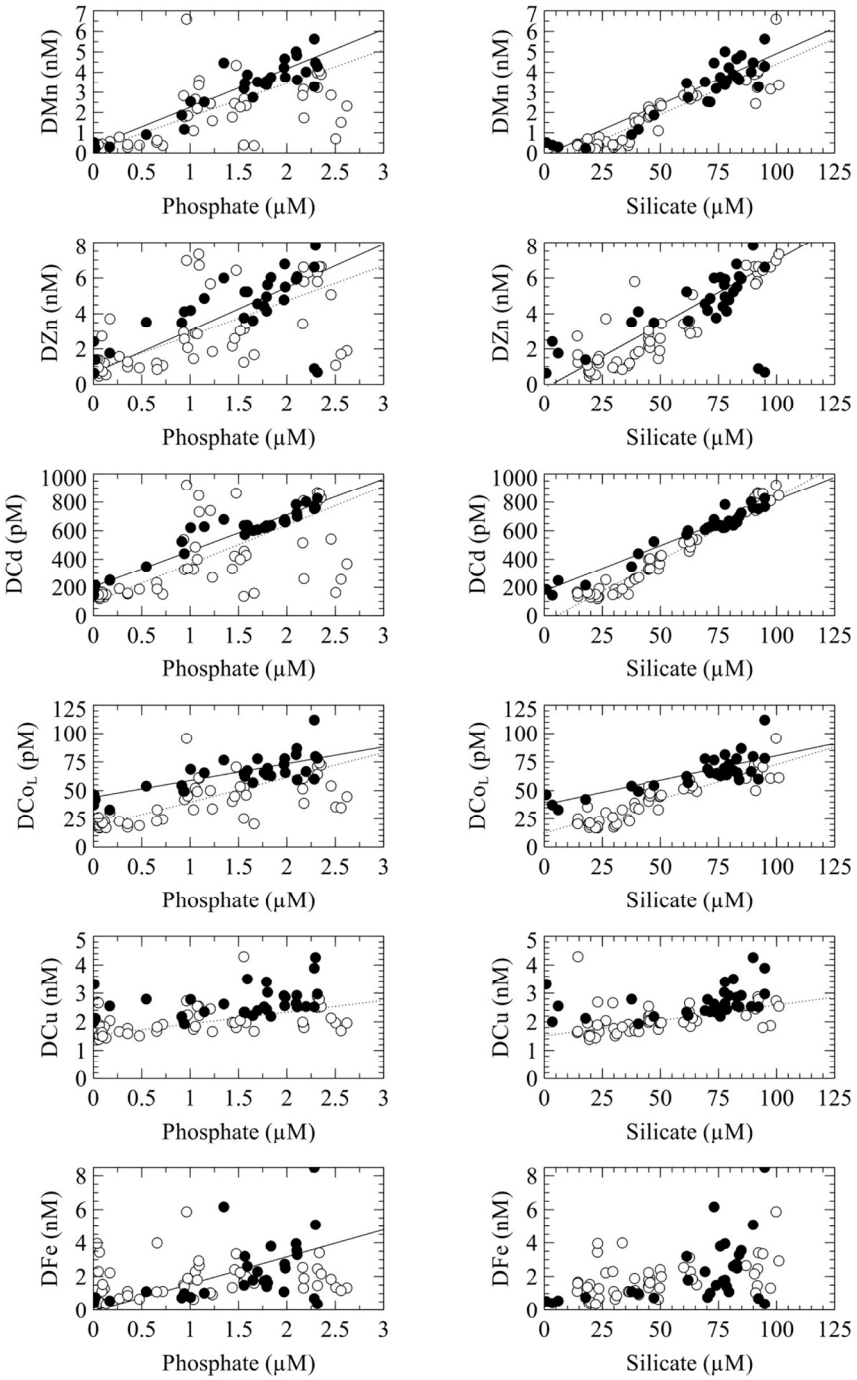

Figure 8: Trace elements concentrations versus phosphate and silicate during So2. Solid lines and dotted lines illustrate linear regression of DMe vs. Nutrient during B3 (black dots) and B4 (white dots). Equations of each linear regression are reported in Table 2.

layer dropped to 0.40 and 0.60 nM for DFe and DZn, 0.22 nM and 146 pM for DMn and DCd respectively (Fig. 6). The DCo_L also exhibited very low concentration (19 pM). On the other hand the depletion of DCu was less sharp and DCu mean reached a less pronounced minimum of 1.48 nM (Fig. 6).

Relationships of bioactive trace metals with major nutrients

The S01 time series of the first season shows similar trends between nitrate, phosphate and DMn and DCd, whereas for the other trace elements such as DFe or DZn the relation with major nutrients is less obvious. Likeness between DMn, DCd, DZn and DCo_L and major nutrients was even more striking during the second season S02 (Figs. 5 & 6). The correlations of DFe concentrations with phosphate were weak during eventsB2 and B3 (R^2~0.40; $p<0.001$; Table 2) while there was no significant relationship for events B1 and B4 (Figs. 7 & 8; Table 2). DFe was not significantly correlated with silicate for any event (Table 2). During the B2 and B4 events, the drawdown of DCu was proportional to the net removal of phosphate and silicate but correlations were fairly weak ($0.40<R^2<0.55$; $p<0.001$; Table 2; Figs. 7 & 8). Throughout the B1, B2 and B3 events, the plots of DCo_L versus phosphate and silicate also showed weak relationships ($0.40<R^2<0.63$; $p<0.001$; Table 2; Figs. 7 & 8). However during B4 the DCo_L showed stronger correlations with both phosphate and silicate ($R^2=0.73$; $p<0.001$ and $R^2=0.84$; $p<0.001$ respectively; Table 2). Finally, the DMn, DCd and DZn did show stronger correlation with phosphate and silicate during both seasons S01 and S02 ($0.52<R^2<0.94$; $p<0.001$; Table 2; Figs. 7 & 8).

Discussion

Bioactive trace metals concentrations ranges

A number of studies have been conducted to study the biogeochemistry of DFe in different coastal regions of Antarctica (Ardelan *et al.*, 2010; Alderkamp *et al.*, 2012b; de Jong *et al.*, 2012; Gerringa *et al.*, 2012; Annett *et al.*, 2015). In the present study, concentrations of DFe throughout both summer seasons ranged from 0.35 nM to 4.0 nM in the 0-40 m depth layer during bloom maximal intensity and higher concentrations (4-8 nM) were always found in the deeper 40-75 m depth layer. Recently, a study conducted at the RaTS site during Austral summer (January-February

2010; Annett et al. (2015)) showed higher DFe concentrations at 15 m depth (DFe ~ 4-8 nM) than the DFe ranges presented here at 15 m (DFe ~ 0.35-3.5 nM) while biological activity appears to be similar in term of chlorophyll concentrations. Another recent study presents DFe data for contrasted sites located in the Pine Island Glacier Region, in the Amundsen Sea (Alderkamp *et al.*, 2012b; Gerringa *et al.*, 2012). In that study concentrations of DFe in the 0-100 m layer ranged from 0.2 to 1.1 nM nearby Pine Island Glacier, 0.08 and 0.70 nM nearby Crosson and Dotson iceshelf and 0.04 and 0.10 nM in the Amundsen Sea polynya, which is generally much lower that DFe measured in the present study. The main difference between the Pine Island Glacier and Ryder Bay is that the former is mostly covered by ice (ice shelf and sea ice) while the latter is a seasonally ice free area surrounded by land and islands thus likely to be impacted by several sources of trace metals. Few studies have reported the distributions of other bioactive trace elements (Zn, Cd, Mn, Cu) in the Antarctic Ocean (Westerlund & Öhman, 1991; Fitzwater *et al.*, 2000; Saito *et al.*, 2010; Croot *et al.*, 2011; Middag *et al.*, 2011, 2013; Noble *et al.*, 2013; Baars *et al.*, 2014; Zhao *et al.*, 2014; Sherrell *et al.*, 2015) and even fewer articles report nearshore or time series datasets (Westerlund & Öhman, 1991; Fitzwater *et al.*, 2000; Grotti *et al.*, 2001; Hendry *et al.*, 2008). Datasets generally showed dissolved trace metals concentrations within similar wide concentration ranges to those reported for S01 and S02, with perhaps higher concentrations for the upper limit of DFe, DZn and DCd (0.35 <DFe< 8.50 nM; 0.15 <DMn< 6.50 nM; 0.4 <DZn< 7.8 nM; 115 <DCd< 921 pM; 5 <DCu< 7.1 nM; and 17 <DCo< 112 pM). For example, here the reported range of DCd in Ryder Bay surface waters (0-75 m depth; 115 <DCd< 921 pM) was very similar to DCd ranges recently found in the whole water column (0-5000 m depth) of the Atlantic sector of the Southern Ocean (150-900 pM; Baars et al. (2014)). Concentrations of DCd that ranged from 350 to 800 pM have previously been reported for the RaTS site during summer season (January-March 2006; Fig. 9) at 15 m depth (Hendry *et al.*, 2008). These concentrations were slightly higher compared with the same 15 m depth of the present study (DCd~130-680 pM; Fig. 9) which could be due to either differences in analytical methods (Hendry *et al.*, 2008) and/or differences in phytoplankton activity, bloom behaviour, total chlorophyll concentrations and environmental conditions.

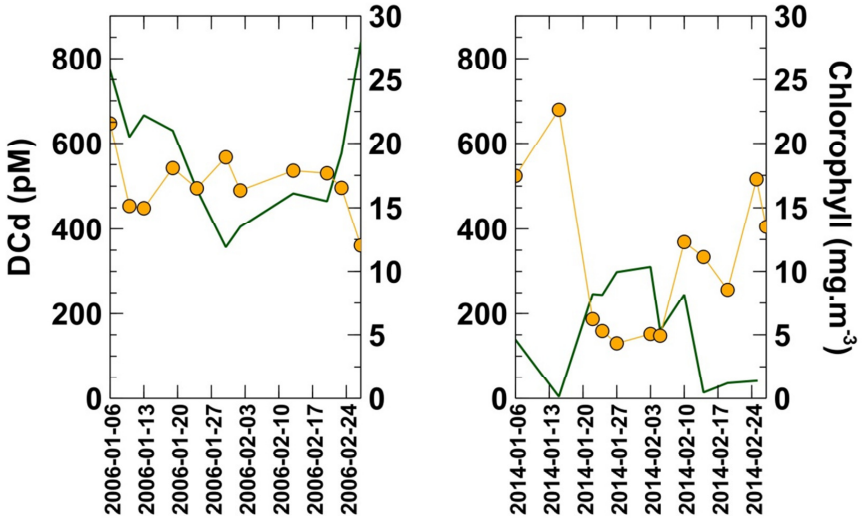

Figure 9: DCd concentrations comparison between Hendry et al., 2008 (on the left) and the present study (right panel) for RaTS site (15 m depth). The green line represents Chlorophyll concentrations (data from BAS).

Wide concentration ranges of the bio-active trace metals were detected in a much thinner layer of the water column (0-75 m depth) than in previous work at 0-400 m (Westerlund & Öhman, 1991; Fitzwater *et al.*, 2000; Grotti *et al.*, 2001) and with higher temporal (during a whole season with weekly sampling) and spatial resolution (4 to 6 samples in the 0-75m depth layer). Such higher resolution in space and time appears to be crucial to adequately document the variability and dynamics of bio-essential trace metals in this coastal ecosystem.

Ratios of bioactive trace metals versus the major nutrients

Linear relationships described in the results section (3.3) strongly suggest that the surface distributions of DMn, DCd, DZn, DCo_L, and to a lesser extent DCu, were mainly driven by biological uptake and remineralization during austral spring and summer in Ryder Bay. Plots of the linear relationships of trace metals (Me) versus nutrients also suggest that, most of the time (exception made for silicate during B1 and B2, further discussed below in 4.2.2 section), phosphate and silicate would be depleted before the bio-active trace elements studied here. This would indicate that abiotic supplies of bio-active trace elements, notably from (i) the glacier, or (ii) by upwelling

and mixing of trace-metal-richer waters from below, or (iii) atmospheric deposition, were high enough to prevent phytoplankton stress during blooms.

Below we discuss the ensuing ratio values of Metal/Nutrient in units of nmol.µmol^{-1} (i.e. 10^{-3}) or pmol.µmol^{-1} (i.e. 10^{-6}).

Trace metals and phosphate

Considering the strong decrease of DFe concentrations in the 0-25 m depth layer between spring and summer bloom conditions (from 2< DFe <3.5 nM to 0.39< DFe <1.10 nM; Fig. 6), there is little doubt that DFe was used by phytoplankton cells during each of the bloom events. The complex chemistry of DFe in combination with variable intensities of several sources of DFe into Ryder Bay (Bown et al., in prep.) likely causes higher variability of DFe as compared to the other trace elements. This in turn would explain the non-linearity of most of the relationships of DFe versus the major nutrients. Nevertheless, weak yet obvious linear relationships gave a DFe/P ratio of 1.1 and 1.76 nmol.µmol^{-1} during B2 and B3 events (R^2~0.40; p<0.001; Table 2). These ratios of 1.1 and 1.76 Fe atom per 1000 P atoms are 5.5 to 8.8 fold higher than the ratio DFe/P = 0.2 nmol.µmol^{-1} calculated from vertical profiles of DFe and phosphate in an Fe-limited region of the Southern Ocean (Twining *et al.*, 2004). On the one hand, this may suggest that phytoplankton growth was not limited by Fe during B2 and B3 events. On the other hand, one still cannot rule out the hypothesis that coastal phytoplankton species may have evolved to have a higher cellular iron requirement than oceanic diatoms, this presumably due to adaptive evolution to a relatively high iron versus low iron environment, respectively (Sunda *et al.*, 1991; Sunda & Huntsman, 1995). If so, then perhaps the phytoplankton growth was in fact sub-optimal or limited during B2 and B3 events due to Fe having become depleted in seawater. Fe limitation is in essence a diffusive limitation by the surface/volume ratio of a plankton cell, which means that, at any given DFe concentration in seawater and same cellular Fe requirement, large diameter cells will be Fe limited whereas small cells will be not limited (Timmermans *et al.*, 2001, 2004). The coastal diatoms in general being very large, may therefore perhaps suffer from inadequate Fe supply much sooner than smaller phytoplankton.

Similarly, the linear relationship between DCu and P was quite weak but still obvious during the B2 and yields a DCu/P drawdown ratio of 0.71 nmol.µmol^{-1} (R^2=0.55; p<0.001; Table 2). This ratio was remarkably similar to the DCu/P ratio determined during a *Phaeocystis antarctica* dominated bloom in Amundsen Sea Polynya by Sherrell et al., 2015 (0.69 nmol.µmol^{-1}) and slightly higher than the P-normalized Cu stoichiometry for diatom dominated assemblages in the Southern Ocean (0.53 ± 0.13; Twining and Baines (2013). The DCu/P ratio determined here for B2 event is also in line with phytoplankton abundances that showed that diatoms and haptophytes dominated during S01 (Fig. 4).

For cobalt, the DCo_L/P drawdown ratios ranged from 7 to 20 pmol.µmol^{-1} during the two seasons with a slight but noticeable increase during S02 (from 16 to 19 pmol µmol^{-1}, Table 2). These DCo_L/P ratio values (7.6, 12, 16 and 19 pmol.µmol^{-1}, Table 2) were lower but still in fair agreement with those reported in the Ross Sea with phytoplankton assemblage including diatoms and *Phaeocystis antarctica* (DCo/P = 37.6 pmol.µmol^{-1}; Saito et al. (2010), and a DCo/P ~ 40 pmol.µmol^{-1} calculated for the Atlantic sector of the Southern Ocean (Bown *et al.*, 2011). The DCo being usually higher than DCo_L, it would make sense to indeed observe a lower drawdown ratio of DCo_L relative to DCo versus the same P value.

For manganese, the Mn/P ratio values showed a small decrease during S01 (from 1.71 to 1.45 nmol.µmol^{-1}, Table 2) and can be slightly higher during S02 (B3 ~1.89 nmol.µmol^{-1}, B3 ~1.48 nmol.µmol^{-1}; Table 2). Here the Mn/P ratios were much higher than the elemental ratio in oceanic diatoms (0.42 nM.µM^{-1}; Twining et al. (2004) and those calculated in the Atlantic Sector of the Southern Ocean (ranging from 0.3 to 0.6 nmol.µmol^{-1}; (Middag *et al.*, 2011; Boye *et al.*, 2012) but matched the elemental ratio measured with bulk analysis of natural phytoplankton assemblages from the Southern Ocean (1.68 nM.µM^{-1}; Cullen et al. (2003). The highest Mn/P depletion rates were found during S02 (B3) when DFe exhibited lower concentrations than in S01. The higher Mn/P uptake ratio at lower ambient availability of DFe is consistent with recent observations in the Weddell Gyre, the Antarctic Circumpolar Current and in a Fe fertilization experiment in the Pacific sector (Middag et al. (2013) their Fig. 9). The underlying biochemistry is that under Fe limitation the electron transport pathway of

the photosystem is hampered, as a result the captured solar energy is transferred into excess superoxide radicals that are very damaging within the plant cell, and hence the cell produces more superoxide-dismutase enzyme to break down these superoxides; this enzyme has Mn as its central atom. Indeed in laboratory experiments, diatoms have been shown to require more Mn under iron-deplete conditions (Peers & Price, 2006). If it is unlikely that Fe was limiting during So2 bloom events, it is also possible that the DFe was low enough (sub-optimal) to induce such higher Mn requirement by the diatoms community. In addition, or alternatively, it also is conceivable that diatom growth would in time be stressed by low concentrations of DMn as indeed observed during So2 (0.15-0.30 nM, 20 and 27 January, 2014, and 5 February, 2014, supplementary material).

For zinc, the Zn/P depletion ratio values for both So1 and So2 ranged between 2.0 and 2.5 nmol.µmol^{-1} and agree well with the lower part of ratio values that have been previously determined for different sectors of the Southern Ocean (1.60<Zn/P<8.20 nmol.µmol^{-1}; Martin et al. (1990); Nolting et al. (1991); Croot et al. (2011)). Low Zn/P values tend to suggest that phytoplankton was not limited by either DFe or light during the time of our study. Indeed, Croot et al. (2011) showed that an increase of Zn/P drawdown ratio could be due to slower phytoplankton growth rates as a result of iron and/or light limitation along the Zero and Drake transects, on the basis of preceding various bio assays on diatoms cultures, and deck incubations studies on Southern Ocean natural assemblages (Sunda & Huntsman, 1998; Cullen *et al.*, 2003).

For cadmium, the Cd/P both increased during So1 and So2, from 222 to 265 pmol.µmol^{-1} and from 241 to 270 pmol.µmol^{-1} respectively (Table 2). These values were lower than those calculated from linear regressions in the Southern Ocean (Cd/P~ 550-600 pmol.µmol^{-1};Twining et al. (2004); Boye et al. (2012); Baars et al. (2014)), from a Cd and phosphate time series data at the RaTS site (15 m depth; Cd/P~ 400-1800 pmol.µmol^{-1}; Hendry et al. (2008)) and one obtained from bulk analysis (1290 pmol.µmol^{-1}; Cullen et al. (2003).

Cd versus P relationships did not show any discontinuity when phosphate concentrations ranged between 0.75 µM and 1.0 µM (Figs. 7 & 8) as found in other

studies (Ellwood, 2008; Boye *et al.*, 2012). In surface waters, such a discontinuity is usually associated to differences in phytoplankton communities (Boye *et al.*, 2012) and/or sources intensities (Ellwood, 2008; Boye *et al.*, 2012). In general the discontinuity is attributed to the mixing of waters of (North) Atlantic origin with relatively low Cd/P ratio with waters of Antarctic origin with relatively high Cd/P ratio (de Baar et al. (1994); Middag personal communication). Indeed the studies of Boye et al. (2012) and Ellwood et al. (2008) both were in or including sub-Antarctic waters influenced by low Cd/P waters of Atlantic origin. Our study in truly Antarctic waters lacks such waters of originally low Cd/P ratio. Also our regressions are representative of bloom evolution instead of resulting from water mass mixing. Therefore, if we considered that Cd inputs were consistent during both seasons and that Ryder Bay phytoplankton blooms were dominated by diatoms during both S01 and S02 seasons (Fig. 4), it would be possible that phytoplankton assemblages had similar requirements regarding Cd during the time of the present study.

The consistency of Mn/P; Cd/P, Zn/P and Co/P ratio values during two consecutive summers indicates that over-winter scavenging removal was slow relative to mixing. This is in agreement with the description made for the behaviour of DCo in the Ross Sea (Saito *et al.*, 2010; Noble *et al.*, 2013). All three metals Cd, Zn, and Co are known to be involved in carbonic anhydrase activity and culture experiments showed that some species were able to substitute one for another when this other is lacking (Price & Morel, 1990; Sunda & Huntsman, 1998; Saito & Goepfert, 2008). It is interesting to notice that during S02, both the Zn/P and DMn/P ratios decreased from B3 to B4 while the Cd/P and Co/P conversely increased (Table 2). If DZn concentrations decreased below 1 nM occasionally during B3 (3 times) it happened more frequently during B4 (10 times). In such instances, it is possible that DZn concentrations below ~ 1nM would trigger the uptake of Cd or Co as substitutions for Zn, and hence an increase of the DCd/P and DCo/P depletions ratio values. This is in agreement with the fact that *Phaeocystis antarctica* was more abundant during the B4 event (Fig. 4) and that culture studies of this species have shown *Phaeocystis antarctica* to be able to substitute Zn for Co in the case of Zn limitation and vice versa, with a preference of Zn uptake in Zn replete conditions (Saito & Goepfert, 2008). Also Löscher (1999)

estimated that ~70% of DCd and 40% of P removed from surface waters in the Southern Ocean by biological uptake were recycled within the mixed layer. This would be another mechanism that accounts for the increased Cd/P drawdown ratio.

Trace metals and silicate

In the second summer (So2), the mean value of the Zn/Si depletion ratio was ~ 0.07 nmol.µmol^{-1}. This is in the same order of magnitude but generally higher than those reported for the Southern Ocean (Zn/Si = 0.030-0.06 nmol.µmol^{-1}; Martin et al. (1990); Westerlund and öhman (1991); Löscher (1999); Zhao et al. (2014)) and lower than in the Ross Sea (0.098 nmol.µmol^{-1}; Fitzwater et al.(2000)) or in the Weddell Sea upper layer (0.10 nmol.µmol^{-1}; Nolting et al. (1991)).

Comparison of the metal/silicate ratio between both season gave approximately two to three times lower values for the second season So2 (Mn/Si ~ 0.10 and ~0.05 nmol.µmol^{-1}; Cd/Si ~ 16 and 8.0 pmol.µmol^{-1}; Zn/Si ~ 0.17 and 0.07 nmol.µmol^{-1}; Table 2). Interestingly, B1 and B2 were the only events that showed that DMn, DZn and DCd would be depleted before silicate (Fig. 7) while B3 and B4 indicated almost simultaneous depletion between DMn, DZn and silicate (Fig. 8). Trace metals appeared to have the same concentrations dynamics during both seasons but silicate concentrations were much higher and steady during So1 (40 - 85 µmol.L^{-1}) compared to So2 (0.80 - 100 µmol.L^{-1}; Figs. 5 & 6) which is most likely due to different phytoplankton assemblages. During So1, diatoms were the most abundant during the second half, cryptophytes dominated in the first half and haptophytes were also present in significant numbers while diatoms dominated for almost 3 months during So2 (Fig. 4). Such differences in dominance and composition might impact on Me/Si drawdown ratios. Moreover, at the beginning of So2 during B3 event, the strong decrease of silicate was due to a major bloom of diatoms (Fig. 4) associated with their sudden release from a large sea ice plate causing the final low silicate ~ 1 µM, and is deemed to be growth limiting. The size of diatoms and their potential growth limitation by silicate might also induce changes in Me/Si and introduce variability at the bloom and the summer season timescales.

Trace-metals pre-bloom and bloom integrated concentrations

Integrated concentrations (IC) of each trace metal in the 0-75 m layer for each RaTS sampling event are presented in Fig. 10. During the B3 event, IC of DFe, DMn and DZn and DCu showed a progressive decrease from what could be called pre-bloom values (Fig. 10; integrated DMe concentrations calculated during early spring conditions while phytoplankton activity was still negligible). In contrast,, during the same event, IC of DCd and DCo_L showed fairly constant values close to their pre-bloom values (Fig. 10). During the B4 event, DFe, DMn and DZn IC variations were more scattered suggesting higher variability on short timescale of inputs and removal terms associated with Fe, Mn and Zn biogeochemical cycles, while IC of DCd, DCu and DCo_L were more steady (Fig. 10). During the B4 event the IC of DFe, DMn, DZn, DCd and DCo_L were lower than those calculated for both pre-bloom and B3 event. This indicates that the B4 event was most likely characterized by higher trace metals removal terms and/or lower sources intensities (Fig. 10).

These trends exclude three anomalies (15 January, 10 and 25 February, 2014) which did experience an increase in IC of trace metals as high or higher than values determined in pre-bloom conditions (Fig. 10). These anomalies correspond to sampling days that occurred after or in between storms as shown by salinity, temperature, density and fluorescence time series (Fig. 3). Storm events can quickly disturb the surface layer at the RaTS site and can deepen the surface mixed layer (e.g. to 11 m, 15 January; to 24.5 m, 27 January; to 16 m, 25 February; to 54 m, 27 February). This kind of event might be an important mechanism that supplies dissolved trace metals to the euphotic layer by vertical mixing of metal-enriched deeper water. Moreover, the 40-75 m layer happened to account for 40 to 90 % of the 0-75 m layer IC of trace metals, which strengthens the idea of a deeper trace metals reservoir, agreeing with the hypothesis of Annett et al. (2015). Sources of trace elements to the surface layers will be discussed in a future publication.

Trace metals fluxes during S02

Relative budgets were calculated for the 0-75 m depth layer during So2 and are presented in Fig. 11. These budgets provide additional information about trace metal flux dynamics at RaTS. The closer the DMe fluxes approach zero, the more the sources

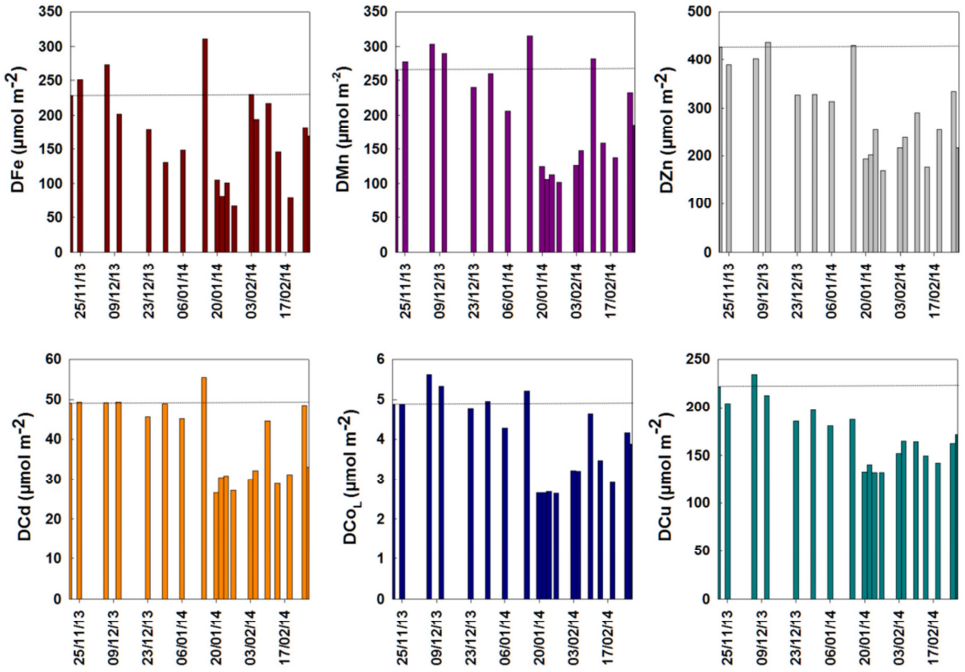

Figure 10: Integrated concentrations (IC) of each trace metals in the 0-75 m layer for each RaTS sampling event during S02. The dotted line represents the IC calculated during pre-bloom conditions (21st November 2013).

and sinks are balanced. Similarly, positive fluxes should reflect more DMe inputs than DMe removal and vice versa.

In the present study trace metals distributions have been shown to be driven by biological uptake and this sink probably accounts for most of the negative fluxes reported here (Fig. 11). The removal fluxes of DMn, DZn, DCd, DCu and DCo_L calculated during B2 event were relatively low and in this period the budgets were fairly balanced. One of the two highest negative fluxes determined for all of the studied trace metals occurred during a sharp increase of fluorescence when diatoms and haptophytes represented ~80 and ~15 % of the biomass (Figs. 4 & 11). At this time, the fluxes of DFe, DMn and DZn reached ~-40 µmol $m^{-2}d^{-1}$ while DCd and DCu were about -10 and -5 µmol $m^{-2}d^{-1}$ respectively. Dissolved Zn and Cd reached their high negative flux (-67 and -7.7 µmol $m^{-2}d^{-1}$; Fig. 11) at the very end of the season while fluorescence increased sharply.

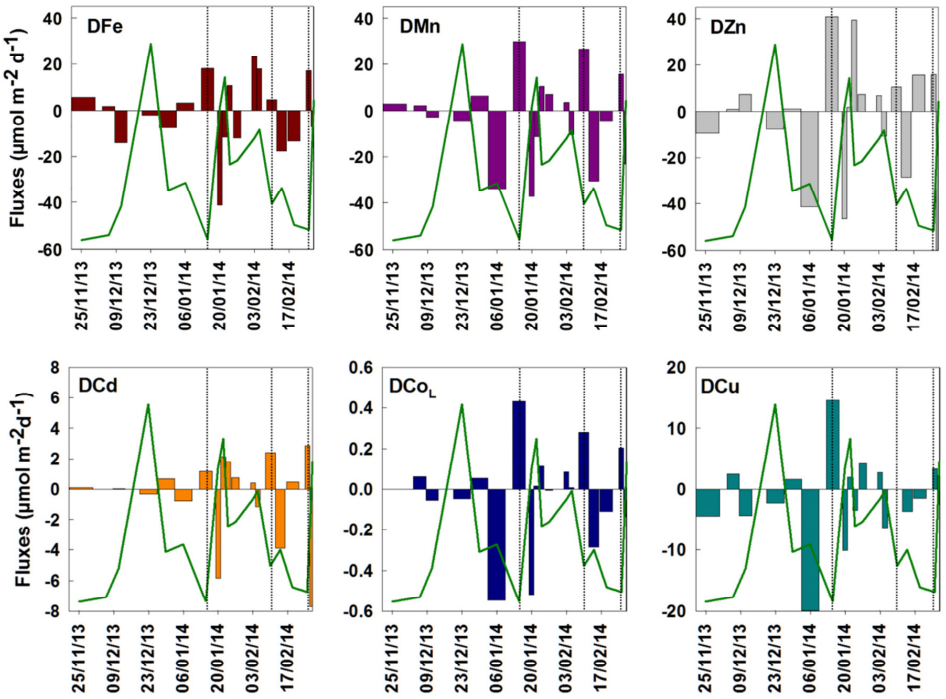

Figure 11: Dissolved trace metals relative budgets during So2 calculated between two consecutive sampling events. Fluxes were calculated by subtracting integrated concentrations of two consecutive sampling days ($\delta_{IC} = IC_{T_1} - IC_{T_0}$) and divided by time periods that separates each sampling events giving fluxes in µmol.m^{-2}.d^{-1} (Fig. 9). A negative flux is indicating a net removal while a positive flux is showing a net input of trace metals. The green line represent fluorescence signal from the CTD (fluorescence maximum within the 0-75 m depth layer). Vertical dotted lines correspond to sampling events conducted after storm episodes.

In such a coastal region, there are numerous high intensity sources of trace metals (atmospheric inputs, glacier and sea ice melt and inputs from shelf sediments, remineralization) as reflected by the highest positive fluxes calculated for all the trace elements (DFe, DZn, DMn and DCu fluxes were up to 18, 30, 41, 14.5 µmol m^{-2}d^{-1}, respectively, between the 6-15 January 2014; Fig. 11). Here the sampling occurred a day after the end of a storm episode which enhanced the upward mixing of deeper waters that are enriched in trace metals with surface water as explained in the previous section. Vertical mixing events have been previously described as partially responsible for renewing surface waters with nutrients coupled to dissolved Al (Hendry *et al.*, 2010), which confirms that storm-induced mixing can have generated inputs of trace

metal in the surface waters during the time of the present study. Higher inputs of trace metals were found from the beginning of January towards the end of February when the surface layer is the warmest (Fig. 3) which might increase glacier and sea ice melt (Meredith *et al.*, 2008) that can also be a significant source of trace metals.

Conclusions

Time series of six bio-active trace metals have been investigated during two Austral summers in Ryder Bay, a small coastal embayment located on the Western Antarctic Peninsula. Most of the studied trace elements (Fe, Mn, Zn, Cd and Co) showed wide ranges of concentrations and this dynamic appears to be driven by phytoplankton uptake, remineralization and occasional vertical mixing associated with storm episodes. The biological uptake of DMn, DZn, DCd, DCo_L and DCu was proportional to the uptake of phosphate and silicate. DMn and DCd exhibited the strongest linear relationship with phosphate and silicate further indicating their key role as trace nutrient and the coupling of their biogeochemical cycles. The weaker relationship of Fe with macronutrients (and to some extent Zn, Cu and Co) suggests that additional sources and sinks are driving their distributions in the present area of study. The consistency of trace metals / nutrient ratios during two consecutive summers indicates that over-winter scavenging was slow relative to mixing. The abundances of diatoms, which tend to vary both at the season and bloom time scale, ruled the relationships of trace elements versus silicate. At the summer season scale, the increase of DCd/P and DCo_L/P drawdown ratios during the two consecutive blooms monitored during the second season could reflect trace metals substitution of Zn due to lowered DZn concentrations after the first bloom. The growth of the phytoplankton assemblage might occasionally be stressed by simultaneous short-term events of depletions of both nutrients and bio-active trace metals.

Calculations of dissolved trace metals integrated concentrations during one bloom event with high temporal resolution indicate that DFe, DMn and DZn show higher variability of their sources and sinks intensities compared DCd, DCu and DCo_L. Comparison of dissolved trace metals integrated concentrations during two consecutive bloom events showed that, during one season, higher removal terms and/or lower sources intensities could drive trace elements stocks lower. Integrated

concentrations anomalies evidenced that storm episodes appear to be an important mechanism to supply dissolved trace metals to the euphotic layer by vertical mixing of enriched deeper water. The relative budget calculated for S02 indicates that the apparent lack of trace metal removal during the second half of the season (January-February) could be due to more significant inputs such as storm driven mixing and ice melt.

Acknowledgements

The authors gratefully acknowledge the British Antarctic Survey, Royal Netherlands Institute for Sea Research (NIOZ) and the Netherlands Organization for Scientific Research (NWO) for the opportunity to conduct field work at the Dirck Gerritsz and Bonner laboratories at Rothera. Particular thanks to our colleagues Amber Annett, Mairi Fenton and Elisabeth Jones, for their wonderful help during trace metals samples collection, and to Ronald Visser and Pim Sprong for collecting and filtering samples for the analysis of phytoplankton pigments. We also would like to thank Rothera's boat officers Timothy Fox and Paul Samways, and Rothera Technical Services for their assistance. We thank Katharine Hendry and one anonymous reviewer for their constructive comments and suggestions that improved the manuscript. Support was gratefully received from Sven Ober (NIOZ), for CTD maintenance and data calibration. This work is part of postdoctoral research (J. Bown) at NIOZ under the research programme 866.20.031, which was financed by the Netherlands Organisation for Scientific Research (NWO).

5

Chapter 6

Niche partitioning in Antarctic haptophyte and cryptophyte ecotypes.

P. D. Rozema
L.A. Amaral-Zettler
W.H. van de Poll
A. G. J. Buma
M.P. Meredith
J. Bown
H. Bolhuis

Abstract

The phytoplankton community along the west Antarctic Peninsula is shifting from a diatom to a phytoflagellate dominated community as a result of current climatic trends. However, many relations between phytoplankton taxa and environmental parameters remain unclear or difficult to reproduce. Here, we strongly improved the taxonomic resolution of the abundant phytoflagellate diversity using 18S rRNA gene sequencing at the Rothera Oceanographic and Biological Time Series station in northern Marguerite Bay in combination with a traditional pigment fingerprinting technique (HPLC with CHEMTAX) and environmental characteristics. Spatial and temporal diversity were included by sampling at five different stations during two summers (2012-2014). This approach yielded information on various members of the *Hacrobia* group, in particular ecotypes from the flagellated, photosynthesizing genera *Chrysochromulina, Phaeocystis* (both dominant haptophytes), and *Geminigera* (cryptophytes). Relative abundance of these ecotypes co-occurred with specific environmental conditions governed by variations in nutrients, water column stability, salinity, and/or temperature, suggesting a strong niche partitioning within each species. For example, three distinct *G. cryophila* ecotypes showed different preferences of sea water temperature and water column stability. Furthermore, a *Geminigera*-specific grazer (*Prorocentrum* sp.) was suggested to assert top down control while no specific grazers were identified for the haptophytes. We conclude that bottom-up controls result in niche partitioning in the phytopflagellate ecotypes, adding an extra layer of complexity the understanding phytoplankton community responses to local climate trends.

Apendices are available upon request.

Introduction

Phytoplankton community composition and dynamics therein along the west Antarctic Peninsula (WAP) is rapidly changing (Montes-Hugo *et al.*, 2009). Decreasing sea ice extent, deeper mixed layers, increasing glacial run off and higher sea water temperatures are considered to be the main causes of these community changes (Cook *et al.*, 2016; Meredith *et al.*, 2017; Stammerjohn & Maksym, 2017). A frequently reported trend along the WAP is the increased abundance of nanophytoflagellates, such as haptophytes and cryptophytes, at the expense of larger diatom species (Montes-Hugo *et al.*, 2009; Saba *et al.*, 2014; Rozema *et al.*, 2017a; Schofield *et al.*, 2017). However, local variations are also observed. In the northern part of the WAP, deeper, wind-induced water mixing occurs due to a decrease in sea ice cover in combination with stronger northerly winds. This results in a decrease in phytoplankton biomass and average phytoplankton cell size (Montes-Hugo *et al.*, 2009). In contrast, phytoplankton biomass is increasing in the southern part of the WAP. Yet, a decreasing winter ice extent may result in deeper mixed layers which persist to the following spring and summer, decreasing overall summer productivity by preventing diatom biomass accumulation (Venables *et al.*, 2013; Rozema *et al.*, 2017a). In addition, at more coastal and sheltered regions along the WAP, melt water lenses are formed by glacial runoff, an increasing dominance of cryptophytes and haptophytes is observed (Moline *et al.*, 2004; Saba *et al.*, 2014; Rozema *et al.*, 2017a). Thus, despite local variability, the overall WAP phytoplankton community is gradually shifting from large diatoms to small phytoflagellates.

The observed transitions within the phytoplankton community have a documented negative impact on grazers and predators within the Antarctic foodweb (Saba *et al.*, 2014). Most notable is the decline in krill (*Euphausia superba*) biomass/numbers, the main grazers of larger phytoplankton. In contrast, gelatinous species such as salps (*Salpa thompsoni*) increase in numbers with negative consequences for Adélie penguins (*Pygoscelis adeliae*), iconic Antarctic species that are currently declining in population size (Atkinson *et al.*, 2004; Ducklow *et al.*, 2007). Albeit meso- and macrograzers, such as krill, are considered pivotal within the Antarctic foodweb, yet microzooplankton are the main herbivores in the world's oceans (Calbet & Landry,

2004; Steinberg & Landry, 2017). While data suggest that this is not different in the WAP (Burkill *et al.*, 1995; Tsuda & Kawaguchi, 1997; Garzio *et al.*, 2013), there is relatively limited information regarding the impact, composition and role of the microzooplankton community or the dynamics therein (reviewed in Ducklow *et al.*, 2012).

Long term monitoring is an essential tool to study phytoplankton community dynamics and to explore future scenarios. Using space-for-time substitution allows to look beyond the span of the currently established timer series (Pickett, 1989). Since the early '90s samples taken along the WAP are being analyzed by pigment fingerprinting and resolved with CHEMTAX, a program using pigment fingerprints that allows identification of major taxonomic groups at approximately the *Class* level, (Mackey *et al.*, 1996; Kozlowski *et al.*, 2011; Rozema *et al.*, 2017a; Schofield *et al.*, 2017). An advantage of the CHEMTAX approach is the long time series analyzed, methodological consistency and use in many oceanic ecosystems allowing comparative studies. However, one of the major limitations is its low taxonomic resolution. For example, the haptophyte group is considered to be dominated by the nano-flagellate *Phaeocystis antarctica* (e.g. Petrou *et al.*, 2016;Trimborn *et al.*, 2015; Rozema *et al.*, 2017c; Ducklow *et al.*, 2012). However, sparse sequencing data suggest the presence of other genera and species in this group, nearly undistinguishable from the dominant species using (pigment or DNA) fingerprinting techniques or microscopy. Moreover, *P. antarctica* is attributed great plasticity with regards to e.g. nutrient uptake, morphology (colony vs flagellate states), photophysiology, temperature and salinity tolerance making identification difficult and time consuming (Arrigo *et al.*, 1999, 2010; Schoemann *et al.*, 2005; DiTullio *et al.*, 2007; Alderkamp *et al.*, 2012b; van Leeuwe *et al.*, 2014; Trimborn *et al.*, 2015). This plasticity is frequently observed when comparing different strains in laboratory experiments but the different properties of these strains are not studied in the field (Medlin & Zingone, 2007; Arrigo *et al.*, 2010; Gäbler-Schwarz *et al.*, 2015). Given the high diversity in locally evolved genotypes in the Southern Ocean (Gäbler-Schwarz *et al.*, 2015), it is highly plausible that some of these local genotypes became specialized in particular environmental conditions, thus filling different niches induced by environmental variability and giving rise to different ecotypes (Cohan,

2002). As such, these processes could be considered the first steps into speciation in phytoplankton. Moreover, exploring different species/ecotypes of haptophytes/*P. antarctica* using CHEMTAX is challenging, if not impossible, and often more a product of high plasticity in pigment composition and not niche partitioning (DiTullio *et al.*, 2007; Wright *et al.*, 2010; van Leeuwe *et al.*, 2014). Refining the taxonomic resolution to which the most abundant flagellates, cryptophytes and haptophytes which are members of the *Hacrobia*-group, are resolved should give us a better understanding of the different ecological niches that these groups frequently occupy, as it has in the case of e.g. *Prochlorococcus* (Rocap *et al.*, 2003; Prosser *et al.*, 2007). Such understanding would allow for a better translation of laboratory based to studies to the Antarctic ecosystems.

The aim of this study was to untangle different strains from the major taxonomic groups, to partition these data to identify specific niches for these strains and finally to identify grazers who might specifically target the observed major strains. A better understanding of phytoflagellate representatives, to which the WAP ecosystem is shifting, will allow for a better prediction of the impact of the current climatic trends. Samples for 18S rRNA MiSeq sequencing were collected over two summer seasons at the Rothera Oceanographic and Biological Time Series (RaTS) in Ryder Bay, northern Marguerite Bay (WAP). We sampled Ryder Bay at three stations and depths to ensure an environmental gradient within each of our time points. Our DNA and pigment samples were supplemented by the sampling for and measurement of a range of environmental parameters ensured sufficient context to our biological samples. Taxonomic resolution was increased by Minimum Entropy Decomposition (MED) of the 18S rRNA sequences (Eren *et al.*, 2015). Additionally, sampling for high pressure liquid chromatography (HPLC) analysis with CHEMTAX allowed for incorporation of our results with the observations from longer running temporal and spatial investigations (Mackey *et al.*, 1996; Kozlowski *et al.*, 2011; Rozema *et al.*, 2017a).

Materials and methods

Sampling sites and collection protocol

Samples were collected during two field campaigns (Jan-Mar 2013 (S01) and Nov 2013-March 2014 (S02)) at three fixed depths (2, 15 and 75m) and three sites near Rothera research station (Ryder Bay, Adelaide Island, Antarctica). The stations were located near the Sheldon Glacier (G), the RaTS site (R, 67.570°S 68.225°W) in the middle of the bay, and at the edge of the boating limit outside of the bay (O) (Figure 1). This ~12 km transect was supplemented with two additional outside stations (O1 and O2) that were sampled once during S02 with help from the *ARSV Lawrence M. Gould* in the open Marguerite Bay. Sampling frequency was approximately once every two weeks resulting in a total of 20 events (S01 = 9 and S02 = 11). Fluorescence, turbidity, conductivity and temperature profiles were recorded to ~95m depth using a CTD package (19+, SeaBird, US) equipped with an in-line fluorometer (WS3S, WETLabs, US) and a turbidity sensor measuring at 700 nm (ECO NTU, WETLabs, US). Occasionally macronutrient analysis were collected using 4 L polyvinyldifluoride bottles, operated via a Kevlar cable connected to a titanium electric winch as described previously (Bown *et al.*, 2017). All other samples (macronutrients, pigments and DNA) were collected using a single 16L Niskin bottle deployed from a small boat equipped with a

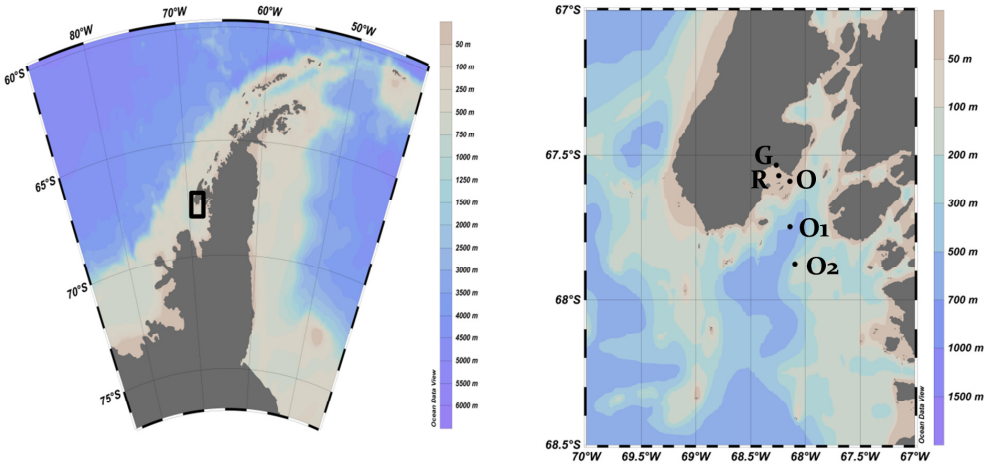

Figure 1: Left: a map of the west Antarctic Peninsula, marked is the study region. Right: the study region with the marked stations.

hand winch as described previously in (Rozema *et al.*, 2017c). Sampling from the *ARSV Lawrence M. Gould* was performed using a rosette sampler equipped with 12L Niskin bottles while sample processing remained identical. After collection, the samples were transported in dark, insulated boxes to the laboratories at Rothera station for further processing. CTD water column profiles, and macronutrient, pigment and DNA samples were processed, stored, and analyzed as described previously and as further explained in the methods supplement (Bown *et al.*, 2017; Carvalho *et al.*, 2017; Rozema *et al.*, 2017a, 2017c).

Pigment fingerprinting and taxonomic assignment

Water samples (3.0-7.0 L) were filtered through 47mm GF/F filters (Whattman, US) after which filters were immediately snap frozen in liquid nitrogen and stored at -80°C. Reverse phased HPLC was executed to separate phytoplankton pigments, as previously described for the RaTS samples (Rozema *et al.*, 2017a). In short, samples were freeze dried before extraction in 90% acetone at 4°C for 48h. Pigments were separated using a Waters 2695 HPLC system equipped with a Zorbax Eclipse XDB-C8 column (van Heukelem & Thomas, 2001; Perl, 2009) and quantified using a Diode array spectroscope (type 996, Waters, US). Calibration of the system was performed using standards for the pigments of interest (Supplement Table 1, DHI Lab Products, Denmark).

CHEMTAX v1.95 software was used to calculate the abundance of major phytoplankton groups using the recommended settings, as previously used for the analysis of RaTS dataset (Mackey *et al.*, 1996; Kozlowski *et al.*, 2011; Rozema *et al.*, 2017a). The included taxonomic groups were expanded in comparison to previously published data from the RaTS as our 18S rRNA sequences suggested unexpectedly large proportions of chrysophytes and pelagophytes (Bown *et al.*, 2017; Rozema *et al.*, 2017a, 2017b). These two groups were combined due to their similar pigment structure. Initial pigment ratios were as used previously and supplemented with field ratios for the Chryso/Pelago-group (Higgins *et al.*, 2011; Rozema *et al.*, 2017c). Samples were binned by depth and season, creating a total of 6 bins (Mackey *et al.*, 1996). CHEMTAX was run 60 times with variable initial ratios, varied randomly by +-35% (Wright *et al.*, 2009). Finally, we summed the abundance results of the various haptophyte and

diatom groups and present this as "Pooled haptophytes" and "Pooled diatoms", respectively. CHEMTAX abundances measured at 15 m depth were compared to 18S OTUs at the taxonomic resolution (phylum or class, supplement Table 2) of CHEMTAX using linear regressions and SIMPER (see Methods supplement).

Collection and processing of DNA and sequences thereof

Samples for DNA analysis (1.7-3.0 L, 176 unique samples) were collected in duplicate and each replicate was filtered in two steps over a 3.0 µm and a 0.2 µm pore size polycarbonate filter membranes (47mm, Millipore, US) using a mild vacuum in a temperature controlled laboratory (~2°C). Filters were stored in 3 mL cryovials before being snap frozen in liquid nitrogen and storage at -80°C. DNA was extracted as specified in (Rozema *et al.*, 2017b) with 0.02% sodium dodecyl sulfate and 0.1% polyvinylpyrrolidone added to the 2% CTAB extraction buffer. Extraction efficiency and quality were estimated using a NanoDrop 2000 (Thermo Scientific, US) before pooling of the DNA from both filter sizes to obtain a DNA sample representing the full community composition. The DNA extracts were transported on dry ice to the Marine Biological Laboratory (Woods Hole, US) for 18S rRNA amplicon sequencing. The variable V4 region of the 18S rRNA gene for all the unique samples plus 10% of the duplicates was amplified from the DNA samples using the universal forward primer V4F (5'-CCA GCA SCY GCG GTA ATT CC-3') and reverse primer V4RB (5'-ACT TTC GTT CTT GAT YRR-3') with PCR conditions as specified in the methods supplement (Balzano *et al.*, 2015). The amplicons were sequenced on a MiSeq sequencer (Illumina, US). The sequences were demultiplexed, trimmed, quality assessed, and rarified (to n = 25,237) before Minimum Entropy Decomposition (MED) to construct operational taxonomic units (OTU_{MED}) (Eren *et al.*, 2013, 2015). MED iteratively decomposes our dataset using only highly variable nucleotide positions to create highly resolved units, oligiotypes (OTU_{MED}), which circumvents the need to set a global sequence similarity cut-off (Bálint *et al.*, 2016). Representative sequences for the final MED nodes were annotated using BLAST+ (v2.2.31) against the Protist Ribosomal Reference database (PR^2, v4.5; Guillou *et al.*, 2013; Camacho *et al.*, 2009).

Identify ecotypes and niches

To investigate temporal and spatial dynamics within the different OTU_{MED} , we calculated relative abundance within every OTU_{MED} to identify periods and stations with strongly elevated presence of that OTU_{MED}. Thus, we divided the count per samples per ecotype by the total number of counts for all samples per ecotype. This method standardized the observations to allow for a comparison of occurrence patterns between different OTU_{MED} within genera differing in total abundance. Clusters were proposed based on spearman-rank based dendrograms, inspected and presented using non-metric multidimensional scaling (NMDS) with Bray-Curtis similarity distances and tested using NP-MANOVA (Bray & Curtis, 1957; Anderson, 2001; Taguchi & Oono, 2005). Derived p-values were deemed significant if the conservative Bonferroni-corrected $p < 0.05$ (Dunn, 1961). If so, the OTU_{MED} within each cluster were pooled and these are presented as suspected ecotypes. Thereafter, the relative abundances were recalculated per ecotype as above before canonical correspondence analysis (CCA) using Bray-Curtis similarity distances with environmental parameters to identify preferred niches per ecotype in the different taxonomic groups (Legendre & Legendre, 1998). All aforementioned statistical analyses were executed using PAST 2.17c (Hammer *et al.*, 2001).

Co-occurrence network analysis

A co-occurrence network was creating using the CoNet app in Cytoscape for the samples taken at 2m depth (Shannon *et al.*, 2003; Faust *et al.*, 2012; see methods supplement). This depth was chosen because changes in environmental conditions, and thus expected niche differentiation, is likely to be highest at the surface. Such an analysis allows to estimate the incorporation of the groups of interest into the microbial foodweb. All OTU_{MED} , not clustered in ecotypes, with at least 1000 counts in the 2m samples were included to reduce the influence of low abundance OTU_{MED} . A stringent threshold ($r \geq 0.8$) was set to identify dependencies between species. The resulting network was analyzed for (sub)clusters using Cytocluster (Wang *et al.*, 2011; see methods supplement), which were then considered an ecological meaningful subset and evaluated in this manuscript

Results

Environmental and biological variability within the natural laboratory

Spatial differences in temperature and salinity between the G, R and O stations (2m) on the same day were at most 0.93 °C and 0.56, respectively. Although our stations were located at increasing distance from the glacial freshwater input, this did not necessarily result in an increasing salinity along this transect. For example, station O was occasionally less saline than station G if O was situated in the wake of a large melting ice berg. Both investigated seasons were more extensively described elsewhere and with a higher temporal resolution (Bown *et al.*, 2017; Jones *et al.*, 2017; Rozema *et al.*, 2017c; Venables *et al.*, 2017). Thus in short, during the 2012-2013 summer, the inspected waters were described as medium stratified, phytoplankton biomass was low-to-medium biomass and sea surface temperature (SST) was relatively high. In contrast, in the 2013-2014 summer, water temperatures were lower, with weaker stratification, above average sea ice melt and medium levels of biomass. The phytoplankton community was largely composed of three major taxonomic groups, namely diatoms, haptophytes and cryptophytes as determined by CHEMTAX (Fig. 2). Diatoms were dominating with generally >60% abundance at 15m at site R. Only during January and February 2013 diatoms dropped in abundance to 20% in favour of cryptophytes which increased to 71%. Smaller, yet noteworthy, increases in cryptophyte abundances occurred early December 2013, mid-January and February 2014. Haptophytes did not reach contributions as high as cryptophytes, giving a maximum relative contribution of 24%, but were more abundant than cryptophytes in February 2013, early December 2013 and the second half of February 2014. Stations O and G were highly similar in seasonal dynamics of the phytoplankton community relative to station R.

Comparison of pigment- and 18S-based taxonomy

Sequencing of 173 unique samples resulted in a total of 7.4 million sequences and were decomposed into ~1200 OTU_{MED} after subsampling. Forty different genera of known photosynthetic microeukaryotes were observed, constituting on average 35% of the total sequences per samples (Appendix table 2, appendix figure 1). When comparing to

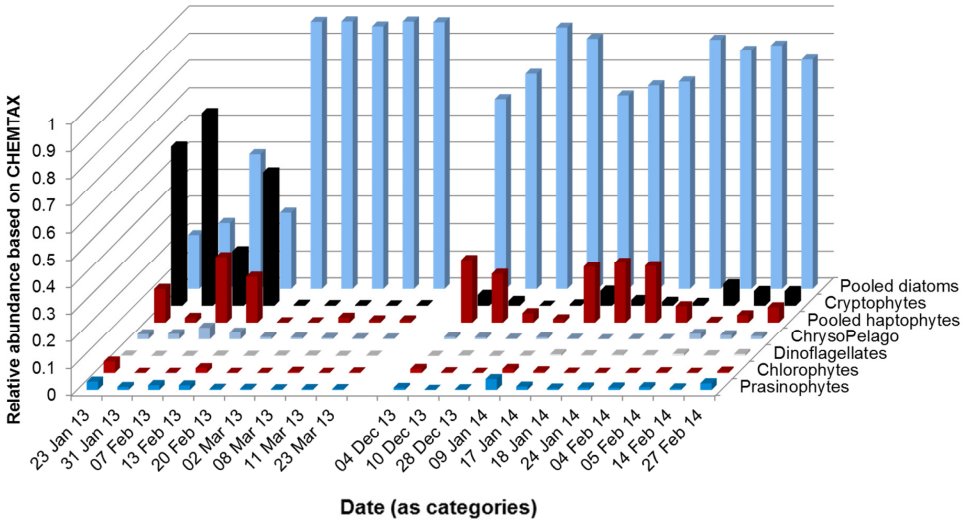

Figure 2: The relative abundance in the major taxonomic groups as estimated by HPLC-CHETMAX. These data are obtained from 15 m at the long term monitoring site (R).

the CHEMTAX data, an 18% lower contribution of diatoms to the community was measured in the sequence dataset, while haptophytes were estimated to be 20% higher in the sequence dataset (Table 1, supplement figure 3). Cryptophytes and less abundant taxonomic groups were highly similar between the two methods. The overall dissimilarity between the two datasets was estimated at 39.5% (SIMPER) and could be largely attributed to the observed difference in estimations for haptophytes and diatoms (Table 1).

Homogeneity within the top surface layer

Comparison (SIMPER) of photosynthetic *Hacrobia* related OTU_{MED} abundances at 2 and 15m depth revealed a dissimilarity of 49.9% (Supplement Table 1) of which 64.8% could be explained by the abundant OTU_{MED} (*P. antarctica* e1, *Geminigera cryophila* e1 and *Chrysochromulina* sp. e1). Further exploration using NMDS and NP-MANOVA did not yield a significant difference between these depths (data not shown, $p > 0.05$). As such, temporal and spatial dynamics were described below for the 15m samples as 2m samples followed the same trends, as such CCAs were conducted using the combination of the 2 and 15m datasets.

Table 1: A comparison between 18S rRNA and HPLC-CHEMTAX relative abundance of the major taxonomic groups as resulted from a SIMPER analysis

Group	Av. dissim	Contrib. %	Mean abund. CHEMTAX	Mean abund. 18S rRNA
Pooled diatoms	17.32	43.79	0.747	0.563
Pooled haptophytes	12.38	31.31	0.1	0.302
Cryptophytes	8.065	20.39	0.114	0.108
ChrysoPelago	0.729	1.843	0.0146	0.0125
Prasinophytes	0.5814	1.47	0.012	0.0142
Chlorophytes	0.4739	1.198	0.00949	8.88E+05

Dynamics in the photosynthetic hapto- and cryptophytes using 18S rRNA

In this manuscript we discuss the dynamics in haptophytes and cryptophytes from 18S rRNA sequences. We reiterated that we define OTU_{MED} as the our lowest unit derived from sequence annotation. OTU_{MED} with different temporal and spatial dynamics but annotated to the same species are defined as ecotypes. Different OTU_{MED} within an ecotype we call genotypes. Finally, "database entries" are full length 18S rRNA gene sequences from the PR² or NCBI databases. The first is based on the second but with curated, standardized taxonomy.

Haptophytes

Overall the haptophyte community was dominated by *Phaeocystis* and *Chrysochromulina. Phaeocystis* absolute abundance was highest on January 23 and in February 2013 (Figure 3). Yet, overall *Phaeocystis* was observed more frequently during the second, 2013-2014, season especially early December 2013 and in the second halves of January and February 2014. *Chrysochromulina* occurred predominantly during two periods; February 2013 when the genus was observed as frequent (21.5%) as *Phaeocystis* and February 2014 but only up to 1.8% of the total microbial community.

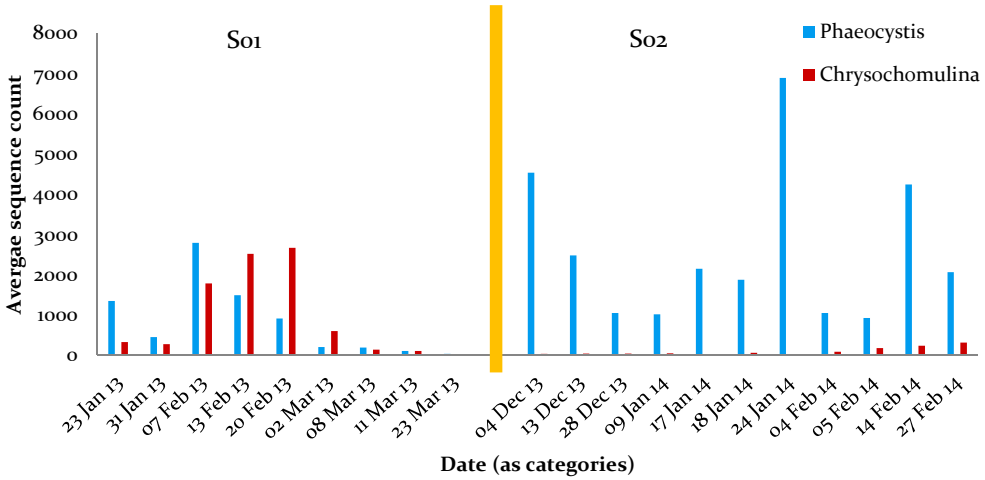

Figure 3: Absolute sequence abundance of the two major genera of haptophyte photoflagellates. The orange bar marks the difference between the two seasons.

Five different OTU_{MED}, all annotated to the same taxonomy (*Chrysochrolumina* sp.*)* but different database entries, were found in *Chrysochromulina* (supplement figure 3) Yet dynamics in standardized relative abundances indicated only two ecotypes (Figure 4). *Chrysochromulina* e1 (mostly KJ763331, 100% identity) was numerically dominant over e2 (KF130215 and JX680407, both 99.7% identity) and peaked in abundance on February 7th (Figure 5). Shortly thereafter a peak of e2 (February 13th – 20th) was found.

Within the *Phaeocystis* genus the 37 different OTU_{MED} revealed high identity to three different database entries (supplement figure 3). Numerically dominant, both in total sequence counts and genotypes (19), was *Phaeocystis antarctica* e1 (Figure 4, mainly JX680433, 100% identity). The second *P. antarctica* ecotype (e2, also JX680433, 99.7% identity) showed near identical dynamics in S01 as e1 but was nearly absent in S02. Two other database entries were abundant which were both attributed to *Phaeocystis* sp.. These ecotypes included 6 (e1, JX660995, 100% identity) and 7 genotypes (e2, JX680367, 99.7% identity). The original independent studies of these database entries placed these sequences in the *Phaeocystis jahnii* clade, as such we will refer to these sequences as *Phaeocystis cf. jahnii* (Decelle *et al.*, 2012; Simon *et al.*, 2013). Temporal variability showed that *P. antarctica* e1 dominated the general dynamics of the haptophytes, as estimated with CHEMTAX (Fig. 2 and 5). However, *Phaeocystis cf.*

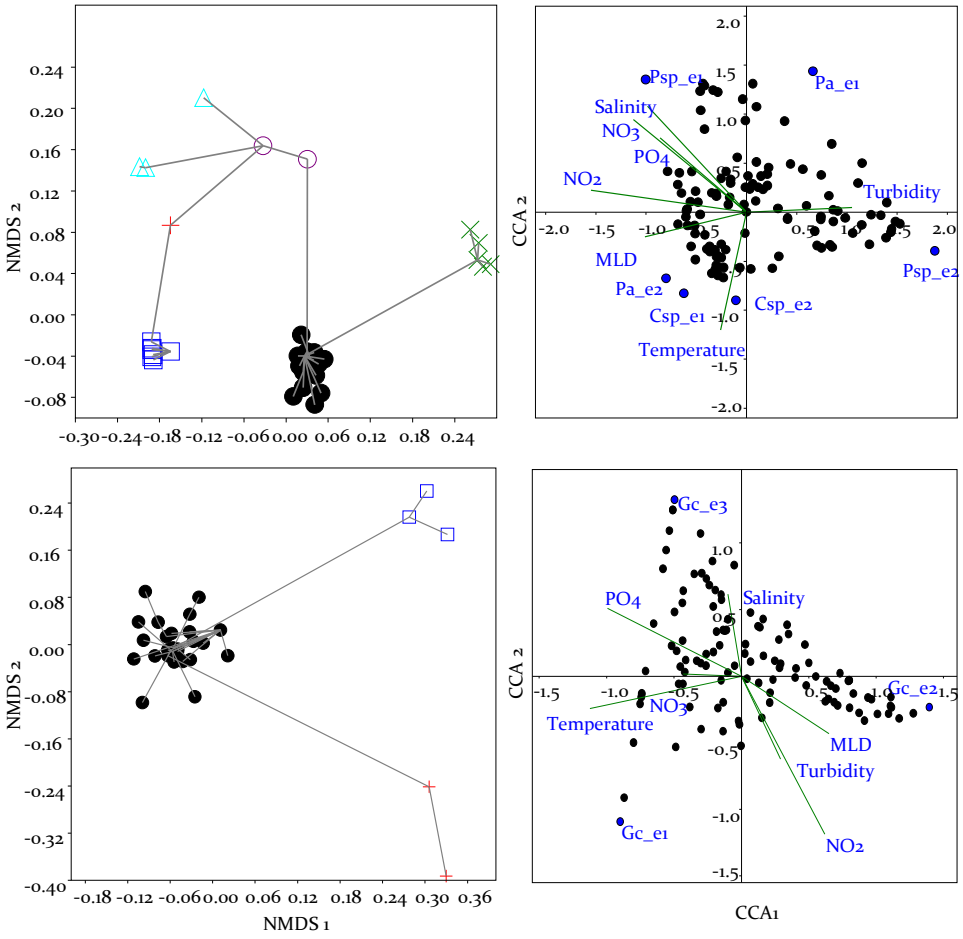

Figure 4: Left: NMDS with bray-curtis similarity for the difference genotypes of haptophyte photoflagellates (top) and cryptophytes (bottom). The different symbols and colors indicate the different genotype clusters and thus ecotypes. Right: CCA for the different ecotypes of haptophyte photoflagellates (top) and cryptophytes (bottom) and environmental parameters. Blue dots are the ecotype centroids whereas black dots represent individual environmental samples.

jahnii e1 abundance was only elevated in S02 and started to increase on January 9. Maximal abundance was observed on January 17. *Phaeocystis cf. jahnii* e2 abundance peaked mainly in S01, most closely associated with the increase in *Chrysochromulina,* but was also observed in elevated numbers in the first sample of S02 on December 4. The combination of the different peaks in maximum abundance of the haptophytes ecotypes strongly resembled the different increases in haptophyte relative abundance as estimated with CHEMTAX (Table 1, Figures 2 and 5).

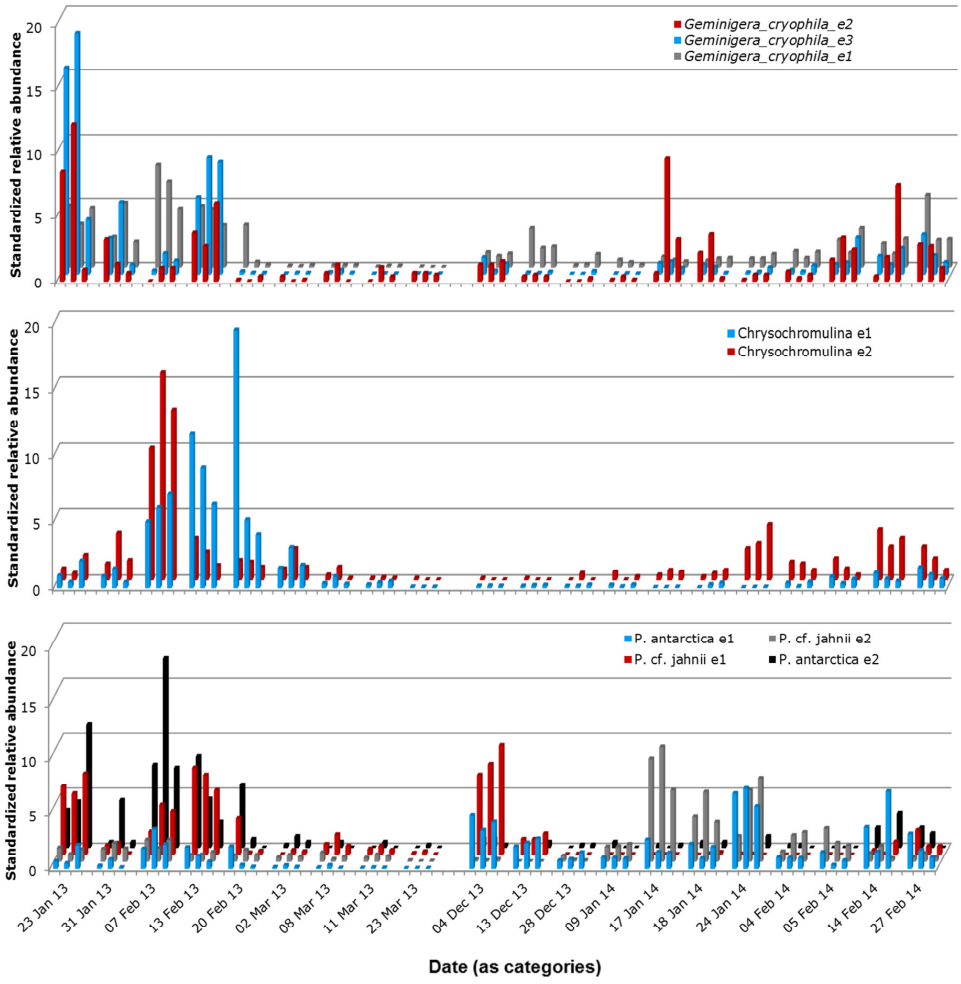

Figure 5: Standardized relative abundances of the different ecotypes. Top: Geminigera cryophila, middle: Chrysochromulina sp., and bottom: Phaeocystis antarctica and cf. jahnii.

The CCA divided the six different haptophyte species/ecotypes into different quadrantsin relation to environmental parameters (Figure 4). As suggested from the temporal dynamics, the *Chrysochromulina* ecotypes and *P. antarctica* e2 were highly similar, only differentiated slightly by a difference in MLD, nutrient concentrations and salinity. The conditions characterizing these ecotypes were a deep MLD and relatively high water temperature. In contrast, the previous ensemble was *P. antarctica* e1, which was associated with a high turbidity, salinity and nutrient concentrations yet shallow MLD and relatively low temperatures. The samples with the two ecotypes of

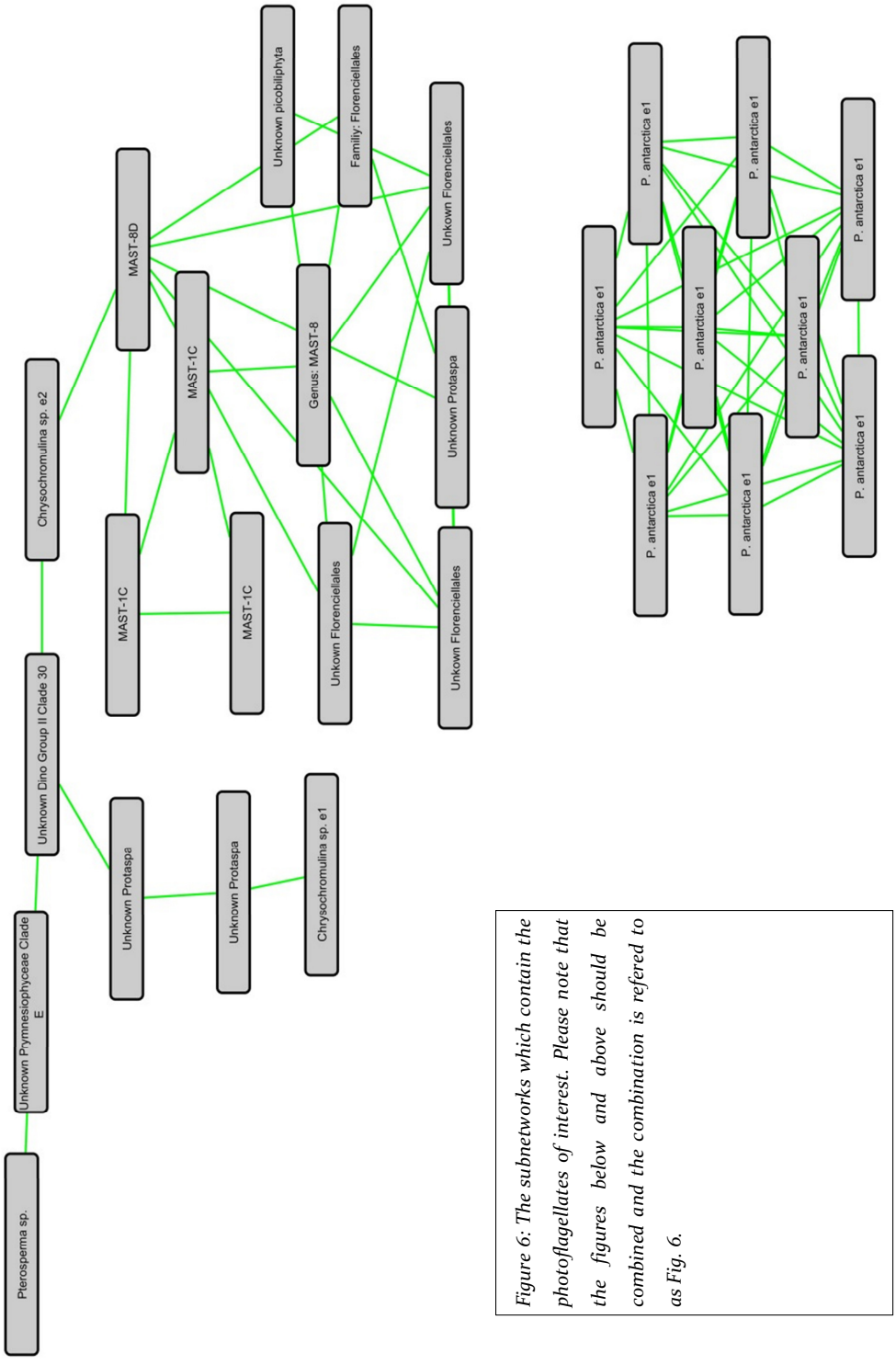

Figure 6: The subnetworks which contain the photoflagellates of interest. Please note that the figures below and above should be combined and the combination is refered to as Fig. 6.

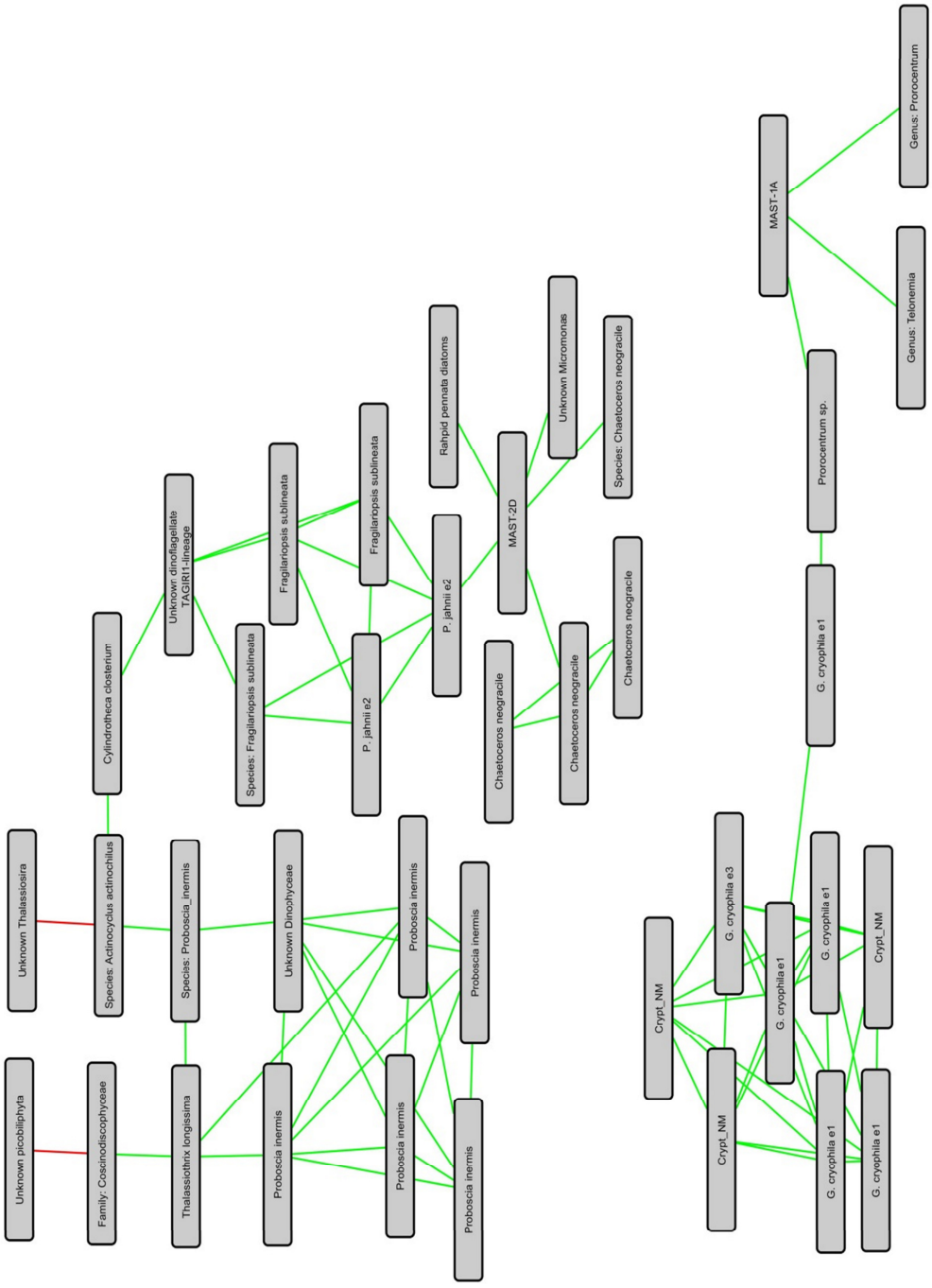
Unknown picobiliphyta
Unknown Thalassiosira
Family: Coscinodiscophyceae
Species: Actinocyclus actinochilus
Cylindrotheca closterium
Thalassiothrix longissima
Species: Proboscia_inermis
Unknown: dinoflagellate TAGIR11-lineage
Proboscia inermis
Unknown Dinophyceae
Species: Fragilariopsis sublineata
Fragilariopsis sublineata
Proboscia inermis
Proboscia inermis
P. jahnii e2
Fragilariopsis sublineata
Proboscia inermis
P. jahnii e2
Rahpid pennata diatoms
Chaetoceros neogracile
MAST-2D
Unknown Micromonas
Chaetoceros neogracile
Species: Chaetoceros neogracile
Chaetoceros neogracile
Crypt_NM
G. cryophila e3
Crypt_NM
G. cryophila e1
G. cryophila e1
Crypt_NM
G. cryophila e1
G. cryophila e1
Prorocentrum sp.
MAST-1A
Genus: Prorocentrum
Genus: Telonemia

Phaeocystis cf. jahnii also showed opposite preferences, e1 was observed in samples with a low temperature and turbidity, but high salinity, nutrient concentrations and deep MLD. The other ecotype, *Phaeocystis cf. jahnii* e2, showed opposite preferences albeit al lower temperature influence.

Cryptophytes

Only one genus of cryptophytes was found, namely *Geminigera*, and temporal dynamics suggested three ecotypes belonging to the species *Geminigera cryophila* (Figure 4). Cryptophytes were more abundant during S01 than in S02. During S01, two periods of increasing abundances (January 23rd and February 13th) were observed and sequences of *Geminigera* were more numerous than *Phaeocystis* and *Chrysochromulina* combined. In contrast, absolute and standardized abundance of *Geminigera* in S02 were only somewhat elevated in the early summer before reaching a low on January 9th (Figure 5). Thereafter, the cryptophytes slowly increased towards the end of the summer. Variability in temporal dynamics of the three cryptophyte ecotypes revealed that S01 was characterized by opposing trends in e1 (HQ111513, 99.3% similarity) and e2 (also HQ111513, 99.5% similarity) + e3 (AB058366, 100% similarity). The dynamics of the three ecotypes were somewhat similar during S02, but more in temporal than spatial scales. Also, the coupling between e2 and e3 was not as strong as in S01, they differed more in relative abundance.

Each of the three ecotypes were associated with strongly different water column properties as indicated by the maximum distance between the species nodes (Figure 4). *Geminigera* e1, the most abundant ecotype, was observed under low salinity, abundant nutrients, deep MLD and high water temperatures. Ecotype 2 also seemed to prefer a lower salinity and deep MLD but low PO_4, NO_3 and sea water temperature. Finally, e3 was observed in samples with a high salinity, elevated NO_3 and PO_4, low turbidity and shallow MLD. As a result of these differences, we further explored how *G. cryophila* e1 and e2 related to fresh water from different sources.

Embedding ecotypes in the micro-eukaryotic food web

The co-occurrence of the most abundant, and presumably most important, ecotypes of the haptophytes and cryptophytes were analysed together with the full OTU_{MED} table

of our dataset (Figure 6). Firstly, we observed a separation of all the cryptophyte OTU_{MED} into a subnetwork. The nearest neighbours were sequences which we were not able to annotate (~85% similarity to the best hit) which we labelled as "Unknown". Yet we suspected to have identified the nucleomorph of the cryptophytes (see discussion), as such we label this sequences "Crypt_NM". The correlation between the most observed cryptophyte and "Crypt_NM" sequences yielded a strong linear relationship and a ratio of 1 copy per every 10 cryptophyte sequences. The grazer associated to the cryptophytes was the dinoflagellate *Prorocentrum* sp.. In addition, *Telonemia* sp. and MAST-1A sequences were also connected to the dinoflagellate. Within the subnetwork we observed both *G. cryophila* e1 and e3. Also, *Prorocentrum* sp. persisted after the demise of the cryptophytes, most specifically at 75 m (Fig. 7).

P. antarctica e1 was not incorporated into the co-occurrence network, in contrast to *P. cf. jahnii* e2 (Figure 6). The latter species, represented by two OTU_{MED}, fitted between one MAST-2D member and various *Fragillariopsis sublineata* OTU_{MED}. The short MAST-2D side of the subnetwork has members belonging to *Chaetoceros neogracile* and *Micromonas* sp. whereas the other longer part of the subnetwork included *Cylindrotheca closterium, Actinocyclus actinochilus, Proboscia inermis, Thalassiothryx*

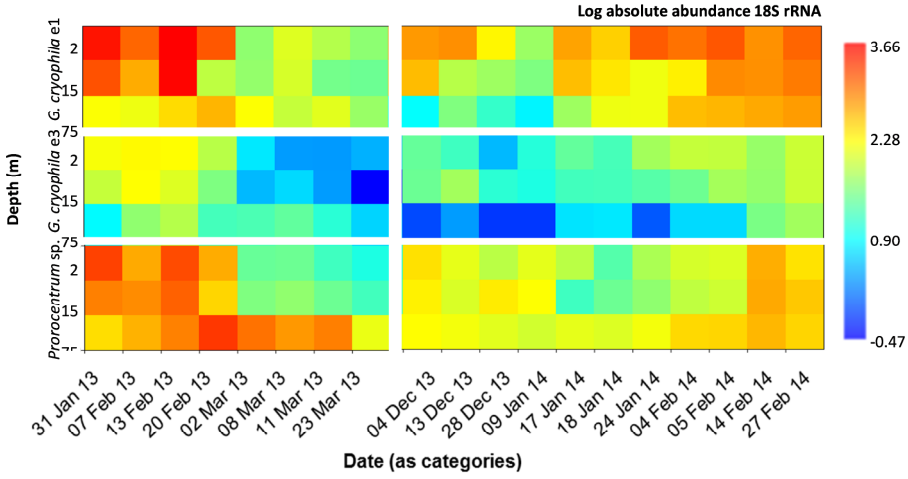

Figure 7: Depth distribution of log transformed abundances of Geminigera cryophila e1 and e3, and Prorocentrum sp. The values are the averages of three stations (G, R, and O).

longissima and an OTU_{MED} belonging to *Dinophyceae*. Yet, only in the immediate surrounding of *P. cf. jahnii* e2 no candidate specific grazers was observed, as nodes further away from these OTU_{MED} are somewhat disconnected due to the temporal aspect.

Chrysochromulina sp. e1 is closely associated with *Florenciellales* yet these two groups were excluded after the establishment of the subnetwork. Thus, the edges between *Florenciellales* and the subnetwork discussed below collapsed at MAST-8D. *Chrysochromulina* sp. e2 however did remain in this subnetwork and was surrounded by members from *Prymnesiophyceae* clade E, a group 2 dinoflagellate from clade 30, and members from the *Protaspa* genus. Further away in the subnetwork more members of the aforementioned genera in addition to *Florenciellales,* MAST-1C and picobiliphytes were observed.

Discussion

Dynamics of major taxonomic groups

In the present study we compared the classical and frequently-used HPLC-CHEMTAX based pigment analysis to sequencing of the 18S rRNA gene to estimate phytoplankton community composition. This might ensure compatibility between long term trends and our two-year dataset. The study site was generally dominated by diatoms. Cryptophytes briefly accounted for a large fraction of the community while haptophyte abundance strongly varied (Fig. 1 and 5). This range of variability is typically observed along the latitudinal gradient along the WAP using CHEMTAX or 18S (Kozlowski *et al.*, 2011; Piquet *et al.*, 2011; Luria *et al.*, 2014; Rozema *et al.*, 2017a, 2017b; Schofield *et al.*, 2017). Yet, studies employing both techniques at the same time are scarce and limited in temporal and/or spatial coverage (Rozema *et al.*, 2017b). Selecting photosynthetic genera for a comparison to CHEMTAX based results is challenging given the widespread existence of mixotrophy within the *Hacrobia* and stramenopiles. While the comparison of cryptophyte relative abundances using both approaches (Table 3) was shown to be accurate, this was less so for diatoms and haptophytes (Supplement figure 2). Although the trends between the two methods were similar, the large variability within these groups suggests a difference in estimated abundances of various species

within these groups. When considering the sequence-based analysis, diatom abundances were underestimated in favor of haptophytes. This might be related with differences in cell size ranges. Diatoms can range from ~1 to ~500 µm while haptophytes typically range between 4 and 12 µm. Previous studies have shown a relationship between 18S rRNA gene copy number and size/volume with copy numbers varying ~3 orders of magnitude (Zhu *et al.*, 2005; Godhe *et al.*, 2008). On the other hand, biovolume normalized Chl-a concentration within the aforementioned size range of diatoms also varies although less pronounced than the 18S rRNA gene copy number per biovolume (Kulk et al. submitted). The difference between these ratios is ~30% which would correct the diatom abundance to approximately a 1:1 ratio between the two approaches which would consequently lead to a decrease in relative haptophyte abundance. Despite the observed differences, we have shown in the present study that both techniques identify the same trends at the class level making our observations and deductions valid for extrapolation onto longer running time series.

Dynamics in ecotypes

We successfully identified different ecotypes within all three major genera of flagellated phytoplankton species. Our method of untangling ecotypes by identifying OTU_{MED} which have (near) identical temporal and spatial distributions is appropriate as both time and space present a unique combination of environmental conditions (Cohan, 2002). Previous studies have often assumed *P. antarctica* to be the dominant haptophyte species in the Southern Ocean, including a wide range of environments such as sea ice, coastal areas and the deep open ocean (e.g. Petrou *et al.,* 2016; Trimborn *et al.*, 2015; Ducklow *et al.*, 2012). These environments greatly differ in e.g. light regime, (micro)nutrient concentrations and salinity. Different *P. antarctica* populations, and potential ecotypes, as identified using microsatellites were described earlier for different parts of the Southern Ocean, including the WAP (Gäbler-Schwarz *et al.*, 2015). Our identification of different ecotypes within one water samples thus supports the co-oocurance of genotypes. Yet, we show that these also have distinctly different dynamics, supporting ecotypes as an ecological meaningful unit and not merely naturally occurring genetic variability.

Assigning OTUs by MED, and consequently abandon traditional clustering in 97% identity clusters, yielded ecological relevant information (Bálint *et al.*, 2016). For example, our most abundant *P. antarctica* sequence of 380 bp revealed >97% identity to two *P. cf. jahnii* ecotypes. If, we would have had full length 18S rRNA gene sequences, we would have identified the two different *Phaeocystis* species as these are 96% identical between the two full length entries in PR² but not the ecotypes within each species. Thus, while future sequencing techniques will yield longer reads (e.g. full length 18S rRNA), approaches such as MED will still be needed to understand niche separation if only the 18S rRNA gene is studied. It is widely established that traditional techniques, such as CHEMTAX, cannot go beyond the *class* level and therefore miss dynamics at the lower taxonomic levels. Light microscopy has the same challenges when studying variability in flagellated species within one single genus, let alone in different ecotypes. As such, we advocate using less stringent approaches to enumerated community composition using a range of methods to ensure and test for future compatibility with valuable time series data (Bálint *et al.*, 2016).

Niche separation between species and ecotypes

Phaeocystis in the Southern Ocean is often associated with deeply mixed layers (Arrigo *et al.*, 1999). Yet they can also persist in a strongly stratified, sea ice dominated ecosystem (Alderkamp *et al.*, 2012b). Also, *P. antarctica* is known to be abundant in sea ice (Tison *et al.*, 2010). These environments are highly different and require a highly plasticity or different ecotypes. The latter is supported by cultivation efforts where different isolates from the same region behaved differently under standardized lab experiments (Arrigo *et al.*, 2010). Not only is this the case for *Phaeocystis* but also for the cryptophyte *G. cryophila* as we observed three ecotypes. The most abundant ecotype (e1) is closely related to a well described isolate from Ace Lake (East-Antarctica) and observed in other lakes (van den Hoff & Bell, 2015). This ecotype was most abundant in our dataset and associated with a lowered salinity. Yet, the second most abundant *Geminigera* ecotype (e3) is more related to a marine isolate from Ongul Island (East-Antarctica).

Here we established different ecotypes, their temporal distribution as well as preferred environmental conditions. Therefore, we can postulate discrete niches for these

ecotypes (Cohan, 2002; Prosser *et al.*, 2007). Such a bottom-up control, where environmental conditions determine phytoflagellate abundance, is often suggested and explored for Antarctic phytoplankton but a lack of taxonomic resolution strongly complicated the generation of evidence. First and foremost, for phytoflagellates to become dominant, the conditions should not favor diatoms. Thus, the water column should be relatively unstable as prolonged stratified conditions promote diatom growth (e.g. reviewed in Petrou *et al.*, 2016). Driving the different dynamics in occurrence of flagellates were rapid, pronounced changes in the MLD, ending or starting periods with elevated contributions of the different ecotypes. Prolonged unstable water column conditions, or in contrast a high influx of melt water or relatively warm surface water, promoted growth of *Chrysochromulina* and *Geminigera* (except e2) ecotypes. *Chrysochromulina* is not often observed yet microscopic studies frequently report high numbers of unidentified flagellates. Moreover, the genus has previously been reported to be a highly abundant nanophytoflagellate in the Southern Ocean and underneath Artic sea ice (Hallfors & Niemi, 1974; Hall & Safi, 2001; Garibotti *et al.*, 2005; Annett *et al.*, 2010; Georges *et al.*, 2014). Both *Chrysochromulina* ecotypes were highly similar in standardized dynamics except that e2 peaked before e1, suggesting a small difference in preferred environmental conditions. These differentiating conditions were a deeper MLD and thus possibly a slightly higher nutrient concentration benefitting e1 over e2.

Dissimilarities between the most abundant *G. cryophila* ecotypes were more evident, as already suggested by the high similarity with isolates from contrasting Antarctic environments. E1, similar to the Ace lake isolate, was most abundant and preferred a low salinity and high sea water temperature over a relative unstable water column. These conditions are highly similar to those frequently observed north of Adelaide island where cryptophyte abundances are generally high (Moline *et al.*, 2004; Montes-Hugo *et al.*, 2009; Schofield *et al.*, 2017; Mendes *et al., in press*). Here, increasing wind speeds and decreasing ice cover destabilize the water column preventing diatom domination. Subsequent establishment of warm, fresh surface melt layers instigated by presumably glacial melt allow cryptophytes to prevail (Moline *et al.*, 2004; Montes-Hugo *et al.*, 2009; Saba *et al.*, 2014). In contrast, abundances of *G. cryophila* e3 are

opposing those of e1 in S01. A strong association with a higher salinity could suggests a more open ocean origin, where cryptophytes have also been observed (Kozlowski *et al.*, 2011). *G. cryophila* e2 was similar to e3 but only a minor ecotype which could explain our difficulty in identifying its niche. Yet, noteworthy is the increase in abundance coinciding with a strong influx of sea ice melt in S02 and increase in *P. cf. jahnii* e2. This could explain the co-occurrence in a long term dataset off the coast of Alexander Island and near dominance in the marginal ice zone in the Weddell Scotia confluence (Buma *et al.*, 1992; Kozlowski *et al.*, 2011).

For *Phaeocystis*, we observed two species with two ecotypes each. The *P. antarctica* e1 was most abundant, was always observed and increased in abundance under typical open ocean conditions. Thus, preferred environmental conditions were low sea water temperature (<0.5°C), elevated salinity and deeper mixed layers where high nutrient stocks were maintained. These conditions are classically associated with *P. antarctica* (Arrigo *et al.*, 1999; Alderkamp *et al.*, 2012a). As mentioned above, *P. antarctica* e2 dynamics were nearly identical to *Chrysochromulina* sp. e1 , preferring warm water conditions. The distribution of *P. antarctica* is limited to the Southern Ocean but is present throughout this vast ocean. To our knowledge, the geographical variability within this highly abundant species and related different genotypes, and thus potentially ecotypes, to different regions of the Southern Ocean was studied only once (Gäbler-Schwarz *et al.*, 2015).

The distribution of the second *Phaeocystis* species, *P. cf. jahnii* was not similar to that of *P. antarctica* (e1). Yet, the major *P. cf. jahnii* ecotype (e1) did strongly resemble the dynamics of both *P. antarctica* e2 and *Chrysochromulina* sp. e1. Unique in its distribution was *P. cf. jahnii* e2 as abundances peaked after a large influx of sea ice melt. While the species only slowly increased when sea ice sheets entered the region (Rozema *et al.*, 2017c), it did so rapidly when sea ice melt became prominent and furthermore increased immediately after a wind mixing event. This suggests that this ecotype is related to sea ice, possibly originating from slushy top layers, but was not a major contributor of biomass therein. The distribution of *P. jahnii* generally seems limited to the more northern regions of the WAP, yet it was also observed earlier in northern Marguerite Bay, the Ross Sea and the open Southern Ocean (Gast *et al.*, 2004;

Piquet *et al.*, 2011; Wolf *et al.*, 2013; Abele *et al.*, 2017). At the northern WAP, water temperatures are higher, less ice covered and presumably more unstable due to stronger winds although melt water of meteoric origin might stabilize the top layer. Moreover, the diversity in *P. jahnii* is remarkable given the initial isolation of this species in the Mediterranean Sea (Zingone *et al.*, 1999). This reflects a great plasticity within this species and illustrates the need for more thorough ecotype studies.

Incorporation into the micro-eukaryotic community

The cryptophyte *G. cryophila* co-occurred strongly with *Prorocentrum* sp., a small mixotrophic dinoflagellate that is known as cryptophyte grazer in temperate waters, often during periods of nutrient limitation or deviation from the Redfield ratios (Johnson, 2015 and references therein). Moreover, *Prorocentrum* sp. is also widely distributed throughout the Southern Ocean (Kopczyńska *et al.*, 1998; Díez *et al.*, 2001; Assmy *et al.*, 2007; Piquet *et al.*, 2008, 2011; Shields & Smith, 2009; Mendes *et al.*, 2013). *Prorocentrum* is a potential toxin producer affecting coastal regions around the globe and could therefore influence the WAP ecosystem (as reviewed in Ajani *et al.*, 2017).

The two often observed haptophyte genera, *Phaeocystis* and *Chrysochromulina*, were contrasting in their ecosystem positioning. *P. antarctica* derived OTU_{MED} did not show a significant co-occurrence with other OTU_{MED}, suggesting no specific interactions or dependencies on this species. We consider this in line with observations of *Phaeocystis* in other ecosystems where it showed a wide array in consumer-specific defenses (Long *et al.*, 2007; Nejstgaard *et al.*, 2007). In contrast, *P. cf. jahnii* and *Chrysochromulina* sp. were well incorporated with various OTU_{MED} of potential mixotrophs and small bacterial grazers neighboring their OTU_{MED}. As such, we considered the changes in the species of these genera to affect microzooplankton community composition whereas *Phaeocystis antarctica* does not. The stringent threshold on the inclusion of OTU_{MED} into our co-occurrences network allowed for an assessment of the positioning of the major photosynthetic members of the *Hacrobia* within the micro-eukaryotic community. We could infer strong dependencies between species and thus identify specific relations. The downside of using a stringent threshold would be the inability to identify more generalist relations. While our network did not empirically establish the type of relationship between OTU_{MED}, e.g. grazer-prey interactions, a high similarity in

dynamics coupled to an established relationship based on the literature could justify coupling in terms of trophic links. Additionally, generalist grazers such as krill and salps did not occur in our networks suggesting they do not rely on a sole prey. As such, these grazers could still graze on e.g. *P. antarctica*. Yet these grazers were apparently not solely dependent on specific phytoplankton species. Also, we did not see strong differences between ecotypes within each genus, in part because some ecotypes were not sufficiently abundant in the 2m samples.

Cryptophyte nucleomorph

Additionally, we suspect to have identified a nucleomorph (Crypt_NM) of *Geminigera* with the sequences highly dissimilar to anything in the PR² database (Douglas *et al.*, 2001). This second eukaryotic nucleus is a remnant from the enslavement of a small photosynthetic eukaryote by cryptophytes and holds an array of genes involved in photosynthesis. The identification of this extra genome allows for a number of evolutionary calculations within the global cryptophyte species pool. Additionally, it could provide an independent insight into the 18S rRNA gene copy number. The three chromosomes in the nucleomorph each hold a copy of the 18S rRNA gene per DNA strain. Given the high similarity in dynamics between these two OTUs we established that there are 10x as many 18S copies in the genome of *G. cryophila* in comparison to its nucleomorph. Given the importance of this nucleomorph, we expect it will be well conserved between species. Thus, we suspect to have 60 rDNA copies of the 18S gene in the genome of this species if the nucleomorph holds six, slightly less than expected based on the cell length (Zhu *et al.*, 2005).

Conclusions

In light of the current climatic trends, which include decreasing sea ice cover, higher SSTs and more unstable water columns, a shift towards phytoflagellates at the expense of diatoms is likely. In an environment with a less stable water column, *Phaeocystis antarctica* e1 will become more abundant if SSTs will remain low, for example due to deeper mixing. Unstable conditions but with higher SST will most likely stimulate growth of *Chrysochromulina* sp. and *Geminigera cryophila*. Which ecotypes of *G. cryophila* will prevail will likely depend on surface salinity. If the higher SSTs coincide with more sea ice melt than we expect to observe more *Phaeocystis jahnii*. We suspect

less thropic levels in the ecosystems when *P. antarctica* becomes more abundant while the other groups appear to be well incorporated into the microbial network. Higher cryptophyte abundance will likely cause an increase in *Prorocentrum*, a potentially toxic genus. To keep track of potential changes, future monitoring should include DNA analysis and cultivate different phytoplankton ecotypes. Evident from our niche propositions for the different ecotypes is that experimental settings should include multiple isolates of the same species if the goal is to compare the lab results to field observations.

We conclude to have successfully increased the taxonomic resolution which has increased our insight in the changing phytoplankton community as a function of environmental drivers. Also, we show that studies can successfully align long running pigment-based taxonomy studies to new sequencing approaches. Genera such as *Chrysochromulina* and *Prorocentrum* are understudied in the Southern Ocean ecosystems and have the potential to have a severe impact given the widespread production of toxins within more temperate species of these genera. Thus, aside from changes in the food web due to the shift from diatoms, warming conditions could also become more important in a warmer WAP.

Acknowledgements

We are grateful for the support by the BAS and the staff of Rothera research stations for the ability to conduct this research. We would like to thank Hein de Baar for initial discussions regarding the exploitation of Ryder Bay as a natural laboratory. Amber Annett, Mairi Fenton and Libby Jones are thanked for their assistance with sample collection. Also, Martijn Scharrenburg for assisting with DNA extractions, Wendy Bollen and Sean de Graaf for assisting with HPLC analysis and Leslie Murphy for preparing the samples for sequencing are thankfully acknowledged. We thank the captain, scientists, officers and crew of the *ARSV Lawrence M. Gould* for the support and opportunity to extend our sampling efforts further into northern Marguerite Bay. This research was funded by the Dutch Polar Programme of NWO (866.10.105) and NSF (OPP-1142114). Sequencing was conducted at the Keck sequencing facility facilitated by the technical expertise of Leslie Murphy and the MBL bioinformatics

core. Also, this work was facilitated by the framework of the EU research network IMCONet funded by the Marie Curie Action IRSES (FP7 IRSES, Action No. 319718).

Apendices are available upon request.

6

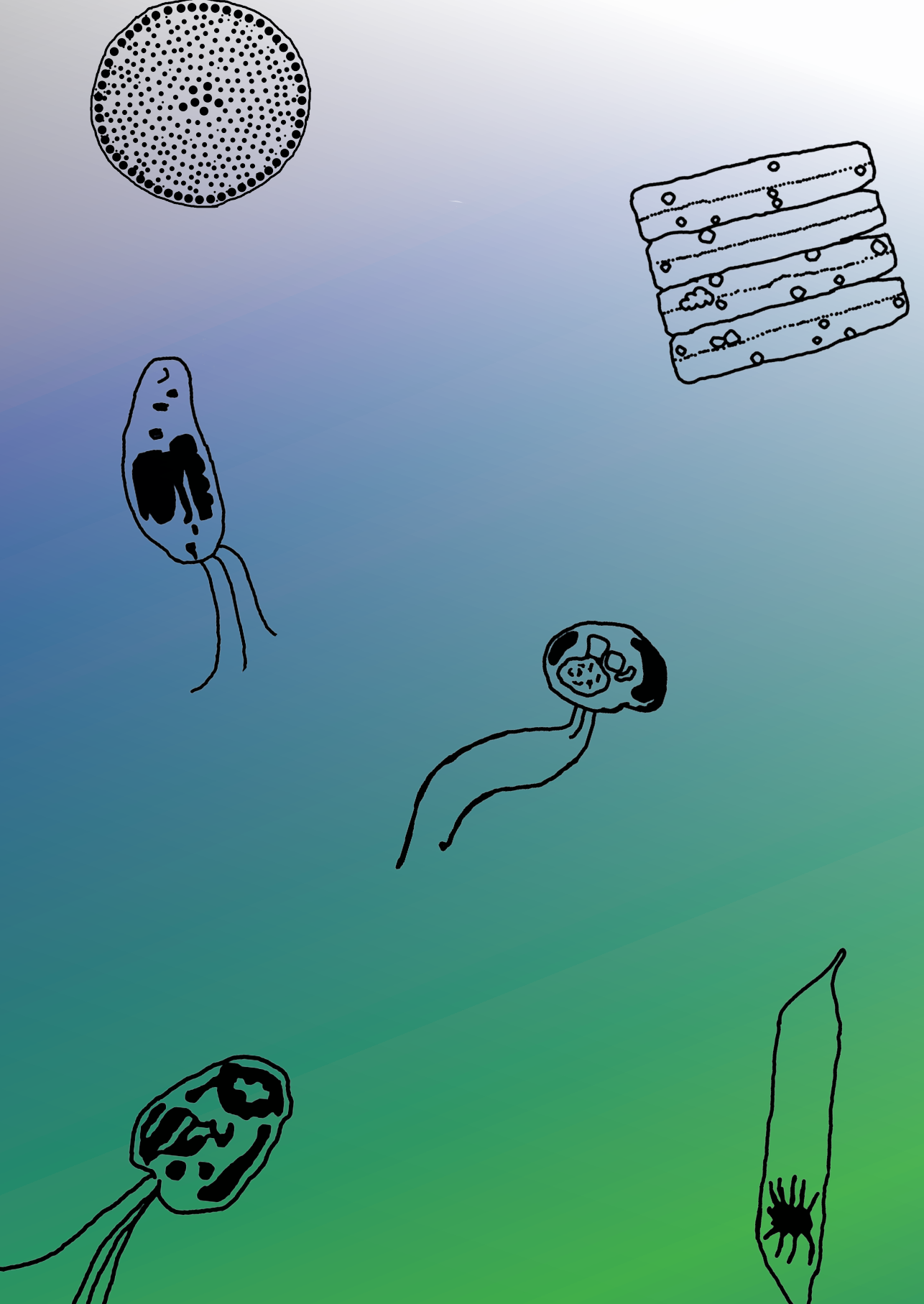

Samenvatting
Summary
References
Acknowledgements &
Dankwoord
Bibliography

Samenvatting

Het klimaat op onze planeet is aan het veranderen en dit heeft vergaande gevolgen voor een groot aantal regio's. Een zeer kwetsbaar continent is Antarctica, een wereld van sneeuw en ijs omringd door de Zuidelijke Oceaan. Op dit continent is het goed voorstelbaar dat de veranderingen in lucht- en watertemperatuur grote gevolgen hebben. Immers, of de temperatuur enkele graden boven of onder 0°C ligt maakt een groot verschil voor de ijsbedekking. Door opwarming zijn in sommige gebieden rond Antarctica zowel zee-ijsvelden die op de oceaan drijven als uiteinden van gletsjers zich aan het terugtrekken.

Van de verschillende regio's veranderen op dit moment de kustgebieden van het Antarctisch Schiereiland, het noordelijkst gelegen gedeelte van Antarctica, het snelst. Het Antarctisch Schiereiland bestaat uit een bergrug van vulkanische herkomst, die van Zuid-Amerika wordt gescheiden door de meer dan 5000m diepe Straat Drake. Ten westen van het Antarctisch Schiereiland neemt het zee-ijs tijdens de winter steeds verder af doordat het zich later in het jaar vormt en het in het voorjaar eerder smelt. Dit heeft tot gevolg dat de wind gemiddeld genomen meer grip krijgt op de oceaan wat zorgt voor een diepere verticale menging. Naast de verandering in zee-ijs, trekt het merendeel van de gletsjers aan de westkant van het schiereiland zich terug. Dit wordt vooral veroorzaakt doordat het warmere water uit de diepten van de oceaan de gletsjers van onderen doen afsmelten, met als gevolg dat deze dunner en korter worden. Dit smeltwater zorgt vooral in de zomer voor zogenaamde stratificatie (gelaagdheid; *Strata* in het Grieks) van de waterkolom doordat omdat dit zoete water veel lichter is dan het onderliggende zeewater.

Zolang deze verschillende lagen (bijna) niet mengen, kunnen de populaties van micro-organismen die in het water leven per laag verschillend zijn. Bovendien wordt dit effect versterkt omdat deze gelaagdheid er ook voor kan zorgen dat bijvoorbeeld de beschikbaarheid van voedingsstoffen en zonlicht per laag verschillen. Stratificatie kan overigens wel worden doorbroken: harde wind kan zorgen voor een menging van de bovenste waterlagen, waardoor de verschillende lagen een homogene dichtheid krijgen. Kortom, de opwarming van het Antarctisch Schiereiland zorgt voor complexe

veranderingen, naast de verhoging van de temperatuur zelf. Al deze veranderingen hebben gevolgen voor het voedselweb doordat het fysieke milieu allesbepalend is voor de mariene productiviteit en structuur van het ecosysteem.

Mariene micro-organismen zijn wereldwijd zeer divers, zowel in vorm, afmeting als functie. Net als op land, staan die organismen die energie uit zonlicht gebruiken om CO_2 vast te leggen middels fotosynthese aan de basis van de voedselketen. In de oceaan zijn het hoofdzakelijk microscopisch kleine algen (fytoplankton genoemd), die de fotosynthese verzorgen. Dit fytoplankton wordt gegeten door kleine en grote grazers (herbivoren). De meest bekende algen-eter rond Antarctica is het Antarctische krill garnaal-achtigen die een paar centimeter groot kunnen worden. Deze grazers vormen een spil in het klassieke Antarctische voedselweb omdat zij kunnen worden gegeten door bijvoorbeeld pinguïns en walvissen. Wanneer fytoplankton niet wordt opgegeten zinkt het uit naar de diepe oceaan, waar het vastgelegde CO_2 dus voor lange tijd kan worden opgeslagen. Echter, wanneer de algen te licht zijn om snel uit te zinken, dit geldt vooral voor de kleine fytoplanktonsoorten, wordt de algenbiomassa grotendeels in de waterkolom door bacteriën afgebroken. Hierdoor blijft de vastgelegde koolstof dus in de bovenste waterlaag. Kortom, de soortensamenstelling, en de gemiddelde grootte van de algen, bepaalt hoe de algenbiomassa verder in het voedselweb wordt verwerkt.

Wereldwijd zorgt het fytoplankton voor 50% van de totale zuurstofproductie en tegelijkertijd voor de gedeeltelijke opslag van CO_2 in de diepe oceaan. Sommige fytoplanktonsoorten (flagellaten) zijn klein en mobiel, ze hebben een staart (zweepstaartje of flagel) waarmee ze kunnen zwemmen. Andere soorten zijn groot en in het bezit van een zwaar omhulsel van silica (diatomeeën of kiezelwieren genoemd). Het is bekend dat beide groepen fytoplankton veelvuldig voorkomen in de kustgebieden van het Antarctisch Schiereiland. Niet alleen verschillen deze microalgen in eigenschappen als vorm en mobiliteit, maar ook in hun capaciteit om opgeloste voedingsstoffen, zoals nitraat en fosfaat, op te nemen, en hun specifieke voorkeur voor lichtintensiteit en -stabiliteit. Bovendien worden diatomeeën door krill geprefereerd ten opzichte van flagellaten.

De open Zuidelijke Oceaan staat bekend als een gebied waar belangrijke voedingsstoffen als nitraat, fosfaat en silicaat de groei van fytoplankton niet limiteren. Echter, sporenelementen zoals ijzer en zink zijn wel limiterend in de open oceaan. Voor kustgebieden wordt verondersteld dat limitatie door sporenelementen niet voorkomt. Dit omdat de nabijheid van rotsen en sedimenten in ondiepere wateren dienen als bron van elementen, waaronder bijvoorbeeld ijzer. De contrasterende omstandigheden tussen de open oceaan en de kustgebieden leggen druk op de aanwezige fytoplanktonsoorten om zich aan te passen aan de specifieke en ook zeer variabele omstandigheden. Bij dat laatste kan men denken aan variabiliteit in zee-ijsbedekking, zoutgehalte, stratificatie, lichtinval, seizoen dynamiek, en beschikbaarheid van nutriënten. Tenslotte zijn er nog soorten organismen die een combinatie van verschillende strategieën gebruiken. Er zijn bijvoorbeeld microalgen die fotosynthese gebruiken, maar daarnaast ook bacteriën kunnen eten. Daarom is het dus eenvoudig voor te stellen dat er veel verschillende soorten fytoplankton geëvolueerd zijn, elk met hun eigen set optimale voorkeursomstandigheden, flexibiliteit, strategie en vorm. De combinatie van al deze verschillende factoren bepaalt de plek die een soort in het ecosysteem inneemt. Deze plek wordt ook wel niche genoemd.

Hoewel de “soort” het laagste taxonomische niveau vormt dat we kennen, zijn niet alle individuen binnen een soort identiek. We gebruiken voor micro-organismen vaak een definitie van 97% gelijkheid op basis van vergelijking van het DNA voordat we organismen tot dezelfde soort rekenen. Zo kunnen er binnen soorten varianten zijn die een voorkeur hebben voor net iets andere milieucondities. Er zijn bijvoorbeeld van enkele fytoplanktonsoorten een hoog licht en een laag licht variant beschreven. Deze varianten zijn genetisch bijna identiek, daarom zijn ze ook van dezelfde soort, maar zij bezetten dus wel verschillende niches binnen een ecosysteem. Dergelijke varianten van een soort worden ook wel ecotypes genoemd. Omdat deze ecotypes dus onder verschillende condities voorkomen, kunnen ze ook verschillende functies vervullen in het ecosysteem.

In dit proefschrift behandel ik een aantal vragen met betrekking tot deze micro-organismen. De overstijgende vraag achter dit proefschrift was: “Hoe varieert de

microbiële gemeenschap van een kustgebied van het Antarctisch Schiereiland in aantal en samenstelling, en hoe wordt dit gestuurd door de fysisch/chemische veranderingen?". Om dit uit te zoeken werden meerdere concrete deelvragen geformuleerd, die in de verschillende onderzoekshoofdstukken worden beantwoord. Er is in dit onderzoek gebruik gemaakt van zowel eerder verzamelde monsters (Hoofdstukken 2 en 4), als metingen en monsters verzameld tijdens dit door NWO gefinancierde onderzoeksproject (Hoofdstukken 3, 5 en 6). Deze laatste gegevens zijn verzameld tijdens twee Antarctische zomers (Jan 2013-Mar 2013 en Nov 2013-Mar 2014) bij Rothera, een Brits onderzoeksstation. Dit station ligt aan Ryder Bay, met daarin een meetpunt dat al 20 jaar door Britse collega's wordt bemonsterd, de RaTS-locatie. Op en rondom deze locatie zijn alle monsters, gebruikt voor dit proefschrift, verzameld.

In **hoofdstuk 2** werd bestudeerd in welke mate de zee-ijs bedekking tijdens de winter, en ook de stabilisatie van de waterkolom tijdens de lente en zomer de soortsamenstelling van het fytoplankton bepaalde. Door eerder onderzoek was al duidelijk geworden dat de biomassa van het fytoplankton afhangt van de waterkolom stabiliteit. De geformuleerde hypothese was dat er bovendien significante verschillen in soortensamenstelling optreden tussen jaren met een hoge of lage gemiddelde biomassa tijdens voorjaar en zomer. Door het analyseren van een tijdserie verzameld sinds 1997 bleek dit daadwerkelijk het geval. Winters met weinig zee-ijs, resulterend in een instabiele waterkolom, resulteerden in een zomer met een lage fytoplanktonbiomassa, verder gekarakteriseerd door een relatief laag aandeel aan grotere diatomeeën en dus een hoog aandeel aan kleine flagellaten. De resultaten van deze tijdserie werden samengevat in een conceptueel model waarin zomers volgend op winters met verschillende mate van zee-ijs bedekking duidelijk van elkaar kunnen worden onderscheiden. Ook werd een tussenvorm gedefinieerd: winters met weinig zee-ijs, maar toch een versterkte mate van waterkolom stabilisatie tijdens het voorjaar, door bijvoorbeeld mooi weer resulteren in zomers met gemiddelde fytoplankton-biomassa zonder een verlaging van de fractie diatomeeën.

In **hoofdstuk 3** werd de productiviteit van het fytoplankton op de RaTS locatie in de zomer van 2013-2014 als functie van omgevingsfactoren beschreven. Er bestaan verschillende (klimaat)modellen te bereken hoeveel CO_2 er door fytoplankton wordt

opgenomen, maar het is belangrijk om dergelijke modellen met metingen in het veld te verifiëren en verbeteren. In de poolgebieden wordt het productieproces (de fotosynthese) vooral door de beschikbaarheid van licht gecontroleerd: deze is namelijk een groot deel van het jaar beperkend voor de groei, door de lage zonnestand of bedekking door zee-ijs. Tegelijkertijd kan ook de beschikbaarheid van voedingsstoffen (nitraat, fosfaat, ijzer) een rol spelen. Om deze abiotische, sturende factoren verder te ontrafelen werden CO_2 opname experimenten gedaan met natuurlijk fytoplankton. Deze resultaten werden met een zelflerend model geanalyseerd om te kijken welke parameters het meeste invloed hadden op CO_2 opname. Hieruit bleek verrassend genoeg dat de hoeveelheid stikstof (nitraat en nitriet) een belangrijke sturende factor is. Waarschijnlijk was de ijzer-beschikbaarheid voldoende om de fytoplanktonbiomassa te verhogen tot een punt waarop het stikstof beperkend werd. Een opvallend resultaat was verder dat het niet belangrijk is welke fytoplankton groepen aanwezig zijn. We weten uit lab experimenten dat er bijvoorbeeld verschillen zijn tussen de flagellaten en diatomeeën. Deze verschillen maakten in het veld dus veel minder uit, de omgevingsfactoren bleken vele malen belangrijker. Al met al kon met slechts drie parameters, licht intensiteit, totale fytoplankton biomassa en stikstof beschikbaarheid, een goede schatting van de fytoplankton productiviteit worden gemaakt.

In **hoofdstuk 4** werd onderzocht welke omgevingsfactoren gedurende het zomerseizoen van 2010-2011 de soortensamenstelling van zowel de bacteriële- als de fytoplanktongemeenschap bepalen. Voorheen werd de fytoplanktongemeenschap beschreven met behulp van de microscoop, dit is erg tijdsintensief en daarom kostbaar of pigmenten, dit heeft een lagere taxonomische resolutie. Nu kijken we naar een klein gedeelte van het genetische materiaal om de soorten te identificeren en een idee te hebben in welke hoeveelheid deze soorten aanwezig zijn. Bovendien doen we dit in combinatie met het bestudeerden van de bacteriën. Hierdoor kunnen we de beide componenten van het microbiële leven vergelijken en zien hoe de omgeving dezen beïnvloeden. De resultaten gaven sterke aanwijzingen dat, in tegenstelling tot wat er vaak wordt aangenomen, limitatie van voedingsstoffen tijdens de zomer plaatsvindt. Welke voedingsstof limiterend was verschilde per fase in het zomer seizoen. Zowel

fosfaat als nitraat waren tijdens onderzoek soms (bijna) onder het detectieniveau. Tegelijkertijd werd aangetoond dat ook de fytoplankton soortensamenstelling tijdens de zomer sterk wordt gestuurd door de beschikbaarheid van voedingsstoffen. Een andere belangrijke sturende factor bleek de stabiliteit van de waterkolom. Stormen kunnen zorgen voor een abrupte verandering in de stratificatie van de waterkolom. Hierdoor beïnvloedt de wind indirect de beschikbaarheid van licht en voedingsstoffen: momenten van diepe menging door de wind bleken binnen enkele dagen een grote invloed te hebben op de fytoplankton soortensamenstelling. Veranderingen in de samenstellingen van de bacteriële gemeenschap bleken voornamelijk afhankelijk van de hoeveelheid fytoplankton. Ook leek de bacteriële samenstelling afhankelijk zijn van de fytoplankton soortensamenstelling hoewel met een vertraging van twee weken. Deze afhankelijkheid is begrijpelijk omdat de samenstelling van het organische materiaal waarop bacteriën groeien verschilt tussen de verschillende fytoplankton soorten.

In **hoofdstuk 5** werd de beschikbaarheid van verschillende sporenelementen en belangrijke voedingsstoffen tijdens de zomers van 2012-2014 in kaart gebracht. Op verschillende dieptes op de RaTS-locatie werden monsters genomen voor analyse van verscheidene nutriënten (nitraat, nitriet, fosfaat, silicaat, ijzer, mangaan, zink, cadmium, kobalt en koper). Ten eerste lieten we zien dat verscheidene sporenelementen (waaronder ijzer en zink) soms in dusdanig lage concentraties aanwezig kan zijn dat het de groei van fytoplankton kan beperken. Daarbij lieten we wederom (zoals in **Hoofdstuk 3**) zien dat de belangrijkste nutriënten (nitraat, fosfaat en silicaat) door opname door het fytoplankton soms tot zeer lage concentraties kunnen worden teruggebracht. Al met al werden er grote verschillen in nutriënt dynamiek tussen de beide zomers gevonden. Tenslotte konden we aantonen dat flagellaten en diatomeeën in verschillende mate nutriënten en sporenelementen opnemen. Dat maakt dus dat de beschikbaarheid van een groot aantal elementen relevant is voor het bepalen van de soortsamenstelling maar vooral voor de abundantie van de verschillende fytoplankton groepen.

In **Hoofdstuk 6** werd de mogelijkheid van het voorkomen van verschillende ecotypes binnen een aantal flagellaten-soorten onderzocht. Voorgaande studies (inclusief eigen

studies beschreven in **hoofdstukken 2, 3** en **5)** maakten vooral gebruik van specifieke pigmenten om verschillende groepen fytoplankton te onderscheiden. Echter, in **hoofdstuk 6** maakten we gebruik van nieuwe DNA technieken om soorten en ecotypes te detecteren en te beschrijven. Veelal wordt aangenomen dat de haptofyt *Phaeocystis antarctica* en de cryptofyt *Geminigera cryophila* de twee dominante flagellaten-soorten zijn in het bestudeerde kustsysteem. Wij toonde echter aan dat er ook een andere *Phaeocystis* soort aanwezig is, waarschijnlijk *P. jahnii*. Bovendien vonden we een tweede, erg talrijke haptofyten genus, namelijk *Chrysochromulina*. Tevens vonden we verschillende ecotypes binnen alle voorgenoemde soorten. Zo werd er een drietal *G. cryophila* ecotypes gevonden. Hiervan bleken twee ecotypes contrasterende voorkeuren voor zoutgehalte te hebben, een ecotype geassocieerd met zoetwater en een andere met het zoute water van de open oceaan. Het bestaan van deze verschillende ecotypes betekent dat ze verschillende niches, en dus functies, in het ecosysteem kunnen hebben. Tot slot vonden we een vermoedelijke grazer (*Prorocentrum*) die sterk gekoppeld lijkt te zijn aan de aanwezigheid van *G. cryophila*. Dit zou kunnen betekenen dat abundantie van *G. cryophila* kan worden gereguleerd door deze grazer, terwijl we geen aanwijzing van een dergelijk mechanisme vonden voor de andere aanwezige flagellaten soorten.

Met het in dit proefschrift beschreven onderzoek zijn duidelijke stappen gemaakt om de sterke dynamiek in microbiële samenstelling, abundantie en productie bij een veranderend klimaat rond het Antarctisch Schiereiland beter te kunnen begrijpen. De meeste factoren die de soortsamenstelling sturen, zoals bijvoorbeeld zee-ijs bedekkingsgraad, smeltende gletsjers, menging door wind en nutriëntbeschikbaarheid, zijn hier aan het veranderen. In dit proefschrift zijn al jaren beschreven die een afwijkende fytoplanktonbiomassa en -samenstelling laten zien ten opzichte van het meer klassieke beeld. Deze afwijkende jaren werden met name gerelateerd aan warme winters met een lage zee-ijs bedekking, Dergelijke afwijkende patronen zullen waarschijnlijk vaker voor gaan komen, en dus in toenemende mate een impact gaan hebben op het voedselweb en de potentie om CO_2 op te slaan in de diepe Antarctische oceaan.

Summary

The changing climate of our planet holds extensive consequences for many regions. Antarctica is a continent mostly covered by snow and ice, and is surrounded by the Southern Ocean, and therefore highly vulnerable. It is easy to imagine that changes in air and water temperature strongly affect this continent. After all, a temperature slightly above or below 0°C is a world of difference on an ice covered continent. As a consequence of this warming marine-terminating glaciers and ice sheets floating on the ocean are retreating of collapsing.

One of the most strongly affected regions is the coastal region of the Antarctic Peninsula, the northernmost area of Antarctica. The Antarctic Peninsula is of volcanic origin and is separated from South America by the 5000m deep Drake Passage. Winter sea ice cover is declining along the west Antarctic Peninsula as the onset of ice formation is delayed while ice melt in spring occurs earlier. Consequently, the increase in open water area results in deeper vertical mixing as the ocean surface is exposed to the strong winter winds. In addition to the changes in sea ice, the majority of the glaciers on the west side of the Antarctica Peninsula are in retreat. This is mostly due to warmer waters originating from deep water layers which melt the glaciers from underneath, therefore thinning and shorting them. This fresh melt water promotes stratification (formation of different water layers) of the water column during summer because the fresh water is lighter than the underlying sea water.

As the different water layers hardly mix, the populations of micro-organisms can be different between the water layers. Moreover, this effect is enhanced by for example differences in nutrient and/or sun light availability. Yet, the stratification of the water column can be undone: strong winds could mix of the surface layers and therefore homogenize the surface ocean. Thus, the warming of the Antarctic Peninsula causes complex changes, beyond only increasing the temperature. These changes affect the marine food web as the physical and chemical environment controls marine productive and structuring of the ecosystem.

Marine micro-organisms are globally extremely divers in shape, size and function. As in the terrestrial system, organisms that fix use solar energy to fix CO_2 in a process

called photosynthesis form the bottom of the food chain. In the ocean, these are microscopically small algae called phytoplankton which are eaten by small and large grazers (herbivores). The best known of these grazers in the Southern Ocean are krill, shrimp-like creatures only a few centimeters long. These grazers are pivotal in the classical Antarctic food web as these are readily edible by for example penguins and whales. When phytoplankton are not consumed, it sinks to the deep ocean where the fixed CO_2 can be stored for a long time, offsetting some of the CO_2 input into the atmosphere. Yet, small and light algae species sink too slow and therefore their algal biomass is mostly broken-down by bacteria. Thus, the previously fixed CO_2 remains in the upper water layers. Therefore, species composition, and average size, of the phytoplankton community determine how algal biomass is processed in the food web.

Phytoplankton are responsible for 50% of the global oxygen production and a large part of the storage of CO_2 in the deep ocean. Some phytoplankton species (flagellates) are small, light and mobile, they have tail (flagellate) used for swimming. Other species are large and have a heavy silica cell wall. These species are often referred to as "algae in a glass house" and are called diatoms. We know that both groups of phytoplankton are common in the coastal waters of the Antarctic Peninsula. Not only do these micro-algal groups differ size and mobility, but also in their uptake capacity of dissolved nutrients, such as nitrate and phosphate, and their preferences for variability in light intensity. Moreover, krill prefer diatoms over flagellates as their main food source.

The open Southern Ocean is known as a region where the most important nutrients (nitrate, phosphate and silicate) are not limiting to phytoplankton growth. Yet, trace elements such as iron and zinc are limiting. In contrast, it is assumed that coastal regions are not limited by trace elements due to the proximity to sources such as rocks and sediment. The overall contrasting conditions between the open and coastal ocean force the phytoplankton species to adept to these different, yet specific and highly variable conditions. Not only can nutrient concentrations vary greatly, but also the variability sea-ice cover, salinity, stratification, light intensity and seasonal dynamics in grazing contribute to a highly variable environment of the coastal ocean and therefore drive the adaption of the different phytoplankton species. These species employ a range of strategies to cope with these conditions, for example certain phytoplankton

species combine photosynthesis with the eating of bacteria. Therefore, it is easy to imagine the evolution of a large number of phytoplankton species, each with a different shape, flexibility and function optimized for a specific set of preferred conditions. The combination of these properties and conditions determines the place, also known as niche, a certain species fulfills within the ecosystem.

While “species” is the lowest taxonomic level that we know, not all individuals within a species are identical. We often use the definition of 97% similarity in DNA before attributing micro-organisms to the same species. As such, there can be variants within species which prefer slightly different environmental conditions. For example, we know of some phytoplankton species with a high-light and a low-light variant. These variants are genetically nearly identical, therefore they belong to the same species, but occupy different niches in the ecosystem. Such variants of a species are also known as ecotypes. Because these ecotypes occur under different environmental conditions, they can also fulfill different ecosystem functions.

In this thesis I discuss a number of questions related to these micro-organisms. The over-arching question is: ”How does the microbial community in the coastal region of the west Antarctic Peninsula vary in abundance and composition, and how is this driven by changes in the physical and chemical environment?” This question was subdivided into multiple smaller, and more specific questions which are discussed in the different chapters. For this research we made use of both previously collected samples (Chapters 2 and 4),, and measurements and samples collected specifically for this research funded by NWO (Chapters 3, 5, and 6). These latter samples were collected during two Antarctic summers (Jan 2013-Mar 2013 and Nov 2013-Mar 2014) at Rothera, a British research station. This station is situated on the west Antarctic Peninsula at Ryder Bay, where a study site occupied since 1997 is situated, the RaTS-site. At and round this site is where all of the samples discussed in this thesis are collected.

In **Chapter 2** we studied to what extent sea-ice cover during winter, and water column stabilization during spring and summer governed phytoplankton species composition. Previous research has established that total phytoplankton biomass depended on water

column stability. I hypothesized that phytoplankton species composition also varied between years with high or low total summer phytoplankton biomass. We confirmed this hypothesis through the analysis of a time series collecting data since 1997. Winters with low sea ice cover, and therefore a deeply mixed water column, resulted in less phytoplankton biomass and a lower contribution of large diatoms in favor of small flagellates. The results of this study were summarized in a conceptual model where summers resulting from winters differing in sea ice cover are clearly separated. Moreover, we have added summers of intermediate levels of biomass: for example a winter with low sea ice cover but relative warm and stable spring conditions can still result in average phytoplankton biomass levels without a reduction in relative diatom abundances.

In **Chapter 3** the productivity of phytoplankton at the RaTS-site during the summer of 2013-2014 was analyzed as a function of the environmental conditions. Different (climate)models calculate how much CO_2 is absorbed by phytoplankton, yet it is important to calibrated and improve those models using field measurements. In the polar regions, the production process (photosynthesis) is primarily regulated by light availability as this limits growth due to low angles of irradiance, it is nearly dark during winter, or sea ice cover. Moreover, it is likely that the availability of nutrients, such as nitrate or iron, is relevant. To unravel these abiotic factors , but also the importance of phytoplankton species composition, CO_2 uptake experiments were conducted using natural phytoplankton communities. These results were analyzed using a self-learning model to understand which parameters influenced CO_2 uptake most strongly. Surprisingly, we learned that nitrogen (nitrate and nitrite) availability was a governing factor. Probably because iron-availability was high enough to allow biomass accumulation to a level where nitrogen became the limiting element. Also, the results show that phytoplankton community composition does not directly affect uptake. This is unexpected as we know from laboratory studies that different species have different uptake rates. Thus, environmental conditions are many times more important than biological variability with regards to CO_2 uptake. Therefore, we could accurately estimate phytoplankton productivity by only three parameters, light, total biomass and nitrogen availability.

In **Chapter 4** was investigated which environmental parameters influenced the species composition of the bacterial and phytoplankton communities. Previous investigations of the phytoplankton community used microscope or pigments analyses, yet these techniques are costly or lack taxonomic resolution. Here, we investigated a small piece of the genetic material of these species to identify them and get an idea of their abundance. Moreover, using this approach we could study the bacteria and phytoplankton simultaneously. This allowed us to compare both components of the microbial system and study how these are controlled by their environment. Our results suggest that, in contrast to what is generally assumed, limitation of nutrients does occur during summer. Which nutrient varied between the different phases of the summer season. Both nitrogen and phosphorus concentrations were occasionally near or below the detection levels. Also, the variations in these different nutrients strongly influenced phytoplankton diversity while water column stability (stratification) was another strong influence. Storms can cause abrupt changes in the water column stability by mixing the water. These moments of strong wind mixing influenced nutrient and light availability and drastically changed the phytoplankton community within days. Changes in the bacterial community were mostly depended on total phytoplankton biomass. Also, the data suggests that bacterial diversity was depended on phytoplankton community composition albeit delayed by two weeks. This dependency is understandable as the composition of the organic material on which bacteria grow varies between different phytoplankton species.

In **Chapter 5** was the availability of various trace elements and major nutrients during the summer over 2012-2014 investigated. Samples were collected at multiple depths at the RaTS-location for the measurement of nitrate, nitrite, phosphate, silicate, iron, manganese, zinc, cadmium, cobalt and copper. First of all, we showed that several trace elements were present in such low concentrations that they most likely hampering phytoplankton growth. Moreover, we confirmed our earlier findings (from **Chapter 3**) and showed that all major nutrients (thus nitrate, phosphate and silicate) can be reduced by phytoplankton to very low concentrations. Also, nutrient dynamics differed greatly between the two different summers. Finally, we showed that flagellates and diatoms take up major nutrients and trace elements in different ratios. Thus, these

results underline that the majority of the measured nutrients and trace elements are relevant for determining species composition but more importantly: they control phytoplankton abundance to a great extent.

In **Chapter 6** we investigated the existence of different ecotypes for the flagellated species. Previous studies, including **Chapters 2, 3** and **5** of this thesis, have mainly used pigments to assess crude phytoplankton species composition. Yet, in **Chapter 6** we employed new DNA techniques to detect and describe species during two austral summers (2012-2014). It is generally assumed that the haptophyte *Phaeocystis antarctica* and the cryptophyte *Geminigera cryophila* are the two dominant flagellated species. Yet, we showed the presences of a second haptophyte species, probably *P. jahnii*. Additionally, we observed a second haptophyte genus, namely *Chrysochromulina* that was equally abundant as *Phaeocystis* during the first summer. We also confirm the presence of different ecotypes within all the investigated species. For example, for *G. cryophila* we observed three different ecotypes of which two had contrasting preferences for salinity, thus suggesting an open ocean ecotype and one associated with fresher water. The existence of these different ecotypes means that they occupy different niches, and potentially fulfill different roles in the ecosystem. Finally, we strongly suspect to have identified a cryptophyte specific grazer, the dinoflagellate *Prorocentrum.* This could mean that *G. cryophila* is thightly regulated by top-down grazing pressure, a mechanism we did not identify for the other flagellated species.

The research conducted in this thesis has increased our understanding of the strong dynamics in microbial species composition, abundance, and production along the rapidly changing Antarctic Peninsula. Most of these factors, such as: sea-ice cover, melting glaciers, wind mixing and nutrient availability, are all governing the microbial community and are undergoing rapid change. This thesis already shows years where the phytoplankton community composition has shifted away from the classical coastal Antarctic system. Such deviations are likely to occur more frequently in the near future given the current trends in the local and global climate. Therefore, the impact on the food web and CO_2 storage capabilities of the Southern Ocean will only become more evident.

References

Abele D, Vazquez S, Buma AGJ et al. (2017) Pelagic and benthic communities of the Antarctic ecosystem of Potter Cove: Genomics and ecological implications. *Marine Genomics*, **33**, 1–11.

Abell GCJ, Bowman JP (2005) Ecological and biogeographic relationships of class Flavobacteria in the Southern Ocean. *FEMS Microbiology Ecology*, **51**, 265–277.

Ackley SF, Sullivan CW (1994) Physical controls on the development and characteristics of Antarctic sea ice biological communities- a review and synthesis. *Deep-Sea Research Part I*, **41**, 1583–1604.

Ajani P, Harwood DT, Murray A (2017) Recent trends in marine phycotoxins from Australian coastal waters. *Marine Drugs*, **15**.

Alderkamp AC, de Baar HJW, Visser RJW, Arrigo KR (2010) Can photoinhibition control phytoplankton abundance in deeply mixed water columns of the Southern Ocean? *Limnology and Oceanography*, **55**, 1248–1264.

Alderkamp AC, Kulk G, Buma AGJ, Visser RJW, van Dijken GL, Mills MM, Arrigo KR (2012a) The effect of iron limitation on the photophysiology of phaeocystis antarctica (prymnesiophyceae) and fragilariopsis cylindrus (bacillariophyceae) under dynamic irradiance. *Journal of Phycology*, **48**, 45–59.

Alderkamp AC, Mills MM, van Dijken GL et al. (2012b) Iron from melting glaciers fuels phytoplankton blooms in the Amundsen Sea (Southern Ocean): Phytoplankton characteristics and productivity. *Deep-Sea Research Part II: Topical Studies in Oceanography*, **71–76**, 32–48.

Alderkamp AC, Mills MM, van Dijken GL, Arrigo KR (2013) Photoacclimation and non-photochemical quenching under in situ irradiance in natural phytoplankton assemblages from the Amundsen Sea, Antarctica. *Marine Ecology Progress Series*, **475**, 15–34.

Amann RI, Binder BJ, Olson RJ, Chisholm SW, Devereux R, Stahl DA (1990) Combination of 16S rRNA-targeted oligonucleotide probes with flow cytometry for analyzing mixed microbial populations. *Applied and Environmental Microbiology*, **56**, 1919–1925.

Anderson MJ (2001) A new method for non-parametric multivariate analysis of variance. *Austral Ecology*, **26**, 32–46.

Annett AL, Carson DS, Crosta X, Clarke A, Ganeshram RS (2010) Seasonal progression of diatom assemblages in surface waters of Ryder Bay, Antarctica. *Polar Biology*, **33**, 13–29.

Annett AL, Skiba M, Henley SF, Venables HJ, Meredith MP, Statham PJ, Ganeshram RS (2015) Comparative roles of upwelling and glacial iron sources in Ryder Bay, coastal western Antarctic Peninsula. *Marine Chemistry*, **176**, 21–33.

Annett AL, Fitzsimmons JN, Séguret MJM, Lagerström M, Meredith MP, Schofield O, Sherrell RM (2017a) Controls on dissolved and particulate iron distributions in surface waters of the Western Antarctic Peninsula shelf. *Marine Chemistry*.

Annett AL, Henley SF, Venables HJ, Meredith MP, Clarke A, Ganeshram RS (2017b) Silica cycling and isotopic composition in northern Marguerite Bay on the rapidly-warming western Antarctic Peninsula. *Deep-Sea Research Part II: Topical Studies in Oceanography*, **139**, 132–142.

Ardelan MV, Holm-Hansen O, Hewes CD et al. (2010) Natural iron enrichment around the Antarctic Peninsula in the Southern Ocean. *Biogeosciences*, **7**, 11–25.

Armbrust EV (2009) The life of diatoms in the world's oceans. *Nature*, **459**, 185–192.

Arrigo KR (1997) Primary Production in Antarctic Sea Ice. *Science*, **276**, 394–397.

Arrigo KR (2005) Marine microorganisms and global nutrient cycles. *Nature*, **437**, 343–348.

Arrigo KR (2016) Sea ice as a habitat for primary producers. In: *Sea Ice*, 3rd edn (ed Thomas DN), pp. 352–369. Chichester.

Arrigo KR, Robinson DH, Worthen DL, Dunbar RB, DiTullio GR, van Woert M, Lizotte MP (1999) Phytoplankton Community Structure and the Drawdown of Nutrients and CO_2 in the Southern Ocean. *Science*, **283**, 365–367.

Arrigo KR, van Dijken GL, Pabi S (2008) Impact of a shrinking Arctic ice cover on marine primary production. *Geophysical Research Letters*, **35**.

Arrigo KR, Mills MM, Kropuenske LR, van Dijken GL, Alderkamp AC, Robinson DH (2010) Photophysiology in two major southern ocean phytoplankton taxa: Photosynthesis and growth of phaeocystis antarctica and fragilariopsis

cylindrus under different irradiance levels. *Integrative and Comparative Biology*, **50**, 950–966.

Arrigo KR, Brown ZW, Mills MM (2014) Sea ice algal biomass and physiology in the Amundsen Sea, Antarctica. *Elementa: Science of the Anthropocene*, **2**.

Assmy P, Henjes J, Klaas C, Smetacek V (2007) Mechanisms determining species dominance in a phytoplankton bloom induced by the iron fertilization experiment EisenEx in the Southern Ocean. *Deep-Sea Research Part I: Oceanographic Research Papers*, **54**, 340–362.

Atkinson A, Siegel V, Pakhomov EA, Rothery P (2004) Long-term decline in krill stock and increase in salps within the Southern Ocean. *Nature*, **432**, 100–103.

Atkinson A, Siegel V, Pakhomov EA et al. (2008) Oceanic circumpolar habitats of Antarctic krill. *Marine Ecology Progress Series*, **362**, 1–23.

Atkinson A, Ward P, Hunt BP V, Pakhomov EA, Hosie GW (2012) an Overview of Southern Ocean Zooplankton Data: Abundance, Biomass, Feeding and Functional Relationships. *Ccamlr Science*, **19**, 171–218.

Aumont O, Ethé C, Tagliabue A, Bopp L, Gehlen M (2015) PISCES-v2: An ocean biogeochemical model for carbon and ecosystem studies. *Geoscientific Model Development*, **8**, 2465–2513.

de Baar HJW, La Roche J (2003) Trace Metals in the Oceans: Evolution, Biology and Global Change. In: *Marine Science Frontiers for Europe* (eds Wefer G, Lamy F, Mantoura F), pp. 79–105. Springer Berlin Heidelberg, Berlin, Heidelberg.

de Baar HJW, Saager PM, Nolting RF, van der Meer J (1994) Cadmium versus phosphate in the world ocean. *Marine Chemistry*, **46**, 261–281.

de Baar HJW, de Jong JTM, Bakker DCE, Löscher BM, Veth C, Bathmann U V., Smetacek V (1995) Importance of iron for plankton blooms and carbon dioxide drawdown in the Southern Ocean. *Nature*, **373**, 412–415.

de Baar HJW, Boyd PW, Coale KH et al. (2005) Synthesis of iron fertilization experiments: From the iron age in the age of enlightenment. *Journal of Geophysical Research C: Oceans*, **110**, 1–24.

Baars O, Abouchami W, Galer SJG, Boye M, Croot PL (2014) Dissolved cadmium in the Southern Ocean: Distribution, speciation, and relation to phosphate. *Limnology and Oceanography*, **59**, 385–399.

Bálint M, Bahram M, Eren AM et al. (2016) Millions of reads, thousands of taxa: Microbial community structure and associations analyzed via marker genesa. *FEMS Microbiology Reviews*, **40**, 686–700.

Balzano S, Abs E, Leterme SC (2015) Protist diversity along a salinity gradient in a coastal lagoon. *Aquatic Microbial Ecology*, **74**, 263–277.

Banse K (1992) Grazing, Temporal Changes of Phytoplankton Concentrations, and the Microbial Loop in the Open Sea BT - Primary Productivity and Biogeochemical Cycles in the Sea. *Primary productivity and biogeochemical cycles in the sea*, 409–440.

Barrand NE, Vaughan DG, Steiner N, Tedesco M, Kuipers Munneke P, van den Broeke MR, Hosking JS (2013) Trends in Antarctic Peninsula surface melting conditions from observations and regional climate modeling. *Journal of Geophysical Research: Earth Surface*, **118**, 315–330.

Barton AD, Dutkiewicz S, Flierl G, Bragg J, Follows MJ (2010) Patterns of Diversity in Marine Phytoplankton. *Science*, **327**, 1509–1511.

Behrenfeld MJ (2010) Abandoning sverdrup's critical depth hypothesis on phytoplankton blooms. *Ecology*, **91**, 977–989.

Behrenfeld M, Falkowski PG (1997) A consumer's guide to phytoplankton primary productivity models. *Limnology and Oceanography*, **42**, 1479–1491.

Belcher A, Tarling GA, Manno C et al. (2017) The potential role of Antarctic krill faecal pellets in efficient carbon export at the marginal ice zone of the South Orkney Islands in spring. *Polar Biology*, 1–13.

Billen G, Becquevort S (1991) Phytoplankton Bacteria Relationship in the Antarctic Marine Ecosystem. *Polar Research*, **10**, 245–253.

Biller D V, Bruland KW (2012) Analysis of Mn, Fe, Co, Ni, Cu, Zn, Cd, and Pb in seawater using the Nobias-chelate PA1 resin and magnetic sector inductively coupled plasma mass spectrometry (ICP-MS). *Marine Chemistry*, **130**, 12–20.

Bird DF, Karl DM (1991) Spatial patterns of glutamate and thymidine assimilation in Bransfield Strait, antarctia during and following the austral spring bloom. *Deep Sea Research*

Part A, Oceanographic Research Papers, **38**, 1057–1075.

Bird DF, Karl DM (1999) Uncoupling of bacteria and phytoplankton during the austral spring bloom in Gerlache Strait, Antarctic Peninsula. *Aquatic Microbial Ecology*, **19**, 13–27.

Boelen P, de Boer MK, Kraay GW, Veldhuis MJW, Buma AGJ (2000) UVBR-induced DNA damage in natural marine picoplankton assemblages in the tropical Atlantic Ocean. *Marine Ecology Progress Series*, **193**, 1–9.

Bown J, Boye M, Baker A et al. (2011) The biogeochemical cycle of dissolved cobalt in the Atlantic and the Southern Ocean south off the coast of South Africa. *Marine Chemistry*, **126**, 193–206.

Bown J, Laan P, Ossebaar S, Bakker K, Rozema PD, de Baar HJW (2017) Bioactive trace metal time series during Austral summer in Ryder Bay, Western Antarctic Peninsula. *Deep Sea Research Part II: Topical Studies in Oceanography*, **139**, 103–119.

Boye M, Wake BD, Lopez Garcia P, Bown J, Baker AR, Achterberg EP (2012) Distributions of dissolved trace metals (Cd, Cu, Mn, Pb, Ag) in the southeastern Atlantic and the Southern Ocean. *Biogeosciences*, **9**, 3231–3246.

Brainerd KE, Gregg MC (1995) Surface mixed and mixing layer depths. *Deep-Sea Research Part I*, **42**, 1521–1543.

Bray RJ, Curtis JT (1957) An ordination of the upland forest communities of southern Wisconsin. *Ecological Monographs*, **27**, 325–349.

Breiman L (2001) Random forests. *Machine Learning*, **45**, 5–32.

Brum JR, Hurwitz BL, Schofield O, Ducklow HW, Sullivan MB (2015) Seasonal time bombs: dominant temperate viruses affect Southern Ocean microbial dynamics. *Isme J*, **10**, 1–13.

Brzezinski MA (2008) Mining the diatom genome for the mechanism of biosilicification. *Proceedings of the National Academy of Sciences* , **105**, 1391–1392.

Buma AGJ, Gieskes WWC, Thomsen HA (1992) Abundance of cryptophyceae and chlorophyll b-containing organisms in the Weddell-Scotia Confluence area in the spring of 1988. *Polar Biology*, **12**, 43–52.

Buma AGJ, de Boer MK, Boelen P (2001) Depth distributions of DNA damage in antarctic marine phyto and bacterioplankton exposed to summertime UV radiation. *Journal of Phycology*, **37**, 200–208.

Burkill PH, Edwards ES, Sleight MA (1995) Microzooplankton and their role in controlling phytoplankton growth in the marginal ice zone of the Bellingshausen Sea. *Deep-Sea Research Part II*, **42**, 1277–1290.

Calbet A, Landry MR (2004) Phytoplankton growth, microzooplankton grazing, and carbon cycling in marine systems. *Limnology and Oceanography*, **49**, 51–57.

Camacho C, Coulouris G, Avagyan V, Ma N, Papadopoulos J, Bealer K, Madden TL (2009) BLAST+: architecture and applications. *BMC Bioinformatics*, **10**, 421.

Caporaso JG, Kuczynski J, Stombaugh J et al. (2010) QIIME allows analysis of high-throughput community sequencing data. *Nature methods*, **7**, 335–6.

Caron DA, Countway PD, Jones AC, Kim DY, Schnetzer A (2011) Marine Protistan Diversity. *Annual Review of Marine Science*, **4**, 467–493.

Carvalho F, Kohut J, Oliver MJ, Schofield O (2017) Defining the ecologically relevant mixed-layer depth for Antarctica's coastal seas. *Geophysical Research Letters*, **44**, 338–345.

Cassarino L, Hendry KR, Meredith MP, Venables HJ, De La Rocha CL (2017) Silicon isotope and silicic acid uptake in surface waters of Marguerite Bay, West Antarctic Peninsula. *Deep-Sea Research Part II: Topical Studies in Oceanography*, **139**, 143–150.

Castro CG, Ríos AF, Doval MD, Pérez FF (2002) Nutrient utilisation and chlorophyll distribution in the Atlantic sector of the Southern Ocean during Austral summer 1995-96. *Deep-Sea Research Part II: Topical Studies in Oceanography*, **49**, 623–641.

Chao A, Jost L (2012) Coverage-based rarefaction and extrapolation: Standardizing samples by completeness rather than size. *Ecology*, **93**, 2533–2547.

Chao A, Gotelli NJ, Hsieh TC, Sander EL, Ma KH, Colwell RK, Ellison AM (2014) Rarefaction and extrapolation with Hill numbers: A framework for sampling and estimation in species diversity studies. *Ecological Monographs*, **84**, 45–67.

Clarke A, Meredith MP, Wallace MI, Brandon MA, Thomas DN (2008) Seasonal and interannual variability in temperature,

chlorophyll and macronutrients in northern Marguerite Bay, Antarctica. *Deep-Sea Research Part II: Topical Studies in Oceanography*, **55**, 1988–2006.

Claustre H, Moline MA, Prezelin BB (1997) Sources of variability in the column photosynthetic cross section for Antarctic coastal waters. *Journal of Geophysical Research-Oceans*, **102**, 25047–25060.

Clem KR, Fogt RL (2013) Varying roles of ENSO and SAM on the Antarctic Peninsula climate in austral spring. *Journal of Geophysical Research Atmospheres*, **118**, 11481–11492.

Cohan FM (2002) What are bacterial species? *Annual Review of Microbiology*, **56**, 457–487.

Cole J, Findlay S, Pace M (1988) Bacterial production in fresh and saltwater ecosystems: a cross-system overview. *Marine Ecology Progress Series*, **43**, 1–10.

Constable AJ, Melbourne-Thomas J, Corney SP et al. (2014) Climate change and Southern Ocean ecosystems I: How changes in physical habitats directly affect marine biota. *Global Change Biology*, **20**, 3004–3025.

Cook AJ, Fox A. J, Vaughan DG, Ferrigno JG (2005) Retreating glacier fronts on the Antarctic Peninsula over the past half-century. *Science*, **308**, 541–544.

Cook AJ, Holland PR, Meredith MP, Murray T, Luckman A, Vaughan DG (2016) Ocean forcing of glacier retreat in the western Antarctic Peninsula. *Science*, **353**, 1261–1273.

Corps C (2011) *Chapter 16: Memories of changes in renal care over three decades - The human perspective on registry statistics*, Vol. 119. North Pacific Marine Science Organization, Sidney, 191 pp.

Craig H, Gordon L (1965) Deuterium and oxygen 18 variations in the ocean and the marine atmosphere. In: *Stable Isotopes in Oceanographic Studies and Paleotemperatures* (ed Tongiorgio E), pp. 9–130. Spoleto, Italy.

Croot PL, Baars O, Streu P (2011) The distribution of dissolved zinc in the Atlantic sector of the Southern Ocean. *Deep Sea Research Part II: Topical Studies in Oceanography*, **58**, 2707–2719.

Cullen JT, Chase Z, Coale KH, Fitzwater SE, Sherrell RM (2003) Effect of iron limitation on the cadmium to phosphorus ratio of natural phytoplankton assemblages from the Southern Ocean. *Limnology and Oceanography*, **48**, 1079–1087.

Curson ARJ, Rogers R, Todd JD, Brearley CA, Johnston AWB (2008) Molecular genetic analysis of a dimethylsulfoniopropionate lyase that liberates the climate-changing gas dimethylsulfide in several marine alpha-proteobacteria and Rhodobacter sphaeroides. *Environmental Microbiology*, **10**, 757–767.

Decelle J, Probert I, Bittner L et al. (2012) An original mode of symbiosis in open ocean plankton. *Proceedings of the National Academy of Sciences of the United States of America*, **109**, 18000–5.

Delmont TO, Hammar KM, Ducklow HW, Yager PL, Post AF (2014) Phaeocystis antarctica blooms strongly influence bacterial community structures in the Amundsen Sea polynya. *Frontiers in Microbiology*, **5**.

Depoorter MA, Bamber JL, Griggs JA, Lenaerts JTM, Ligtenberg SRM, van den Broeke MR, Moholdt G (2013) Calving fluxes and basal melt rates of Antarctic ice shelves. *Nature*, **502**, 89–92.

Dierssen HM, Smith RC (2000) Bio-optical properties and remote sensing ocean color algorithms for Antarctic Peninsula waters. *Journal of Geophysical Research: Oceans*, **105**, 26301–26312.

Dierssen HM, Smith RC, Vernet M (2002) Glacial meltwater dynamics in coastal waters west of the Antarctic peninsula. *Proceedings of the National Academy of Sciences of the United States of America*, **99**, 1790–5.

Díez B, Pedrós-Alió C, Marsh TL, Pedro C (2001) Application of Denaturing Gradient Gel Electrophoresis (DGGE) To Study the Diversity of Marine Picoeukaryotic Assemblages and Comparison of DGGE with Other Molecular Techniques Application of Denaturing Gradient Gel Electrophoresis (DGGE) To Study the. *Applied and environmental microbiology*, **67**, 2941–2951.

Díez B, Massana R, Estrada M, Pedrós-Alió C (2004) Distribution of eukaryotic picoplankton assemblages across hydrographic fronts in the Southern Ocean, studied by denaturing gradient gel electrophoresis. *Limnology and Oceanography*, **49**, 1022–1034.

Ding Q, Steig EJ, Battisti DS, Küttel M (2011) Winter warming in West Antarctica caused by

central tropical Pacific warming. *Nature Geoscience*, **4**, 398–403.

DiTullio GR, Garcia N, Riseman SF, Sedwick PN (2007) Effects of iron concentration on pigment composition in Phaeocystis antarctica grown at low irradiance. *Biogeochemistry*, **83**, 71–81.

Dixon DA, Mayewski PA, Goodwin ID, Marshall GJ, Freeman R, Maasch KA, Sneed SB (2012) An ice-core proxy for northerly air mass incursions into West Antarctica. *International Journal of Climatology*, **32**, 1455–1465.

Dolan JR, Yang EJ, Lee SH, Kim SY (2013) Tintinnid ciliates of amundsen sea (Antarctica) plankton communities. *Polar Research*, **32**, 1–12.

Dore JE, Tien G, Letelier R, Parrish G, Szyper J, Burgett J, Karl DM (1992) RACER: Distributions of nitrogenous nutrients near receding pack ice in Marguerite Bay. *Antarctic Journal of the United States*, **27**, 177–179.

Douglas S, Zauner S, Fraunholz M et al. (2001) The highly reduced genome of an enslaved algal nucleus. *Nature*, **410**, 1091–1096.

Ducklow HW, Baker K, Martinson DG et al. (2007) Marine pelagic ecosystems: the West Antarctic Peninsula. *Philosophical Transactions of the Royal Society B: Biological Sciences*, **362**, 67–94.

Ducklow H, Clarke A, Dickhut R et al. (2012a) The Marine System of the Western Antarctic Peninsula. In: *Antarctic Ecosystems: An Extreme Environment in a Changing World* (eds Rogers AD, Johnston NM, Murphy EJ, Clarke A), pp. 121–159. John Wiley & Sons, Ltd, Chichester.

Ducklow HW, Schofield O, Vernet M, Stammerjohn S, Erickson M (2012b) Multiscale control of bacterial production by phytoplankton dynamics and sea ice along the western Antarctic Peninsula: A regional and decadal investigation. *Journal of Marine Systems*, **98–99**, 26–39.

Ducklow H, Fraser W, Meredith M et al. (2013) West Antarctic Peninsula: An ice-dependent coastal marine ecosystem in transition. *Oceanography*, **26**, 190–203.

Dulaiova H, Ardelan M V, Henderson PB, Charette MA (2009) Shelf-derived iron inputs drive biological productivity in the southern Drake Passage. *Global Biogeochemical Cycles*, **23**, GB4014.

Dunn OJ (1961) Multiple Comparisons Among Means. *Journal of the American Statistical Association*, **56**, 52–64.

Ellwood MJ (2008) Wintertime trace metal (Zn, Cu, Ni, Cd, Pb and Co) and nutrient distributions in the Subantarctic Zone between 40-52°S; 155-160°E. *Marine Chemistry*, **112**, 107–117.

Eren AM, Vineis JH, Morrison HG, Sogin ML (2013) A Filtering Method to Generate High Quality Short Reads Using Illumina Paired-End Technology. *PLoS ONE*, **8**.

Eren AM, Morrison HG, Lescault PJ, Reveillaud J, Vineis JH, Sogin ML (2015) Minimum entropy decomposition: unsupervised oligotyping for sensitive partitioning of high-throughput marker gene sequences. *Isme J*, **9**, 968–979.

Everson I (2000) Role of Krill in Marine Food Webs. 7.3 The Southern Ocean. In: *Krill: Biology, Ecology, and Fisheries*, Fish and A edn (ed Everson I), pp. 194–201. Blackwell Science, Oxford.

Faust K, Sathirapongsasuti JF, Izard J, Segata N, Gevers D, Raes J, Huttenhower C (2012) Microbial co-occurrence relationships in the Human Microbiome. *PLoS Computational Biology*, **8**.

Fernández-Gómez B, Richter M, Schüler M, Pinhassi J, Acinas SG, González JM, Pedrós-Alió C (2013) Ecology of marine Bacteroidetes: A comparative genomics approach. *The ISME Journal*, **7**, 1026–37.

Fitzwater SE, Johnson KS, Gordon RM, Coale KH, Smith WO (2000) Trace metal concentrations in the Ross Sea and their relationship with nutrients and phytoplankton growth. *Deep Sea Research Part II: Topical Studies in Oceanography*, **47**, 3159–3179.

Flores H, Atkinson A, Kawaguchi S et al. (2012) Impact of climate change on Antarctic krill. *Marine Ecology Progress Series*, **458**, 1–19.

Frank KL, Rogers DR, Olins HC, Vidoudez C, Girguis PR (2013) Characterizing the distribution and rates of microbial sulfate reduction at Middle Valley hydrothermal vents. *The ISME Journal*, **7**, 1391–1401.

Fripiat F, Meiners KM, Vancoppenolle M et al. (2017) Macro-nutrient concentrations in Antarctic pack ice: Overall patterns and overlooked processes. *Elem Sci Anth*, **5**, 13.

Gäbler-Schwarz S, Medlin LK, Leese F (2015) A puzzle with many pieces: the genetic structure and diversity of Phaeocystis antarctica Karsten (Prymnesiophyta). *European Journal of Phycology*, **50**, 112–124.

Garibotti IA, Vernet M, Kozlowski WA, Ferrario ME (2003) Composition and biomass of phytoplankton assemblages in coastal Antarctic waters: A comparison of chemotaxonomic and microscopic analyses. *Marine Ecology Progress Series*, **247**, 27–42.

Garibotti IA, Vernet M, Ferrario ME (2005) Annually recurrent phytoplanktonic assemblages during summer in the seasonal ice zone west of the Antarctic Peninsula (Southern Ocean). *Deep-Sea Research Part I: Oceanographic Research Papers*, **52**, 1823–1841.

Garrison DL, Mathot S (1996) Pelagic and sea ice microbial communities. **70**, 155–172.

Garzio LM, Steinberg DK, Erickson M, Ducklow HW (2013) Microzooplankton grazing along the Western Antarctic Peninsula. *Aquatic Microbial Ecology*, **70**, 215–232.

Gast RJ, Dennett MR, Caron DA (2004) Characterization of Protistan Assemblages in the Ross Sea, Antarctica, by Denaturing Gradient Gel Electrophoresis. *Applied and Environmental Microbiology*, **70**, 2028–2037.

Gentile G, Giuliano L, D'Auria G, Smedile F, Azzaro M, De Domenico M, Yakimov MM (2006) Study of bacterial communities in Antarctic coastal waters by a combination of 16S rRNA and 16S rDNA sequencing. *Environmental Microbiology*, **8**, 2150–2161.

Georges C, Monchy S, Genitsaris S, Christaki U (2014) Protist community composition during early phytoplankton blooms in the naturally iron-fertilized Kerguelen area (Southern Ocean). *Biogeosciences*, **11**, 5847–5863.

Gerringa LJA, Alderkamp AC, Laan P et al. (2012) Iron from melting glaciers fuels the phytoplankton blooms in Amundsen Sea (Southern Ocean): Iron biogeochemistry. *Deep Sea Research Part II: Topical Studies in Oceanography*, **71–76**, 16–31.

Gerringa LJA, Laan P, van Dijken GL, van Haren H, de Baar HJW, Arrigo KR, Alderkamp AC (2015) Sources of iron in the Ross Sea Polynya in early summer. *Marine Chemistry*, **177**, 447–459.

Ghiglione JF, Murray AE (2012) Pronounced summer to winter differences and higher wintertime richness in coastal Antarctic marine bacterioplankton. *Environmental Microbiology*, **14**, 617–629.

Giovannoni SJ, DeLong EF, Olsen GJ, Pace NR (1988) Phylogenetic group-specific oligodeoxynucleotide probes for identification of single microbial cells. *Journal of Bacteriology*, **170**, 720–726.

Godhe A, Asplund ME, Härnström K, Saravanan V, Tyagi A, Karunasagar I (2008) Quantification of diatom and dinoflagellate biomasses in coastal marine seawater samples by real-time PCR. *Applied and Environmental Microbiology*, **74**, 7174–7182.

Grotti M, Soggia F, Abelmoschi ML, Rivaro P, Magi E, Frache R (2001) Temporal distribution of trace metals in Antarctic coastal waters. *Marine Chemistry*, **76**, 189–209.

Grzymski JJ, Riesenfeld CS, Williams TJ et al. (2012) A metagenomic assessment of winter and summer bacterioplankton from Antarctica Peninsula coastal surface waters. *The ISME Journal*, **6**, 1901–1915.

Guillou L, Bachar D, Audic S et al. (2013) The Protist Ribosomal Reference database (PR2): A catalog of unicellular eukaryote Small Sub-Unit rRNA sequences with curated taxonomy. *Nucleic Acids Research*, **41**, 597–604.

Haberman KL, Ross RM, Quetin LB (2003) Diet of the Antarctic krill (Euphausia superba Dana): II. Selective grazing in mixed phytoplankton assemblages. *Journal of Experimental Marine Biology and Ecology*, **283**, 97–113.

Hall JA, Safi K (2001) The impact of in situ Fe fertilisation on the microbial food web in the Southern Ocean. *Deep-Sea Research Part II: Topical Studies in Oceanography*, **48**, 2591–2613.

Hallfors G, Niemi A (1974) A chrysochromulina (Haptophyceae) bloom under the ice in the Tvarminne Archipelago, southern coast of Finland. *Memoranda Soc. Fauna Flora Fennica*, **50**, 89–104.

Hammer Ø, Harper DAT, Ryan PD (2001) PAST: Paleontological statistics sofware package for education and data analysis. *Palaeontologia Electronica*, **4**, 1–9.

Harangozo SA (2006) Atmospheric circulation impacts on winter maximum sea ice extent in the west Antarctic Peninsula region (1979-2001). *Geophysical Research Letters*, **33**, L02502.

Hatta M, Measures CI, Selph KE, Zhou M, Hiscock WT (2013) Iron fluxes from the shelf

regions near the South Shetland Islands in the Drake Passage during the austral-winter 2006. *Deep-Sea Research Part II: Topical Studies in Oceanography*, **90**, 89–101.

Hendry KR, Rickaby REM, de Hoog JCM, Weston K, Rehkämper M (2008) Cadmium and phosphate in coastal Antarctic seawater: Implications for Southern Ocean nutrient cycling. *Marine Chemistry*, **112**, 149–157.

Hendry KR, Meredith MP, Measures CI, Carson DS, Rickaby REM (2010) The role of sea ice formation in cycling of aluminium in northern Marguerite Bay, Antarctica. *Estuarine, Coastal and Shelf Science*, **87**, 103–112.

Henley SF, Tuerena RE, Annett AL et al. (2017) Macronutrient supply, uptake and recycling in the coastal ocean of the west Antarctic Peninsula. *Deep-Sea Research Part II: Topical Studies in Oceanography*, **139**, 58–76.

Heuer H, Wieland G, Schönfeld J, Schönwälder A, Gomes NCM, Smalla K (2001) *Bacterial community profiling using DGGE or TGGE analysis*, Vol. 9 (ed Rouchelle I. P.). Horizon Scientific Press, Wymondham, 177-190 pp.

van Heukelem L, Thomas CS (2001) Computer-assisted high-performance liquid chromatography method development with applications to the isolation and analysis of phytoplankton pigments. *Journal of Chromatography A*, **910**, 31–49.

Higgins HW, Wright SW, Schlüter L (2011) Chapter 6: Quantitative interpretation of chemotaxonomic pigment data. In: *Phytoplankton Pigments: Characterization, Chemotaxonomy and Applications in Oceanography*, Vol. 1 (eds Roy S, Llewellyn CA, Egeland ES, Johnsen G), p. 890. Cambridge University Press, Cambridge.

van den Hoff J, Bell E (2015) The ciliate Mesodinium rubrum and its cryptophyte prey in Antarctic aquatic environments. *Polar Biology*, **38**, 1305–1310.

Holm S (1979) A Simple Sequentially Rejective Multiple Test Procedure. *Scandinavian Journal of Statistics*, **6**, 65–70.

Huang K, Ducklow H, Vernet M, Cassar N, Bender ML (2012) Export production and its regulating factors in the West Antarctica Peninsula region of the Southern Ocean. *Global Biogeochemical Cycles*, **26**, 1–13.

Huisman J, Weissing FJ (1999) Biodiversity of plankton by species oscillations and chaos. *Nature*, **402**, 407–410.

Huse SM, Mark Welch DB, Voorhis A, Shipunova A, Morrison HG, Eren AM, Sogin ML (2014) VAMPS: a website for visualization and analysis of microbial population structures. *BMC bioinformatics*, **15**, 41.

IPCC (2007) *Contribution of Working Group I to the Fourth Assessment Report of the Intergovernmental Panel on Climate Change*. 996 pp.

Johnson MD (2015) Inducible Mixotrophy in the Dinoflagellate Prorocentrum minimum. *Journal of Eukaryotic Microbiology*, **62**, 431–443.

Johnson KM, Sieburth JM, Williams PJL, Brändström L (1987) Coulometric total carbon dioxide analysis for marine studies: Automation and calibration. *Marine Chemistry*, **21**, 117–133.

Jones EM, Fenton M, Meredith MP et al. (2017) Ocean acidification and calcium carbonate saturation states in the coastal zone of the West Antarctic Peninsula. *Deep Sea Research Part II: Topical Studies in Oceanography*, **139**, 181–194.

de Jong J, Schoemann V, Lannuzel D, Croot P, de Baar H, Tison JL (2012) Natural iron fertilization of the Atlantic sector of the Southern Ocean by continental shelf sources of the Antarctic Peninsula. *Journal of Geophysical Research: Biogeosciences*, **117**, 25pp.

Karl DM, Holm-Hansen O, Taylor GT, Tien G, Bird DF (1991) Microbial biomass and productivity in the western Bransfield Strait, Antarctica during the 1986-87 austral summer. *Deep Sea Research Part A, Oceanographic Research Papers*, **38**, 1029–1055.

Kim H, Ducklow HW (2016) A Decadal (2002–2014) Analysis for Dynamics of Heterotrophic Bacteria in an Antarctic Coastal Ecosystem: Variability and Physical and Biogeochemical Forcings. *Frontiers in Marine Science*, **3**, 214.

Kim JG, Park SJ, Quan ZX et al. (2014) Unveiling abundance and distribution of planktonic Bacteria and Archaea in a polynya in Amundsen Sea, Antarctica. *Environmental microbiology*, **16**, 1566–1578.

Kirk J (1983) *Light and photosynthesis in aquatic ecosystems*. Cambridge University Press.

Klunder MB, Laan P, de Baar HJW, Middag R, Neven I, van Ooijen J (2014) Dissolved Fe across the Weddell Sea and Drake Passage: Impact of

DFe on nutrient uptake. *Biogeosciences*, **11**, 651–669.

Kopczyńska EE, Fiala M, Jeandel C (1998) Annual and interannual variability in phytoplankton at a permanent station off Kerguelen Islands, Southern Ocean. *Polar biology*, **20**, 342–351.

Korhonen H, Carslaw KS, Forster PM, Mikkonen S, Gordon ND, Kokkola H (2010) Aerosol climate feedback due to decadal increases in southern hemisphere wind speeds. *Geophysical Research Letters*, **37**, 0–5.

Kozlowski WA, Deutschman D, Garibotti I, Trees C, Vernet M (2011) An evaluation of the application of CHEMTAX to Antarctic coastal pigment data. *Deep-Sea Research Part I: Oceanographic Research Papers*, **58**, 350–364.

Kropuenske LR, Mills MM, van Dijken GL, Bailey S, Robinson DH, Welschmeyer NA, Arrigo KR (2009) Photophysiology in two major Southern Ocean phytoplankton taxa: Photoprotection in Phaeocystis antarctica and Fragilariopsis cylindrus. *Limnology and Oceanography*, **54**, 1176–1196.

Kulk G, Buist A, van de Poll WH, Rozema PD, Buma AGJ (submitted) Size scaling of photophysiology and growth in four freshly isolated diatom species from Ryder Bay, West Antarctic Peninsula. *Journal of Phycology*.

Ladau J, Sharpton TJ, Finucane MM et al. (2013) Global marine bacterial diversity peaks at high latitudes in winter. *The ISME journal*, **7**, 1669–77.

Lagerström ME, Field MP, Séguret M, Fischer L, Hann S, Sherrell RM (2013) Automated on-line flow-injection ICP-MS determination of trace metals (Mn, Fe, Co, Ni, Cu and Zn) in open ocean seawater: Application to the GEOTRACES program. *Marine Chemistry*, **155**, 71–80.

Landa M, Blain S, Christaki U, Monchy S, Obernosterer I (2016) Shifts in bacterial community composition associated with increased carbon cycling in a mosaic of phytoplankton blooms. *The ISME …*, **10**, 39–50.

Lannuzel D, Bowie AR, van der Merwe PC, Townsend AT, Schoemann V (2011) Distribution of dissolved and particulate metals in Antarctic sea ice. *Marine Chemistry*, **124**, 134–146.

Latasa M, Scharek R, Vidal M, Vila-Reixach G, Gutiérrez-Rodríguez A, Emelianov M, Gasol JM (2010) Preferences of phytoplankton groups for waters of different trophic status in the northwestern Mediterranean sea. *Marine Ecology Progress Series*, **407**, 27–42.

van Leeuwe MA, Villerius LA, Roggeveld J, Visser RJW, Stefels J (2006) An optimized method for automated analysis of algal pigments by HPLC. *Marine Chemistry*, **102**, 267–275.

van Leeuwe MA, Visser RJW, Stefels J (2014) The pigment composition of Phaeocystis antarctica (Haptophyceae) under various conditions of light, temperature, salinity, and iron. *Journal of Phycology*, **50**, 1070–1080.

Legendre P, Legendre LFJ (1998) *Numerical Ecology*, 2nd edn. Elsevier, Amsterdam, 1-839 pp.

Legge OJ, Bakker DCE, Meredith MP, Venables HJ, Brown PJ, Jones EM, Johnson MT (2017) The seasonal cycle of carbonate system processes in Ryder Bay, West Antarctic Peninsula. *Deep-Sea Research Part II: Topical Studies in Oceanography*, **139**, 167–180.

Lewis M, Smith J (1983) A small volume, short-incubation-time method for measurement of photosynthesis as a function of incident irradiance . *Marine Ecology Progress Series*, **13**, 99–102.

Liaw A, Wiener M (2002) Classification and Regression by randomForest. *R news*, **2**, 18–22.

Ligowski R, Godlewski M, Łukowski A (1992) Sea ice diatoms and ice edge planktonic diatoms at the nothern limit of the Weddell Sea pack ice. *Polar Biol*, **5**, 9–20.

Lin S, Zhang H, Hou Y, Miranda L, Bhattacharya D (2006) Development of a dinoflagellate-oriented PCR primer set leads to detection of picoplanktonic dinoflagellates from Long Island Sound. *Applied and Environmental Microbiology*, **72**, 5626–5630.

Long JD, Smalley GW, Barsby T, Anderson JT, Hay ME (2007) Chemical cues induce consumer-specific defenses in a bloom-forming marine phytoplankton. *Proceedings of the National Academy of Sciences of the United States of America*, **104**, 10512–10517.

Löscher BM (1999) Relationships among Ni, Cu, Zn, and major nutrients in the Southern Ocean. *Marine Chemistry*, **67**, 67–102.

Luria CM, Ducklow HW, Amaral-Zettler LA (2014) Marine bacterial, archaeal and eukaryotic diversity and community structure on the

continental shelf of the western Antarctic Peninsula. *Aquatic Microbial Ecology*, **73**, 107–121.

Luria CM, Amaral-Zettler LA, Ducklow HW, Rich JJ (2016) Seasonal succession of free-living bacterial communities in coastal waters of the western antarctic peninsula. *Frontiers in Microbiology*, **7**, 1731.

MacIntyre H, Cullen J (2005) Using cultures to investigate the physiological ecology of microalgae. In: *Algal Culturing Techniques* (ed Andersen RA), pp. 287–326. Academic Press.

Mackey MD, Mackey DJ, Higgins HW, Wright SW (1996) CHEMTAX - A program for estimating class abundances from chemical markers: Application to HPLC measurements of phytoplankton. *Marine Ecology Progress Series*, **144**, 265–283.

Malmstrom RR, Kiene RP, Cottrell MT, Kirchman DL (2004) Contribution of SAR11 bacteria to dissolved dimethylsulfoniopropionate and amino acid uptake in the North Atlantic Ocean. *Applied and Environmental Microbiology*, **70**, 4129–4135.

Marshall GJ, Orr A, van Lipzig NPM, King JC (2006) The impact of a changing Southern Hemisphere Annular Mode on Antarctic Peninsula summer temperatures. *Journal of Climate*, **19**, 5388–5404.

Martin JH, Gordon RM, Fitzwater SE (1990) Iron in Antarctic waters. *Nature*, **345**, 156–158.

Martinson DG, Stammerjohn SE, Iannuzzi RA, Smith RC, Vernet M (2008) Western Antarctic Peninsula physical oceanography and spatio–temporal variability. *Deep Sea Research Part II: Topical Studies in Oceanography*, **55**, 1964–1987.

Maxwell K, Johnson GN (2000) Chlorophyll fluorescence—a practical guide. *Journal of Experimental Botany*, **51**, 659–668.

McMurdie PJ, Holmes S (2014) Waste Not, Want Not: Why Rarefying Microbiome Data Is Inadmissible. *PLoS Computational Biology*, **10**.

Medlin LK, Kaczmarska I (2004) Evolution of the diatoms: V. Morphological and cytological support for the major clades and a taxonomic revision. *Phycologia*, **43**, 245–270.

Medlin L, Zingone A (2007) A taxonomic review of the genus Phaeocystis. In: *Biogeochemistry*, Vol. 83, pp. 3–18.

Medlin L, Elwood HJ, Stickel S, Sogin ML (1988) The characterization of enzymatically amplified eukaryotic 16S-like rRNA-coding regions. *Gene*, **71**, 491–499.

Mendes CRB, Tavano VM, Dotto TS, Kerr R, de Souza MS, Garcia CAE, Secchi ER New insights on the dominance of cryptophytes in Antarctic coastal waters: A case study in Gerlache Strait. *Deep-Sea Research Part II: Topical Studies in Oceanography*.

Mendes CRB, de Souza MS, Garcia VMT, Leal MC, Brotas V, Garcia CAE (2012) Dynamics of phytoplankton communities during late summer around the tip of the Antarctic Peninsula. *Deep-Sea Research Part I: Oceanographic Research Papers*, **65**, 1–14.

Mendes CRB, Tavano VM, Leal MC, de Souza MS, Brotas V, Garcia CAE (2013) Shifts in the dominance between diatoms and cryptophytes during three late summers in the Bransfield Strait (Antarctic Peninsula). *Polar Biology*, **36**, 537–547.

Meredith MP, King JC (2005) Rapid climate change in the ocean west of the Antarctic Peninsula during the second half of the 20th century. *Geophysical Research Letters*, **32**, 1–5.

Meredith MP, Renfrew IA, Clarke A, King JC, Brandon MA (2004) Impact of the 1997/98 ENSO on upper ocean characteristics in Marguerite Bay, western Antarctic Peninsula. *Journal of Geophysical Research C: Oceans*, **109**, 1–19.

Meredith MP, Brandon MA, Wallace MI et al. (2008) Variability in the freshwater balance of northern Marguerite Bay, Antarctic Peninsula: Results from δ18O. *Deep-Sea Research Part II: Topical Studies in Oceanography*, **55**, 309–322.

Meredith MP, Wallace MI, Stammerjohn SE et al. (2010) Changes in the freshwater composition of the upper ocean west of the Antarctic Peninsula during the first decade of the 21st century. *Progress in Oceanography*, **87**, 127–143.

Meredith MP, Venables HJ, Clarke A et al. (2013) The freshwater system west of the antarctic peninsula: Spatial and temporal changes. *Journal of Climate*, **26**, 1669–1684.

Meredith MP, Stammerjohn SE, Venables HJ et al. (2017) Changing distributions of sea ice melt and meteoric water west of the Antarctic Peninsula. *Deep-Sea Research Part II: Topical Studies in Oceanography*, **139**, 40–57.

Middag R, de Baar HJW, Laan P, Cai PH, van Ooijen JC (2011) Dissolved manganese in the

Atlantic sector of the Southern Ocean. *Deep Sea Research Part II: Topical Studies in Oceanography*, **58**, 2661–2677.

Middag R, de Baar HJW, Klunder MB, Laan P (2013) Fluxes of dissolved aluminum and manganese to the Weddell Sea and indications for manganese co-limitation. *Limnology and Oceanography*, **58**, 287–300.

Mitchell BG, Holm-Hansen O (1991) Observations of modeling of the Antartic phytoplankton crop in relation to mixing depth. *Deep Sea Research Part A, Oceanographic Research Papers*, **38**, 981–1007.

Moffat C, Beardsley RC, Owens B, van Lipzig N (2008) A first description of the Antarctic Peninsula Coastal Current. *Deep-Sea Research Part II: Topical Studies in Oceanography*, **55**, 277–293.

Moline MA, Prezelin BB (1996) Long-term monitoring and analyses of physical factors regulating variability in coastal Antarctic phytoplankton composition over seasonal and interannual timescales. *Marine Ecology Progress Series*, **145**, 143–160.

Moline MA, Claustre H, Frazer TK, Schofield O, Vernet M (2004) Alteration of the food web along the Antarctic Peninsula in response to a regional warming trend. *Global Change Biology*, **10**, 1973–1980.

Montes-Hugo MA, Vernet M, Smith R, Carder K (2008a) Phytoplankton size-structure on the western shelf of the Antarctic Peninsula: a remote-sensing approach. *International Journal of Remote Sensing*, **29**, 801–829.

Montes-Hugo MA, Vernet M, Martinson D, Smith R, Iannuzzi R (2008b) Variability on phytoplankton size structure in the western Antarctic Peninsula (1997–2006). *Deep Sea Research Part II: Topical Studies in Oceanography*, **55**, 2106–2117.

Montes-Hugo M., Doney SC, Ducklow HW, Fraser W, Martinson D, Stammerjohn SE, Schofield O (2009) Recent Changes in Phytoplankton Communities Associated with Rapid Regional Climate Change Along the Western Antarctic Peninsula. *Science*, **323**, 1470–1473.

Moran XAG, Gasol JM, Estrada M, Pedros-Alio C (2001) Dissolved and particulate primary production and bacterial production in offshore antarctic waters during austral summer:coupled or uncoupled? *Marine Ecology Progress Series*, **222**, 25–39.

Moreno AM, Matz C, Kjelleberg S, Manefield M (2010) Identification of ciliate grazers of autotrophic bacteria in ammonia-oxidizing activated sludge by RNA stable isotope probing. *Applied and Environmental Microbiology*, **76**, 2203–2211.

Muyzer G (1999) DGGE/TGGE a method for identifying genes from natural ecosystems. *Current Opinion in Microbiology*, **2**, 317–322.

Neilson JW, Jordan FL, Maier RM (2013) Analysis of artifacts suggests DGGE should not be used for quantitative diversity analysis. *Journal of Microbiological Methods*, **92**, 256–263.

Nejstgaard JC, Tang KW, Steinke M, Dutz J, Koski M, Antajan E, Long JD (2007) Zooplankton grazing on Phaeocystis: A quantitative review and future challenges. *Phaeocystis, Major Link in the Biogeochemical Cycling of Climate-Relevant Elements*, **83**, 147–172.

Nielsen ES (1952) The Use of Radio-active Carbon (C14) for Measuring Organic Production in the Sea. *ICES Journal of Marine Science*, **18**, 117–140.

Nielsen GA, Bresta AM (1984) Guidelines for the measurement of phytoplankton primary production (ed Baltic Marine Biologists). *The Baltic Marine Biologists*, **1**, **2nd Edi**, 1–23.

Nishikawa J, Naganobu M, Ichii T, Ishii H, Terazaki M, Kawaguchi K (1995) Distribution of salps near the South Shetland Islands during austral summer , 1990 – 1991. *Polar Biology*, **15**, 1990–1991.

Noble AE, Moran DM, Allen AE, Saito MA (2013) Dissolved and particulate trace metal micronutrients under the McMurdo Sound seasonal sea ice: basal sea ice communities as a capacitor for iron. *Frontiers in chemistry*, **1**, 25.

Nolting RF, de Baar HJW, van Bennekom AJ, Masson A (1991) Cadmium, copper and iron in the Scotia Sea, Weddell Sea and Weddell/Scotia Confluence (Antarctica). *Marine Chemistry*, **35**, 219–243.

Nübel U, Engelen B, Felske A et al. (1996) Sequence heterogeneities of genes encoding 16S rRNAs in Paenibacillus polymyxa detected by temperature gradient gel electrophoresis. *Journal of bacteriology*, **178**, 5636–5643.

Oksanen J, Blanchet FG, Friendly M et al. (2017) Community Ecology Package.

Parkinson CL (2014) Global sea ice coverage from satellite data: Annual cycle and 35-yr trends. *Journal of Climate*, **27**, 9377–9382.

Parkinson CL, Cavalieri DJ (2012) Antarctic sea ice variability and trends, 1979-2010. *Cryosphere*, **6**, 871–880.

Pebesma EJ (2004) Multivariable geostatistics in S: The gstat package. *Computers and Geosciences*, **30**, 683–691.

Peck LS, Barnes DKA, Cook AJ, Fleming AH, Clarke A (2010) Negative feedback in the cold: Ice retreat produces new carbon sinks in Antarctica. *Global Change Biology*, **16**, 2614–2623.

Peers G, Price NMN (2006) Copper-containing plastocyanin used for electron transport by an oceanic diatom. *Nature*, **441**, 341–4.

Perissinotto R, Pakhomov EA (1998a) The trophic role of the tunicate Salpa thompsoni in the Antarctic marine ecosystem. *Journal of Marine Systems*, **17**, 361–374.

Perissinotto R, Pakhomov EA (1998b) Contribution of salps to carbon flux of marginal ice zone of the Lazarev Sea, southern ocean. *Marine Biology*, **131**, 25–32.

Perl J (2009) The SDU (CHORS) Method. In: *The Third SeaWiFS HPLC Analysis Round-Robin Experiment (SeaHARRE-3)*, pp. 89–91. NASA, Greenbelt.

Petrou K, Kranz SA, Trimborn S et al. (2016) Southern Ocean phytoplankton physiology in a changing climate. *Journal of Plant Physiology*, **203**, 135–150.

Pickett STA (1989) Space-for-time substitution as an alternative to long-term studies. In: *Long-term studies in ecology* (ed Likens GE), pp. 110–135. Springer, New York.

Pike J, Crosta X, Maddison EJ, Stickley CE, Denis D, Barbara L, Renssen H (2009) Observations on the relationship between the Antarctic coastal diatoms Thalassiosira antarctica Comber and Porosira glacialis (Grunow) Jørgensen and sea ice concentrations during the late Quaternary. *Marine Micropaleontology*, **73**, 14–25.

Piquet AMT, Bolhuis H, Davidson AT, Thomson PG, Buma AGJ (2008) Diversity and dynamics of Antarctic marine microbial eukaryotes under manipulated environmental UV radiation. *FEMS Microbiology Ecology*, **66**, 352–366.

Piquet AMT, Bolhuis H, Meredith MP, Buma AGJ (2011) Shifts in coastal Antarctic marine microbial communities during and after melt water-related surface stratification. *FEMS Microbiology Ecology*, **76**, 413–427.

Piquet AMT, van de Poll WH, Visser RJW, Wiencke C, Bolhuis H, Buma AGJ (2014) Springtime phytoplankton dynamics in Arctic Krossfjorden and Kongsfjorden (Spitsbergen) as a function of glacier proximity. *Biogeosciences*, **11**, 2263–2279.

Platt T, Gallegos CL, Harrison WG (1980) Photoinibition of photosynthesis in natural assemblages of marine phytoplankton. *Journal of Marine Research (USA)*, **38**, 687–701.

van de Poll WH, Janknegt PJ, van Leeuwe MA, Visser RJW, Buma AGJ (2009) Excessive irradiance and antioxidant responses of an Antarctic marine diatom exposed to iron limitation and to dynamic irradiance. *Journal of Photochemistry and Photobiology B: Biology*, **94**, 32–37.

van de Poll WH, Lagunas M, de Vries T, Visser RJW, Buma AGJ (2011) Non-photochemical quenching of chlorophyll fluorescence and xanthophyll cycle responses after excess PAR and UVR in Chaetoceros brevis, Phaeocystis antarctica and coastal Antarctic phytoplankton. *Marine Ecology Progress Series*, **426**, 119–131.

Polvani LM, Waugh DW, Correa GJP, Son SW (2011) Stratospheric Ozone Depletion: The Main Driver of Twentieth-Century Atmospheric Circulation Changes in the Southern Hemisphere. *Journal of Climate*, **24**, 795–812.

Price NM, Morel FMM (1990) Cadmium and cobalt substitution for zinc in a marine diatom. *Nature*, **344**, 658–660.

Prosser JI, Bohannan BJM, Curtis TP et al. (2007) The role of ecological theory in microbial ecology. *Nature Reviews Microbiology*, **5**, 384–392.

Quast C, Pruesse E, Yilmaz P et al. (2013) The SILVA ribosomal RNA gene database project: Improved data processing and web-based tools. *Nucleic Acids Research*, **41**, 590–596.

Quéroué F, Townsend A, van der Merwe P, Lannuzel D, Sarthou G, Bucciarelli E, Bowie A (2014) Advances in the offline trace metal extraction of Mn, Co, Ni, Cu, Cd, and Pb from open ocean seawater samples with

determination by sector field ICP-MS analysis. *Analytical Methods*, **6**, 2837.

Quetin LB, Ross RM (1985) Feeding by Antarctic Krill, Euphausia superba: Does Size Matter? *Antarctic Nutrient Cycles and Food Webs*, 372–377.

R Core Team (2016) R package. *R Foundation for Statistical Computing*, **739**.

Ramette A (2007) Multivariate analyses in microbial ecology. *FEMS Microbiology Ecology*, **62**, 142–160.

Redfield AC (1958) The biological control of chemical factors in the environment. *American Scientific*, **46**, 205–222.

Reisch CR, Moran MA, Whitman WB (2011) Bacterial catabolism of dimethylsulfoniopropionate (DMSP). *Frontiers in Microbiology*, **2**, 172.

Reiss CS, Walsh J, Goebel ME (2015) Winter preconditioning determines feeding ecology of Euphausia superba in the antarctic peninsula. *Marine Ecology Progress Series*, **519**, 89–101.

Riebesell U, Schloss I, Smetacek V (1991) Aggregation of algae released from melting sea ice: implications for seeding and sedimentation. *Polar Biology*, **11**, 239–248.

Rignot E, Casassa G, Gogineni P, Krabill W, Rivera A, Thomas R (2004) Accelerated ice discharge from the Antarctic Peninsula following the collapse of Larsen B ice shelf. *Geophysical Research Letters*, **31**.

Rignot E, Jacobs S, Mouginot J, Scheuchl B (2013) Ice-shelf melting around Antarctica. *Science*, **341**, 266–70.

Rijkenberg MJA, de Baar HJW, Bakker K et al. (2015) "PRISTINE", a new high volume sampler for ultraclean sampling of trace metals and isotopes. *Marine Chemistry*, **177**, 501–509.

Rocap G, Larimer FW, Lamerdin J et al. (2003) Genome divergence in two Prochlorococcus ecotypes reflects oceanic niche differentiation. *Nature*, **424**, 1042–1047.

Rognes T, Flouri T, Nichols B, Quince C, Mahé F (2016) VSEARCH: a versatile open source tool for metagenomics. *PeerJ*, **4**, e2409v1.

Ross RM, Quetin LB, Haberman KL (1998) Interannual and seasonal variability in short-term grazing impact of Euphausia superba in nearshore and offshore waters west of the Antarctic Peninsula. *Journal of Marine Systems*, **17**, 261–273.

Ross RM, Quetin LB, Martinson DG, Iannuzzi RA, Stammerjohn SE, Smith RC (2008) Palmer LTER: Patterns of distribution of five dominant zooplankton species in the epipelagic zone west of the Antarctic Peninsula, 1993-2004. *Deep-Sea Research Part II: Topical Studies in Oceanography*, **55**, 2086–2105.

Rozema PD, Venables HJ, van de Poll WH, Clarke A, Meredith MP, Buma AGJ (2017a) Interannual variability in phytoplankton biomass and species composition in northern Marguerite Bay (West Antarctic Peninsula) is governed by both winter sea ice cover and summer stratification. *Limnology and Oceanography*, **62**, 235–252.

Rozema PD, Biggs T, Sprong PAA et al. (2017b) Summer microbial community composition governed by upper-ocean stratification and nutrient availability in northern Marguerite Bay, Antarctica. *Deep-Sea Research Part II: Topical Studies in Oceanography*, **139**, 151–166.

Rozema PD, Kulk G, Veldhuis MP, Buma AGJ, Meredith MP, van de Poll WH (2017c) Assessing drivers of coastal phytoplankton productivity in northern Marguerite Bay, Antarctica. *Frontiers in Marine Science*, **4**.

Russell A, McGregor GR (2010) Southern hemisphere atmospheric circulation: Impacts on Antarctic climate and reconstructions from Antarctic ice core data. *Climatic Change*, **99**, 155–192.

Saba GK, Fraser WR, Saba VS et al. (2014) Winter and spring controls on the summer food web of the coastal West Antarctic Peninsula. *Nature communications*, **5**, 4318.

Saito MA, Goepfert TJ (2008) Zinc-cobalt colimitation of Phaeocystis antarctica. *Limnology and Oceanography*, **53**, 266–275.

Saito MA, Goepfert TJ, Noble AE, Bertrand EM, Sedwick PN, DiTullio GR (2010) A seasonal study of dissolved cobalt in the Ross Sea, Antarctica: micronutrient behavior, absence of scavenging, and relationships with Zn, Cd, and P. *Biogeosciences*, **7**, 4059–4082.

Sakshaug E, Holm-Hansen O (1986) Photoadaptation in Antarctic phytopfankton: Variations in growth rate, chemical composition and P versus I curves. *Journal of Plankton Research*, **8**, 459–473.

Schlitzer R (2016) Ocean Data View. http://odv.awi.de.

Schoemann V, Becquevort S, Stefels J, Rousseau V, Lancelot C (2005) Phaeocystis blooms in the global ocean and their controlling mechanisms: A review. *Journal of Sea Research*, **53**, 43–66.

Schofield O, Ducklow HW, Martinson DG, Meredith MP, Moline MA, Fraser WR (2010) How Do Polar Marine Ecosystems Respond to Rapid Climate Change? *Science*, **328**, 1520–1523.

Schofield O, Saba G, Coleman K et al. (2017) Decadal variability in coastal phytoplankton community composition in a changing West Antarctic Peninsula. *Deep Sea Research Part I: Oceanographic Research Papers*, **124**, 42–54.

Sedwick PN, DiTullio GR, Mackey DJ (2000) Iron and manganese in the Ross Sea, Antarctica: Seasonal iron limitation in Antarctic shelf waters. *Journal of Geophysical Research*, **105**, 11321.

Shannon P, Markiel A, Ozier O et al. (2003) Cytoscape: A software Environment for integrated models of biomolecular interaction networks. *Genome Research*, **13**, 2498–2504.

Shelley RU, Zachhuber B, Sedwick PN, Worsfold PJ, Lohan MC (2010) Determination of total dissolved cobalt in UV-irradiated seawater using flow injection with chemiluminescence detection. *Limnology and Oceanography: Methods*, **8**, 352–362.

Sherr EB, Sherr BF (1994) Bacterivory and herbivory: Key roles of phagotrophic protists in pelagic food webs. *Microbial Ecology*, **28**, 223–235.

Sherr EB, Sherr BF (2002) Significance of predation by protists in aquatic microbial food webs. *Antonie van Leeuwenhoek, International Journal of General and Molecular Microbiology*, **81**, 293–308.

Sherr EB, Sherr BF (2007) Heterotrophic dinoflagellates: A significant component of microzooplankton biomass and major grazers of diatoms in the sea. *Marine Ecology Progress Series*, **352**, 187–197.

Sherrell RM, Lagerström ME, Forsch KO, Stammerjohn SE, Yager PL (2015) Dynamics of dissolved iron and other bioactive trace metals (Mn, Ni, Cu, Zn) in the Amundsen Sea Polynya, Antarctica. *Elementa: Science of the Anthropocene*, **3**, 71.

Shi T, Horvath S (2006) Unsupervised Learning With Random Forest Predictors. *Journal of Computational and Graphical Statistics*, **15**, 118–138.

Shields AR, Smith WO (2009) Size-fractionated photosynthesis/irradiance relationships during Phaeocystis antarctica-dominated blooms in the Ross Sea, Antarctica. *Journal of Plankton Research*, **31**, 701–712.

Simon M, López-García P, Moreira D, Jardillier L (2013) New haptophyte lineages and multiple independent colonizations of freshwater ecosystems. *Environmental Microbiology Reports*, **5**, 322–332.

Simpson EH (1949) Measurement of Diversity. *Nature*, **163**, 688–688.

Simpson JH, Allen CM, Morris NCG (1978) Fronts on the continental shelf. *Journal of Geophysical Research*, **83**, 4607.

Smith RC, Stammerjohn SE (2001) Variations of surface air temperature and sea-ice extent in the western Antarctic Peninsula region. *Annals of Glaciology*, **33**, 493–500.

Sogin ML, Gunderson JH (1987) Structural Diversity of Eukaryotic Small Subunit Ribosomal RNAs: Evolutionary Implications. *Annals of the New York Academy of Sciences*, **503**, 125–139.

Sohrin Y, Urushihara S, Nakatsuka S et al. (2008) Multielemental determination of GEOTRACES key trace metals in seawater by ICPMS after preconcentration using an ethylenediaminetriacetic acid chelating resin. *Analytical Chemistry*, **80**, 6267–6273.

Stammerjohn S, Maksym T (2017) Gaining (and losing) Antarctic sea ice: variability, trends and mechanisms. In: *Sea Ice*, 3rd edn (ed Thomas DN), pp. 261–289. John Wiley & Sons, Ltd, Chichester.

Stammerjohn SE, Martinson DG, Smith RC, Iannuzzi RA (2008a) Sea ice in the western Antarctic Peninsula region: Spatio-temporal variability from ecological and climate change perspectives. *Deep-Sea Research Part II: Topical Studies in Oceanography*, **55**, 2041–2058.

Stammerjohn SE, Martinson DG, Smith RC, Yuan X, Rind D (2008b) Trends in Antarctic annual sea ice retreat and advance and their relation to El Niño–Southern Oscillation and Southern Annular Mode variability. *Journal of Geophysical Research*, **113**, 1–20.

Steig EJ, Schneider DP, Rutherford SD, Mann ME, Comiso JC, Shindell DT (2009) Warming of the Antarctic ice-sheet surface since the 1957 International Geophysical Year. *Nature*, **457**, 459–462.

Steig EJ, Ding Q, White JWC et al. (2013) Recent climate and ice-sheet changes in West Antarctica compared with the past 2,000 years. *Nature Geoscience*, **6**, 372–375.

Steinberg DK, Landry MR (2017) Zooplankton and the Ocean Carbon Cycle. *Annual Review of Marine Science*, **9**, 413–444.

Steinberg DK, Ruck KE, Gleiber MR et al. (2015) Long-term (1993-2013) changes in macrozooplankton off the western antarctic peninsula. *Deep-Sea Research Part I: Oceanographic Research Papers*, **101**, 54–70.

Stoecker DK, Silver MW, Michaels AE, Davis LH (1988) Obligate mixotrophy in Laboea strobila, a ciliate which retains chloroplasts. *Marine Biology*, **99**, 415–423.

Stoecker DK, Hansen PJ, Caron DA, Mitra A (2017) Mixotrophy in the Marine Plankton. *Annual Review of Marine Science*, **9**, 311–335.

Straza TRA, Ducklow HW, Murray AE, Kirchman DL (2010) Abundance and single-cell activity of bacterial groups in Antarctic coastal waters. *Limnology and Oceanography*, **55**, 2526–2536.

Stukel MR, Asher E, Couto N, Schofield O, Strebel S, Tortell P, Ducklow HW (2015) The imbalance of new and export production in the western Antarctic Peninsula, a potentially "leaky" ecosystem. *Global Biogeochemical Cycles*, **29**, 1400–1420.

Sunda WG, Huntsman SA (1995) Iron uptake and growth limitation in oceanic and coastal phytoplankton. *Marine Chemistry*, **50**, 189–206.

Sunda WG, Huntsman SA (1998) Processes regulating cellular metal accumulation and physiological effects: Phytoplankton as model systems. *Science of The Total Environment*, **219**, 165–181.

Sunda WG, Swift DG, Huntsman SA (1991) Low iron requirement for growth in oceanic phytoplankton. *Nature*, **351**, 55–57.

Sverdrup H (1953) On conditions for the vernal blooming of phytoplankton. *Journal du Conseil Permanent International pour l'Exploration de la Mer*, **18**, 287–295.

Taguchi YH, Oono Y (2005) Relational patterns of gene expression via non-metric multidimensional scaling analysis. *Bioinformatics*, **21**, 730–740.

Takao S, Hirawake T, Wright SW, Suzuki K (2012) Variations of net primary productivity and phytoplankton community composition in the Indian sector of the Southern Ocean as estimated from ocean color remote sensing data. *Biogeosciences*, **9**, 3875–3890.

Takeda S (1998) Influence of iron availability on nutrient consumption ratio of diatoms in oceanic waters. *Nature*, **393**, 774–777.

Thompson DWJ, Solomon S (2002) Interpretation of Recent Southern Hemisphere Climate Change. *Science*, **296**, 3995–399.

Timmermans KR, Gerringa LJA, de Baar HJW et al. (2001) Growth rates of large and small Southern Ocean diatoms in relation to availability of iron in natural seawater. *Limnology and Oceanography*, **46**, 260–266.

Timmermans KR, van der Wagt B, de Baar HJW (2004) Growth rates, half saturation constants, and silicate, nitrate, and phosphate depletion in relation to iron availability of four large open-ocean diatoms from the Southern Ocean. *Limnology and Oceanography*, **49**, 2141–2151.

Tison JL, Brabant F, Dumont I, Stefels J (2010) High-resolution dimethyl sulfide and dimethylsulfoniopropionate time series profiles in decaying summer first-year sea ice at Ice Station Polarstern, western Weddell Sea, Antarctica. *Journal of Geophysical Research: Biogeosciences*, **115**, G04044.

Torbjørn R (2016) Vsearch: VSEARCH version 1.1.3. Zenodo.

Trimborn S, Hoppe CJM, Taylor BB, Bracher A, Hassler C (2015) Physiological characteristics of open ocean and coastal phytoplankton communities of Western Antarctic Peninsula and Drake Passage waters. *Deep Sea Research Part I: Oceanographic Research Papers*, **98**, 115–124.

Trivelpiece WZ, Hinke JT, Miller AK, Reiss CS, Trivelpiece SG, Watters GM (2011) Variability in krill biomass links harvesting and climate warming to penguin population changes in Antarctica. *Proceedings of the National Academy of Sciences of the United States of America*, **108**, 7625–8.

Tsuda A, Kawaguchi S (1997) Microzooplankton grazing in the surface water of the Southern

Ocean during an austral summer. *Polar Biology*, **18**, 240–245.

Turner J, Colwell SR, Marshall GJ et al. (2005) Antarctic climate change during the last 50 years. *International Journal of Climatology*, **25**, 279–294.

Turner J, Bindschadler R, Convey P et al. (2009) *Antarctic Cliamte Change and the Environment*. 555 pp.

Turner J, Maksym T, Phillips T, Marshall GJ, Meredith MP (2013) The impact of changes in sea ice advance on the large winter warming on the western Antarctic Peninsula. *International Journal of Climatology*, **33**, 852–861.

Turner J, Lu H, White I et al. (2016) Absence of 21st century warming on Antarctic Peninsula consistent with natural variability. *Nature*, **535**, 411–415.

Twining BS, Baines SB (2013) The trace metal composition of marine phytoplankton. *Annual review of marine science*, **5**, 191–215.

Twining BS, Baines SB, Fisher NS (2004) Element stoichiometries of individual plankton cells collected during the Southern Ocean Iron Experiment (SOFeX). *Limnology and Oceanography*, **49**, 2115–2128.

Uitz J, Claustre H, Griffiths FB, Ras J, Garcia N, Sandroni V (2009) A phytoplankton class-specific primary production model applied to the Kerguelen Islands region (Southern Ocean). *Deep-Sea Research Part I: Oceanographic Research Papers*, **56**, 541–560.

Vaughan DG, Marshall GJ, Connolley WM et al. (2003) Recent rapid regional climate warming on the Antarctic Peninsula. *Climatic Change*, **60**, 243–274.

Venables HJ, Meredith MP (2014) Feedbacks between ice cover, ocean stratification, and heat content in Ryder Bay, western Antarctic Peninsula. *Journal of Geophysical Research: Oceans*, **119**, 5323–5336.

Venables HJ, Clarke A, Meredith MP (2013) Wintertime controls on summer stratification and productivity at the western Antarctic Peninsula. *Limnology and Oceanography*, **58**, 1035–1047.

Venables HJ, Meredith MP, Brearley JA (2017) Modification of deep waters in Marguerite Bay, western Antarctic Peninsula, caused by topographic overflows. *Deep-Sea Research Part II: Topical Studies in Oceanography*, **139**, 9–17.

Vernet M, Martinson D, Iannuzzi R et al. (2008) Primary production within the sea-ice zone west of the Antarctic Peninsula: I-Sea ice, summer mixed layer, and irradiance. *Deep-Sea Research Part II: Topical Studies in Oceanography*, **55**, 2068–2085.

Vernet M, Wendy AK, Lynn RY, Alexander TL, Robin MR, Langdon BQ, Christian HF (2012) Primary production throughout austral fall, during a time of decreasing daylength in the western Antarctic Peninsula. *Marine Ecology Progress Series*, **452**, 45–61.

Wang Q, Garrity GM, Tiedje JM, Cole JR (2007) Naive Bayesian classifier for rapid assignment of rRNA sequences into the new bacterial taxonomy. *Applied and Environmental Microbiology*, **73**, 5261–5267.

Wang J, Li M, Chen J, Pan Y (2011) A fast hierarchical clustering algorithm for functional modules discovery in protein interaction networks. *IEEE/ACM transactions on computational biology and bioinformatics / IEEE, ACM*, **8**, 607–20.

Westerlund S, Öhman P (1991) Cadmium, copper, cobalt, nickel, lead, and zinc in the water column of the Weddell Sea, Antarctica. *Geochimica et Cosmochimica Acta*, **55**, 2127–2146.

Weston K, Jickells TD, Carson DS et al. (2013) Primary production export flux in Marguerite Bay (Antarctic Peninsula): Linking upper water-column production to sediment trap flux. *Deep-Sea Research Part I: Oceanographic Research Papers*, **75**, 52–66.

Williams TJ, Long E, Evans F et al. (2012) A metaproteomic assessment of winter and summer bacterioplankton from Antarctic Peninsula coastal surface waters. *The ISME journal*, **6**, 1883–900.

Williams CM, Dupont AM, Loevenich J, Post AF, Dinasquet J, Yager PL (2016) Pelagic microbial heterotrophy in response to a highly productive bloom of Phaeocystis antarctica in the Amundsen Sea Polynya ,. *Elementa: Science of the Anthropocene*, **4**, 102.

Wolf C, Frickenhaus S, Kilias ES, Peeken I, Metfies K (2013) Protist community composition in the Pacific sector of the Southern Ocean during austral summer 2010. *Polar Biology*, **37**, 375–389.

Wood LW (1985) Chloroform–Methanol Extraction of Chlorophyll a. *Canadian Journal of Fisheries and Aquatic Sciences*, **42**, 38–43.

Wright SW, Ishikawa A, Marchant HJ, Davidson AT, van den Enden RL, Nash G V. (2009) Composition and significance of picophytoplankton in Antarctic waters. *Polar Biology*, **32**, 797–808.

Wright SW, van den Enden RL, Pearce I, Davidson AT, Scott FJ, Westwood KJ (2010) Phytoplankton community structure and stocks in the Southern Ocean (30-80°E) determined by CHEMTAX analysis of HPLC pigment signatures. *Deep-Sea Research Part II: Topical Studies in Oceanography*, **57**, 758–778.

Yu L, Zhang W, Liu L, Yang J (2015) Determining microeukaryotic plankton community around Xiamen Island, Southeast China, using Illumina MiSeq and PCR-DGGE techniques (ed Chiang T-Y). *PLoS ONE*, **10**, e0127721.

Zhang J, Kobert K, Flouri T, Stamatakis A (2014) PEAR: A fast and accurate Illumina Paired-End reAd mergeR. *Bioinformatics*, **30**, 614–620.

Zhao Y, Vance D, Abouchami W, de Baar HJW (2014) Biogeochemical cycling of zinc and its isotopes in the Southern Ocean. *Geochimica et Cosmochimica Acta*, **125**, 653–672.

Zhu F, Massana R, Not F, Marie D, Vaulot D (2005) Mapping of picoeucaryotes in marine ecosystems with quantitative PCR of the 18S rRNA gene. *FEMS Microbiology Ecology*, **52**, 79–92.

Zingone A, Chrétiennot-Dinet MJ, Lange M, Medlin L (1999) Morphological and Genetic Characterization of Phaeocystis Cordata and P. Jahnii (Prymnesiophyceae), Two New Species From the Mediterranean Sea. *Journal of Phycology*, **35**, 1322–1337.

Acknowledgements and Dankwoord

WOW, I'm writing the acknowledgements! That means I am almost done with the journey that started over 5 years ago. And what a ride has it been. From the chilling ocean spray of the Antarcitic ocean in my face while speeding between ice bergs and whales to the late hours behind a computer screen in a desolated building. Humbled by the icy beauty of the Antarctic continent and motivated by interesting results and people, I now see the fruits of my labors which have led to the culmination of this project, a PhD thesis to defend. Many people have contributed to this research or made life even more enjoyable whilst doing this. I am sure I will forget many, for that I apologize, but I will have a go at thanking as many people as I can.

First and foremost I would like to thank Anita, my promotor, for giving me the opportunity to partake in this endeavor. While we have had our differences, I greatly appreciate the advice and guidance you have given me. I was lucky to have a promotor which allowed a great sense of freedom with regards to the topics and approaches I explored during this project. Over the course of the project, Henk became my go to advisor for everything related to DNA. Henk, your drive, creativity and understanding stimulated me to pursue an open mind and sparked my creativity. Willem, my second co-promotor, stepped into the role of daily advisor, for which I am very grateful. Thanks, for your approachability and reality check. Many times we have acted as each other's sounding board which resulted in interesting and relevant science being pursued. Also, I would like to thank Anouk Piquet, although we only shared an office for a brief moment I appreciate you sharing your experience with field work and in the molecular lab.

Much of the success of this project depended on the Antarctic fieldwork. Organizing, executing and preparing the continuous collection of data and samples for a 2.5 year period combined with two additional extensive summer campaigns is something I could not and have not done by myself. First and foremost, I would like to thank Ronald for sharing his extensive knowledge as a field technician and polar field guide. Together we designed and build new equipment, executed a large part of the summer campaigns and went through the extensive piles of paperwork. And perhaps more importantly, thanks for teaching me the names of all non-microbial fauna we have

observed during the exciting sampling trips. And of course Pim, as a student you've joined for the second summer campaign. Your determination and dedication to the project were marvelous and I think you've had a great experience despite the long hours of filtrations in a chilly container. Our sampling programme continued throughout two Antarctic winters, while I was absent, and for this I am grateful to Amber Annett and Mairi Fenton. You were both very enthusiastic for staying and despite a demanding sampling schedule you've managed to collect a unique set of winter samples. And there are many, many more people that assisted in these campaign preparations: the RuG logistics (Dirk-Jan and colleagues) and purchase departments (Froukje and colleagues), the RAD lab (Arjo and Mieke). Moreover, the campaigns were impossible without the support from the British Antarctic Survey, most specially Sharon Duggan, thanks for your seemingly endless support both on site and through email, Mike Brian (station leader), the boatmen, the Marine assistants (Sabrina and Mairi), and all the support staff and fellow scientists on station. A very big thank you.

Not only I, but many other scientists worked at or from Rothera, there were too many to name and everybody added to a great atmosphere in the Bonner and Gerritsz labs. Sharing cookies and coffees, often going on boats together and many fun times. Also, many were affiliated with the Dutch Programme: Jacqueline, Maria, Tristan, Libby, Désirée, Nikki, Zoi, Dorien, Patrick and Hein. Especially Johann is thanked as we shared many hours on the Sea Rover helping eachother to collect samples for our research. Thanks for all the fun and help, but also the feedback and exchange of ideas that only improved my PhD!

After the collection on the samples and data, the tedious process of analyses began. Coffee breaks, and the occasional Friday afternoon beer, broke up this process and fueled my inspiration. Especially Peter, thank you for sharing your great perpectives on life and the job as a scientists. Also, a big thank you for sharing those coffees and beers to many of my marine biology colleagues: Eize, Dennis, Jan, Karin, Ika, Henk, Loes, Klaas, Stella, Gezien, Han, Steven, Cecilia, Sem, Azim and the many MSc students throughout the years. Alison, thank you for introducing me to the wonderful world of geocaching. It has been a wonderful distraction from writing my thesis! Martijn,

Wendy and Sean are thanked for their helping with pigment analysis and/or DNA extraction. Cindy, of course I want to say a special thanks to you. Not only for all of coffee breaks but also for all the paperwork with regards to my thesis defense and every other "small" question I have had.

Once all the samples were processed I came to the data analysis part and I was lucky to be collaborating with a large number of inspiring, kind and helpful scientists that gave their views on my work. I am grateful for Anita her introduction into the IMCONET framework where I've met many interesting and kind scientists including Edy Hernandez, Irene Schloss and Doris Abele. Also, this framework allowed me to visit Woods Hole and work in the lab of Linda Amaral-Zettler. Linda, thank you for facilitating such an inspiring environment and being a very curious person! I'm sure you like your new position on Texel! Finally, I would like to thank my BAS collaborators, Mike Meredith and Hugh Venables. Mike, thank you for always being helpful! Hugh, thanks for all the talks we've had on site about our research but also help with the RaTS data. It was great fun to shoot the occasional game of pool after lunch, thanks!

Obviously I also want to thank both my paranymiphs, Gemma and Michiel. Gemma, we've met when you were a PhD student at Ocean Ecosystems and we've followed highly similar paths during our studies. You worked in the Atlantic Ocean but you had the the great idea of starting new project at Rothera and thus shared an office for the past two years. Many laughs and frustrations were shared and you were an inspiration and example as a fellow junior scientist. Michiel, you're one of the guys with whom I started studying biology 10,000 years ago. Thanks for the many disussions we've had which resulted in an expansion of my horizon. You also wanted to work at Rothera, something I fully understand and you somewhat did. I had the good fortune of working with both my paranymiphs and sharing authorships on the same paper (Chapter 3). All kidding aside, I'm very glad to have you both standing by my side during the last minutes before my defense.

Completing a PhD thesis is not only about the work part, but also the mind set and relaxation outside of work hours. Daarom wil ik graag nog een aantal vrienden

bedanken. Ten eerste mijn bio-vrienden, Hanneke, Arne, Inge, Michiel, Maya, Chris, Anna, Remco en Floor, het merendeel ook (bijna) gepromoveerd. En natuurlijk ook de nieuwe introducees, Boris, Hugo en Rosemare! Een hechte groep met een sterk relativerend vermogen en die elkaar erg goed kent. In goede en slechte tijden werd er gelachen, gespot en gesteund. Een betere vriendengroep kan ik mij niet wensen. Daarnaast natuurlijk ook Maarten. Het is inmiddels een traditie geworden om éénmaal per jaar een avond in Den Haag door te brengen, altijd voor het Nederlands Pool Symposium. (Ik zal je nog even bellen over dit jaar….). Je bent altijd erg geïnteresseerd in wat ik een dag later ga vertellen of laat zien. Bedankt voor je interesse! Daarnaast natuurlijk ook Daniel, Myrthe, Liesbeth, Rianne, Frank en de buren van de Oranjerie! Bedankt voor alle steun en belangstelling. Ik hoop dat mijn promotie meer samenhang geeft aan alle dingen waar ik steeds mee bezig ben geweest.

Naast mijn vrienden is er natuurlijk ook mijn (schoon)familie, bedankt voor alle steun die we hebben gehad tijdens het veldwerk en het schrijven. Veelal stelden jullie vragen over Antarctica, het werk dat ik daar deed of de “waarom daar dan?”-vraag. Erg leuk hoe iedereen zo betrokken was bij dit onderzoek. Pa, mam, Sylvia, Miriam en Chris en ook mijn tweede familie, Anita, Roel, Karlien, Frank en Fokkejan excuses voor het missen van allerlei familie events en diner, maar ik ben blij zoals jullie voor mijn gezin hebben gezorgd tijdens mijn vele excursies en het laatste schrijven. Pa, het was leuk om samen de photosynthetron te bouwen, een apparaat dat nog steeds veelvuldig wordt gebruikt en waar veel publicaties uit zijn gekomen. Mam, hoewel je er niet bij kan zijn weet ik hoe trots je was en vandaag zou zijn geweest. Ik zal nooit vergeten hoe het interview uit het Dagblad boven je bed hing en je iedereen in Emmen glunderend vertelde wanneer ik weer eens in het buitenland zat. Roel, je interesse in mijn werk is altijd erg leuk en bedankt voor het dienen als klankbord! Het heeft mij enorm geholpen in het structureren van mijn boodschap. Een speciaal en groot dankjewel voor Karlien, het ontwerp van de voorkant en de hoofdstukpaginas is heel erg mooi geworden. Het boekje had zonder je hulp er nooit zo uit kunnen zien.

Tenslotte wil ik op het einde Aline en Merijn bedanken! Hoewel genoemd als laatste is hier zeker mijn grootste dank verschuligd. Aline, ik heb gelukkig altijd op je steun mogen rekenen om mijn doctorsgraad te behalen. Door dik en door dun, dichtbij of

ver weg heb je mij daarin gesteund en daarvoor ben ik je zeer dankbaar. De afgelopen vijf jaar hebben we een verscheidenheid aan life events meegemaakt, de meeste zeer positief maar helaas niet alle. Ik vind het heel erg leuk om te zien hoe je, met google er naast, mijn proefschrift zit te lezen! Merijn, wat leuk dat je er ook bij bent gekomen! Helaas eens een boekje zonder wolven, brandweer, dino's en auto's maar wel met algen!

Bibliography

Kim H, Ducklow HW, Abele D, Barlett ER, Buma AGJ, Meredith MP, Rozema PD, Schofield OM, Venables HJ, Schloss IR (submitted) Interdecadal variability of phytoplankton biomass accumulation along the coastal West Antarctic Peninsula. *Philosophical Transactions of the Royal Society A*.

Kulk G, Buist A, van de Poll WH, Rozema PD, Buma AGJ (submitted) Size scaling of photophysiology and growth in four freshly isolated diatom species from Ryder Bay, West Antarctic Peninsula. *Journal of Phycology*.

van de Poll WH, Kulk G, Rozema PD, Brussaard C, Visser RJW, Buma AGJ (submitted) Nutrient limitation in a melt water gradient affects composition but not productivity of post-bloom phytoplankton in Kongsfjorden, Spitsbergen. *Elementa: Science of the Anthropocene*.

Rozema PD, Kulk G, Veldhuis MP, Buma AGJ, Meredith MP, van de Poll WH (2017) Assessing drivers of coastal primary productivity in northern Marguerite Bay, Antarctica. *Frontiers in Marine Science*, **4**.

Rozema PD, Biggs T, Sprong PAA, Buma AGJ Venables HJ, Evans C, Meredith MP, Bolhuis H (2017) Summer microbial community composition governed by upper-ocean stratification and nutrient availability in northern Marguerite Bay, Antarctica. *Deep-Sea Research Part II: Topical Studies in Oceanography*, **139**, 151–166.

Bown J, Laan P, Ossebaar S, Bakker K, Rozema PD, de Baar HJW (2017) Bioactive trace metal time series during Austral summer in Ryder Bay, Western Antarctic Peninsula. *Deep Sea Research Part II: Topical Studies in Oceanography*, **139**, 103–119.

Rozema PD, Venables HJ, van de Poll WH, Clarke A, Meredith MP, Buma AGJ (2017) Interannual variability in phytoplankton biomass and species composition in northern Marguerite Bay (West Antarctic Peninsula) is governed by both winter sea ice cover and summer stratification. *Limnology and Oceanography*, **62**, 235–252.

van de Poll WH, Maat D, Fischer P, Rozema PD, Daly OB, Koppelle S, Visser RJW, Buma AGJ (2016) Atlantic advection driven changes in glacial meltwater: Effects on phytoplankton chlorophyll-a and taxonomic composition in Kongsfjorden, Spitsbergen. *Frontiers in Marine Science*, **3**, 200.

van de Poll WH, Boute PG, Rozema PD, Buma AGJ, Kulk G, Rijkenberg MJA (2015) Sea surface temperature control of taxon specific phytoplankton production along an oligotrophic gradient in the Mediterranean Sea. *Marine Chemistry*, **177**, 536–544.

van de Poll WH, Kulk G, Timmermans KR, Brussaard CPD, van der Woerd HJ, Kehoe MJ, Mojica KDA, Visser RJW, Rozema PD, Buma AGJ (2013) Phytoplankton chlorophyll *a* biomass, composition, and productivity along a temperature and stratification gradient in the northeast Atlantic Ocean. *Biogeosciences*, **10**, 4227–4240.